

Organic geochemical characteristics of coal deposits in  
Lampang Province



Mr. Patthapong Chaiseanwang

จุฬาลงกรณ์มหาวิทยาลัย  
CHULALONGKORN UNIVERSITY

A Thesis Submitted in Partial Fulfillment of the Requirements  
for the Degree of Master of Science in Geology  
Department of Geology  
FACULTY OF SCIENCE  
Chulalongkorn University  
Academic Year 2019  
Copyright of Chulalongkorn University

ลักษณะเฉพาะทางธรณีเคมีอินทรีย์ของแหล่งถ่านหินในจังหวัดลำปาง



วิทยานิพนธ์นี้เป็นส่วนหนึ่งของการศึกษาตามหลักสูตรปริญญาวิทยาศาสตรมหาบัณฑิต

สาขาวิชาธรณีวิทยา ภาควิชาธรณีวิทยา

คณะวิทยาศาสตร์ จุฬาลงกรณ์มหาวิทยาลัย

ปีการศึกษา 2562

ลิขสิทธิ์ของจุฬาลงกรณ์มหาวิทยาลัย



ปัฐพงษ์ ไชยแสนวัง : ลักษณะเฉพาะทางธรณีเคมีอินทรีย์ของแหล่งถ่านหินในจังหวัดลำปาง. ( Organic geochemical characteristics of coal deposits in Lampang Province) อ.ที่ปรึกษาหลัก : ศศ. ดร.ปัฐพงษ์ เชนรัมย์

ถ่านหินและหินตะกอนจำนวน 31 ตัวอย่างจากแหล่งถ่านหินแม่ติบและแหล่งถ่านหินแม่ทานที่ตั้งอยู่ในจังหวัดลำปางทางตอนเหนือของประเทศไทยถูกนำมาศึกษาลักษณะเฉพาะทางธรณีเคมีอินทรีย์ (Organic geochemistry) ผลจากการวิเคราะห์ปริมาณสารอินทรีย์ทั้งหมด (Total organic carbon) พบว่าตัวอย่างถ่านหินจากแหล่งแม่ติบมีค่าระหว่าง 30.12 - 73.71 wt. % และสูงกว่าตัวอย่างถ่านหินของแหล่งแม่ทานซึ่งมีค่าระหว่าง 23.48 - 52.50 wt. % หินดินดานจากทั้งสองแหล่งมีค่าใกล้เคียงกันระหว่าง 4.82 - 19.49 wt. % ในแหล่งแม่ติบ และ 14.00 - 24.87 wt. % ในแหล่งแม่ทาน ค่าที่น้อยที่สุดของปริมาณสารอินทรีย์ทั้งหมดปรากฏในตัวอย่างหินโคลนซึ่งมีค่าระหว่าง 0.88 - 4.92 wt. % ในแหล่งแม่ติบ และค่าระหว่าง 0.59 - 5.98 wt. % การวิเคราะห์ปริมาณสารอินทรีย์ที่สกัดได้ (Extractable organic matter) ในตัวอย่างหินของแหล่งแม่ติบมีค่าระหว่าง 1,277 - 9,764 ppm ในขณะที่ตัวอย่างหินของแหล่งแม่ทานมีค่ามากกว่าโดยอยู่ระหว่าง 1,256-16,421 ppm จากข้อมูลข้างต้นทั้งสองแหล่งมีศักยภาพการเป็นชั้นหินต้นกำเนิดของแหล่งปิโตรเลียมอยู่ในเกณฑ์ดีถึงดีเยี่ยมยกเว้นหินโคลนบางตัวอย่าง ข้อมูลลักษณะเฉพาะทางธรณีเคมีอินทรีย์ศึกษาจากแก๊สโครมาโตแกรม (Gas chromatogram) ได้มาจากการวิเคราะห์โดยใช้เครื่องมือแก๊สโครมาโตกราฟี-แมสสเปกโตรมิเตอร์ (Gas chromatography-mass spectrometer) ซึ่งให้ข้อมูลของตัวชี้วัดทางชีวภาพ (Biomarker and non-biomarker) ที่มีประโยชน์ในการตีความทั้งระดับความพร้อมสมบูรณ์ (Maturity) ชนิดของอินทรีย์วัตถุ (Organic matter input) และสภาพแวดล้อมการสะสมตัวในอดีต (Depositional environment) ในการศึกษาถ่านหินมีระดับความพร้อมสมบูรณ์เทียบเท่ากับระดับถ่านหิน (coal rank) อยู่ในระดับลิกไนต์ถึงบิทูมินัสสารระเหยสูงระดับซี (Lignite – high volatile bituminous C) อ้างอิงจากตัวชี้วัดความพร้อมสมบูรณ์ทางชีวภาพ (Biomarker maturity) ซึ่งบ่งชี้ว่าตัวอย่างถ่านหินมีระดับความพร้อมสมบูรณ์อยู่ในระดับตอนต้น (immature-early mature stage) แก๊สโครมาโตแกรมของแอลเคนสายตรง (n-alkanes) และดัชนีคาร์บอนคูตี (Carbon Preference Index, CPI) ของทั้งสองแหล่งถ่านหินบ่งชี้ถึงที่พบเป็นชนิดของสารอินทรีย์หลักร่วมกับสาหร่ายน้ำจืดที่เป็นชนิดของสารอินทรีย์รอง สภาพแวดล้อมการสะสมตัวโบราณของทั้งสองแหล่งถ่านหินนั้นสะสมตัวบนบกโดยอ้างอิงจากตัวชี้วัดทางชีวภาพของสเตอรินทั่วไป (Regular steranes) และพบว่าวิวัฒนาการที่แตกต่างกันส่งผลมาจากสภาวะการสะสมตัวโบราณที่แตกต่างกัน การเกิดถ่านหินของทั้งสองแหล่งสัมพันธ์กับสภาวะออกซิเจนปานกลางถึงสูงในช่วงระหว่างการสะสมตัว ระดับน้ำในแอ่งมีส่วนสำคัญในการควบคุมชนิดของอินทรีย์วัตถุและการเกิดถ่านหิน ตัวอย่างหินดินดานในการศึกษานี้สะสมตัวภายใต้สภาวะไร้ออกซิเจนซึ่งสัมพันธ์กับระดับน้ำที่สูงโดยเป็นสภาวะที่สามารถให้อินทรีย์วัตถุประเภทสาหร่ายที่อาศัยอยู่ในแอ่งที่มีสภาวะไร้ออกซิเจนถึงออกซิเจนต่ำส่งผลให้เกิดหินน้ำมันขึ้นได้ โดยเฉพาะแหล่งแม่ติบ หินโคลนสามารถสะสมตัวภายใต้สภาวะออกซิเจนปานกลางเป็นส่วนใหญ่ในช่วงที่มีปริมาณสารอินทรีย์

สาขาวิชา ธรณีวิทยา  
ปีการศึกษา 2562

ลายมือชื่อผู้นิสิต .....  
ลายมือชื่อ อ.ที่ปรึกษาหลัก .....

# # 6172004123 : MAJOR GEOLOGY

KEYWORD Biomarker and non-biomarker, Depositional environment, Mae  
D: Teep, Mae Than, Thermal maturity

Patthapong Chaiseanwang : Organic geochemical characteristics of coal  
deposits in Lampang Province. Advisor: Asst. Prof. PIYAPHONG  
CHENRAI, Ph.D.

Thirty-one rocks and coals were collected from Mae Teep and Mae Than coal mines located in Lampang Province, Northern Thailand in order to investigate their geochemical characteristics. The total organic carbon (TOC) contents of Mae Teep coal samples are slightly higher with the range of 30.12 - 73.71 wt. % compared to those from Mae Than samples ranging from 23.48 - 52.20 wt. %. Shales from Mae Teep and Mae Than coal mines exhibit similar values with 4.82 - 19.49 wt. % and 14.00 - 24.87 wt. %, respectively. The lowest TOC contents appear on mudstones, ranging from 0.88 to 4.92 wt. % in Mae Teep coal mine and from 0.59 to 5.98 wt. % in Mae Than coal mine. The extractable organic matter (EOM) from Mae Teep samples vary between 1,277 and 9,764 ppm, while Mae Than samples are higher in the range of 1,256 – 16,421 ppm. The TOC and EOM results indicate coals and shales are good to excellent hydrocarbon generation potential for source rocks, except some mudstone samples. Biomarker and non-biomarker parameters from GC-MS analysis are useful to interpret thermal maturity, organic matter input and depositional environment. The thermal maturity of coal samples from both coal mines are represented in the range of immature to early mature stage at the present day which is equivalent to lignite to high volatile bituminous C based on the American Society for Testing and Materials (ASTM). The distribution of n-alkanes showing the predominance of long-chain n-alkanes and the high CPI values in all samples indicate terrestrial higher plants input. The difference in redox conditions of depositional environments exhibits the different lithology. The coal formation in both basins requires high level of oxygen content, probably related to suboxic to oxic condition during sediment deposits. Local water table within the basins may be controlled the organic matter inputs and coal formation. Shale samples in this study are deposited under anoxic condition during high water level. Consequently, this condition provides algal input originated from blooms of planktonic algae settling to the bottom of the basin where is little to no oxygen content, resulting in the oil shale formation, particularly in Mae Teep basin. During the low productivity, mudstones can be occurred mostly under suboxic condition.

Field of Study: Geology

Student's Signature

Academic 2019

Advisor's Signature

Year:

.....

## ACKNOWLEDGEMENTS

I would like to thank my thesis advisor Asst. Prof. Piyaphong Chenrai for his advice, support in this work. All master students, my colleague and my family are thank for encouragement.

I am grateful to scientists and officers at Department of Geology, Center of Excellence on Hazardous Substance Management (HSM) and Scientific and Technological Research Equipment Centre (STREC) of Chulalongkorn University, who provides and guides laboratory and facilities.

Patthapong Chaiseanwang



# TABLE OF CONTENTS

	<b>Page</b>
.....	iii
ABSTRACT (THAI) .....	iii
.....	iv
ABSTRACT (ENGLISH) .....	iv
ACKNOWLEDGEMENTS .....	v
TABLE OF CONTENTS .....	vi
List of tables.....	ix
List of figures.....	xi
CHAPTER I.....	16
INTRODUCTION .....	16
1.1 Rationales.....	16
1.2 Study area .....	17
1.3 Objectives .....	18
1.4 Theories .....	18
1.4.1 Coal definition.....	18
1.4.2 Coal composition.....	19
1.4.3 Coalification .....	21
1.4.4 Maturation of organic matter.....	24
1.4.5 Quantity of organic matter .....	26
1.4.6 Biomarkers .....	28
CHAPTER II.....	35
LITERATURE REVIEWS .....	35
2.1 Geological setting of Cenozoic basins.....	35
2.2 Stratigraphy.....	41
2.2.1 Mae Teep basin .....	41

2.2.2 Mae Than basin .....	42
2.3 Coal-bearing sedimentary basins in the Cenozoic .....	44
2.4 Cenozoic sedimentary basins in Northern Thailand .....	47
2.5 Organic geochemical characteristics of coal .....	49
2.6 Organic matter in intermontane basins .....	51
2.7 Environmental of coexistence of coal accumulation and oil shale formation and their crucial organic matter materials. ....	54
CHAPTER III .....	57
METHODOLOGY .....	57
3.1 Field observation and sample collection and preparation.....	58
3.2 Organic geochemical analysis .....	58
3.2.1 Total organic carbon (TOC).....	58
3.2.2 Extractable organic matter (EOM).....	60
3.2.3 Column chromatography.....	61
3.2.4 Gas chromatography - Mass spectrometry (GC - MS).....	62
CHAPTER IV .....	64
RESULTS .....	64
4.1 Sample description.....	64
4.2 Total organic carbon (TOC) .....	75
4.3 Extractable organic matter (EOM) .....	75
4.4 Hydrocarbon fractions .....	75
4.5 Gas chromatograms .....	78
4.5.1 n-alkanes and isoprenoids .....	78
4.5.2 Carbon preference index (CPI), average chain length (ACL), terrigenous/aquatic ratio (TAR), natural n-alkanes ratio (NAR) and $P_{aq}$ .....	82
4.5.3 Triterpanes and terpanes.....	85
4.5.4 Steranes .....	88
CHAPTER V .....	91
DISCUSSIONS.....	91
5.1 Quantity of organic matter.....	91



5.2 Type of organic matter.....	95
5.3 Maturity of organic matter related to coal rank .....	101
5.4 Depositional environment.....	106
5.5 Comparison between Mae Teep and Mae Than basins .....	110
Chapter VI.....	117
Conclusions.....	117
Appendix.....	118
REFERENCES .....	150
VITA.....	161



## List of tables

	<b>Page</b>
Table 1 Maceral groups and modes of optical identification (Modified from Bustin et al., 1985; Stach et al., 1982; Styan and Bustin, 1983; Taylor et al., 1998).....	20
Table 2 Petrographic nomenclature and genetic groupings of coal macerals (Compiled from ICCP, 1971, 1998, 2001; Stanton et al., 1989; Sýkorová et al., 2005). ....	20
Table 3 Classification of source rock richness based on total organic carbon (TOC) and extractable organic matter (EOM) contents (Peters and Cassa, 1994).....	28
Table 4 Lithological descriptions from Mae Teep samples.....	65
Table 5 Lithological descriptions from Mae Than samples.....	71
Table 6 The results of TOC, EOM and EOM fractions. ....	77
Table 7 The results of n-alkanes and isoprenoids.....	81
Table 8 The results of CPI, ACL, P <sub>aq</sub> , TAR and NAR ratios. ....	84
Table 9 The results of triterpane and terpane distribution. ....	87
Table 10 The results of sterane distribution.....	90
Table 11 The results of TOC, EOM and EOM fractions of coals compared to the previous studies.....	93
Table 12 The results of TOC, EOM and EOM fractions of shales and oil shales compared to the previous studies.....	94
Table 13 The results of n-alkane distribution, CPI and type of organic matter of coals compared to the previous studies.....	100
Table 14 The results of n-alkane distribution, CPI and type of organic matter of shales and oil shales compared to the previous studies. ....	100
Table 15 The maturity indicator and thermal maturity related to coal rank compared to the previous studies.....	105
Table 16 The depositional environments and their conditions of coals compared to the previous studies.....	114
Table 17 The depositional environments and their conditions of shales and oil shales compared to the previous studies.....	115
Table 18 The organic geochemical characteristics of the studied samples based on biomarkers and related parameters. ....	115

Table 19 The interpretation of organic geochemical characteristics of the studied samples.....	116
Table 20 The peak identification of triterpene and terpane distribution.....	118
Table 21 The peak identification of sterane distribution. ....	118



## List of figures

### Page

Figure 1 The map of the study area located in Lampang province, Northern Thailand. The study area consists of Mae Teep Basin and Mae Than Basin aligned on NE-SW direction in which adjacent to Mae Moh Basin. ....	18
Figure 2 The process of peatification, which occurs on the surface is followed by coalification of the peat upon burial in the subsurface where it is dewatered and exposed to heat and pressure (Modified from Greb, 2006). ....	22
Figure 3 Diagram of coal macerals in relation to hydrogen/carbon and oxygen/carbon atomic ratios, coal types, and direction of coal rank increase. H, hydrogen; O, oxygen; C, carbon (Modified from Hunt, 1991; Mukhopadhyay and Hatcher, 1993; van Krevelen, 1981).....	23
Figure 4 Maturation stages of coals plotted in a Van Krevelen type diagram. Sapropelic coals start with a high H/C atomic ratio due to a high aliphatic content, humic coals start with a high O/C atomic ratio and undergo the coalification stages peat, lignite, sub-bituminous coal and high volatile bituminous coal (Modified from Killops and Killops, 2013).....	24
Figure 5 General scheme of evolution of the organic matter, from the freshly deposited sediment to the metamorphic zone. (CH: carbohydrates, AA: amino acids, FA: fluvic acids, HA: humic acids, L: lipids, HC: hydrocarbons, N,S,O: N, S, O compounds (non-hydrocarbon)) and comparison of the scale of equivalent A.S.T.M. coal rank (Modified from Tissot and Welte, 1984). ....	26
Figure 6 Composition of disseminated organic matter in sedimentary rocks (Tissot and Welte, 1984).....	27
Figure 7 Pristane ( $C_{19}H_{40}$ ) (Stauffer et al., 2008b). ....	28
Figure 8 Phytane ( $C_{20}H_{42}$ ) (Stauffer et al., 2008b). ....	28
Figure 9 Heptadecane ( $n-C_{17}$ ; $C_{17}H_{36}$ ) (Hintze et al., 2010).....	29
Figure 10 Octadecane ( $n-C_{18}$ ; $C_{18}H_{38}$ ) (Hintze et al., 2010).....	29
Figure 11 $C_{20}$ Tricyclic terpane (Greenwood et al., 2000). ....	29
Figure 12 Gammacerane ( $C_{30}H_{52}$ ) (Xiao et al., 2018). ....	30
Figure 13 $18\alpha(H)-22,29,30$ -Trisnorneohopane ( $C_{27}H_{46}$ ; Ts) (Peters et al., 2005). ....	30
Figure 14 $17\alpha(H)-22,29,30$ -Trisnorhopane ( $C_{27}H_{46}$ ; Tm) (Peters et al., 2005). ....	30

Figure 15 17 $\beta$ (H),21 $\alpha$ (H)-moretane (C <sub>30</sub> H <sub>52</sub> ) (Peters et al., 2005).....	31
Figure 16 17 $\alpha$ (H),21 $\beta$ (H)-hopane (C <sub>30</sub> H <sub>52</sub> ) (Xiao et al., 2018). ....	31
Figure 17 Homohopane (C <sub>31</sub> H <sub>54</sub> ) (Peters et al., 2005).....	31
Figure 18 Cholestane (C <sub>27</sub> H <sub>48</sub> ) (Rohrssen et al., 2015). ....	32
Figure 19 Ergostane (C <sub>28</sub> H <sub>50</sub> ) (Rohrssen et al., 2015). ....	32
Figure 20 Stigmastane (C <sub>29</sub> H <sub>52</sub> ) (Rohrssen et al., 2015).....	32
Figure 21 17 $\alpha$ (H),21 $\beta$ (H)-hopane (C <sub>30</sub> H <sub>52</sub> ) (Xiao et al., 2018). ....	33
Figure 22 28,30-Bisnorhopane (C <sub>28</sub> H <sub>48</sub> ) (Peters et al., 2005).....	33
Figure 23 30-Norhopane (C <sub>29</sub> H <sub>50</sub> ) (Peters et al., 2005). ....	33
Figure 24 Hopane (C <sub>30</sub> H <sub>52</sub> ) (Xiao et al., 2018).....	34
Figure 25 Distribution of continental blocks, fragments and terranes, and principal sutures of Southeast Asia. Numbered micro-continental blocks, 1. East Java 2. Bawean 3. Paternoster 4. Mangkalihat 5. West Sulawesi 6. Semitau 7. Luconia 8. Kelabit–Longbowan 9. Spratly Islands–Dangerous Ground 10. Reed Bank 11. North Palawan 12. Paracel Islands 13. Macclesfield Bank 14. East Sulawesi 15. Bangai–Sula 16. Buton 17. Obi–Bacan 18. Buru–Seram 19. West Irian Jaya. LT = Lincang Terrane, ST = Sukhothai Terrane and CT =Chanthaburi Terrane. C–M = Changning–Menglian Suture, C.-Mai = Chiang Mai Suture, and Nan–Utt. = Nan–Uttaradit Suture (Metcalf, 2011).....	36
Figure 26 The tectonic evolution of Sundaland (Thailand–Malay Peninsula) and evolution of the Sukhothai Arc System during Late Carboniferous–Early Jurassic times (Metcalf, 2011). ....	38
Figure 27 Distribution of Cenozoic basins and significant fault systems in Thailand. (MPF = Mae Ping Fault, TPF = Three – Pagoda Fault, NF = Nan Fault, RNF = Ranong Fault, KMF = Klong Marui Fault, SWF = Sri Sawat Fault, MTF = Mae Tha Fault) (Charusiri and Pum-Im, 2009).....	40
Figure 28 Stratigraphy of Mae Teep basin (Modified from Gibling et al., 1981). ....	42
Figure 29 Map of the Basin and Range Province of northern Thailand showing the major Tertiary basins and late Cenozoic-Quaternary normal and strike-slip faults. Towns: CM, Chiand Mai; CR, Chiang Rai; PY, Payao. Faults: MCF, Mae Chan fault; MIF, Mae Ing fault; MKF, Mae Kuang fault; MTF, Mae Tha fault; PRF, Phrae fault; PUF, Pua Fault; PYF, Payao fault; TF, Thoen fault. Basins: CMB, Chiang Mai basin; CRB, Chiang Rai basin; FB, Fang basin; LiB, Li basin; LB, Lampang basin; NB, Nan basin; MIB, Mae Ing basin; MMB, Mae Moh basin; MTB, Mae Teep basin; MTHB,	

Mae Than basin; PB, Phrae basin; PRB, Phrao basin; PYB, Payao basin; WPB, Wiang Pa Pao basin (Rhodes et al., 2005).....	43
Figure 30 Stratigraphy of Mae Than basin (Modified from Muenlek, 1992; Thowanich, 1997). .....	44
Figure 31 Regional division of coal-bearing sedimentary basins in SE Asia (Friederich et al., 2016).....	45
Figure 32 Distribution of peat in the western part of SE Asia (Dommain et al., 2011; Staub and Esterle, 1994). .....	46
Figure 33 Major Cenozoic basins in Northern Thailand (Snansieng, 1979). .....	47
Figure 34 Warm temperate and tropical pollen from Ban Pa Kha and Mae Long Formations (Songtham et al., 2003).....	48
Figure 35 Elementary analysis of Tertiary Thai coals (Songtham et al., 2003). .....	48
Figure 36 Example of log plot of phytane to n-C <sub>18</sub> alkane (Ph/n-C <sub>18</sub> ) against pristane to n-C <sub>17</sub> alkane (Pr/n-C <sub>17</sub> ) (Alias et al., 2012). .....	49
Figure 37 Example of ternary diagram of regular steranes (C <sub>27</sub> -C <sub>29</sub> ) showing the relation of sterane components, source input, and depositional environment for the analyzed (Modified after Huang and Meinschein, 1979). .....	50
Figure 38 Example of cross-plot of two biomarker parameters sensitive to thermal maturity of the Pinangah sediments (Alias et al., 2012). .....	51
Figure 39 Schematic model of lacustrine environment (Setyobudi et al., 2016).....	52
Figure 40 The schematic model of wetland types (Wilcox et al., 2007). .....	55
Figure 41 The flow chart shows methodology of this study.....	57
Figure 42 The flow chart of sample preparation.....	58
Figure 43 Total organic carbon analysis.....	59
Figure 44 Soxhlet extraction for extracting EOM in rocks.....	60
Figure 45 The method of column chromatography. ....	62
Figure 46 The procedure of gas chromatography-mass spectrometry analysis. ....	63
Figure 47 The lithostratigraphy of Mae Teep coal mine. The white circle denotes the collecting samples.....	64
Figure 48 (a) thick bed of shale showing graded bedding (red square) in the uppermost part of lithostratigraphy of Mae Teep coal mine and (b) the gradational change between coal (sample ID MC3) and shale (sample ID MS2).....	65

Figure 49 The lithostratigraphy of Mae Than coal mine. The white circle denotes the collecting samples.....	70
Figure 50 Leaves and wood fragments preserved in shale (sample ID TS6). ....	71
Figure 51 An example of m/z 85 chromatogram showing n-alkane and isoprenoid distribution of oil shale from Mae Teep coal mine (sample ID MS5). ....	78
Figure 52 An example of m/z 85 chromatogram showing n-alkane and isoprenoid distribution of shale from Mae Than coal mine (sample ID TS6). ....	79
Figure 53 An example of m/z 191 chromatogram showing terpane and triterpane distribution of oil shale from Mae Teep coal mine (sample ID MS5). The peak identification shows on Table 20. ....	85
Figure 54 An example of m/z 191 chromatogram showing terpane and triterpane distribution of shale from Mae Than coal mine (sample ID TS5). The peak identification shows on Table 20. ....	86
Figure 55 An example of m/z 217 chromatogram showing sterane distribution of oil shale from Mae Teep coal mine (sample ID MS5). The peak identification shows on Table 21. ....	88
Figure 56 An example of m/z 217 chromatogram showing sterane distribution of shale from Mae Than coal mine (sample ID TS5). The peak identification shows on Table 21.....	89
Figure 57 The lithostratigraphy correlated with TOC (% wt.) and EOM (ppm) contents and EOM fractions of (a) Mae Teep coal mine, (b) Mae Than coal mine. ...	92
Figure 58 The lithology correlates with the percentage of n-alkanes from (a) Mae Teep samples (b) Mae Than samples.....	96
Figure 59 The lithology correlates with CPI, ACL, P <sub>aq</sub> , TAR and NAR of (a) Mae Teep coal mine (b) Mae Than coal mine. ....	99
Figure 60 The intersection of maturity biomarker parameters indicates immature to early mature stage at the present day. ....	104
Figure 61 The ternary diagram showing the relative of C <sub>27</sub> , C <sub>28</sub> and C <sub>29</sub> regular steranes. The red, blue and green circle dots represent coal, shale and mudstone from Mae Teep coal mine. The orange, light blue and light green square dots represent coal, shale and mudstone from Mae Than coal mine (Huang and Meinschein, 1979). ....	107
Figure 62 The log plot of Ph/nC <sub>18</sub> versus Pr/nC <sub>17</sub> of both Mae Teep and Mae Than samples (Shanmugam, 1985). The circle and square points denote Mae Teep and Mae Than samples, respectively. ....	108

Figure 63 The lithostratigraphy correlates with pr/ph ratio and gammacerane index of (a) Mae Teep coal mine, (b) Mae Than coal mine..... 109

Figure 64 The schematic model of three different types units provide the different lithotypes formation including Unit A: Shale and oil shale formation, Unit B: Mudstone formation and Unit C: Coal formation related to deep part, shallow part and marsh/bog in lacustrine environment, respectively (Setyobudi et al., 2016)..... 112

Figure 65 The schematic model of relative water level dependent on environmental conditions in (a) Mae Teep basin and (b) Mae Than basin, showing the difference in basin geometry (Yin et al., 2019)..... 113





# CHAPTER I

## INTRODUCTION

### 1.1 Rationales

Coal is the one of important fossil-fuel resources in Thailand and is widely used to generate electricity in power plant and heating materials for other industries such as cement and iron and steel. Consumption of coal is expected to increase in the future due to industries' expansion. However, domestic coal production in Thailand is not sufficient for higher demand. Importing of coals from other countries can partly solve the high demand problem in Thailand. Thus, coal study and exploration in Thailand is needed for sustainable energy in the future.

Cenozoic sedimentary basins have been found to be widely distributed in several parts of Thailand, especially in the north-western Thailand (Gibling and Ratanasthien, 1980). These basins are mostly formed as half-grabens or grabens of normal fault bounded, N-S trending. It was formed in result of extensional regime influenced by the collision of the Indian Plate and Eurasian Plate which initiated in Oligocene age (Morley et al., 2001; Songtham et al., 2005). These basins are often covered by Quaternary sediments and associated with coal and oil shale deposits (Coster et al., 2010). In Thailand, coal investigation has been studied on physical characteristics by stratigraphy and petrography in order to imply depositional environment, and studied on coal rank and property by using proximate and ultimate analysis (Gibling and Ratanasthien, 1980; Gibling et al., 1985b; Ratanasthien, 2011; Ratanasthien et al., 1999). However, a few organic geochemistry studies of the Cenozoic coals were performed in Thailand, especially biomarker and non-biomarker studies (Gibling et al., 1985a; Petersen et al., 2006). Thus, the organic geochemistry investigation of coal in Thailand is very limited and needed in order to get better understanding of coal deposits in Thailand. These two basins are economically operated as coal mines for power plant and cement industry. There are few geological studies in both Mae Teep and Mae Than basins. This study should be useful for coal mine operation. In addition, the location of these two basins are adjacent to Mae Moh basin where is geologically studied in several previous works in structure,

stratigraphy and geochemistry which can be useful for relate with the study areas. Thus, the aim of this study is to determine coal rank and depositional environment within Mae Teep and Mae Than basins in Lampang, northern Thailand based on organic geochemical characteristics using methods of total organic carbon (TOC) and gas chromatography-mass spectrometry (GC-MS).

## 1.2 Study area

The study areas are located into two coal-bearing sedimentary basins, Mae Teep and Mae Than basins. Mae Teep basin locates about 80 km northeast of Lampang Province (18°35'33.2"N 100°00'43.4"E) and covers about 30 km<sup>2</sup> with 3 km wide and 10 km long. Mae Than basin situates about 50 km southwest of Lampang Province (17°58'04.9"N 99°26'14.2"E) and covers about 10 km<sup>2</sup> with 2 km wide and 5 km long. In this study, rock samples are collected sixteen samples from Mae Teep basin and fifteen samples from Mae Than basin. The map of study area exhibits in Figure 1.

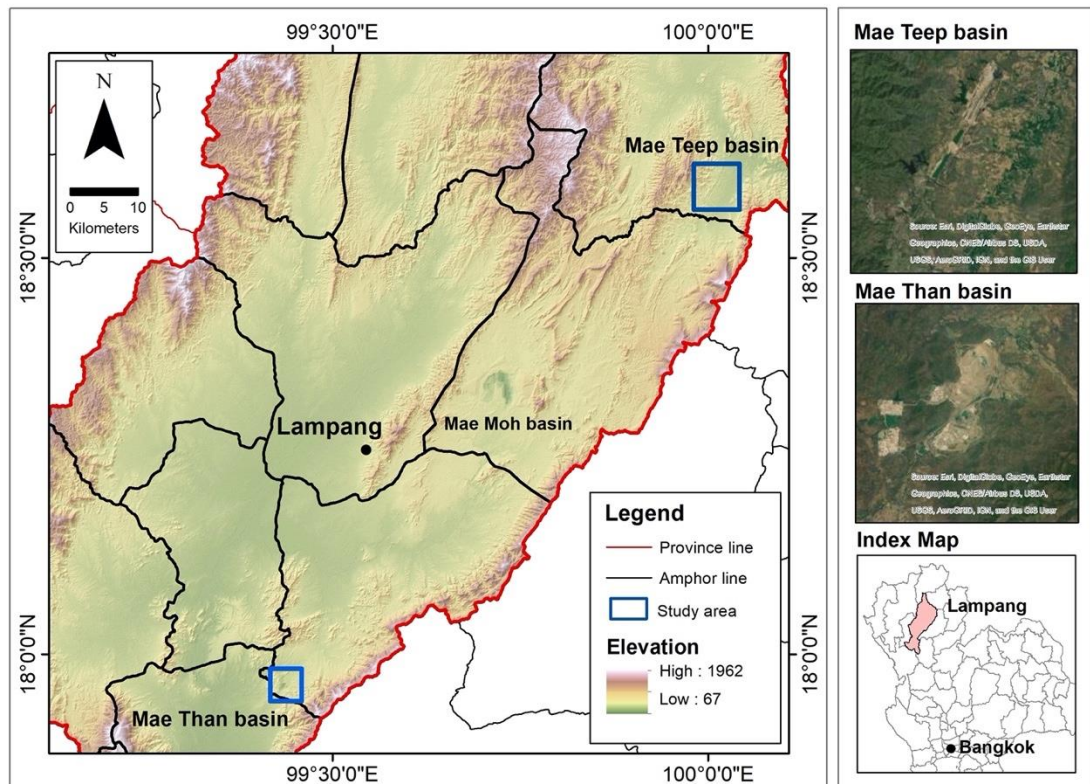


Figure 1 The map of the study area located in Lampang province, Northern Thailand. The study area consists of Mae Teep Basin and Mae Than Basin aligned on NE-SW direction in which adjacent to Mae Moh Basin.

### 1.3 Objectives

The aims of this thesis are to analyze the depositional environments of coal deposits in Lampang province and to understand the organic geochemical characteristics of coal deposits in Lampang province.

### 1.4 Theories

#### 1.4.1 Coal definition

Coal is a readily combustible rock. It consists of carbonaceous material with more than 50% by weight and more than 70% by volume (Schopf, 1956). Coal is formed by compaction of variously altered plant remains which is related to peaty deposits (Schopf, 1956). Coal is a mixture of organic and inorganic matters. It contains original moisture similar to modern peaty swamps or bogs (Bates and

Jackson, 1987). This definition has recognized and accepted from the American Society for Testing and Materials (ASTM, 1991) and many coal specialists.

Coal definition has various viewpoints. For example, to a biologist or botanist, coal is a successor of peat which is mainly composed of organic material derived from plants (Moore, 1989). The plants are accumulated in certain types of ecosystems which are wide-range peat-forming environments. The ecosystems are dynamic of production of biomass (i.e. living or biological materials), resulted from combination of biological, chemical, physical and hydrological processes (Quinty and Rochefort, 2003). In terms of coal petrologist, coal is a rock derived from plant remains which forms due to peatification and coalification or maturation (Teichmüller, 1989). To a sedimentologist, coal is a product of paleoenvironments and tectonic settings (Ferm and Horne, 1979; Ferm and Weisenfluh, 1989). As a geochemist, coal is a peat which has undergone chemical and physical transformation during diagenesis, catagenesis, and metagenesis (Mukhopadhyay and Hatcher, 1993; Tissot and Welte, 1984). Finally, to a petroleum geologist, coal is a source of hydrocarbons which generates gas (e.g. methane and carbon dioxide) and oil (Boreham and Powell, 1993; Clayton, 1993).

#### 1.4.2 Coal composition

Macerals are the organic components in coal (Stopes, 1935). Macerals are defined as their microscopic characteristics under transmitted and reflected lights and fluorescence (Table 1). Macerals show their physical and chemical properties in various reflectance controlled by coalification. Macerals are analyzed microscopically by color, shape, morphology, degree of preservation of cell structure, light reflectance, and the intensity of fluorescence. The origin of macerals can be formed by different parts of plant, depositional environment or preservation (Mastalerz et al., 2012). Macerals are classified into three groups: vitrinite or huminite, inertinite, and liptinite. There are macerals group, maceral subgroups, and maceral entitled in coal nomenclature. The classification of maceral groups is established by the International Committee for Coal and Organic Petrology (ICCP, 1998; Sýkorová et al., 2005), the organization that develops and revises coal petrology, terminology, and nomenclature.

Table 1 Maceral groups and modes of optical identification (Modified from Bustin et al., 1985; Stach et al., 1982; Styan and Bustin, 1983; Taylor et al., 1998)..

<b>Maceral group</b>	<b>Transmitted light</b>	<b>Reflected light</b>	<b>Fluorescence</b>
Vitrinite	Red brown	Intermediate gray	None of yellow (lignites) brown (bituminous)
Liptinite	Yellow	Dark gray	High intensities; very variable with rank
Inertinite	Opaque	White, yellowish, light gray	None

The vitrinite group of macerals compose of woody plant materials such as stems, trunks, roots, and branches derived from lignin and cellulose of plant remains. The liptinite group of macerals represent diverse plant and animal remains derived from phytoplankton (algae), bacteria, cuticles, spore, pollen, resin, waxes, chlorophyll, and detritus. The inertinite group of macerals originate from charred remains formed peat fires and bacterial surface oxidation such as cell walls, fungal cell walls, fish, and other animal relics (Table 2).

Table 2 Petrographic nomenclature and genetic groupings of coal macerals (Compiled from ICCP, 1971, 1998, 2001; Stanton et al., 1989; Sýkorová et al., 2005).

<b>Maceral group</b>	<b>Identification criteria</b>	<b>Origin</b>	<b>Maceral</b>
Vitrinite (huminite)	Fluorescence; response to etching	Cell walls, gelified	Telinite
		Cell structure, poorly defined	Collotelinite
		Vitrinite fragments	Vitrodetrinite
		Vitrinite groundmass, mottled	Collodetrinite
		Vitrinitic colloidal infills	Gelovitrinite

		Cell infills	Corpogelinite
		Infills of cracks and voids	Gelinite
Liptinite	Characteristics fluorescence in blue light	Spores and pollens	Sporinite
		Leaf cuticle, roots, and stems	Cutinite
		Algae	Alginite
		Corkified cell walls	Suberinite
		Plant resins	Resinite
		Liptinite fragments	Liptodetrinite
		Cavity-filling resins, cell lumens, and originating after oil generation	Exsudatinite
		Plant oils	Fluorinite
		Amorphous bitumen	Bituminite
Inertinite	High reflectance in white light	Highly oxidized wood	Fusinite
		Less oxidized wood	Semifusinite
		Oxidized humic gel	Macrinite
		Oxidized fragments of inertinites	Inertodetrinite
		Fungal hyphae, spores, and other fungal remains	Funginite
		Oxidized resin	Secretinite

### 1.4.3 Coalification

Coalification or maturation of coal is the process of coal formation from peat to coal which can be divided into two main stages: the peatification and the coalification. Furthermore, the coalification process can be subdivided into a biochemical phase or early coalification and a geochemical phase or later coalification (Killops and Killops, 2013). Peatification and early coalification stages are mainly dominated by biological process related to diagenesis. Later coalification stage requires high temperature and pressure, which are related to catagenesis and

metagenesis. Coalification is typically process of transformation of peat to various coal ranks or stages of maturation (Figure 2). Coalification can be classified by different coal types including peat, lignite, sub-bituminous, bituminous and anthracite.

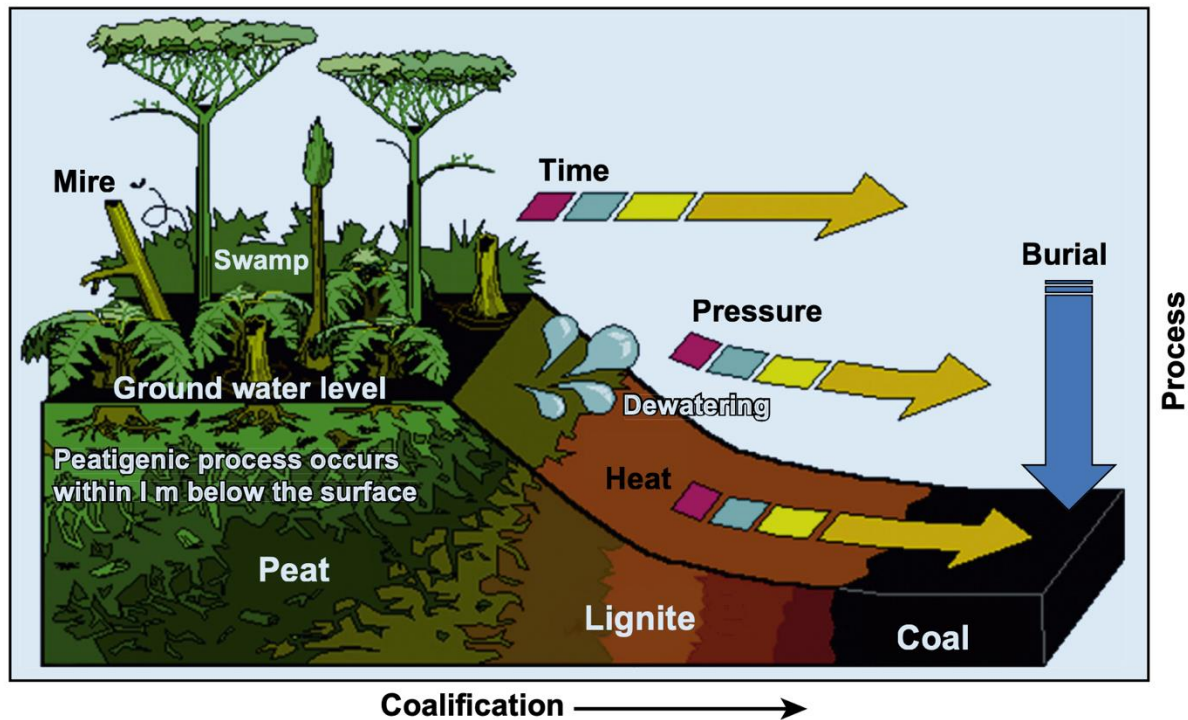


Figure 2 The process of peatification, which occurs on the surface is followed by coalification of the peat upon burial in the subsurface where it is dewatered and exposed to heat and pressure (Modified from Greb, 2006).

The concept of chemical process of coalification is related to maturation of coal that change hydrogen, carbon, and oxygen concentration. These elemental compositions represent organic matter or maceral composition. Carbon content increases and oxygen content decreases with increasing maturation or coalification. Hydrogen content decreases with increasing maturation in the same coal type. In order to determine coal rank and maceral composition, the atomic ratios of hydrogen and carbon (H/C), and oxygen and carbon (O/C) were plotted by van Krevelen (1981) (Figure 3). During coal maturation, oxygen and hydrogen contents reduce related to carbon content.

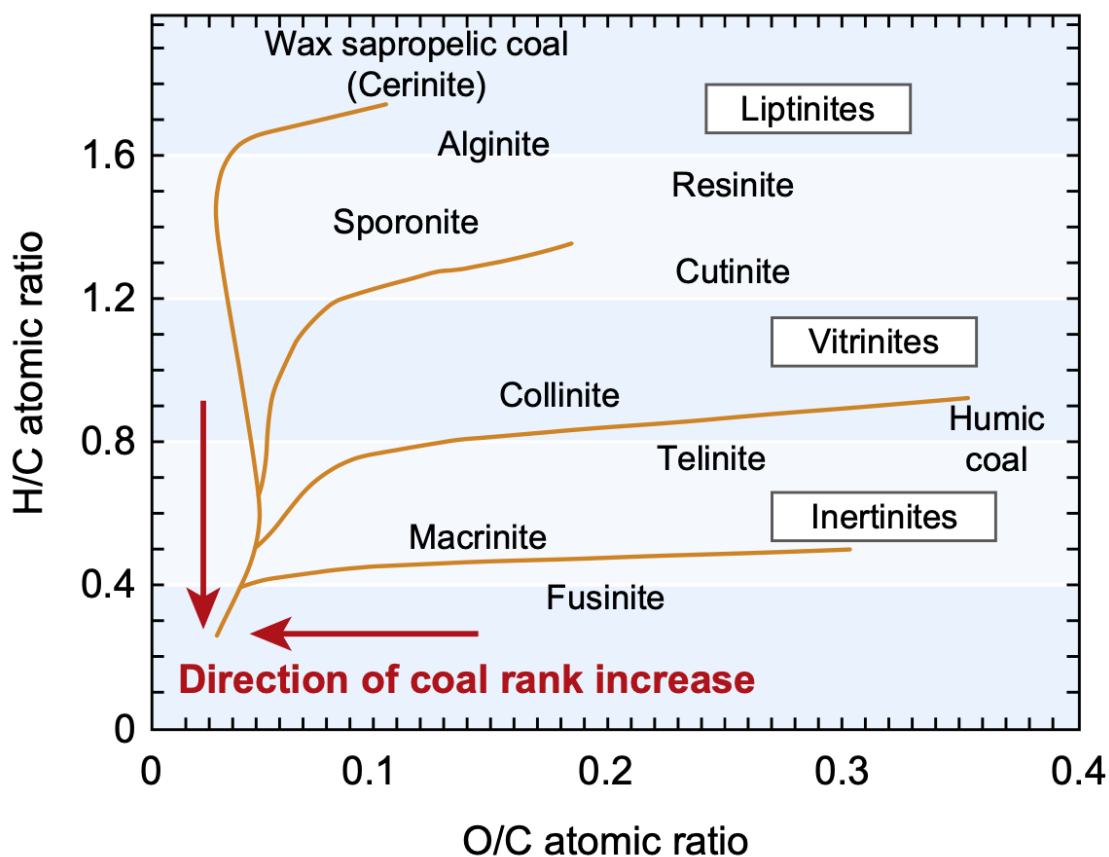


Figure 3 Diagram of coal macerals in relation to hydrogen/carbon and oxygen/carbon atomic ratios, coal types, and direction of coal rank increase. H, hydrogen; O, oxygen; C, carbon (Modified from Hunt, 1991; Mukhopadhyay and Hatcher, 1993; van Krevelen, 1981).

The atomic ratios of H/C and O/C are related to different coal maceral groups, i.e. vitrinites, liptinites and inertinites, and coal types such as humic and sapropelic coals (Figure 3). The group of vitrinite has high O/C atomic ratio, but low H/C atomic ratio. The inertinite group has lower in H/C atomic ratio compared to the vitrinite group. The liptinite group is enriched in H/C atomic ratios compared to the vitrinite and inertinite groups (Mukhopadhyay and Hatcher, 1993).

The proportions of hydrogen, carbon and oxygen are described in the humic and sapropelic coals (Figure 4). Humic and sapropelic coals can be classified by hydrogen, carbon and oxygen contents in the sample. The carbon content increases as hydrogen and oxygen contents decrease during coalification. Humic coals are oxygen rich and hydrogen poor. In contrast, sapropelic coals are initially enriched in



hydrogen, but oxygen poor. The coal types can be separated by using the difference in proportions of hydrogen, carbon, and oxygen. However, the higher rank coals are not able to distinguish (Levine, 1993).

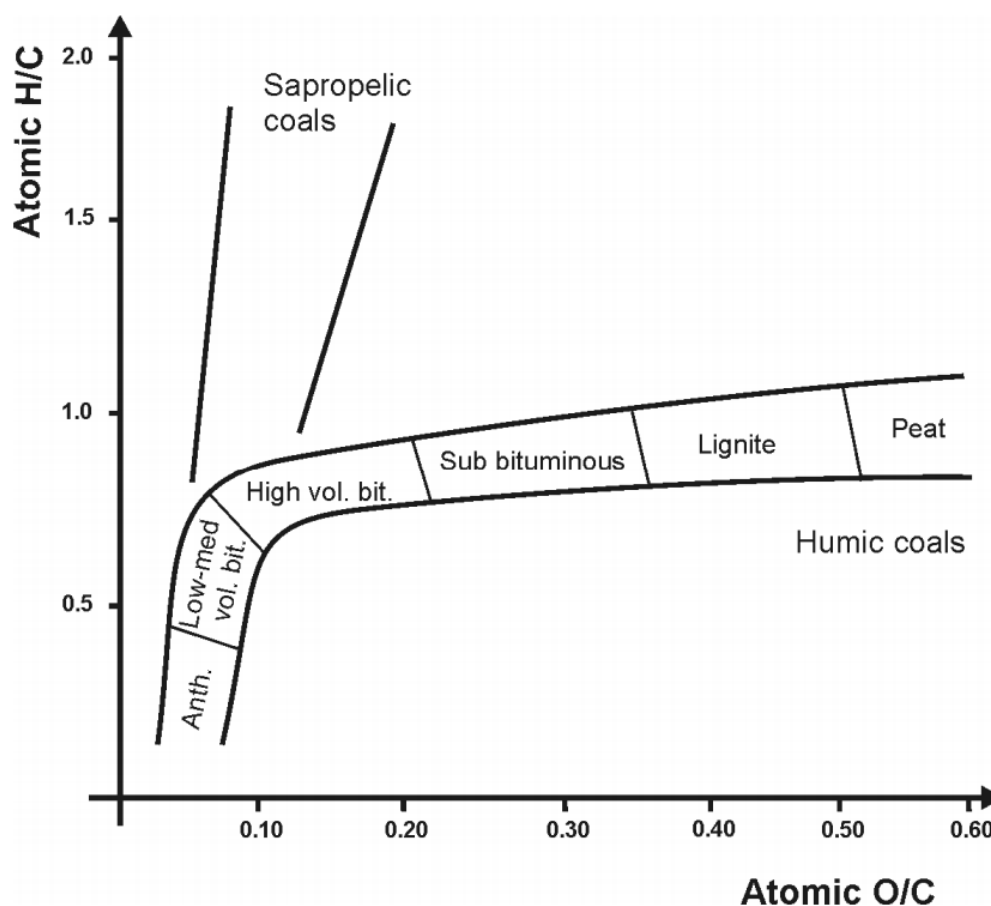


Figure 4 Maturation stages of coals plotted in a Van Krevelen type diagram. Sapropelic coals start with a high H/C atomic ratio due to a high aliphatic content, humic coals start with a high O/C atomic ratio and undergo the coalification stages peat, lignite, sub-bituminous coal and high volatile bituminous coal (Modified from Killops and Killops, 2013).

#### 1.4.4 Maturation of organic matter

Maturation of organic matter or thermal maturity is the degree of transformation from organic matter to hydrocarbon compounds depending on temperature and pressure levels. Increasing deposition depth of sedimentary rock will raise temperature and pressure. There are three levels of thermal maturation; immature, mature and post mature, respectively (Tissot and Welte, 1984).

The immature stage is the first organic maturation affected by diagenesis. This stage starts breaking biogenic polymers (i.e. proteins, carbohydrates) influenced by microbial activity during sedimentation and early diagenesis. Then, their compounds are progressed into new structures (geopolymers) due to polycondensation. When, organic matter mainly derived from plant deposits during this stage forming peat and then brown coals (lignite and sub-bituminous coal). Nevertheless, methane is hydrocarbon compounds forming during diagenesis. At the end of diagenesis, little amount of organic matter is transformed into humic acid related to the boundary between brown coal and hard coal (ICCP, 1971).

The increase in temperature and pressure related burial depth of several kilometers of overburden makes organic matter become matured in catagenesis stage. This stage may be high temperature about 50 – 150 °C, pressure ranges from 300 - 1,500 bars. Mineral composition is remained with some changes. Water content, porosity and permeability start decreasing while rock compaction increases. Organic matter evolution progressively starts cracking of kerogen formed liquid hydrocarbon, then wet gas and condensate in late stage. This organic matter evolution relates to various coal ranks (Figure 5). At the end of catagenesis, aliphatic carbon chain completely disappears in kerogen compound then hydrocarbon generation is limited due to the beginning of subsequent stage metagenesis known as post mature stage. Vitrinite reflectance is about 2% at metagenesis stage indicating a high-rank coal.

Metagenesis is the last stage of the organic matter evolution in sediments within high temperature and high pressure. This stage can be equivalented as over mature and related to anthracite coal. In this stage, organic matter is transformed into only methane and carbon residue. Mineral begins to recrystallize corresponding to 4% of vitrinite reflectance at the end of metagenesis. Residue kerogen is converted to graphite due to carbonization (Figure 5).

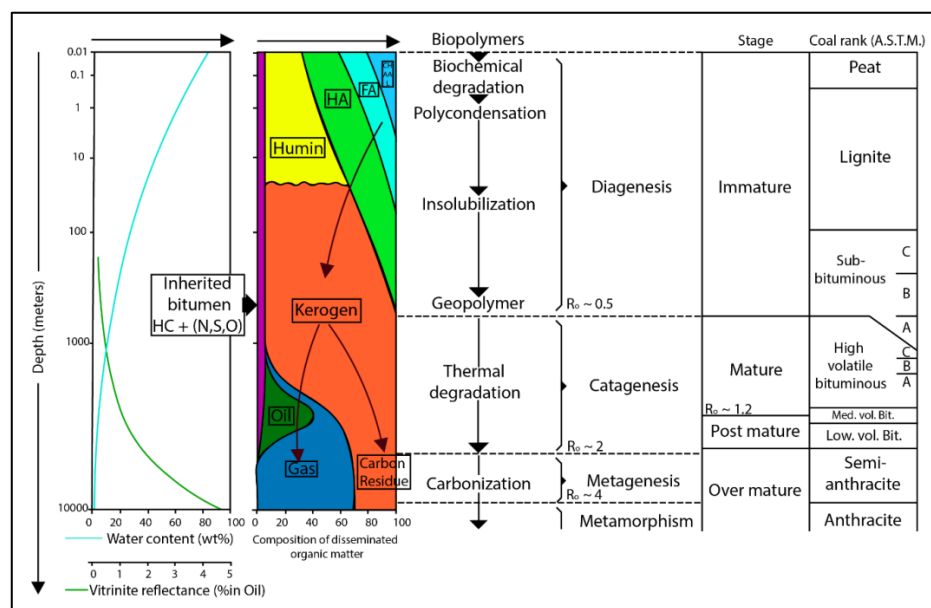


Figure 5 General scheme of evolution of the organic matter, from the freshly deposited sediment to the metamorphic zone. (CH: carbohydrates, AA: amino acids, FA: fluvic acids, HA: humic acids, L: lipids, HC: hydrocarbons, N,S,O: N, S, O compounds (non-hydrocarbon)) and comparison of the scale of equivalent A.S.T.M. coal rank (Modified from Tissot and Welte, 1984).

#### 1.4.5 Quantity of organic matter

The quantitative analysis of organic matter is used to evaluate organic richness of sedimentary rocks. There are two general terms to define quantity of organic matter including total organic carbon (TOC) indicating amount of kerogen and extractable organic matter (EOM) indicating amount of bitumen (Peters and Cassa, 1994).

Kerogen is the macromolecular organic matter which is insoluble in common organic solvents (Durand, 1980). In contrast, bitumen is entitled as a soluble part of organic matter. Kerogen is derived from plant material or algae modified by diverse microbial and thermal alteration processes during burial. Kerogen composes condensed aromatic hydrocarbons and aliphatic chains linked by hetero atoms mainly oxygen and sulfur. Kerogen can be divided into three types: type I, II, and III kerogens depend on its origin and structural composition.

Bitumen or extractable organic matter (EOM) is the fraction extractable with organic solvents (Figure 6). It can be used for evaluating hydrocarbon generation potential in source rocks. The quantitative scale of EOM can be evaluated as a

minimum value at 500 ppm and reach to 4,000 ppm for petroleum source rocks (Table 3). The EOM consists of saturated hydrocarbon, aromatic hydrocarbon and asphaltenes and resins. During diagenesis, free constituents still remain in the bitumen such as molecular fossils and biological markers or biomarkers (Peter and Moldowan, 1993).

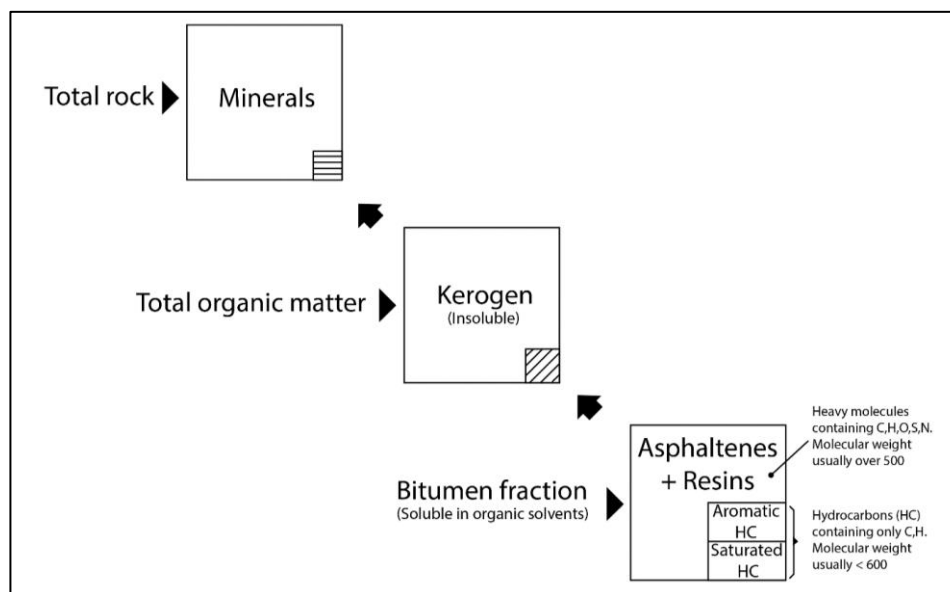


Figure 6 Composition of disseminated organic matter in sedimentary rocks (Tissot and Welte, 1984).

Total organic carbon (TOC) is a measurement of the organic richness of sedimentary rocks. This parameter is used for screening potential petroleum source rocks. Organic carbon is distinguished from a variety of biological origins which deposited and buried through geological time (Hunt, 1995; Tissot and Welte, 1984). TOC content is analyzed by the direct combustion of a crush rock sample. The unit of TOC is shown as percent weight (wt.%) of organic carbon in microgram per rock in gram (Table 3). TOC has different criteria in different lithology such as shale and carbonate rock due to the difference in porosity and permeability (Peters and Cassa, 1994). The TOC content of carbonate rock composes lower value compared to those of shale in same criteria (Jones, 1987). Generally, the minimum value of TOC is about 0.5 wt.% for shale and 0.2 wt.% for carbonate rock to define as a petroleum source rocks (Jarvie, 1991a).

Table 3 Classification of source rock richness based on total organic carbon (TOC) and extractable organic matter (EOM) contents (Peters and Cassa, 1994).

Source Potential	TOC (wt.%)		EOM (ppm)
	Shale	Carbonate	
Poor	< 0.5	< 0.2	< 500
Fair	0.5 - 1.0	0.2 - 0.5	500 - 1,000
Good	1.0 - 2.0	0.5 - 1.0	1,000 - 2,000
Very good	2.0 - 4.0	1.0 - 2.0	2,000 - 3,000
Excellent	> 4.0	> 2.0	> 4,000

#### 1.4.6 Biomarkers

Biomarkers or Biological markers are complex organic compounds consist of carbon, hydrogen and other elements. They remain or slightly change in structure from their parent organic molecules in living organism (Peter and Moldowan, 1993). The characteristic of biomarkers is analyzed by using gas chromatography – mass spectrometry (GC–MS). Some biomarkers can be found in coal and other sedimentary rocks shown as following.

1) The pristane/phytane ratio (Pr/Ph) is used to determine the redox condition of depositional environment. Pr/Ph ratio is less than 1.0 represents anoxic condition whereas oxic condition is more than 3.0 in ratio (Didyk et al., 1978). In addition, intermediate condition values between 1.0 and 3.0 (Didyk et al., 1978).

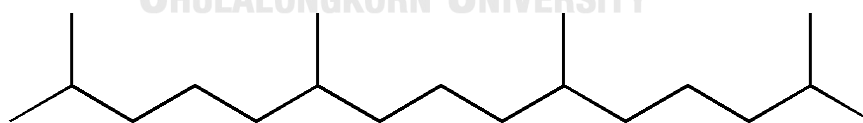


Figure 7 Pristane (C<sub>19</sub>H<sub>40</sub>) (Stauffer et al., 2008b).

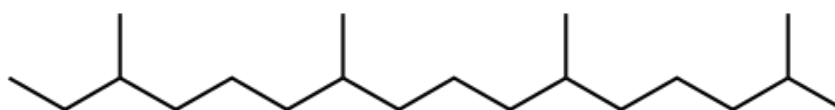


Figure 8 Phytane (C<sub>20</sub>H<sub>42</sub>) (Stauffer et al., 2008b).

2) The isoprenoids/n-alkanes ratio (Pr/n-C<sub>17</sub> and Ph/n-C<sub>18</sub>) represents conditions of biodegradation, maturation and diagenesis. Isoprenoids is more resistant

to microbial degradation than normal alkanes. Ratio is more than 1.0 referring high level of degradation (mature) whereas ratio value has lower than 1.0 means low maturity or low microbial activity.

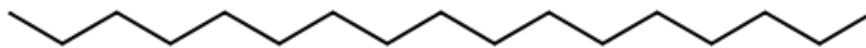


Figure 9 Heptadecane (n-C<sub>17</sub>; C<sub>17</sub>H<sub>36</sub>) (Hintze et al., 2010).

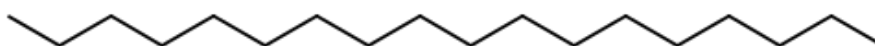


Figure 10 Octadecane (n-C<sub>18</sub>; C<sub>18</sub>H<sub>38</sub>) (Hintze et al., 2010).

3) The tricyclic terpanes (m/z 191) are used to determine input of organic matter and evaluate thermal maturity and biodegradation (Peter and Moldowan, 1993). Predominant C<sub>19</sub> tricyclic terpane represents terrigenous organic matter, whereas C<sub>23</sub> tricyclic terpane indicates marine organic matter (Moldowan et al., 1985).

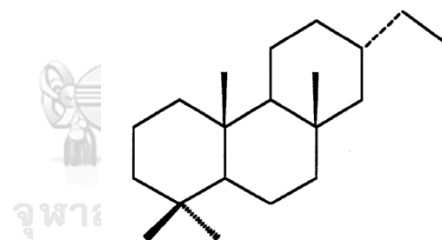


Figure 11 C<sub>20</sub> Tricyclic terpane (Greenwood et al., 2000).

4) Gammacerane (m/z 191) has been found in sediments from Late Proterozoic (Summons et al., 1988). It can be used for indicating transition zone between marine and lacustrine environments (Sinninghe Damsté et al., 1995).

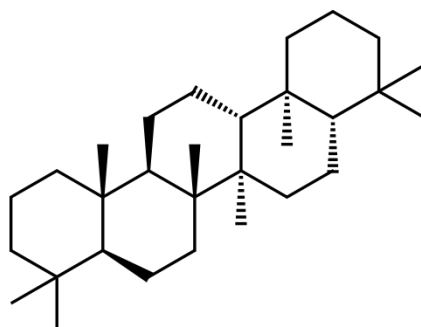


Figure 12 Gammacerane ( $C_{30}H_{52}$ ) (Xiao et al., 2018).

5) The trisnorhopane (Ts) and trisnorhopane (Tm) ratio (Ts/Tm) is used as a maturity indicator. Ts is more stable than Tm at higher maturation (Mackenzie et al., 1981).

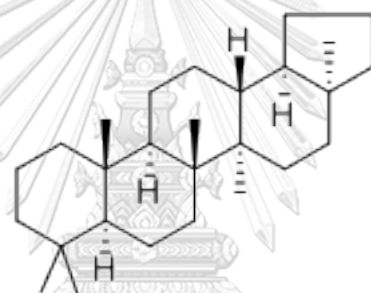


Figure 13  $18\alpha(H)$ -22,29,30-Trisnorhopane ( $C_{27}H_{46}$ ; Ts) (Peters et al., 2005).

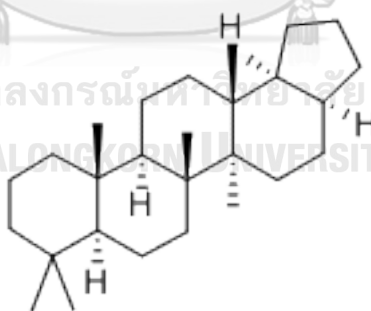


Figure 14  $17\alpha(H)$ -22,29,30-Trisnorhopane ( $C_{27}H_{46}$ ; Tm) (Peters et al., 2005).

6) The  $17\beta(H),21\alpha(H)$ -moretane and  $17\alpha(H),21\beta(H)$ -hopane ratio is used to indicate thermal maturation. Hopane is more stable than moretane. The moretane abundance relatively decreases at higher temperature (Petersen et al., 2004).

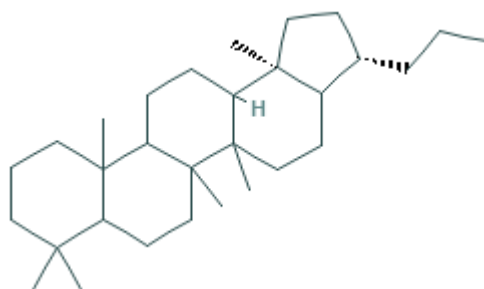


Figure 15 17 $\beta$ (H),21 $\alpha$ (H)-moretane (C<sub>30</sub>H<sub>52</sub>) (Peters et al., 2005).

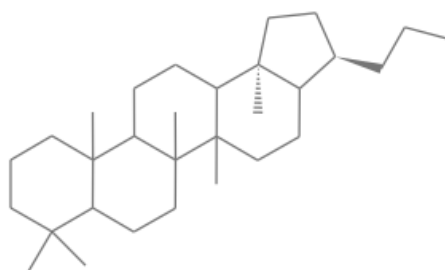


Figure 16 17 $\alpha$ (H),21 $\beta$ (H)-hopane (C<sub>30</sub>H<sub>52</sub>) (Xiao et al., 2018).

7) The homohopanes distribution (m/z 191) is derived from bacteriopolyhopanol of prokaryotic cell membrane. Homohopane index is used to determine type of organic matter and redox condition during and after sediment deposits (Erik and Sancar, 2010).

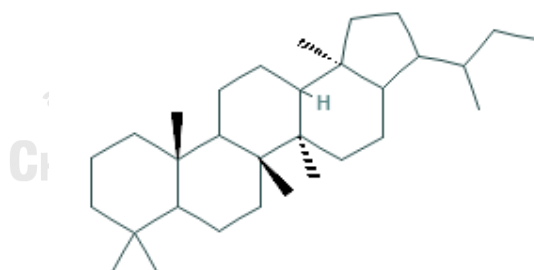


Figure 17 Homohopane (C<sub>31</sub>H<sub>54</sub>) (Peters et al., 2005).

8) The homohopane isomerization ratio (22S/(22S+22R)) is used as an indicator of maturation. The more thermally stable 22S isomer against the biologically derived 22R isomer (Peters and Cassa, 1994).

9) The distribution of steranes (m/z 217) is used to determine organic matter input and sedimentary facies. Steranes are derived from sterols. Predominant C<sub>27</sub> sterane indicates



plankton (algae) input in marine influenced system whereas  $C_{28}$  sterane represents lacustrine deposits.  $C_{29}$  sterane is inferred to swamp shallow water environment with input of terrestrial higher plant (Peter and Moldowan, 1993).

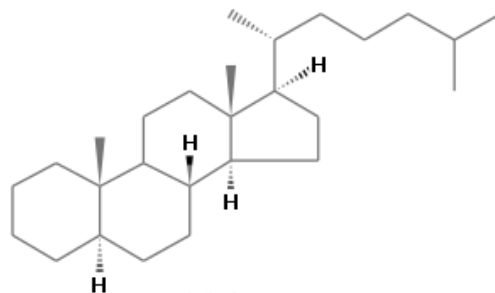


Figure 18 Cholestane ( $C_{27}H_{48}$ ) (Rohrssen et al., 2015).

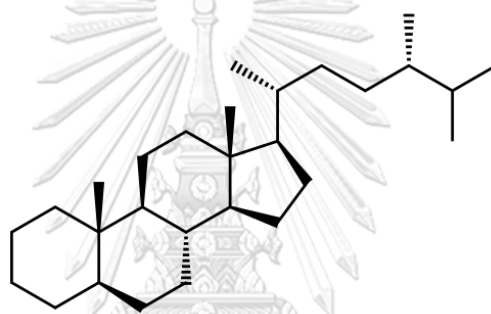


Figure 19 Ergostane ( $C_{28}H_{50}$ ) (Rohrssen et al., 2015).

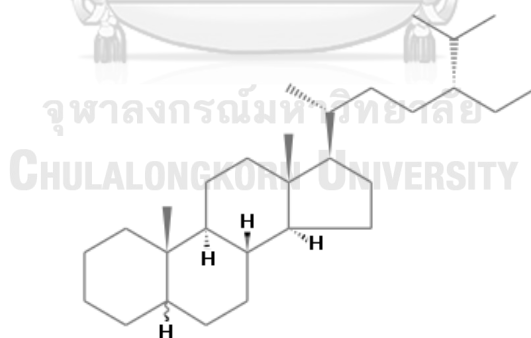


Figure 20 Stigmastane ( $C_{29}H_{52}$ ) (Rohrssen et al., 2015).

10) The regular steranes/ $17\alpha(H)$ -hopane ratio is used as an indicator of eukaryotic input (mainly algae and higher plants) against prokaryotic organism (bacteria) in a source rock (Peter and Moldowan, 1993).

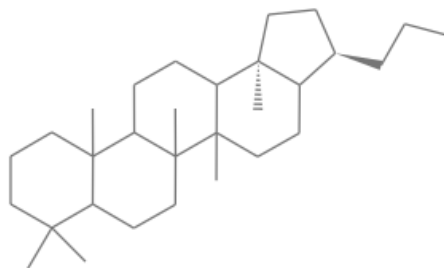


Figure 21 17 $\alpha$ (H),21 $\beta$ (H)-hopane (C<sub>30</sub>H<sub>52</sub>) (Xiao et al., 2018).

11) Bisnorhopanes is used to indicate depositional environment under anoxic conditions containing types of pentacyclic triterpanes (Mello et al., 1988).

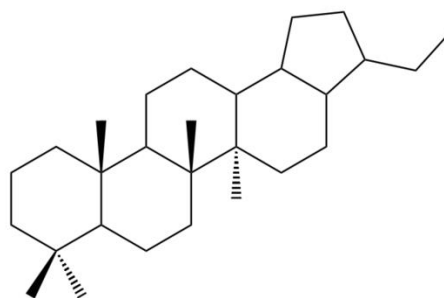


Figure 22 28,30-Bisnorhopane (C<sub>28</sub>H<sub>48</sub>) (Peters et al., 2005).

12) C<sub>29</sub>/C<sub>30</sub> hopanes ratios are generally high (more than 1.0) in oil where is generated from organic rich carbonates and evaporates (Connan et al., 1986).

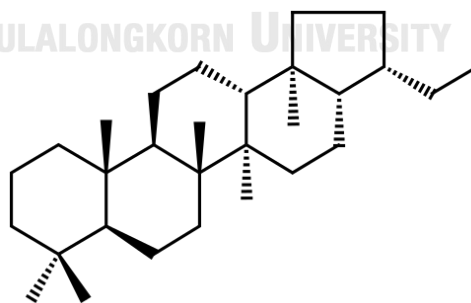


Figure 23 30-Norhopane (C<sub>29</sub>H<sub>50</sub>) (Peters et al., 2005).

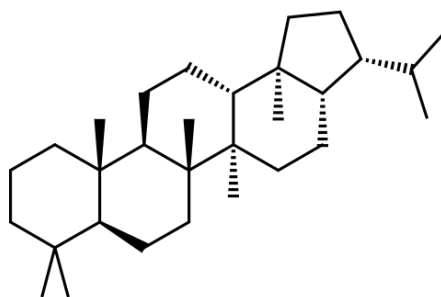


Figure 24 Hopane ( $C_{30}H_{52}$ ) (Xiao et al., 2018).



## CHAPTER II

### LITERATURE REVIEWS

#### 2.1 Geological setting of Cenozoic basins

Cenozoic geological setting in Thailand is complex with sedimentation and deformation on continental core of SE Asia called Sundaland. Sundaland composes a heterogeneous segment of continental blocks derived from the India-Australian margin of eastern Gondwana. Sundaland was assembled by the closure of multiple Tethyan and back-arc ocean basins which is recently shown as suture zones. The continental core of Sundaland consists of a western Sibumasu block and an eastern Indochina-East Malaya block with an island arc terrane, the Sukhothai Island Arc System (Metcalf, 2011). The core of Sundaland includes the South China block, the Indochina-East Malaya blocks, the Sibumasu block, West Burma block and SW Borneo block (Figure 25) (Metcalf, 2011). The West Sumatra block has been recently established outboard of Sibumasu in SW Sumatra (Barber and Crow, 2003; Barber et al., 2005). In addition, a volcanic arc terrane is identified in the middle of Sibumasu and Indochina-East Malaya (Sone and Metcalfe, 2008).

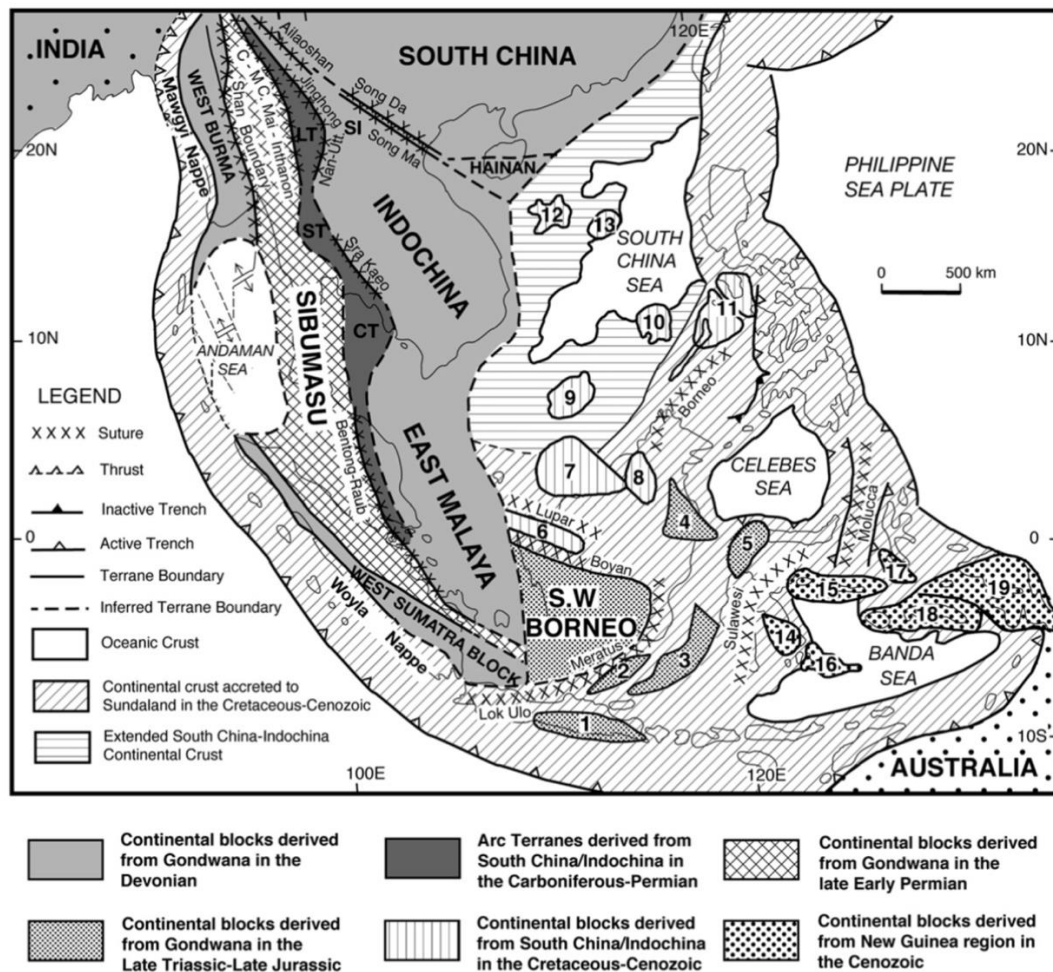
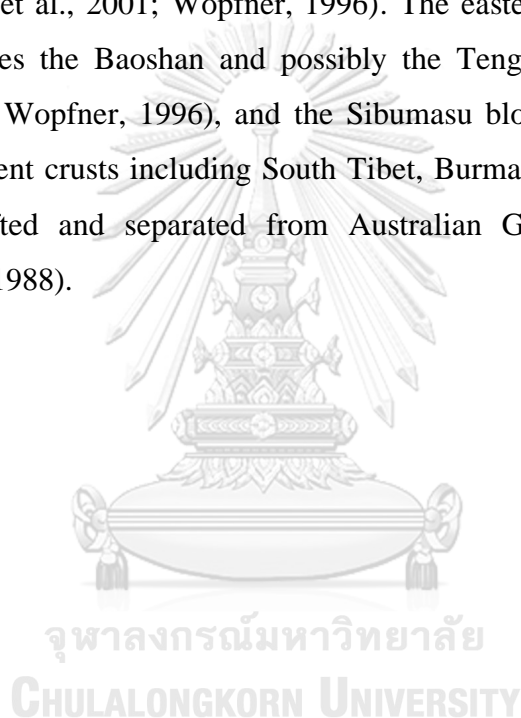


Figure 25 Distribution of continental blocks, fragments and terranes, and principal sutures of Southeast Asia. Numbered micro-continental blocks, 1. East Java 2. Bawean 3. Paternoster 4. Mangkalihat 5. West Sulawesi 6. Semitau 7. Luconia 8. Kelabit–Longbowan 9. Spratly Islands–Dangerous Ground 10. Reed Bank 11. North Palawan 12. Paracel Islands 13. Macclesfield Bank 14. East Sulawesi 15. Bangai–Sula 16. Buton 17. Obi–Bacan 18. Buru–Seram 19. West Irian Jaya. LT = Lincang Terrane, ST = Sukhothai Terrane and CT = Chanthaburi Terrane. C–M = Changning–Menglian Suture, C.-Mai = Chiang Mai Suture, and Nan–Utt. = Nan–Uttaradit Suture (Metcalf, 2011).

The continental terranes of Sundaland and adjacent regions can be divided based on their specific origins and timing of rifting and separation from Gondwana and amalgamation/accretion to form SE Asia. The India-Australian margin of Gondwana comprises the South China, Indochina and East Malaya blocks in the Early

Palaeozoic. These blocks have been rifted and separated from Gondwana by the opening of the Palaeo-Tethys ocean in the Early Devonian (Metcalf, 2006). Sone and Metcalfe (2008) proposed that the Sukhothai Arc System composes the Lincang block in SW China, the Sukhothai block in Central Thailand and the Chanthaburi block derived from the margin of South China-Indochina-East Malaya by back-arc spreading in the Late Carboniferous-Early Permian. The back-arc collapsed in the Late Permian (Figure 26). At the end of the Early Permian, the Cimmerian continent was separated from eastern Gondwana during the Late Carboniferous-Early Permian (Jin, 1994; Wang et al., 2001; Wopfner, 1996). The eastern part of this Cimmerian continent comprises the Baoshan and possibly the Tengchong blocks of Yunnan, China (Jin, 1994; Wopfner, 1996), and the Sibumasu block (Figure 26) (Metcalf, 1991). The continent crusts including South Tibet, Burma, Malaya, SW Borneo and Sumatra were rifted and separated from Australian Gondwana in the Jurassic (Audley-Charles, 1988).



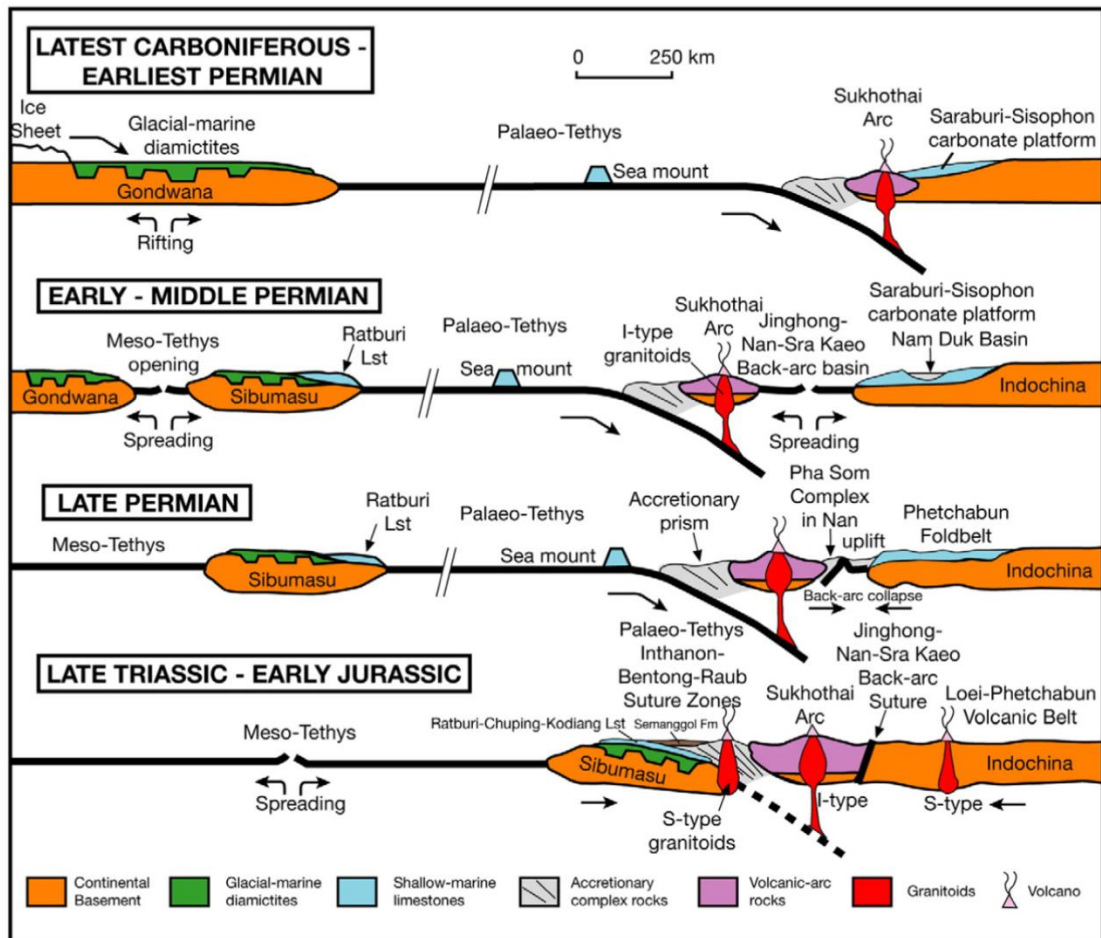


Figure 26 The tectonic evolution of Sundaland (Thailand–Malay Peninsula) and evolution of the Sukhothai Arc System during Late Carboniferous–Early Jurassic times (Metcalf, 2011).

CHULALONGKORN UNIVERSITY

The Cenozoic rift basins in Thailand generally formed a series of N-S trending, typically half-graben basins that can be divided into four regions: (1) the Andaman Sea, (2) Gulf of Thailand (GOT), (3) Central Thailand, and (4) Northern Thailand (Friederich et al., 2016). The complex of regional Cenozoic rift basins in Thailand is initially developed eastern and southern Gulf of Thailand (GOT) during the Eocene and Oligocene. Later development is carried out from Late Oligocene to Miocene in northern and western Thailand (Figure 27) (Morley, 2015; Racey, 2011; Searle et al., 2011; Travena and Clark, 1986). The evidence of basin inversion in some basins, particularly in central and northern Thailand, occurred several phases during Miocene and Early Pliocene (Morley, 2001, 2009; Morley et al., 2011). In

other basins, the result in relatively complex fault patterns restricted rotation of the extension direction during the Miocene. In addition, pre-existing fabrics of rifting basins has resulted in different degrees of faulting oblique to the extension direction which have been built complex fault patterns, fault linkage history, and fault displacement patterns (Morley, 2017; Morley et al., 2004).

The northern Thailand contains a large number of Cenozoic sedimentary basins, which formed between the Oligocene and the Pliocene (Morley et al., 2011). Several models for the formation of the basins have been proposed including their development as strike-slip and/or pull-apart basins (Polachan and Sattayarak, 1989; Tapponnier et al., 1986) and extensional basins related to extensional collapse of thickened crust, and subduction rollback in the Andaman Sea (Watcharanantakul and Morley, 2000). There are more than 40 Cenozoic basins in northern Thailand with basin sizes in the range of 30 – 4,000 km<sup>2</sup> (Polachan et al., 1991). These basins are mainly N-S trending half grabens and grabens with various sediment thickness ranging from 1,000 to 3,000 m overlying with complex basement of igneous, metamorphic and sedimentary rocks (Polachan et al., 1991).



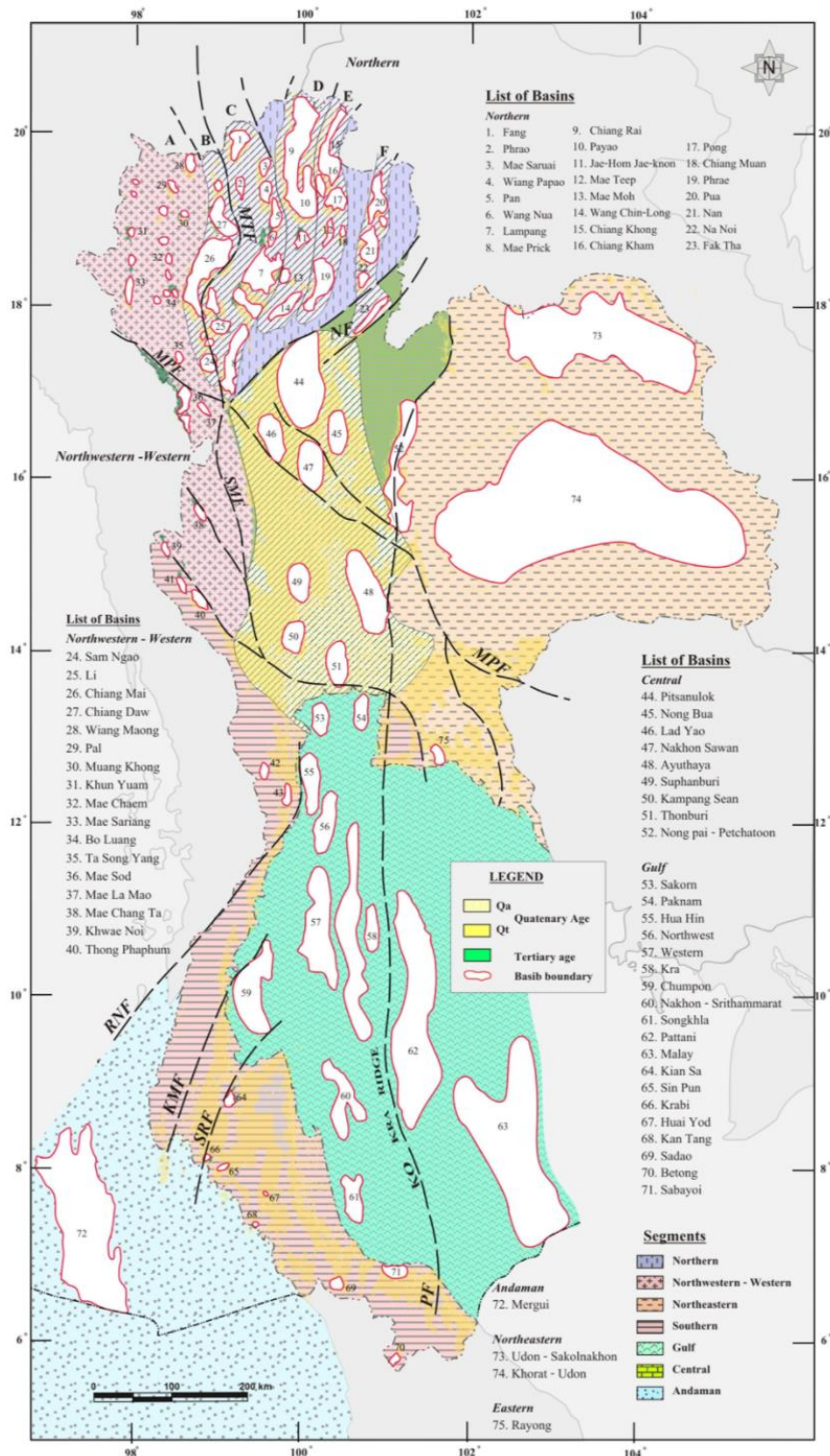


Figure 27 Distribution of Cenozoic basins and significant fault systems in Thailand. (MPF = Mae Ping Fault, TPF = Three – Pagoda Fault, NF = Nan Fault, RNF = Ranong Fault, KMF = Klong Marui Fault, SWF = Sri Sawat Fault, MTF = Mae Tha Fault) (Charusiri and Pum-Im, 2009).

## 2.2 Stratigraphy

Lampang province is located on the northern Thailand (Latitude: 18° 00' N to 18° 45' N and longitude: 99° 00' E to 99° 45' E) covering an area about 850 km<sup>2</sup> (Kwansirikul et al., 2004). It commonly distributes several intermontane basins such as Lampang, Mae Moh, Mae Teep, and Mae Than basins. The general geology of Lampang province mainly consists of Mesozoic basement of marine sediments of Lampang Group and Cenozoic rift basin containing Neogene sedimentary rock (i.e. Mae Moh Group). Mae Moh Group was introduced by Piyasin (1972) as a type section of stratigraphy in Mae Moh basin and used to apply to adjacent areas of other northern Cenozoic basins (Charusiri and Pum-Im, 2009).

### 2.2.1 Mae Teep basin

Mae Teep basin is a small basin located in Ngao district far from Lampang Province about 80 km in northeast direction (Figure 1). It was formed in result of extensional regime influenced by the collision of the Indian Plate and Eurasian Plate which initiated in Oligocene age (Morley, 2001). Mae Teep basin is approximately 30 km<sup>2</sup> with 3 km wide and 10 km long. It is one of intermontane coal-bearing basin in N-S trending with steep and fault-controlled margins (Gibling et al., 1985b; Songtham et al., 2005). The western margin of the basin was operated as a coal mine where Tertiary rocks were uplifted to the surface by post-depositional fault. The Mae Teep coal remaining reserve is recorded approximately 10.115 million tons (Sivavong, 2009).

The sedimentary sequence rocks of Mae Teep basin are more than 200 m thick. The basement rocks are Permo-Triassic volcanics and clastics of the Lampang Group. The successions of Mae Teep Basin can be described as shown in Figure 28 and divided into two sequences including (1) Tertiary coal-bearing sequence consisting limestone, mudstone, coal and carbonaceous mudstone with minor oil shale overlying with (2) Quaternary alluvium sequence containing gravel, pebbly sand, muddy sand and sandy clay (Chaodumrong et al., 1983; Gibling et al., 1985b). The coal-bearing sequences reach up to 35 m in thickness, but laterally variable (Gibling et al., 1985b). The main lignite to bituminous coal bed is about 5 m thick and is interbedded by oil shales and sandstones (Ducrocq et al., 1995). Bivalves, gastropods, fish and plants are

common fossils found in coal-bearing formation in this basin (Ratanasthien, 1984). *Stegolophodon sp.* was found below the main coal seam indicating Early to Middle Miocene age (Buffetaut et al., 1988). However, the study of palynology of coal bearing sequence indicates Senonian or Paleogene age (Ratanasthien, 1984).

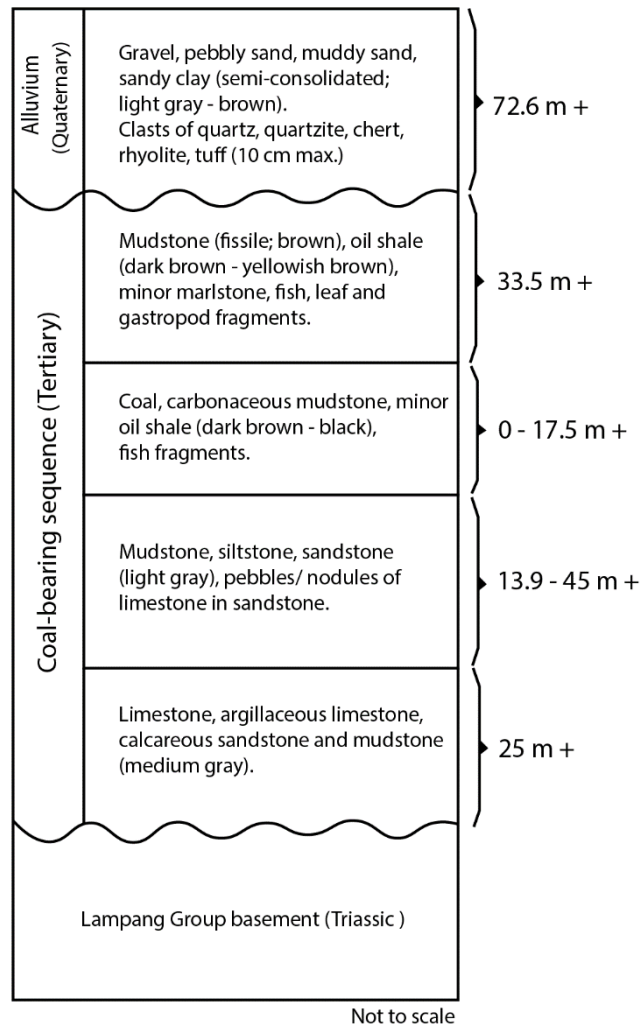


Figure 28 Stratigraphy of Mae Teep basin (Modified from Gibling et al., 1981).

### 2.2.2 Mae Than basin

Mae Than basin is located some 50 km southwest of Lampang Province and closes to the NW-SE Thoen Fault in which is geomorphologically typical of a recently active fault (Figure 29) (Fenton et al., 2003; Morley et al., 2001). It is a small rift basin about 4-5 km wide and 10-12 km long (Figure 1). The basement of basin is Triassic Lampang Group and Permo-Triassic volcanic rocks (Muenlek, 1992a).

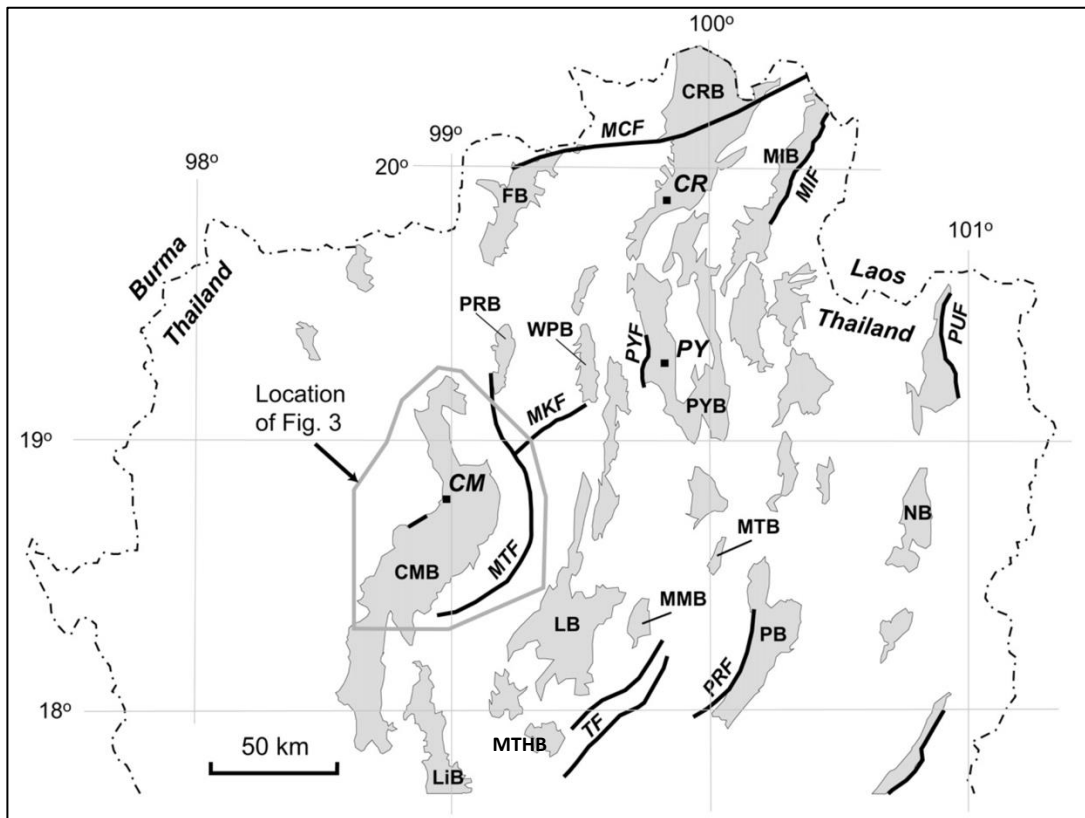


Figure 29 Map of the Basin and Range Province of northern Thailand showing the major Tertiary basins and late Cenozoic-Quaternary normal and strike-slip faults. Towns: CM, Chiand Mai; CR, Chiang Rai; PY, Payao. Faults: MCF, Mae Chan fault; MIF, Mae Ing fault; MKF, Mae Kuang fault; MTF, Mae Tha fault; PRF, Phrae fault; PUF, Pua Fault; PYF, Payao fault; TF, Thoen fault. Basins: CMB, Chiang Mai basin; CRB, Chiang Rai basin; FB, Fang basin; LiB, Li basin; LB, Lampang basin; NB, Nan basin; MIB, Mae Ing basin; MMB, Mae Moh basin; MTB, Mae Teep basin; MTHB, Mae Than basin; PB, Phrae basin; PRB, Phrao basin; PYB, Payao basin; WPB, Wiang Pa Pao basin (Rhodes et al., 2005).

Mae Than basin is described stratigraphy and divided into two sub-basins including northern sub-basin and southern sub-basin (Muenlek, 1992). The sedimentary sequence in this basin can be divided into 3 units (Figure 30). The lower unit consists of reddish-brown sandstone, siltstone and conglomerate about 25-70 m thick (Thowanich, 1997). It is probably equivalent to the Huai King Formation in the Mae Moh basin. The Middle unit composes mudstone, sandstone, ball clay and coal seams (lignite A to sub-bituminous) of fluvio-lacustrine deposits (Thowanich, 1997).

Some vertebrate fossils from this section indicate a Middle Miocene age (Muenlek, 1992). Generally, a single coal seam in the northern part of the basin was found about 10 m thick. There are two coal seams with average thickness about 10-15 m in the southern part of the basin. Furthermore, ball clay is found in SW part of the basin with thickness ranging from 5-20 m within the average depth range of up to 100 m below the ground surface (Thowanich, 1997). The significant abundance of ball clay is presented in Mae Than Basin due to the derivation of the adjacent Triassic granite outcrops and the deposition under humid condition (Donmuang et al., 2014; Muenlek, 1992b). The upper unit is Quaternary of light brown to reddish brown sandstone, siltstone, mudstone and minor conglomerate of alluvial deposits (Thowanich, 1997).

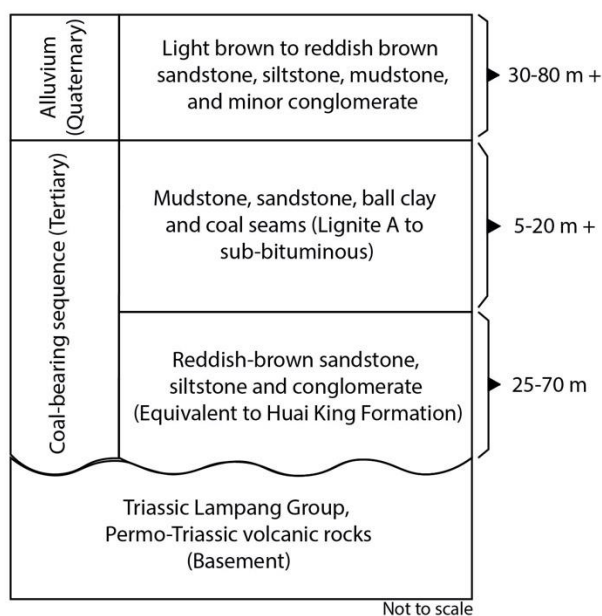


Figure 30 Stratigraphy of Mae Than basin (Modified from Muenlek, 1992; Thowanich, 1997).

### 2.3 Coal-bearing sedimentary basins in the Cenozoic

Friederich et al. (2016) studied coal deposits from Cenozoic basins in Southeast Asia. These basins are mainly coal-bearing sediments and divided into five regions, i.e. Northern Sundaland, Southern Sundaland, the Philippine archipelago, Western Myanmar and eastern Indonesia. Their study focused on three main regions exclude Myanmar and Indonesia (Figure 31).

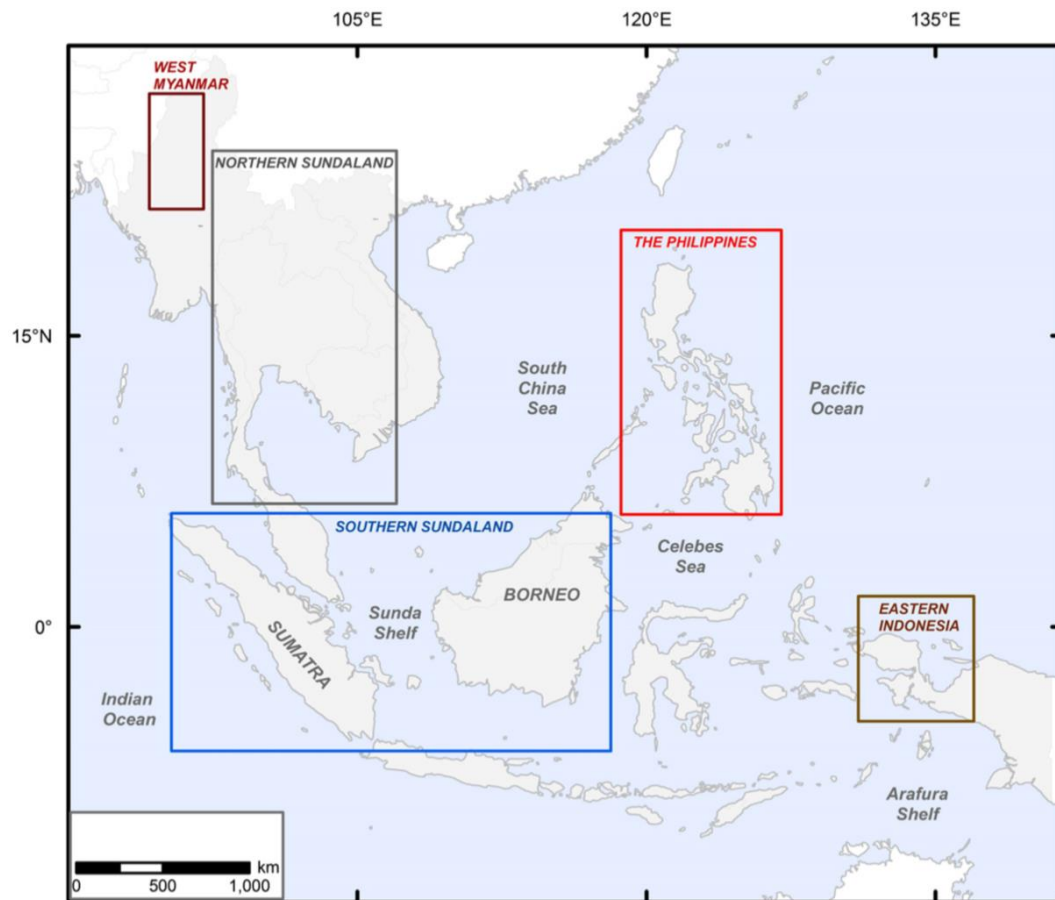


Figure 31 Regional division of coal-bearing sedimentary basins in SE Asia (Friederich et al., 2016).

Each region shows differences in history of tectonics, paleogeography, paleoclimate and paleoenvironment due to unique coal-bearing sedimentary basins and different coal properties. For instance, Northern Sundaland (Thailand) formed limited coal deposits due to small graben and isolated basin, continental fill without influence of sea level change. In addition, the paleoclimate was tropic due to paleogeography in Cenozoic age, thus it is not favorable for peat formation. Tectonics and depositional histories are also the factors of coal contribution within basins. The extensive coal deposits in Southern Sundaland is controlled by post-rift sediments during subsidence phase and marine sediments. In addition, the huge sediment sources are provided from fluvial, deltaic and coastal plain of high hinterland during basin inversion (Friederich et al., 2016).

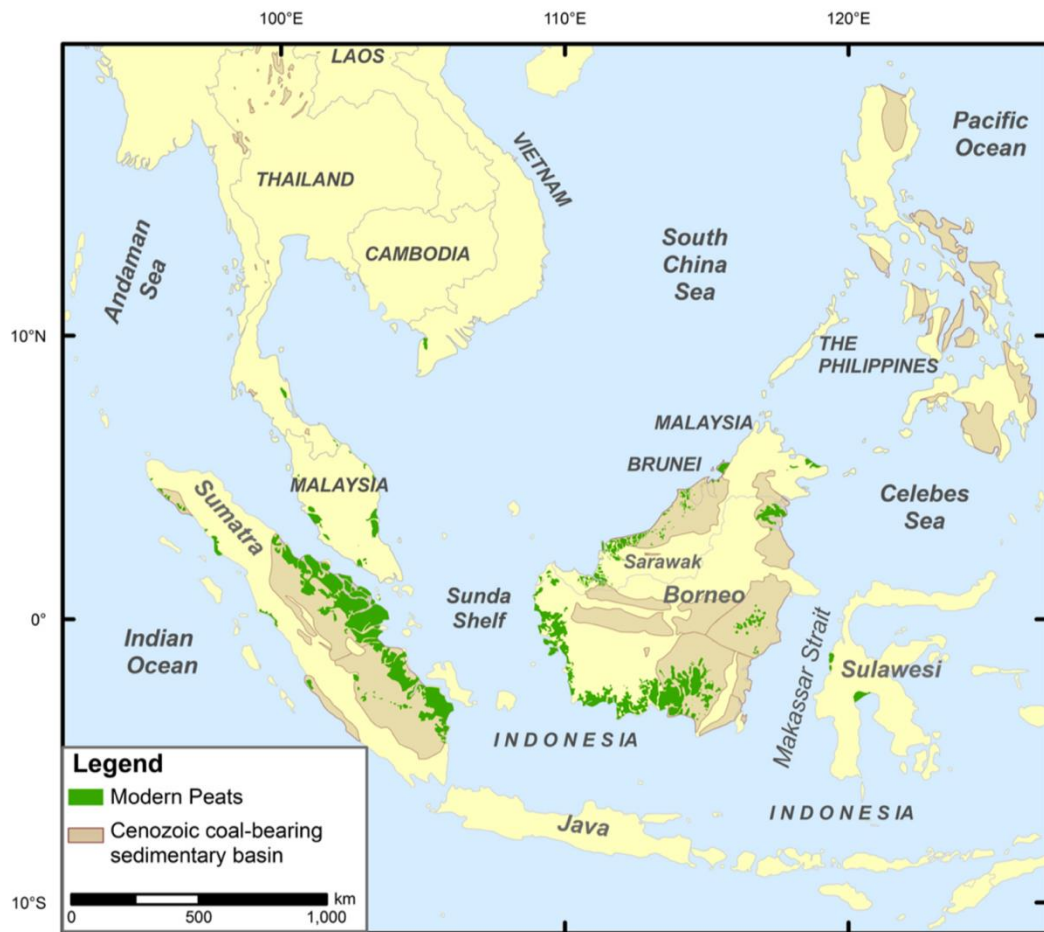


Figure 32 Distribution of peat in the western part of SE Asia (Dommain et al., 2011; Staub and Esterle, 1994).

The tectonic movement, depositional environment, climate and geography play an important role in coal-bearing sediments in the past and in the present day as a peat formation (Friederich et al., 2016). The comparison of modern peat between Southern Sundaland (i.e. Sumatra and Borneo) and Northern Sundaland (i.e. northern Thailand). Southern Sundaland contains both coal-bearing basin and modern peats in widely continuous areas, whereas no area of modern peats in Northern Sundaland (Figure 32). The peat favor depends on input source of organic matter. Then, it has to be a proper climatic and depositional conditions for peat formation in order to change into coals through coalification.

## 2.4 Cenozoic sedimentary basins in Northern Thailand

The study of coal deposits in Cenozoic basin of Thailand can be divided into 3 regions; (1) Eastern basins: Jae Hom, Wang Nua, Mae Than, Mae Teep, Ngao and Mae Moh basins, (2) Western basins: Ban Pa Ka (Li), Ban Wiang Heng, Mae Chaem, Ban Mae Wen and Ban Huay Dua basins, and (3) Westernmost basins: Tha Song Yang and Mae Ramat basins. The stratigraphy of each basin was described from outcrop and borehole data (Figure 33).

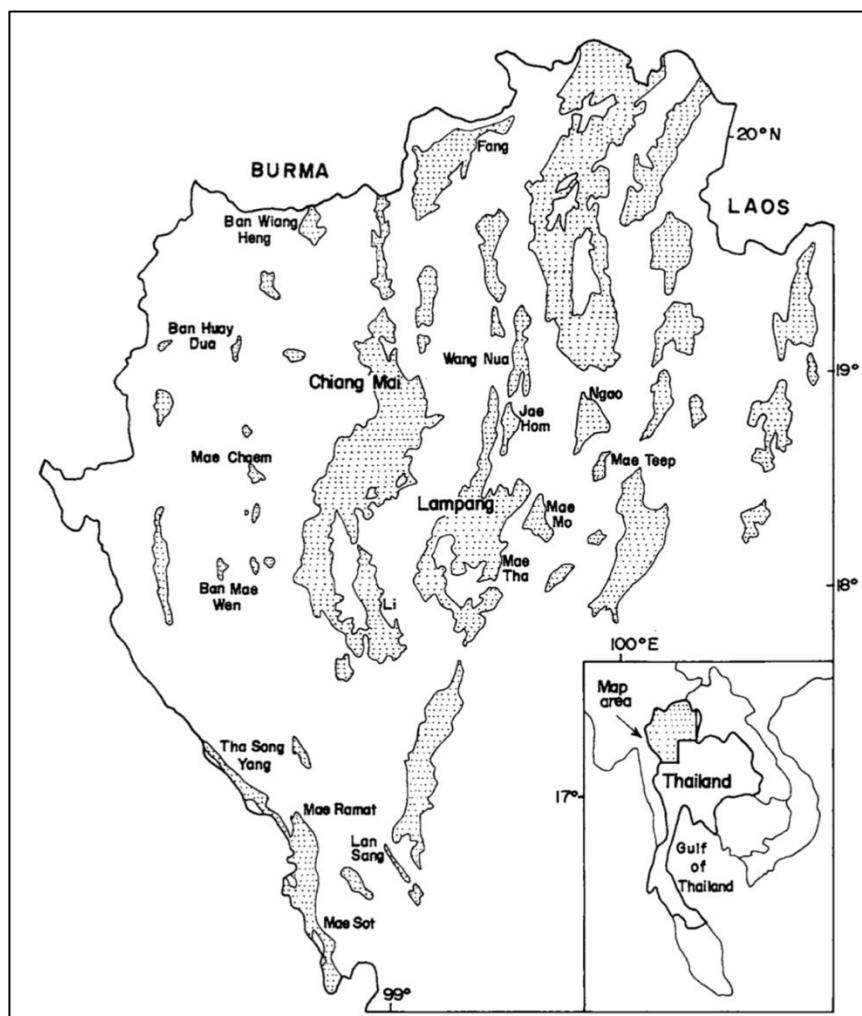


Figure 33 Major Cenozoic basins in Northern Thailand (Snansieng, 1979).

Songtham et al. (2003) studied the palynology of Tertiary basins of northern Thailand including Mae Moh, Li, Na Hong, Mae Lamao, and Chiang muan basins. The fossil pollen specimens were collected from several coalfields in order to group pollen assemblages by using scanning electron microscopy (SEM). The main



palynological assemblages were grouped into tropical climate (Figure 34). The presence of coal conditions and angiosperm pollens are common in trees growing in warm temperate, high latitude, and northern hemisphere climates. The movement of the Southeast Asia was believed to change from southward to southeastward, resulted in the change of the vegetational patterns from warm temperate to tropical forests during the Oligocene to Miocene. In addition, the difference in pollen assemblages can be related to coal quality. The coals in warm temperate contain low ash contents, whereas the tropical coals are relatively high ash contents (Figure 35).

	Warm temperate pollen	Tropical pollen
	<i>Piceapollenites</i> <i>Pinuspollenites</i> <i>Tsugaepollenites igniculus</i> <i>Taxodiaceapollenites</i> <i>Alnipollenites verus</i> <i>Caryapollenites simplex</i> <i>Faguspollenites</i> <i>Ilexpollenites iliacus</i> <i>Juglanspollenites</i> <i>Liquidambarpollenites stigmus</i> <i>Loniceraepollenites</i> <i>Momipites coryloides</i> <i>Pterocaryapollenites</i> <i>Quercoidites</i> <i>Ulmipollenites</i>	<i>Calophyllum cf. C. inophyllum</i> <i>Crudia</i> <i>Dipterocarpaceae</i> <i>Lagerstroemia</i> <i>Radermachera</i>
Mae Long Formation (Middle Miocene)		X X X X X
Ban Pa Kha Formation (Oligocene-Early Miocene)	X X X X X X X X X X X X X X X	

Figure 34 Warm temperate and tropical pollen from Ban Pa Kha and Mae Long Formations (Songtham et al., 2003).

Coal deposit location	Floras and Faunas	Weight percent of elementary analysis					
		Ash free basis					Ash
		H	C	N	O	S	
1. Na Sai, Li, Lamphun	Tropical	5.90	55.81	1.81	33.65	0.99	<b>42.57</b>
4. Na Hong (seam K), Chiang Mai	Warm temperate	5.13	61.13	0.51	32.63	0.43	<b>0.68</b>
5. Na Hong (seam B), Chiang Mai	Warm temperate	4.31	55.97	0.58	38.43	0.64	<b>0.96</b>
6. Ban Pu, Li, Lamphun	Warm temperate	4.11	49.57	0.25	44.56	1.15	<b>2.80</b>
7. Ban Hong, Li, Lamphun	Warm temperate	4.81	57.94	0.31	36.34	0.53	<b>2.92</b>
8. Ban Pa Kha, Li, Lamphun	Warm temperate	4.98	62.13	0.62	32.05	0.52	<b>4.27</b>
9. Nong Ya Plong, Petchaburi	Warm temperate	4.65	69.12	0.84	23.02	0.93	<b>3.87</b>

Figure 35 Elementary analysis of Tertiary Thai coals (Songtham et al., 2003).

## 2.5 Organic geochemical characteristics of coal

Alias et al. (2012) studied the coals from Tertiary Tanjong Formation in onshore Sabah, Malaysia. The coals were analyzed and evaluated by using pyrolysis and bitumen analysis. Furthermore, biomarker distribution was performed on the saturated hydrocarbon fraction by using gas chromatography–mass spectrometry (GC–MS) to characterize the source of organic matter, the thermal maturity and the depositional environment.

The biomarker parameters such as n-alkanes, isoprenoids (pristane and phytane), and steranes are useful to imply type of organic matter. The n-alkane distribution, isoprenoids data represent that the studied coals are derived from terrestrial higher plant input (Figure 36). In addition, the relative abundance of C<sub>27</sub>, C<sub>28</sub>, and C<sub>29</sub> steranes and pristane/phytane ratio are used to study the depositional environment. The studied coals were deposited in a swamp environment under oxic condition due to C<sub>29</sub> sterane dominant and high pristane/phytane ratio (Figure 37).

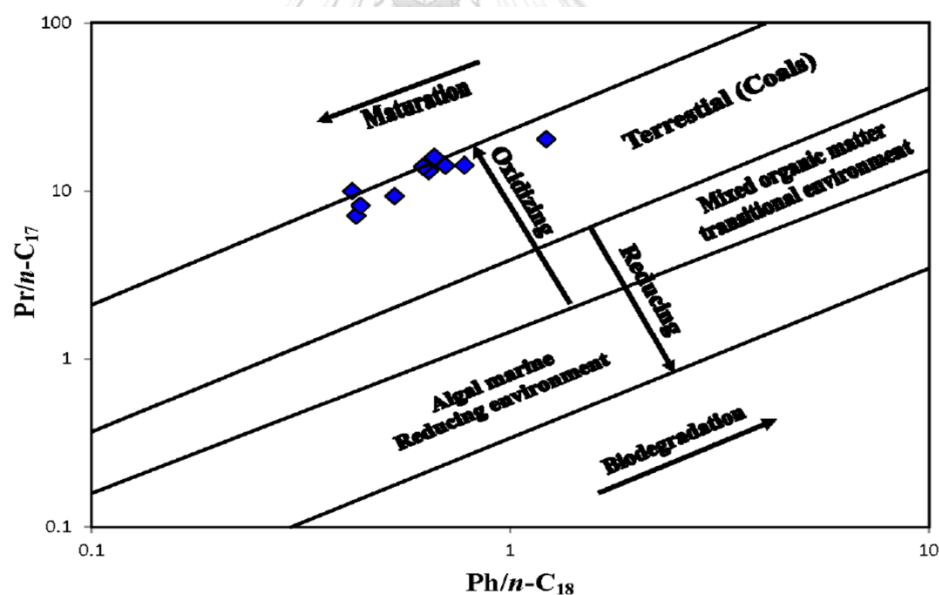


Figure 36 Example of log plot of phytane to n-C<sub>18</sub> alkane (Ph/n-C<sub>18</sub>) against pristane to n-C<sub>17</sub> alkane (Pr/n-C<sub>17</sub>) (Alias et al., 2012).

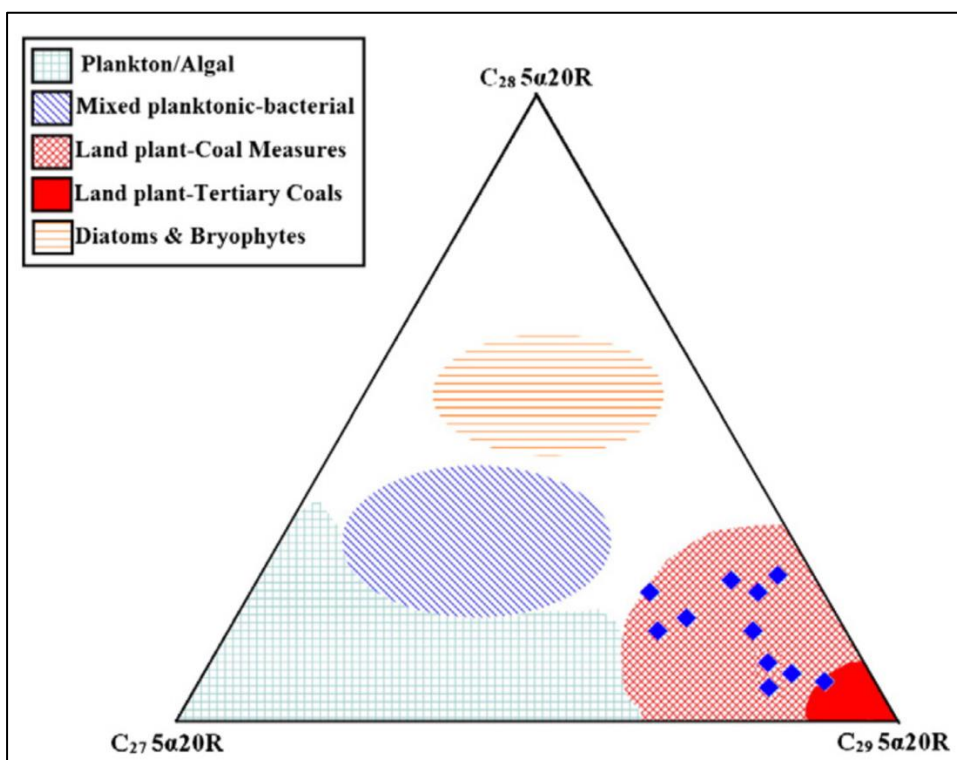


Figure 37 Example of ternary diagram of regular steranes ( $C_{27}$ - $C_{29}$ ) showing the relation of sterane components, source input, and depositional environment for the analyzed (Modified after Huang and Meinschein, 1979).

The thermal maturity can be evaluated by using biomarker parameters such as  $C_{32} 22S/(22S + 22R)$  homohopane,  $20S/(20S + 20R)$   $C_{29}$  sterane, moretane/hopane. The studied coals are in the range of early mature stage which are related to subbituminous B-A and high volatile bituminous C rank (Figure 38).

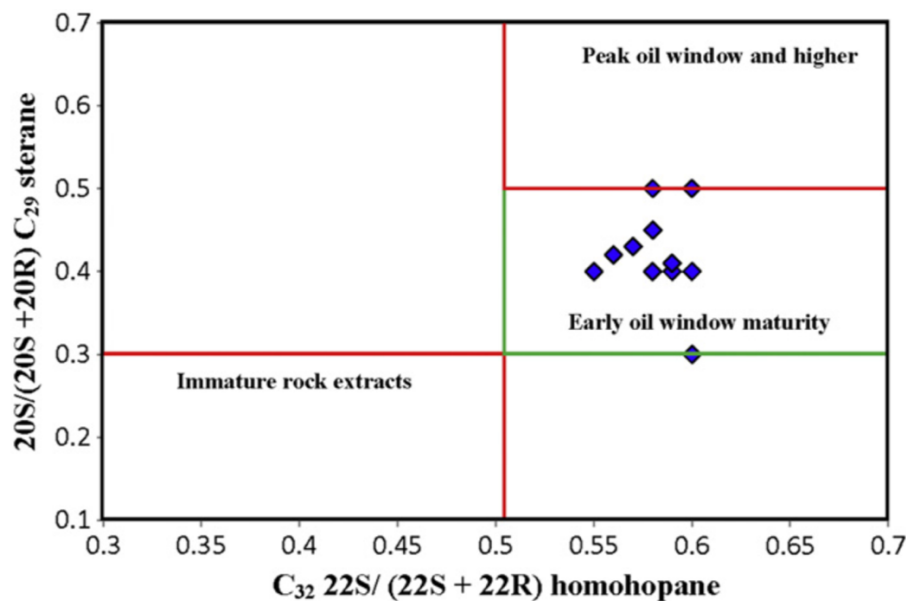


Figure 38 Example of cross-plot of two biomarker parameters sensitive to thermal maturity of the Pinangah sediments (Alias et al., 2012).

## 2.6 Organic matter in intermontane basins

Intermontane basins formed during mountain orogeny that basin subsidence, shape and size were mainly controlled by tectonic activities. Water system in intermontane basins generally provides closed or open conditions of lake on terrestrial setting. In addition, the climate conditions (e.g. precipitation rates, solar irradiation) in some basins also influence water system. Oil shale formation prefer to deposit in large lakes, while small lakes with bog and swamps are favorable to coal deposits associated with oil shale (Figure 39) (Tissot and Welte, 1984). Tectonic setting and climate conditions also influence organic matter source and paleoenvironmental conditions associated with local factors such as topography, drainage pattern, physical and chemical water system and variation of biomass in and around basins. Also, water column and its stratification control cycle and decomposition rates of organic matter that preserves organic matter within each basin (Gasse, 1990).

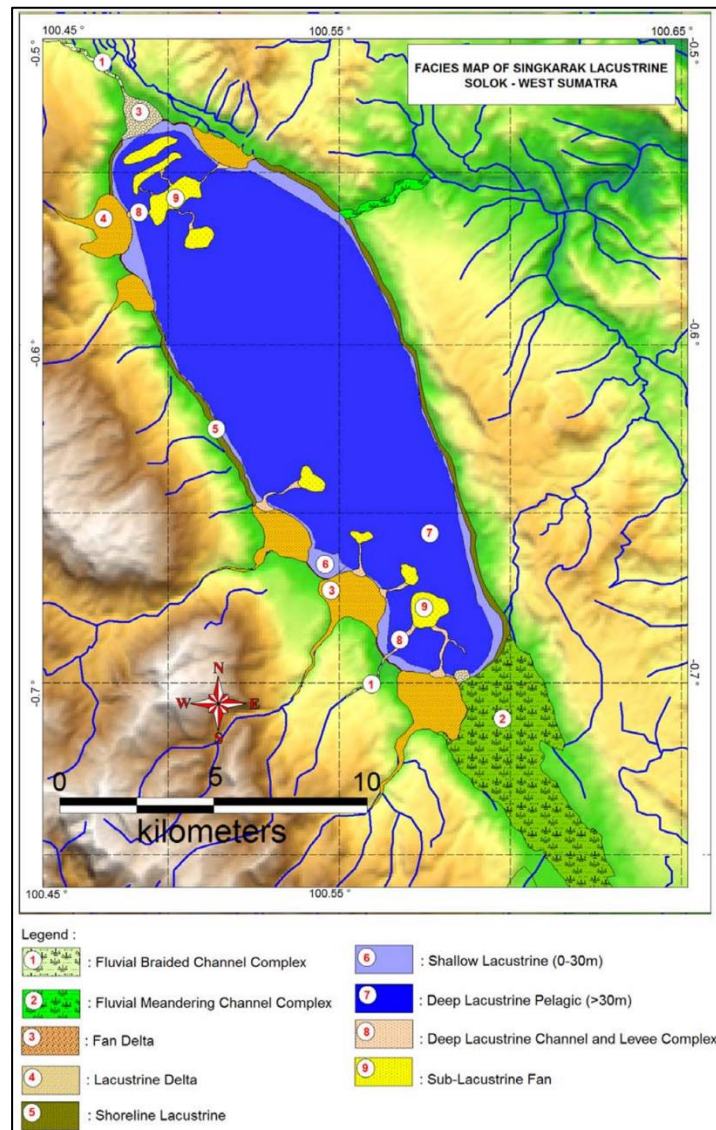


Figure 39 Schematic model of lacustrine environment (Setyobudi et al., 2016).

Plants can be divided into two main types based on biochemical compositions (1) nonvascular plants or lower plants containing low amounts of woody and cellulose (e.g. algae) (2) macrophytic vascular plants or higher plants are tissue structure (e.g. grasses, shrubs and trees) (Meyers and Ishiwatari, 1993). Organic matters that preserved in intermontane basins are combination of allochthonous and autochthonous sources. The allochthonous source is belong to debris of higher plants and dissolved humic compounds pass through media (e.g. water, eolian). The autochthonous source is associated with algae, bacteria and macrophytes. These organic matters undergo via microbial activity to decay and deposited in sediments.

The main microbial agents are bacteria, actinomycetes, fungi and algae (Moore, 1989). Organic compounds consist of carbohydrates and protein easily decomposed by degradation, whereas waxes and resins resistant to decay (Moore, 1989). Carbonization can be change due to highly diagenesis and catagenesis into carbon residue and original decomposition. However, primary characteristics may preserve depend on their composition and degree of decomposition.

The many studies of geochemical and biological markers that provides criteria to determine source of organic matter in sedimentary rocks (Hayes et al., 1990; Hoffmann et al., 1987; Tissot and Welte, 1984). The relative abundance of n-alkanes between short-chain (low molecular weight, LMW) and long-chain n-alkanes (high molecular weight, HMW) and their odd-numbered and even-numbered ratio are considered to differentiate higher plants organic matter input from lower plants contributions (Clark and Blumer, 1967; Cranwell, 1984; Meinschein, 1969; Powell and Mokirdy, 1973; Tissot and Welte, 1984). LMW n-alkanes are characteristics of phytoplankton input, while land plant cuticular waxes are belonged to appear HMW n-alkanes. Some HMW n-alkanes may indicate certain types of land plants (e.g. C<sub>31</sub> n-alkanes is indicative of marsh grasses, C<sub>27</sub> and C<sub>29</sub> are associated with deciduous trees) (Cranwell et al., 1987).

Oxygen levels in aquatic and sedimentary environments also control the degree of degradation of organic matter. The paleoenvironmental conditions (e.g. oxic and anoxic conditions) is provided by using ratio of pristane/phytane (Didyk et al., 1978). Pristane and phytane are derived from chlorophyll that dependent on oxygen content (Brooks et al., 1969; Maxwell et al., 1973). This ratio should be used with caution in hypersaline conditions (Ten Haven et al., 1987). After burial, organic matter preserved in sediments was altered undergone by biochemical and geochemical degradation which is mainly influenced by temperature and pressure. As increasing depth, organic matter gradually changes its color into darker. Thermal alteration associated with diagenesis is determined by using ratios of odd and even carbon number n-alkanes calculated as carbon preference index (CPI) (Bray and Evans, 1965; Philippi, 1965). CPI values more than 1.0 indicating the predominance of odd over even carbon number n-alkanes, while CPI values less than 1.0 representing the higher amounts of even carbon number n-alkanes compare to odd

carbon number n-alkanes. CPI is used to determine the molecular distribution of fatty acids and alcohols in fresh lipids and exhibit the fatty acids alteration dependent on the difference in diagenesis degree (Matsuda and Koyama, 1977). Generally, organic matter source can be characterized as materials for generating coal or hydrocarbon. Higher plants are likely typical of coal formation, while lower plants and microorganisms are predominant for hydrocarbon generation.

## **2.7 Environmental of coexistence of coal accumulation and oil shale formation and their crucial organic matter materials.**

The coal accumulation and oil shale formation are mainly influenced by basin environments and their condition of depositional environment. The formation of coal and shale can be coexisted in same basins. Coal formation is complex that can be formed in situ and/or in stable sedimentary environments. Also, transitional setting can be formed coal seam in peat bog, particularly environment between terrigenous and marine (Li et al., 2016). The main input for coal formation is terrestrial higher plants. Oil shale is typical of aquatic environment dependent on certain depth (Sun et al., 2013). Coal formation may derive from aquatic plants, plankton and debris of terrigenous higher plants. In steady water setting, shale or oil shale can be formed by preservation, aggregation and evolution of lower plankton (Li et al., 2016). Oil shale formed in lakes combining anoxic environments (Xu et al., 2015). The deeper water may form good quality oil shale, while the combination of subaqueous flow and/or fan in lake can cause oil shale with poor organic matter content (Liu et al., 2015). Several factors may control the shale distribution in lake including paleoclimate, paleogeography, the water level change and tectonic and volcanic activity. Semi-deep to deep lake environments are present in the lake of terrestrial plants and benthos (Li et al., 2016). Surface water contains the high amount of organic matter supply into lake, while bottom water is insufficient, salty and oxygen deficient which is favorable for good-quality thick oil shale (Yan et al., 2009).

Coal formation are relatively developed as same as oil shale forming conditions. Their settings may form as the result of peat bogs including alluvial-rivers, lakes, fan/braided streams, meandering rivers, deltas and coastal systems. There are different characteristics of coal in each place dependent on development,

scale, episodes and distribution of peat bog (Chu et al., 2015; Ferm, 1976; Horne et al., 1978). Coal accumulation requires the high amount of organic matter, sediment accommodation and tectonic subsidence/uplift and/or water level change that allow to preserve peat and later coal seams. Generally, temperature and humidity are the main influences for coal formation associated with ample plants, proper paleogeography for development of peat bogs and tectonic conditions (Zhao et al., 2014).

Oil shale is developed under climatic and tectonic settings. The warm climate associated with both humid and drought conditions is well-forming oil shale (Jia et al., 2013). However, the preservation of both coal and oil shale suggests high humidity (Jia et al., 2013). The combination of coal and oil shale formation can be occurred in various settings including fresh water basin with adjacent water-flow system, low oxidizing nearshore and/or low reducing lake swamps (Wang et al., 2011). Transgressive setting is also affected on oil shale formation, particularly in external flow basin. The cooperation of depositional environment, organic matter input and the changes of biological and climatic setting may cause the sequences of coal seams and oil shale formation.

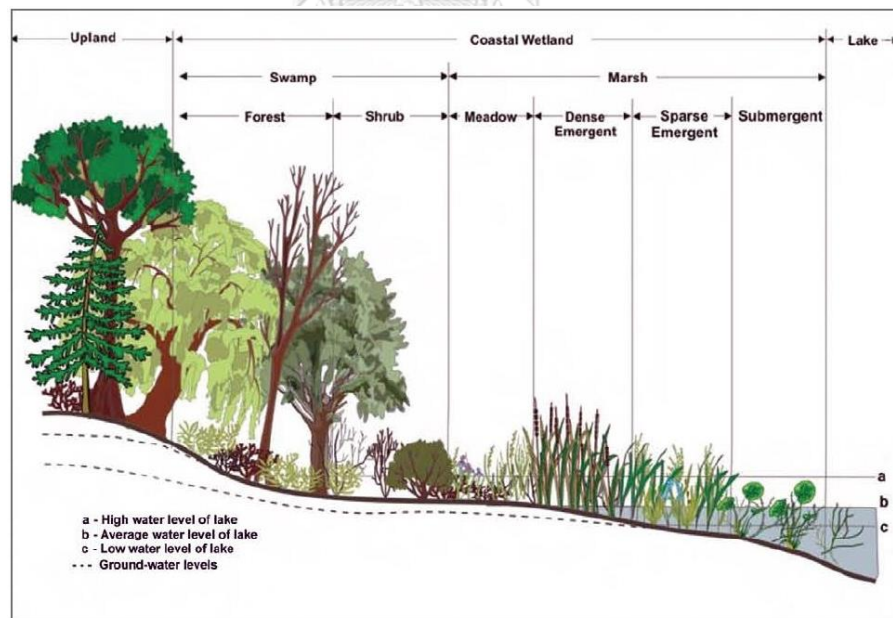


Figure 40 The schematic model of wetland types (Wilcox et al., 2007).

In terms of materials of organic matter input, coal requires materials of higher plants stem, leaf and root parts of the higher woody plants as well as lower plants association (Dai et al., 2020). Coalification is performed to create coal seams that can



be divided into four types depend on coal characterization, as follows: (1) forest swamp; (2) open reed swamp; (3) open basin related in swamp (submerged aquatic plants) and (4) moss marsh (Figure 40) (Wilcox et al., 2007). Generally, plant materials are mostly formed by forest swamp typically with tropical or subtropical areas (Simão and Kalkreuth, 2015). Oil shale is typical of plankton derivation found in lakes or in shallow seas including zooxanthellae algae and cyanobacteria. The blooms of algae in lakes showing the result of high productivity are associated with oil shale formation as autochthonous organic matter (Hutton et al., 1980). The allochthonous such as detrital higher plants growing at the lake edge deposit into lake by wind and/or water flow to supply more organic material (Hardie et al., 1978). The water stratification manifests the effect of marine influence making the different density water due to salinity. This can be led to the high productivity of extinct fresh water organisms and/or marine organisms due to the abrupt change of environments. The lush organic matters provide oil shale formation.

### CHAPTER III

## METHODOLOGY

The method of this study starts with literature reviews including geological history of study area, lithostratigraphy related depositional environment of study area, and organic geochemical analysis methods. The following step is field observation on the study area for lithostratigraphic data and then sample collection needed to be completed. The flow chart exhibits the procedure of this study as shown in Figure 41.

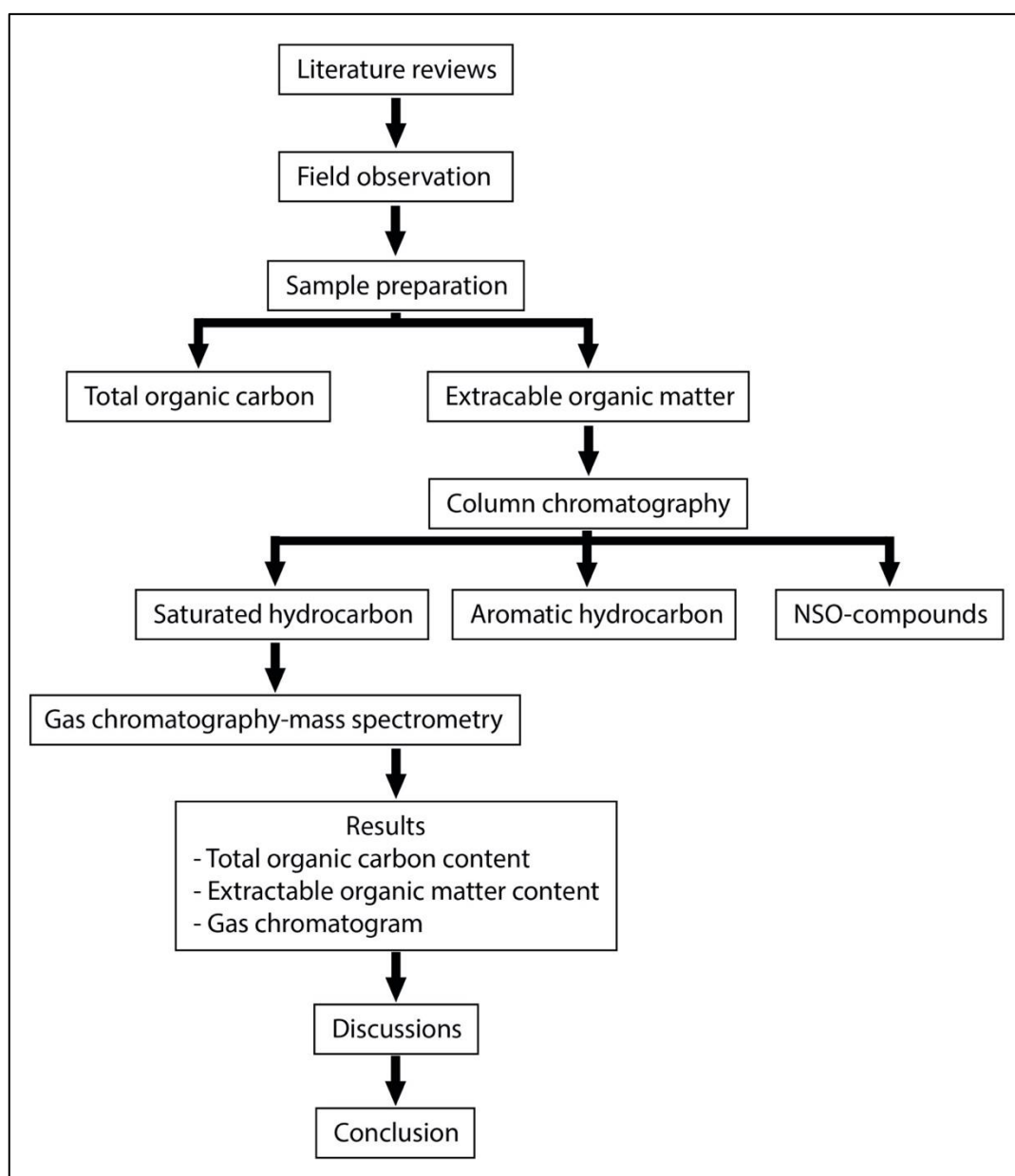


Figure 41 The flow chart shows methodology of this study.

### 3.1 Field observation and sample collection and preparation

The field observation is carried out in order to investigate lithostratigraphy and collect notable rock samples in the study areas. In this study, locations of study areas are operated as a coal mine in two coal mines Mae Teep and Mae Than coal mines. The operated coal mines provide outcrop surfaces that are suitable for making lithostratigraphic column and collecting rock samples. The sample collection is related to lithostratigraphic column by collecting as hand-picked samples from mine surface in which avoid weathered part by digging about 0.10-0.30 meters into outcrop wall. The remaining weathered parts of samples are removed before crushed into small pieces by a hammer and jaw crusher, respectively. Then, samples are ground into powders by a cleaned disc mill by grinding with baked quartz sands. The containing glassware and ball mill are also cleaned with distilled water, acetone and DCM for preventing contamination. The pulverized samples are prepared for geochemical analysis. In this study, TOC analysis uses 10 g of powdered sample to analyze and EOM analysis uses 35 g of powdered sample to analyze. In addition, gas chromatography-mass spectrometry (GC-MS) is analyzed by using saturated hydrocarbon extracted from EOM.

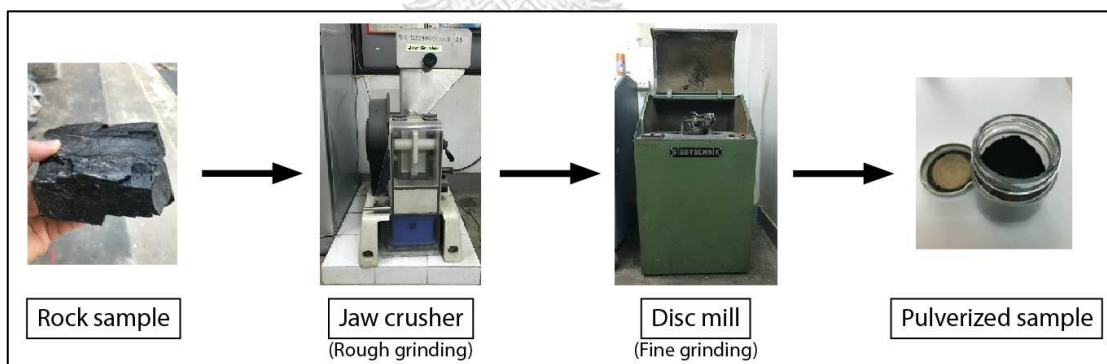


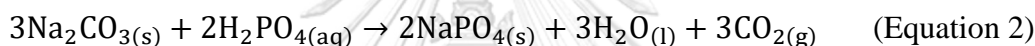
Figure 42 The flow chart of sample preparation.

### 3.2 Organic geochemical analysis

#### 3.2.1 Total organic carbon (TOC)

Total organic carbon content is analyzed by using SHIMADZU TOC analyzer with solid sample module (SSM-5000A) (Sleutel et al., 2007). In this study, TOC analysis is performed at Center of Excellent on Hazardous Substance Management (HSM), Chulalongkorn University. There are two main steps of procedure of TOC

analysis. First, standard calibration curves are set up by preparing standard total carbon curve (TC) from the different concentration of glucose ( $C_6H_{12}O_6$  Mw = 180.156  $g \cdot mol^{-1}$ ) on 5, 10, 20, 50, and 100 mg, respectively and then the crush sample is combusted at 900°C about 2 minutes with atmospheric oxygen (See Equation 1). Similarly, standard inorganic carbon curve (IC) is prepared by sodium carbonate ( $Na_2CO_3$ ; Mw = 105.988  $g \cdot mol^{-1}$ ) with the same concentration as TC and then is neutralized by using phosphoric acid ( $H_3PO_4$ ) 2.5 M (See Equation 2). IC is determined undergo 200°C about 2 minutes. This process provides carbon dioxide as by-product, which can be detected by non-dispersive infrared detector (NDIR). TC and IC can create TOC calibration curve.



After calibration curve is completely set up, there are two main parts for sample measurement. First, the crushed samples are weighted into 10 mg on two ceramic boats for analyzing TC and IC, respectively. In terms of TC, total carbon content in sample is detected by carbon dioxide ( $CO_2$ ) content which is released due to heating. In addition to IC, phosphoric acid reacts with calcium carbonate. Thus, carbonate rocks (calcite) or inorganic carbon can be detected on IC. Finally, TOC analysis is calculated on TC and IC, and exhibits the result as percentage of rock weight (wt. %).

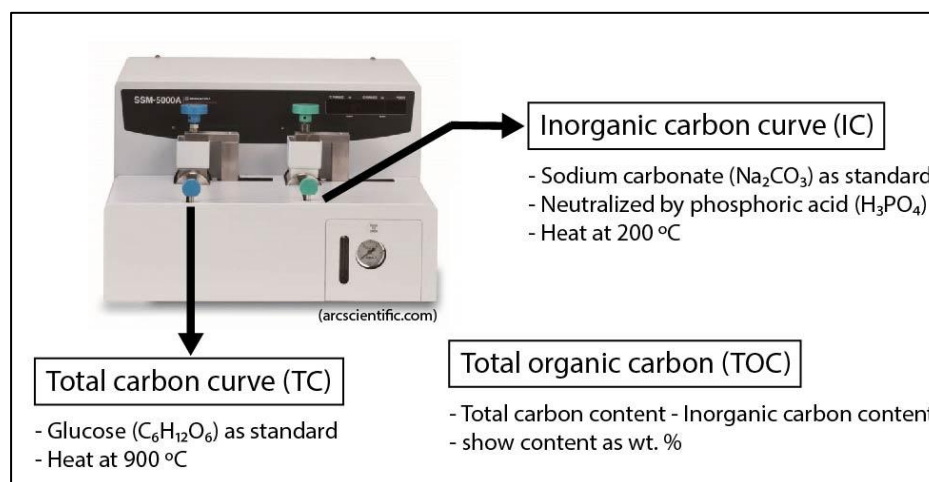


Figure 43 Total organic carbon analysis.

### 3.2.2 Extractable organic matter (EOM)

Extractable organic matter (EOM) or bitumen extraction is a method to extract rock into solution by using soxhlet extraction and mixture organic solvents of dichloromethane (DCM) and methanol (MET) in the ratio 93:7. 35 g of powdered samples are weighted in cellulose thimble (33 x 94 mm<sup>3</sup>). The thimble is covered with cotton wool and then put in soxhlet apparatus by using cleaned tweezers, which is filled with 250 ml of DCM. The soxhlet apparatus is connected with round bottom flask (1,000 ml) filled with the mixture of DCM:MET (93:7) about 200 ml, which is heated by heating mantle using temperature around 40-50 °C due to boiling point of DCM. The soxhlet extraction needs to be completed by cool water circulation system above soxhlet apparatus (6 - 10 °C) for condensing organic solvents. The organic solvents' volume is observed during the process in order to ensure enough volume for recirculation. This process continues for 48 hours, which starts counting since the beginning of first distillation. All glassware, apparatus, flask and tweezers are cleaned by distilled water, acetone and DCM for preventing contamination and sample solution is prepared in beaker for next step. The final product is called EOM or bitumen, which needs to be separated from organic solvents. Rotary evaporator is a tool for separating EOM from organic solvent in vacuum condition, then solution of concentrated EOM remains about 5 ml and leaves to dry for 24 hours. Finally, concentration of EOM can be calculated as milligram per kilograms rock (mg/kg) or part per million (ppm).

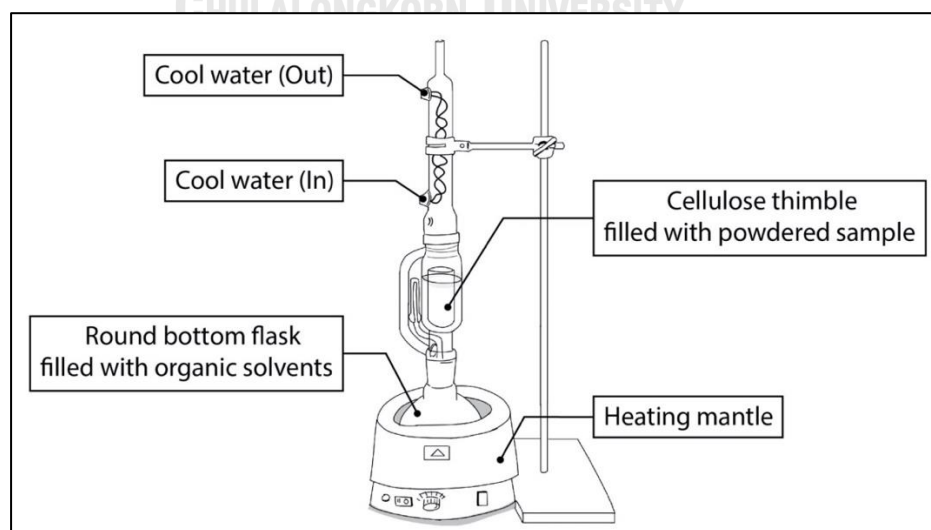


Figure 44 Soxhlet extraction for extracting EOM in rocks.

### 3.2.3 Column chromatography

EOM consists of aliphatic hydrocarbon (saturated hydrocarbon), aromatic hydrocarbon and hetero-aromatic hydrocarbon (NSO-compounds). On the basis of “like dissolves like” rule refers to solubility of both non-polar and polar substances, which can be dissolved in proper solvents. Column chromatography is a procedure of hydrocarbon fractionation by using property of polarity. Saturated hydrocarbon is non-polar substance thus, it can be dissolved in non-polar solvents such as hexane ( $C_6H_{14}$ ) which is used in this study. Similarly, ratio of DCM and hexane (7:3) is used to separate aromatic hydrocarbon, which has low to moderate in polarity. High polarity of hetero-aromatic hydrocarbon is separated by using methyl alcohol ( $CH_3OH$ ). In this study, the method of column chromatography consists of two main phases. First, stationary phase packs silica gel in chromatographic column (50 x 2.5 cm) with the ratio of silica gel and EOM content in weight % being about 20:1 for packing column. Silica gel has to be activated before use by heating at 120 °C for 24 hours and capped with a few centimeters of alumina for a day. Chromatographic column has to be cleaned before use by distilled water, acetone and DCM, respectively. In terms of column packing, the pipe of chromatographic column is plugged with small cotton wool for preventing silica gel leak out. For separating saturated hydrocarbon, hexane is used to be the first mobile phase as a solvent. Packing column needs to be tight by flushing air to release air in pore spaces of silica gel. It might beware of column cracking due to change of solvents in mobile phase. Similarly, separation of aromatic and hetero-aromatic hydrocarbons is completed by 7:3 ratio of DCM: hexane and methyl alcohol, respectively. After that, each hydrocarbon solution is distinguished as saturated, aromatic and hetero-aromatic hydrocarbons in different solvents. Rotary evaporator is used for separating solutions into concentrated substances, which remain about 2 ml filled in cleaned vial and then leave to dry for 24 hours. Finally, concentration of saturated, aromatic and hetero-aromatic hydrocarbons can be calculated as milligram per kilograms rock (mg/kg) or part per million (ppm).

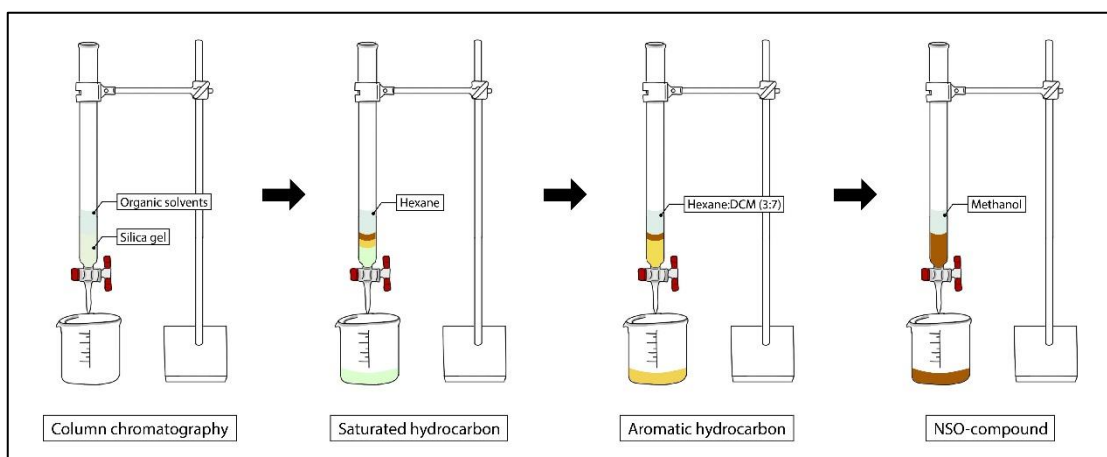


Figure 45 The method of column chromatography.

### 3.2.4 Gas chromatography - Mass spectrometry (GC - MS)

Molecular mass of organic compound is identified by using gas chromatography - mass spectrometry (GC - MS) performed at Scientific and Technological Research Equipment Centre (STREC), Chulalongkorn University. In this study, saturated hydrocarbon is investigated in order to study characteristic biomarker of samples. Firstly, saturated hydrocarbon is dissolved in hexane and then injected into the ionizing chamber by electron impact, then ionized gas flows through the column and is separated into compound by polarity and molecular weight. The separated gas then flows into the mass analyzer equipment which can be identified compound by ratio of mass and charge ( $m/z$ ) under the electromagnetic field. Second, n-alkane is used as standard calibration to dissolve the saturated hydrocarbon. Agilent 7890B GC and Agilent 7000C GC-MS (Triple quadrupole) is a tool for analyze the ratio of mass and charge ( $m/z$ ) under the condition of the ion source temperature of 250°C and 70 eV of ionizing energy. The 30 meters long DB-5 column (5% of Phenyl Methyl Siloxane) with 250  $\mu\text{m}$  inner diameter and 0.25  $\mu\text{m}$  film thickness. The initial temperature is 80°C and hold 3 minutes. The column temperature is heated from 80°C to 310°C at 4°C/minute and hold 30 minutes at 310°C (Chamchoy, 2014; Khositichaisri, 2012). The total analysis time is 90 minutes. Data is acquired in scanning of 35-700 molecular weight. The compound is identified by total-ion-chromatogram (TIC) and selected-ion-monitored (SIM). The difference in ratio of mass and charge provide

integration of n-alkanes and isoprenoids ( $m/z$  85), triterpanes and terpanes ( $m/z$  191) and diasteranes and steranes ( $m/z$  217) (Moustafa and Morsi, 2012).

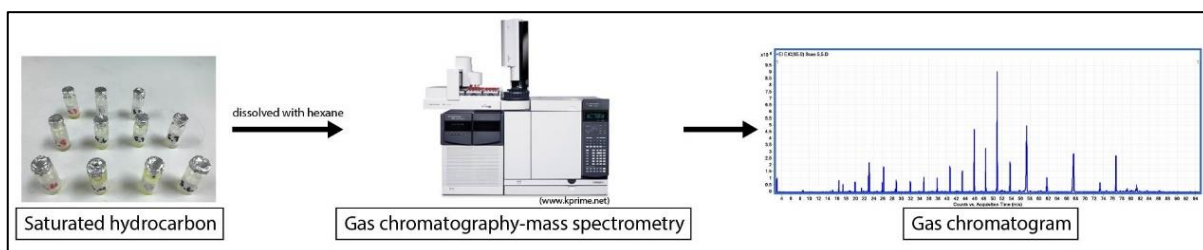


Figure 46 The procedure of gas chromatography-mass spectrometry analysis.





## CHAPTER IV

### RESULTS

#### 4.1 Sample description

This study focuses on the two coal mines including Mae Teep area and Mae Than area. Based on field observation, Mae Teep coal mine consists of three sections of outcrop walls that show lithology, attitude of bedding (210/30°SE) and sedimentary structures. Each section can be correlated to create lithostratigraphic column as shown in Figure 47 with lithological description. There are sixteen rock samples in Mae Teep coal mine collected for analyzing total organic carbon (TOC), extractable organic matter (EOM) and gas chromatography-mass spectrometry (GC-MS) as shown in Table 4.

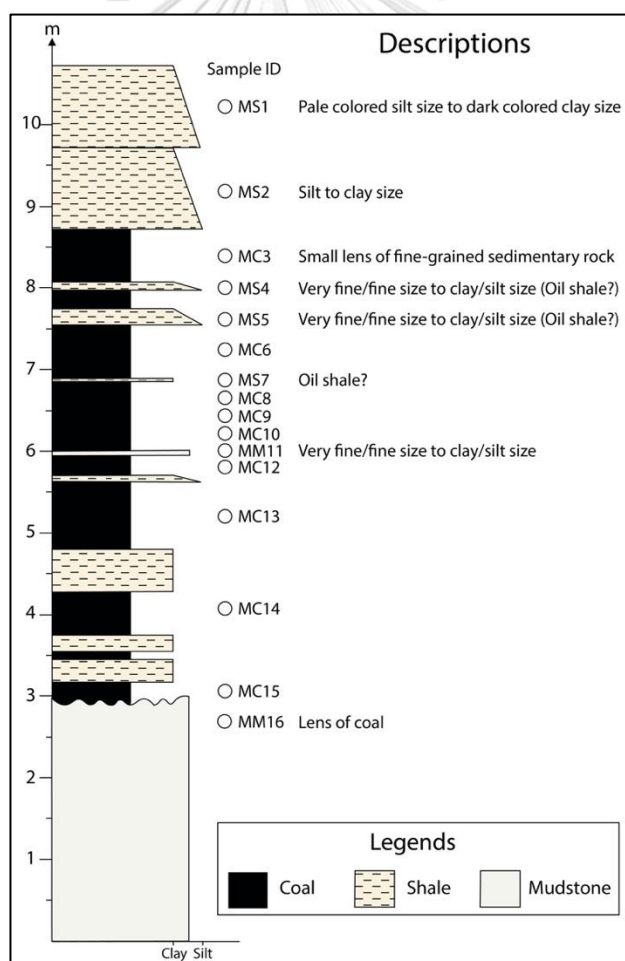


Figure 47 The lithostratigraphy of Mae Teep coal mine. The white circle denotes the collecting samples.

At Mae Teep coal mine, thick bed of shale is observed on the uppermost part of lithostratigraphic column with graded bedding. Grain size varies between silt size in pale colored shale and clay size in dark colored shale (Figure 48a). This shale bed is approximately 2-3 meters in thickness and is covered by overburden sediments. There is gradational change in lithology between coal and shale in the upper part of lithostratigraphy of Mae Teep coal mine (Figure 48b). The shale covers on coal showing coarser grain (silt size) interbedded with finer grain (clay size) and fissility.

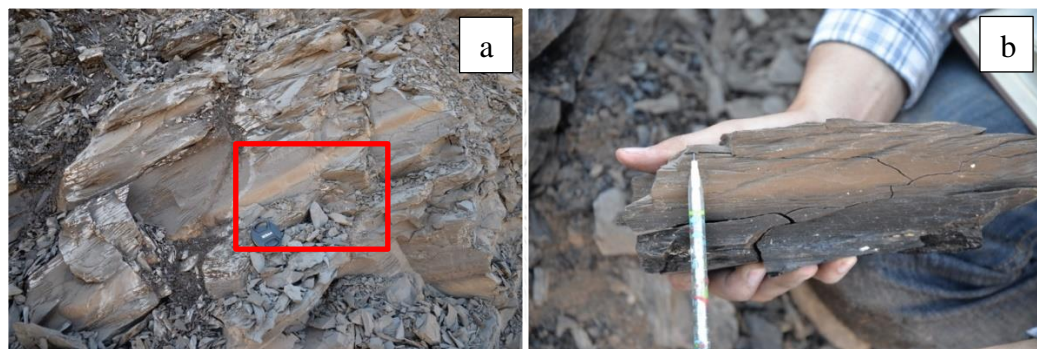
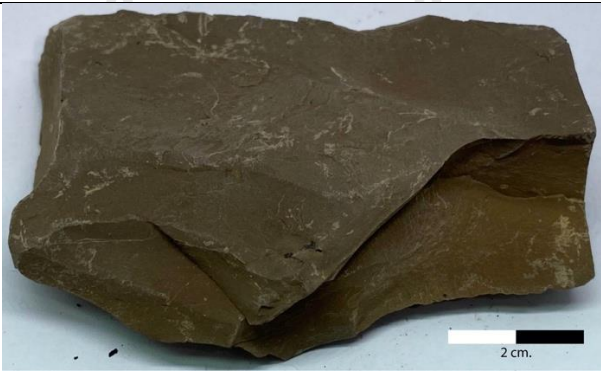
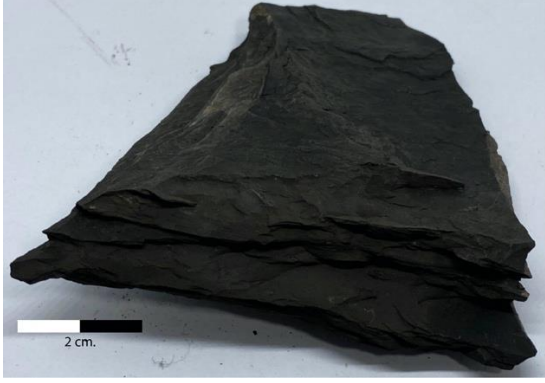









Figure 48 (a) thick bed of shale showing graded bedding (red square) in the uppermost part of lithostratigraphy of Mae Teep coal mine and (b) the gradational change between coal (sample ID MC3) and shale (sample ID MS2).




Table 4 Lithological descriptions from Mae Teep samples.

Sample ID	Rock sample	Lithology
MS1		<ul style="list-style-type: none"> <li>• Shale</li> <li>• Brown color</li> <li>• Clay to silt grain size</li> <li>• Fissility</li> </ul>

MS2		<ul style="list-style-type: none"> <li>• Shale</li> <li>• Dark gray color</li> <li>• Clay to silt grain size</li> <li>• Fissility</li> </ul>
MC3		<ul style="list-style-type: none"> <li>• Coal</li> <li>• Black color</li> <li>• Moderate fracture</li> <li>• Dull</li> </ul>
MS4		<ul style="list-style-type: none"> <li>• Oil shale</li> <li>• Brown color</li> <li>• Clay to silt grain size</li> <li>• Fissility</li> </ul>
MS5		<ul style="list-style-type: none"> <li>• Oil shale</li> <li>• Brown color</li> <li>• Clay to silt grain size</li> <li>• Fissility</li> </ul>

MC6		<ul style="list-style-type: none"> <li>• Coal</li> <li>• Black color</li> <li>• Moderate fracture</li> <li>• Slightly vitreous</li> </ul>
MS7		<ul style="list-style-type: none"> <li>• Oil shale</li> <li>• Brown color</li> <li>• Clay to silt grain size</li> </ul>
MC8		<ul style="list-style-type: none"> <li>• Coal</li> <li>• Black color</li> <li>• High fracture</li> <li>• Vitreous</li> </ul>
MC9		<ul style="list-style-type: none"> <li>• Coal</li> <li>• Black color</li> <li>• High fracture</li> <li>• Dull</li> </ul>

MC10		<ul style="list-style-type: none"> <li>• Coal</li> <li>• Black color</li> <li>• High fracture</li> <li>• Vitreous</li> </ul>
MM11		<ul style="list-style-type: none"> <li>• Mudstone</li> <li>• Brown color</li> <li>• Clay to silt grain size</li> </ul>
MC12		<ul style="list-style-type: none"> <li>• Coal</li> <li>• Black color</li> <li>• High fracture</li> <li>• Vitreous</li> </ul>
MC13		<ul style="list-style-type: none"> <li>• Coal</li> <li>• Black color</li> <li>• Moderate fracture</li> <li>• Slightly vitreous</li> </ul>

MC14		<ul style="list-style-type: none"><li>• Coal</li><li>• Black color</li><li>• High fracture</li><li>• Vitreous</li></ul>
MC15		<ul style="list-style-type: none"><li>• Coal</li><li>• Black color</li><li>• Moderate fracture</li><li>• Vitreous</li></ul>
MM16		<ul style="list-style-type: none"><li>• Mudstone</li><li>• White color</li><li>• Clay to silt grain size</li></ul>

In addition, rock samples from Mae Than coal mine are studied in order to correlate lithostratigraphy with rock samples from Mae Teep coal mine (Figure 49). Organic geochemical analysis is also investigated to compare geochemical results with Mae Teep coal mine. The attitude of bedding shows  $323/16^{\circ}\text{SE}$  based on field observation. In this study, fifteen rock samples are collected for geochemical analyzing as shown in Table 5.

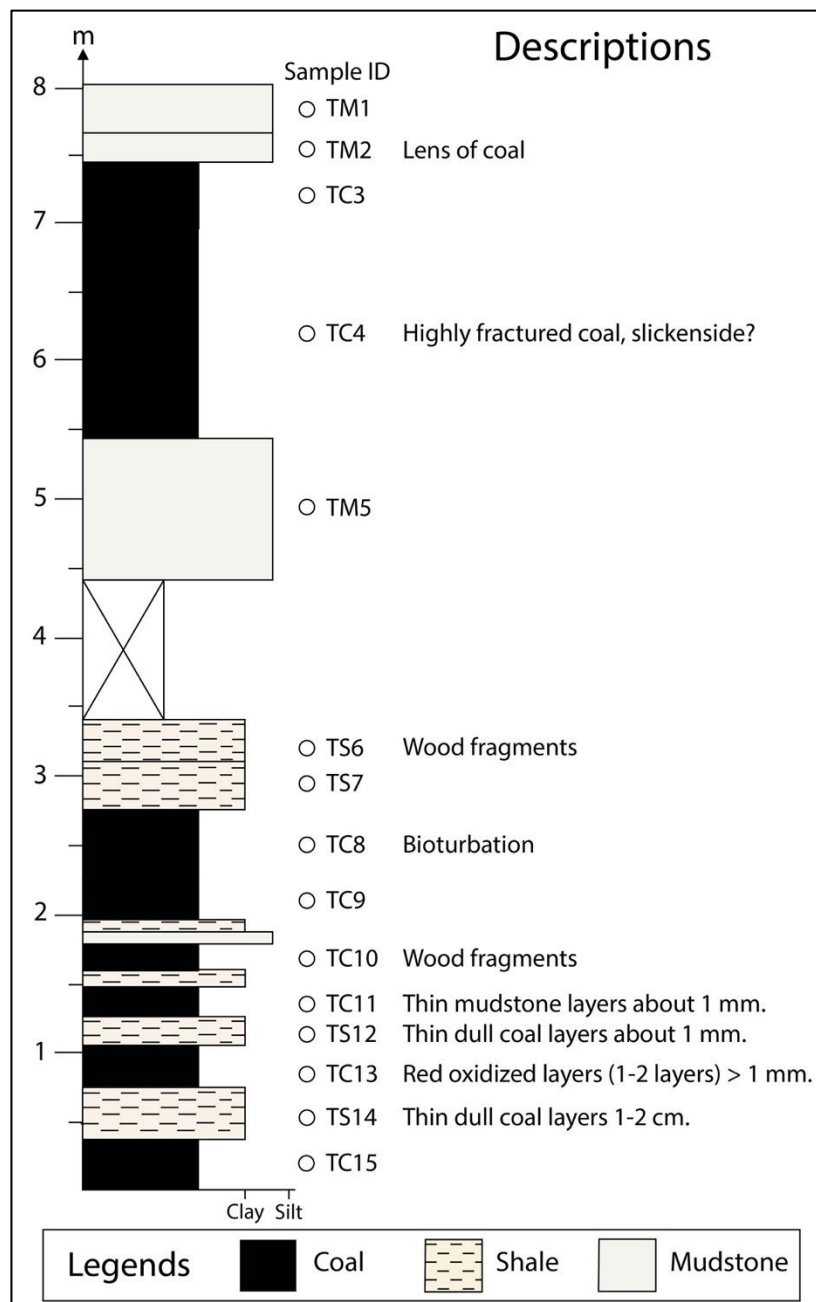



Figure 49 The lithostratigraphy of Mae Than coal mine. The white circle denotes the collecting samples.

There are fragments of leaves and wood preserved in shale (sample ID TS6) showing on the surface at Mae Than coal mine (Figure 50). Due to recent soils cover the middle part of the studied section, there is no data for lithostratigraphic column of Mae Than coal mine in the middle part. Thick mudstone bed presents as the first bed of upper part of this area showing slicken side that provides sub-horizontal fault (0/12°SE) within this area.











Figure 50 Leaves and wood fragments preserved in shale (sample ID TS6).


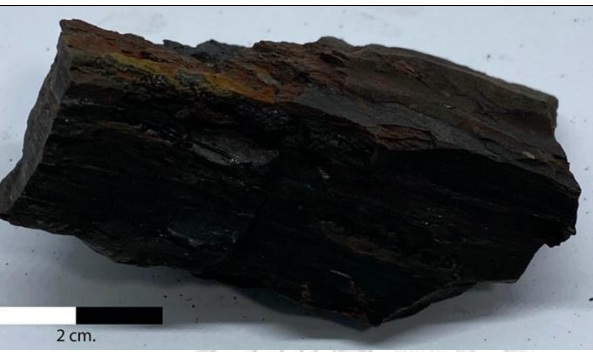

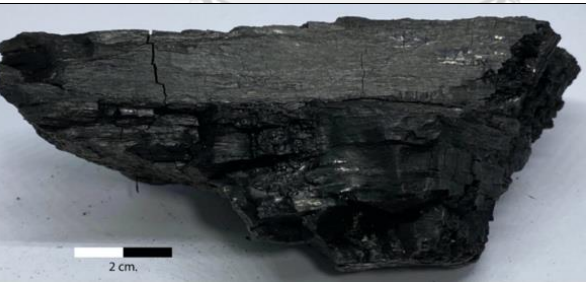

Table 5 Lithological descriptions from Mae Than samples.

Sample ID	Rock sample	Lithology
TM1		<ul style="list-style-type: none"> <li>• Mudstone</li> <li>• White color</li> <li>• Clay to silt grain size</li> </ul>



TM2		<ul style="list-style-type: none"><li>• Mudstone</li><li>• Reddish brown</li><li>• Clay to silt grain size</li></ul>
TC3		<ul style="list-style-type: none"><li>• Coal</li><li>• Black color</li><li>• Low fracture</li><li>• Slightly vitreous</li></ul>
TC4		<ul style="list-style-type: none"><li>• Coal</li><li>• Black color</li><li>• Low fracture</li><li>• Vitreous</li></ul>
TM5		<ul style="list-style-type: none"><li>• Mudstone</li><li>• White color</li><li>• Clay to silt grain size</li></ul>

TS6		<ul style="list-style-type: none"> <li>• Shale</li> <li>• Dark gray color</li> <li>• Clay to silt grain size</li> <li>• Fissility</li> </ul>
TS7		<ul style="list-style-type: none"> <li>• Shale</li> <li>• Reddish gray color</li> <li>• Clay to silt grain size</li> <li>• Fissility</li> </ul>
TC8		<ul style="list-style-type: none"> <li>• Coal</li> <li>• Dark gray color</li> <li>• Low fracture</li> <li>• Dull</li> </ul>
TC9		<ul style="list-style-type: none"> <li>• Coal</li> <li>• Black color</li> <li>• High fracture</li> <li>• Slightly vitreous</li> </ul>

TC10		<ul style="list-style-type: none"> <li>• Coal</li> <li>• Black color</li> <li>• Moderate fracture</li> <li>• Dull</li> </ul>
TC11		<ul style="list-style-type: none"> <li>• Coal</li> <li>• Black color</li> <li>• Low fracture</li> <li>• Slightly vitreous</li> </ul>
TS12		<ul style="list-style-type: none"> <li>• Shale</li> <li>• Dark brown color</li> <li>• Clay to silt grain size</li> <li>• Fissility</li> </ul>
TC13		<ul style="list-style-type: none"> <li>• Coal</li> <li>• Black color</li> <li>• Moderate fracture</li> <li>• Dull</li> </ul>
TS14		<ul style="list-style-type: none"> <li>• Shale</li> <li>• Brownish red color</li> <li>• Clay to silt grain size</li> </ul>

TC15		<ul style="list-style-type: none"> <li>• Coal</li> <li>• Black color</li> <li>• High fracture</li> <li>• Vitreous</li> </ul>
------	---	--

#### 4.2 Total organic carbon (TOC)

The total organic carbon (TOC) is used to provide information of quantity of organic matter in rocks. In Mae Teep coal mine, the highest TOC content appears on coal samples ranging from 30.12 to 73.71 wt.% followed by shale samples in range of 4.82 - 19.49 wt.%. Mudstone samples have the lowest TOC content at about 0.88 - 4.92 wt.%. In addition to Mae Than samples, the TOC results are similar to Mae Teep samples, exhibiting the highest amount on coal samples at about 23.48 - 52.20 wt.%. The shales contain the second place ranging from 14.00 to 24.87 wt.%. The lowest TOC content also appears on mudstone samples in the range of 0.59 - 5.98 wt.% (Table 6).

#### 4.3 Extractable organic matter (EOM)

The extractable organic matter (EOM) is also used to estimate the quantity of organic matter in rocks. Extraction yields obtained from rock samples vary between 313 and 9,764 ppm of Mae Teep coal mine which have the highest EOM on coals ranging from 3,170 to 9,764 ppm followed by shales containing 1,569-5,956 ppm. The lowest EOM content is mudstones ranging between 313 and 1,277 ppm. Also, the EOM contents vary from 228 to 16,421 ppm of rock samples from Mae Than coal mine. The highest EOM content appears on coals in the range of 6,428-16,421 ppm, whereas shales have moderate EOM content ranging from 3,999 to 12,039 ppm. Mudstones contain the lowest EOM content in the range of 507-1,256 ppm (Table 6).

#### 4.4 Hydrocarbon fractions

The EOM can be separated into hydrocarbon fractions including saturated hydrocarbon, aromatic hydrocarbon and NSO-compounds (Nitrogen, sulfur and

oxygen). Each fraction content is shown in Table 6. In Mae Teep samples, NSO-compound fraction shows the highest amount of hydrocarbon fractions in an average of 50.52 wt.% (15.93-79.59 wt.%) followed by aromatic fraction about 43.72 wt.% in average (9.33-61.95 wt.%). The lowest content appears on saturated hydrocarbon fraction in an average of 18.72 wt.% (2.22-34.88 wt.%). In Mae Than samples, the results of hydrocarbon fractions also show the highest content on NSO-compound fraction in an average of 69.91 wt.% (54.82-84.70 wt.%). Aromatic fraction contains moderate content of 22.92 wt.% in average (10.43-34.09 wt.%) and the lowest content appears on saturated fraction in an average of 7.17 wt.% (3.40-13.60 wt.%) (Table 6).



Table 6 The results of TOC, EOM and EOM fractions.

Sample ID	Mae Teeep samples						Mae Than samples						
	Lithology	TOC (wt.%)	EOM (ppm)	Saturated	Aromatic	NSO-compounds	Sample ID	Lithology	TOC (wt.%)	EOM (ppm)	Saturated	Aromatic	NSO-compounds
MS1	Shale	4.82	1,569	18.18	36.36	45.45	TM1	Mudstone	0.75	228	-	-	-
MS2	Shale	6.94	1,998	28.57	31.43	40.00	TM2	Mudstone	5.98	1,256	6.82	34.09	59.09
MC3	Coal	51.86	7,979	20.92	19.86	59.22	TC3	Coal	38.49	12,482	8.43	25.74	65.83
MS4	Oil shale	18.80	5,257	20.11	29.35	50.54	TC4	Coal	37.81	16,421	4.87	10.43	84.70
MS5	Oil shale	16.11	4,568	13.66	24.22	62.11	TM5	Mudstone	0.59	507	-	-	-
MC6	Coal	50.47	6,725	16.53	21.19	62.29	TS6	Shale	21.70	10,360	4.89	17.93	77.17
MS7	Oil shale	19.49	5,956	22.49	29.19	48.33	TS7	Shale	24.87	12,039	6.15	16.31	77.54
MC8	Coal	73.71	4,886	19.65	42.77	37.57	TC8	Coal	38.80	9,846	13.33	28.70	57.97
MC9	Coal	57.66	3,170	22.12	61.95	15.93	TC9	Coal	52.20	12,323	7.13	24.14	68.74
MC10	Coal	44.00	4,819	34.88	51.16	13.95	TC10	Coal	23.48	6,428	13.60	31.58	54.82
MM11	Mudstone	4.92	1,277	2.22	20.00	77.78	TC11	Coal	32.39	11,294	5.56	16.16	78.28
MC12	Coal	35.78	7,852	16.36	17.09	66.55	TS12	Shale	19.83	6,329	7.66	34.23	58.11
MC13	Coal	30.12	9,764	11.08	9.33	79.59	TC13	Coal	46.76	15,909	3.40	13.06	83.54
MC14	Coal	48.37	5,829	16.67	20.59	62.75	TS14	Shale	14.00	3,999	7.04	24.65	68.31
MC15	Coal	50.04	6,132	17.97	23.04	58.99	TC15	Coal	47.87	9,253	4.31	20.92	74.77
MM16	Mudstone	0.88	313	18.18	54.55	27.27							
Average	Average	32.12	4,881	18.72	30.76	50.52	Average	Average	27.03	8,578	7.17	22.92	69.91

-: No data

## 4.5 Gas chromatograms

In mass spectroscopy, the mass-to-charge ratio ( $m/z$ ) of a cation is equal to the mass of the cation divided by its charge. Chemical compounds entering the mass spectrometer are imparted with energy that causes their ionization and fragmentation into many ions. These ions are sorted based on mass-to-charge ratio ( $m/z$ ) and detected (Stauffer et al., 2008a).

In this study, three different mass-to-charge ratios ( $m/z$ ) are studied in order to indicate organic geochemical characteristic of rock samples based on biomarkers and non-biomarkers including  $m/z$  85,  $m/z$  191 and  $m/z$  217 for indicating distributions of n-alkanes and isoprenoids, terpanes and triterpanes and steranes, respectively.

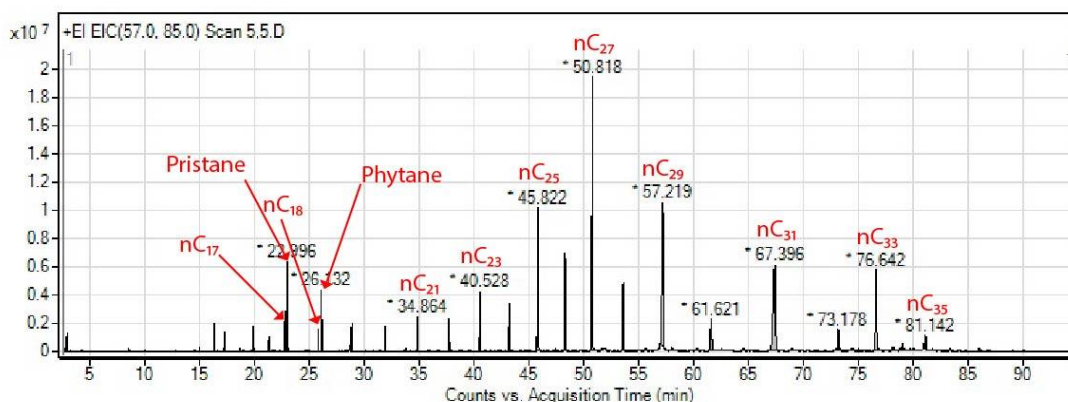


Figure 51 An example of  $m/z$  85 chromatogram showing n-alkane and isoprenoid distribution of oil shale from Mae Teep coal mine (sample ID MS5).

### 4.5.1 n-alkanes and isoprenoids

The n-alkane distributions of the Mae Teep samples are shown in Figure 51 and listed in Table 7. The n-alkanes can be divided into three groups including short-chain range, mid-chain range and long-chain range n-alkanes. The percentage of each n-alkane can be calculated as shown in Equation 3 for the percentage of short-chain n-alkanes. Equation 4 and Equation 5 represent the percentage of mid-chain n-alkanes and long-chain n-alkanes, respectively.

$$\text{short-chain n-alkanes (\%)} = \frac{\sum(C_{13} - C_{19})}{\sum(C_{13} - C_{35})} \times 100 \quad (\text{Equation 3})$$

$$\text{mid-chain n-alkanes (\%)} = \frac{\sum(C_{21} - C_{25})}{\sum(C_{13} - C_{35})} \times 100 \quad (\text{Equation 4})$$

$$\text{long-chain } n\text{-alkanes } (\%) = \frac{\sum(C_{27} - C_{35})}{\sum(C_{13} - C_{35})} \times 100 \text{ (Equation 5)}$$

As the results, the n-alkanes vary in the range of C<sub>13</sub>-C<sub>35</sub> showing long-chain (nC<sub>27-35</sub>) compounds dominate in an average of 73.71% (54.61-86.79%) followed by mid-chain (nC<sub>21-26</sub>) n-alkanes about 16.98% in average (7.39-27.12%). Short-chain n-alkanes (<nC<sub>20</sub>) contain the lowest in an average of 6.47% (1.69-21.61%).

In addition, isoprenoids are significantly presented in pristane (Pr) and phytane (Ph) in term of concentration. Pristane/nC<sub>17</sub> contains an average of 3.70 with the highest ratio shows on shales (2.57-7.74) followed by coals between 1.64 and 7.92. The lowest ratio belongs to mudstones (0.44-0.76). While, phytane/nC<sub>18</sub> ratios have an average of 1.73 showing the low ratios on mudstones (0.06-0.16) and coals (0.50-1.09), whereas shales contain the greatest ratios ranging from 3.31 to 6.37. In addition, Pr/Ph ratios of Mae Teep coal mine are in an average of 3.95 with the greatest ratios on coals (4.83-8.71). Mudstones are in the range of 0.69-2.98, while shales are the lowest pr/ph ratios (0.81-1.34) (Table 7).

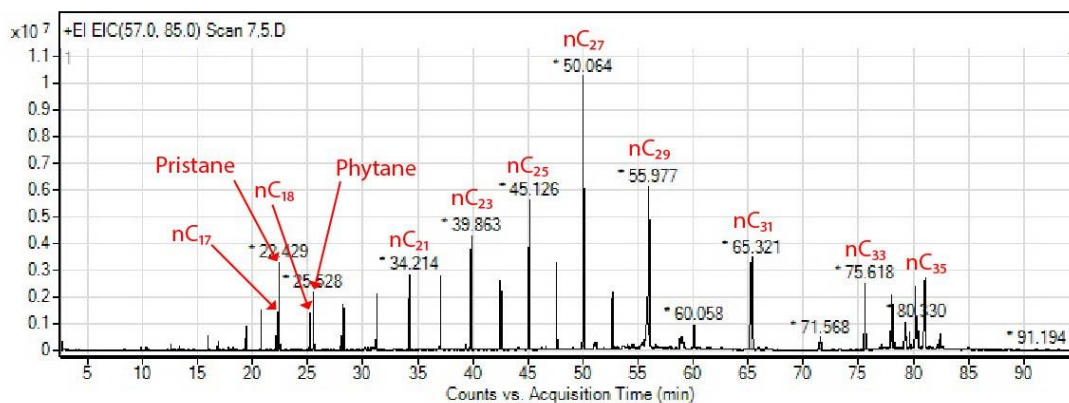


Figure 52 An example of m/z 85 chromatogram showing n-alkane and isoprenoid distribution of shale from Mae Than coal mine (sample ID TS6).

For Mae Than samples, n-alkane distribution is dominant in the range of nC<sub>15</sub>-nC<sub>35</sub> with minor isoprenoid compounds (Figure 52). The highest percentage appears on long-chain n-alkanes (>nC<sub>27</sub>) containing 69.29% in average (54.67-85.80%) while mid-chain n-alkanes (nC<sub>21-26</sub>) show the second highest in an average of 22.28% (12.58-39.04%). Short-chain n-alkanes have low amount of percentage about 5.48%



in average (1.22-10.19%) (Table 7). Also, isoprenoids, pristane and phytane, appear with minor amounts in Mae Than samples showing  $pr/nC_{17}$  with the highest ratios on coals ranging of 0.25-5.00 followed by shales in the 1.61-2.41 range. Mudstones have the lowest  $pr/nC_{17}$  ratios in the 0.51-1.71 range. In addition,  $ph/nC_{18}$  contains lower amounts about 1.43 in average compared to  $pr/nC_{17}$  ratio. Coals and shales have similar  $ph/nC_{18}$  ratios in the range of 0.20-3.82 and 0.75-3.63, respectively. The lowest ratios appear on mudstones ranging from 0.23 to 0.64. Furthermore, the average of  $pr/ph$  ratios in Mae Than samples is about 1.71. Shales show the lowest ratios at 0.80-1.35, whereas mudstones contain moderate ratios of 0.98-1.91. The highest values are about 1.03-5.46 in coals (Table 7).



Table 7 The results of n-alkanes and isoprenoids.

Sample ID	Mae Teep samples										Mae Than samples					
	Lithology	n-Alkanes (%)				Isoprenoids			Sample ID	Lithology	n-Alkanes (%)			Isoprenoids		
		Short-chain	Mid-chain	Long-chain	Pr/n C <sub>17</sub>	Ph/n C <sub>18</sub>	Pr/Ph	Short-chain			Mid-chain	Long-chain	Pr/n C <sub>17</sub>	Ph/n C <sub>18</sub>	Pr/Ph	
MS1	Shale	5.84	20.55	66.43	2.79	3.71	0.82	TM1	Mudstone	4.35	36.22	58.72	1.57	0.33	1.26	
MS2	Shale	3.55	20.37	71.89	2.62	3.31	0.81	TM2	Mudstone	4.10	20.32	74.53	1.71	0.64	0.98	
MC3	Coal	1.69	16.46	80.55	5.08	0.76	6.00	TC3	Coal	2.13	14.71	81.37	3.46	1.66	2.09	
MS4	Oil shale	2.70	16.72	75.35	7.74	6.37	1.34	TC4	Coal	3.41	18.98	75.16	3.13	1.66	2.16	
MS5	Oil shale	6.28	20.16	66.58	2.57	3.32	1.29	TM5	Mudstone	4.47	39.04	54.67	0.51	0.23	1.91	
MC6	Coal	2.02	15.37	80.97	5.17	0.63	6.54	TS6	Shale	8.55	27.49	57.75	2.41	1.69	1.35	
MS7	Oil shale	21.61	16.36	54.61	3.16	4.28	1.07	TS7	Shale	9.07	27.16	58.12	2.02	1.58	1.20	
MC8	Coal	20.00	13.39	65.10	3.78	0.50	8.71	TC8	Coal	8.46	18.13	72.20	0.27	0.25	1.07	
MC9	Coal	16.54	19.07	61.67	3.79	0.80	6.09	TC9	Coal	10.19	24.45	64.67	0.25	0.20	1.03	
MC10	Coal	4.48	7.39	86.79	4.31	0.77	6.29	TC10	Coal	5.21	22.88	64.25	5.00	3.82	1.50	
MM11	Mudstone	5.84	18.38	75.58	0.44	0.16	2.98	TC11	Coal	3.70	16.05	75.54	2.89	2.88	1.11	
MC12	Coal	1.70	11.59	85.65	3.13	0.53	5.56	TS12	Shale	5.65	19.02	69.36	2.83	3.63	0.80	
MC13	Coal	1.71	13.22	84.60	1.64	0.28	5.30	TC13	Coal	1.79	15.35	81.33	4.48	1.68	2.17	
MC14	Coal	1.85	22.49	73.49	7.92	1.09	4.91	TS14	Shale	1.22	12.58	85.8	1.61	0.75	1.50	
MC15	Coal	2.44	12.97	82.62	4.31	1.04	4.83	TC15	Coal	9.96	21.81	65.92	1.67	0.44	5.46	
MM16	Mudstone	5.32	27.12	67.50	0.76	0.06	0.69									
Average		6.47	16.98	73.71	3.70	1.73	3.95	Average		5.48	22.28	69.29	2.25	1.43	1.71	

4.5.2 Carbon preference index (CPI), average chain length (ACL), terrigenous/aquatic ratio (TAR), natural n-alkanes ratio (NAR) and  $P_{aq}$

The Carbon preference index (CPI) is a ratio that use to describe input of organic matter, paleoenvironmental condition, thermal maturity and biodegradation (Tissot and Welte, 1984). The CPI can be calculated from the relative abundance between odd and even carbon numbered n-alkanes from m/z 85 chromatogram (Figure 51 and 52) using the formula purposed by Bray and Evans (1961) (Equation 6). In Mae Teep coal mine, the highest CPI value appears on coals in the range of 3.09-6.39 followed by shales value from 3.27 to 4.20. Mudstones contain low CPI value ranging from 2.47 to 2.67. In Mae Than coal mine, the highest CPI value is in coals in the range of 3.25-4.96. Shales possess CPI values from 2.84 to 4.53 and close to CPI value of mudstones in the range of 3.03-4.03 (Table 8).

$$CPI = \frac{\sum(C_{23} - C_{31})_{odd} + \sum(C_{25} - C_{33})_{odd}}{2\sum(C_{24} - C_{32})_{even}} \quad (\text{Equation 6})$$

The average chain length (ACL) is also applied to indicate source of organic matter in environment based on the relative amounts of odd-numbered n-alkanes between  $C_{25} - C_{33}$  n-alkanes which is mainly derived from higher plant input (Poynter and Eglinton, 1990). The formula of ACL used in this study is presented in Equation 7. The ACL results of Mae Teep samples show the narrow range from 28.14 to 30.29. In Mae Than samples, the ACL ratios also show the narrow range of 27.48-29.64 (Table 8).

$$ACL = \frac{25(C_{25}) + 27(C_{27}) + 29(C_{29}) + 31(C_{31}) + 33(C_{33})}{C_{25} + C_{27} + C_{29} + C_{31} + C_{33}} \quad (\text{Equation 7})$$

$P_{aq}$  is used to differentiate aquatic inputs from terrestrial higher plants. The ratio can be calculated from odd-numbered between  $C_{23}$ - $C_{31}$  n-alkanes (Ficken et al., 2000; Jeng and Huh, 2008). The  $P_{aq}$  formula is shown in Equation 8. As the results, Mae Teep samples contain the  $P_{aq}$  ratio in the range of 0.09-0.35. The  $P_{aq}$  ratios of Mae Than samples value between 0.14 and 0.61 (Table 8).

$$P_{aq} = \frac{C_{23} + C_{25}}{C_{23} + C_{25} + C_{29} + C_{31}} \quad (\text{Equation 8})$$

The terrigenous/aquatic ratio (TAR) is used to differentiate terrestrial derived organic matter from marine organic matter input (Bourbonniere and Meyers, 1996). The ratio can be calculated by using the relative abundance of short-chain and long-chain n-alkanes (Equation 9). In Mae Teep coal mine, the studied samples have a

wide range of 14.46-87.24. Also, Mae Than samples contain high TAR values, ranging from 10.90 to 128.56 (Table 8).

$$TAR = \frac{C_{27} + C_{29} + C_{31}}{C_{15} + C_{17} + C_{19}} \quad (\text{Equation 9})$$

The natural n-alkanes ratio (NAR) is the contribution of relative amounts between natural and petroleum n-alkanes (Mille et al., 2007). The NAR is a ratio that indicates by using n-alkanes related to even-numbered n-alkanes in order to differentiate petroleum hydrocarbons and crude oils from natural n-alkanes (Equation 10). Based on this study, the studied samples from Mae Teep coal mine is in the narrow range of 0.46-0.72. In Mae Than samples, NAR ratios are in the range of 0.46-0.66 (Table 8).

$$NAR = \frac{\sum(C_{19} - C_{32}) - 2\sum(C_{20} - C_{32})_{\text{even}}}{\sum(C_{19} - C_{32})} \quad (\text{Equation 10})$$

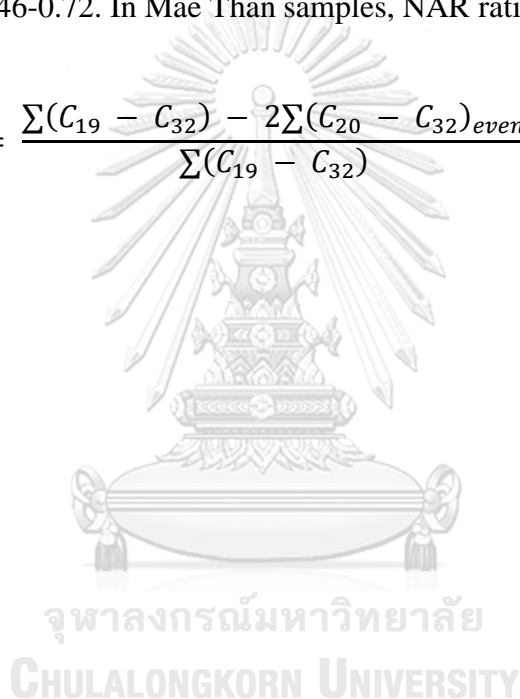


Table 8 The results of CPI, ACL, P<sub>aq</sub>, TAR and NAR ratios.

Sample ID	Mae Teep samples						Mae Than samples						
	Lithology	CPI	ACL	P <sub>aq</sub>	TAR	NAR	Sample ID	Lithology	CPI	ACL	P <sub>aq</sub>	TAR	NAR
MS1	Shale	3.67	28.75	0.29	15.43	0.52	TM1	Mudstone	4.36	27.48	0.52	37.12	0.57
MS2	Shale	3.60	28.51	0.29	30.46	0.53	TM2	Mudstone	4.96	28.86	0.19	41.48	0.60
MC3	Coal	5.60	28.76	0.25	80.74	0.67	TC3	Coal	6.20	30.08	0.17	55.67	0.66
MS4	Oil shale	4.10	28.92	0.21	56.56	0.57	TC4	Coal	5.14	29.10	0.22	37.91	0.63
MS5	Oil shale	3.52	28.74	0.25	14.92	0.52	TM5	Mudstone	3.32	27.64	0.61	22.45	0.46
MC6	Coal	5.09	29.71	0.19	56.57	0.61	TS6	Shale	3.64	28.71	0.33	11.63	0.49
MS7	Oil shale	4.06	28.82	0.26	14.46	0.56	TS7	Shale	3.30	28.56	0.32	10.90	0.46
MC8	Coal	6.38	28.93	0.25	38.20	0.69	TC8	Coal	4.85	28.59	0.15	13.78	0.58
MC9	Coal	7.04	28.14	0.33	25.70	0.72	TC9	Coal	3.44	28.57	0.16	13.59	0.47
MC10	Coal	5.08	30.29	0.09	68.19	0.63	TC10	Coal	3.96	28.88	0.28	20.27	0.53
MM11	Mudstone	2.99	29.43	0.23	49.61	0.46	TC11	Coal	5.57	29.55	0.22	22.91	0.64
MC12	Coal	3.95	29.87	0.13	74.67	0.55	TS12	Shale	5.67	29.43	0.23	18.38	0.63
MC13	Coal	3.60	29.49	0.16	79.44	0.53	TC13	Coal	5.22	29.47	0.16	74.88	0.64
MC14	Coal	6.09	28.47	0.35	72.24	0.69	TS14	Shale	5.26	29.64	0.14	128.56	0.65
MC15	Coal	5.80	29.67	0.16	45.09	0.66	TC15	Coal	5.33	28.11	0.29	14.56	0.65
MM16	Mudstone	3.30	29.06	0.34	87.24	0.48	Average						0.59
Average		4.62	29.10	0.24	50.60	0.59							4.68

#### 4.5.3 Triterpanes and terpanes

The gas chromatogram can be selected by m/z 191 to provide distributions of triterpanes and terpanes including Ts, Tm, Hopane, Moretane, Homohopane. These are biomarkers used for indicating thermal maturity of rocks (Figure 53).

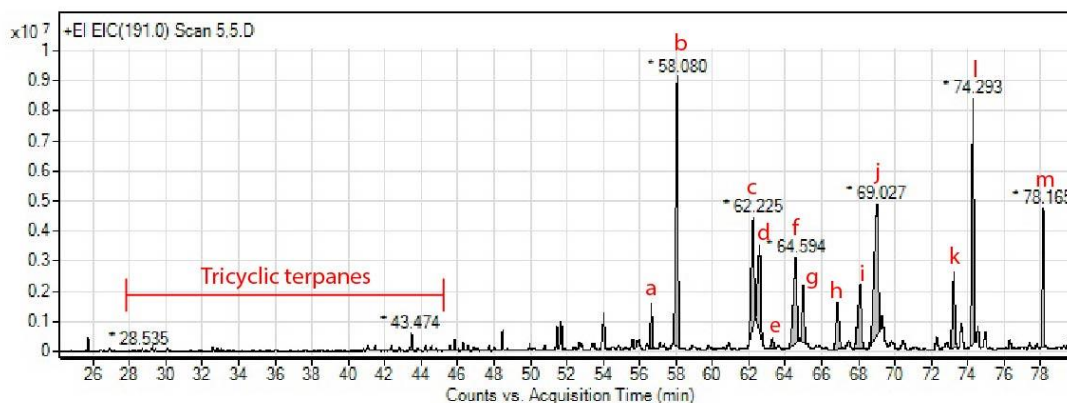


Figure 53 An example of m/z 191 chromatogram showing terpane and triterpane distribution of oil shale from Mae Teep coal mine (sample ID MS5). The peak identification shows on Table 20.

In Mae Teep coal mine, ratios of Ts/(Ts+Tm) trend to be slightly increased with increasing depth from 0.07 to 0.21 (0.12 in average). Moretane/hopane ratios show that coals contain the lowest ratio in the range of 0.10 to 0.24. Shales have higher ratio from 1.30 to 2.55 compared to this ratio of mudstones ranging between 0.22-0.44. In addition, an average C<sub>31</sub> homohopane 22S/(22S+22R) ratio values at 0.39 (0.09-0.75) with the highest ratio of coals in the range of 0.09 to 0.75. Shales and mudstones contain moderate ratio ranging from 0.31 to 0.43 and from 0.25 to 0.35, respectively. In addition, some terpanes provide an indicator of water stratified condition such as gammacerane index that is ratio of gammacerane and hopane. An average of gammacerane index is 1.05 with the highest ratio appears on shales in the range of 1.46-3.20 followed by mudstones ranging from 0.40-2.43. Coals contain the lowest gammacerane index in an average of 1.05 ranging from 0.15 to 0.38 (Table 9).

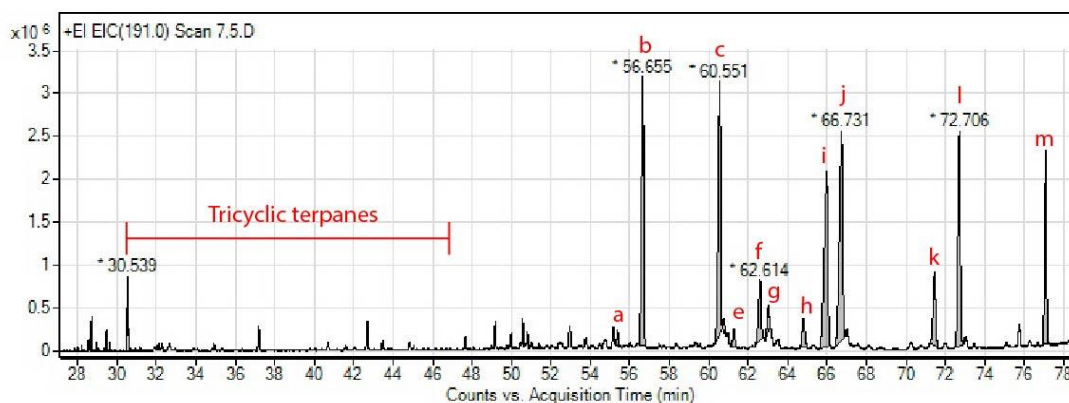


Figure 54 An example of  $m/z$  191 chromatogram showing terpane and triterpane distribution of shale from Mae Than coal mine (sample ID TS5). The peak identification shows on Table 20.

In Mae Than coal mine, the distribution of triterpanes and terpanes is shown in Figure 54. The  $T_s/(T_s+T_m)$  ratio values about 0.11 in average and there is no relationship between  $T_s/(T_s+T_m)$  ratio and depth. The highest  $T_s/(T_s+T_m)$  ratio appears on mudstones in the range of 0.17 to 0.30. Coals and shales are slightly low  $T_s/(T_s+T_m)$  ratios ranging 0.04-0.20 and 0.05-0.08, respectively. An average of moretane/hopane ratio is at 0.54 with the lowest ratio in coals and shales ranging 0.08-0.59 and 0.13-1.10, respectively. The highest moretane/hopane ratio appears on mudstones between 0.11-1.89. In addition to  $C_{31}$  homohopane  $22S/(22S+22R)$ , average ratio is about 0.47 with the highest ratio of coals ranging from 0.31 to 0.85 followed by mudstone in the range of 0.39-0.72. The lowest ratio appears on shales between 0.22 and 0.53. In addition, gammacerane index appears in small amount in an average of 0.57 (0.10-1.77) with mudstones shows the highest value between 0.20 and 1.77. Coals and shales vary in low amounts in the range of 0.15-0.56 and 0.14-0.89, respectively (Table 9). The results of this index contain quite similar value in all samples. There is no difference in value in terms of lithology compared with the gammacerane index results in Mae Teep samples, thus it will be discussed in the discussion chapter.

Table 9 The results of triterpane and terpane distribution.

Sample ID	Mae Teep samples						Mae Than samples					
	Lithology	Ts/(Ts+Tm)	Moretane/hopane	Gamma cerane index	C <sub>31</sub> Homohopane 22S/(22S+22R)	Sample ID	Lithology	Ts/(Ts+Tm)	Moretane/hopane	Gamma cerane index	C <sub>31</sub> Homohopane 22S/(22S+22R)	
MS1	Shale	0.08	1.60	3.20	0.31	TM1	Mudstone	0.29	1.89	1.54	0.40	
MS2	Shale	0.12	0.70	3.14	0.44	TM2	Mudstone	0.30	0.11	0.20	0.72	
MC3	Coal	0.12	0.15	0.23	0.30	TC3	Coal	0.08	0.15	0.15	0.40	
MS4	Oil shale	0.09	1.41	1.46	0.41	TC4	Coal	0.07	0.13	0.16	0.59	
MS5	Oil shale	0.10	2.55	2.22	0.43	TM5	Mudstone	0.17	1.51	1.77	0.39	
MC6	Coal	0.16	0.19	0.36	0.21	TS6	Shale	0.05	1.10	0.85	0.37	
MS7	Oil shale	0.09	1.30	1.76	0.41	TS7	Shale	0.05	0.87	0.89	0.38	
MC8	Coal	0.07	0.11	0.15	0.09	TC8	Coal	0.04	0.55	0.46	0.45	
MC9	Coal	0.12	0.10	0.15	0.58	TC9	Coal	0.04	0.55	0.56	0.85	
MC10	Coal	0.05	0.10	0.17	0.28	TC10	Coal	0.04	0.59	0.47	0.37	
MM11	Mudstone	0.07	0.44	0.40	0.25	TC11	Coal	0.09	0.08	0.10	0.31	
MC12	Coal	0.11	0.15	0.25	0.41	TS12	Shale	0.08	0.13	0.14	0.22	
MC13	Coal	0.10	0.24	0.24	0.29	TC13	Coal	0.09	0.16	0.42	0.63	
MC14	Coal	0.16	0.17	0.38	0.75	TS14	Shale	0.08	0.17	0.33	0.53	
MC15	Coal	0.20	0.10	0.32	0.65	TC15	Coal	0.20	0.16	0.49	0.49	
MM16	Mudstone	0.21	0.22	2.43	0.35							
Average	Average	0.12	0.60	1.05	0.39	Average	Average	0.11	0.54	0.57	0.47	



#### 4.5.4 Steranes

The  $m/z$  217 chromatogram is used to study paleoenvironment and organic matter input. Some biomarkers are generally distributed including  $C_{27}$  regular sterane,  $C_{28}$  regular sterane,  $C_{29}$  regular sterane. In addition,  $C_{29}$  sterane isomerization can be provided as ratios of  $20S/(20S+20R)$  and  $\beta\beta/\beta\beta+\alpha\alpha$  that can be used to imply thermal maturity of petroleum source rocks. These ratios can be calculated from isomerization between biological form (20R) and geological form (20S) which depend on thermal maturity in rocks (Figure 55) (Seifert and Moldowan, 1979; Peters and Moldowan, 1991).

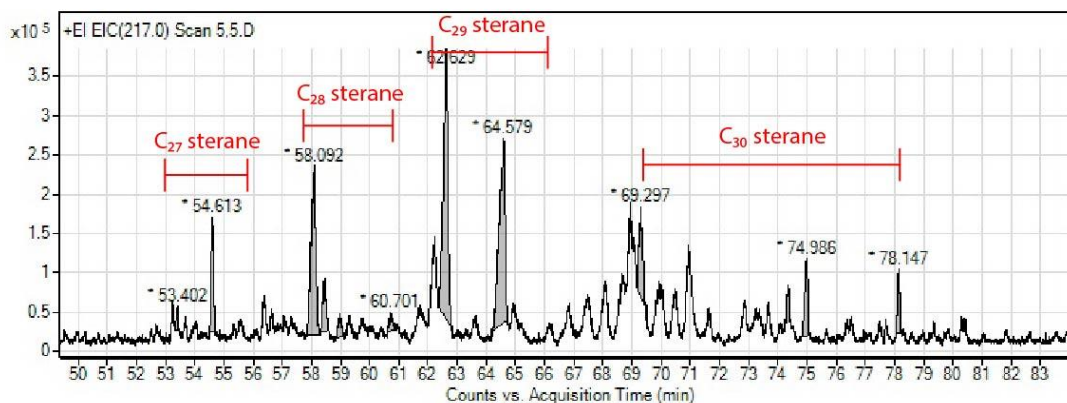


Figure 55 An example of  $m/z$  217 chromatogram showing sterane distribution of oil shale from Mae Teep coal mine (sample ID MS5). The peak identification shows on Table 21.

In Mae Teep coal mine, samples contain the prevalence of  $C_{29}$  regular sterane in an average of 60% (45-74%) followed by  $C_{28}$  regular sterane about 26% in average (12-44%).  $C_{27}$  regular sterane shows the lowest percentage about 14% in average (8-12%). Almost samples have a moderate ratio of  $C_{29}$  sterane  $20S/(20S+20R)$  various from 0.08 to 0.65 (0.41 in average). An average of  $C_{29}$  sterane  $\beta\beta/\beta\beta+\alpha\alpha$  ratio is 0.47 ranging between 0.22 and 0.68 (Table 10).

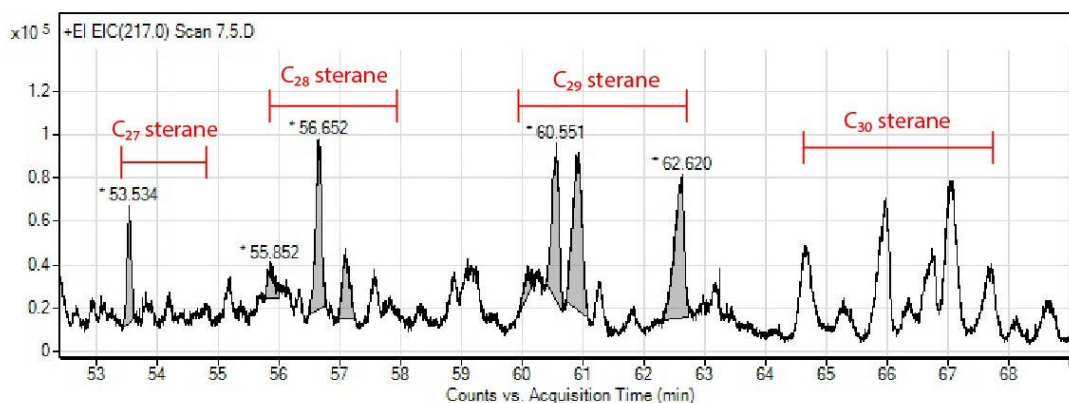


Figure 56 An example of  $m/z$  217 chromatogram showing sterane distribution of shale from Mae Than coal mine (sample ID TS5). The peak identification shows on Table 21.

In Mae Than coal mine, the sterane distribution is shown in Figure 56. C<sub>29</sub> regular sterane shows the prevalent in an average of 61% (48-72%). An average C<sub>28</sub> regular sterane amount is 25% (9-37%) followed by C<sub>27</sub> regular sterane contains the lowest average amount of 14% in the range of 7-31%. In term of C<sub>29</sub> sterane isomerization, 20S/(20S+20R) and  $\beta\beta/(\beta\beta+\alpha\alpha)$  contain moderate values in both ratios about an average of 0.37 (0.27-0.57) and 0.52 (0.28-0.57), respectively (Table 10).

Table 10 The results of sterane distribution.

Sample ID	Mae Teep samples						Mae Than samples						
	Lithology	Regular sterane (%)			C <sub>29</sub> sterane 20S/(20S+20R)	C <sub>29</sub> sterane $\beta\beta/(\beta\beta+\alpha\alpha)$	Sample ID	Lithology	Regular sterane (%)			C <sub>29</sub> sterane 20S/(20S+20R)	C <sub>29</sub> sterane $\beta\beta/(\beta\beta+\alpha\alpha)$
		C <sub>27</sub>	C <sub>28</sub>	C <sub>29</sub>					C <sub>27</sub>	C <sub>28</sub>	C <sub>29</sub>		
MS1	Shale	20	23	57	0.08	0.65	TM1	Mudstone	25	14	61	-	-
MS2	Shale	20	19	61	0.65	0.68	TM2	Mudstone	9	19	72	0.44	0.28
MC3	Coal	8	18	74	0.54	0.31	TC3	Coal	15	37	48	0.31	0.58
MS4	Oil shale	10	25	65	0.47	0.54	TC4	Coal	12	36	51	0.29	0.52
MS5	Oil shale	9	25	66	0.48	0.58	TM5	Mudstone	31	9	61	-	-
MC6	Coal	10	33	57	0.40	0.45	TS6	Shale	8	27	65	0.40	0.63
MS7	Oil shale	21	12	67	0.27	0.23	TS7	Shale	7	21	72	0.37	0.59
MC8	Coal	8	27	65	0.3	0.56	TC8	Coal	10	21	69	0.41	0.47
MC9	Coal	10	32	58	0.32	0.55	TC9	Coal	10	31	59	0.50	0.61
MC10	Coal	14	18	68	0.23	0.56	TC10	Coal	7	21	72	0.32	0.51
MM11	Mudstone	8	35	57	0.51	0.43	TC11	Coal	15	30	55	0.27	0.51
MC12	Coal	15	44	41	0.45	0.43	TS12	Shale	16	26	58	0.19	0.45
MC13	Coal	15	24	61	0.40	0.52	TC13	Coal	9	27	64	0.42	0.57
MC14	Coal	18	37	45	0.48	0.45	TS14	Shale	11	24	65	0.31	0.53
MC15	Coal	17	30	53	0.37	0.43	TC15	Coal	25	27	48	0.57	0.48
MM16	Mudstone	13	18	69	0.53	0.22							
Average	Average	14	26	60	0.41	0.47	Average	Average	14	25	61	0.37	0.52

-: No data

## CHAPTER V

### DISCUSSIONS

#### 5.1 Quantity of organic matter

The TOC and EOM contents provide information of quantity of organic matter in rocks. The studied coals from both basins contains high TOC and EOM contents suggesting high amount of organic matter. The organic richness of Mae Teep shales is lower compared to those of Mae Than shales based on TOC and EOM data. The mudstones are mostly grouped in poor organic richness presented in low TOC and EOM contents. In addition, these contents can be used to evaluate hydrocarbon generation potential for petroleum source rocks. In this study, the Mae Teep samples are mostly suggested as a good to excellent potential for source rocks, except mudstone (sample ID MM16) (Figure 57a) (Tissot and Welte, 1984). On the other hand, the Mae Than samples indicate an excellent potential for petroleum source rocks, except mudstone (sample ID TM1, TM2 and TM3) (Figure 57b) (Jarvie, 1991b; Tissot and Welte, 1984).

Based on this study, the TOC contents coincide with the EOM contents. The samples with high TOC content trend to have high EOM content, while the samples with low TOC content are likely to have low EOM content. In comparison, the EOM contents of coals and shales from Mae Than coal mine are significantly higher than those from Mae Teep coal mine (approximately two times higher). However, mudstones have similar values in both basins (Figure 57). Thus, it can be suggested that Mae Than samples seem to have higher potential for petroleum generation than Mae Teep samples. However, EOM analysis is one of geochemical methods used for evaluation of hydrocarbon potential. It should be supported by other advanced methods.

In terms of EOM fraction, the saturated hydrocarbon compound in this study seems to be relatively low. However, the percentage of saturated hydrocarbon compound extracted from coal samples is usually low and coincides with other reliable works (e.g. Dević and Popović, 2013; Stefanova et al., 1995; Stefanova et al., 1999; Tuo et al., 2003). All samples have similar contents of aromatic hydrocarbon. In addition, NSO-compound hydrocarbon is the highest compound in the EOM

fraction with approximately of more than 50 wt.% from samples of both basins (Figure 57). The high percentage of the NSO-compounds in both basins suggests low maturity stage of the samples (Dević and Popović, 2013).

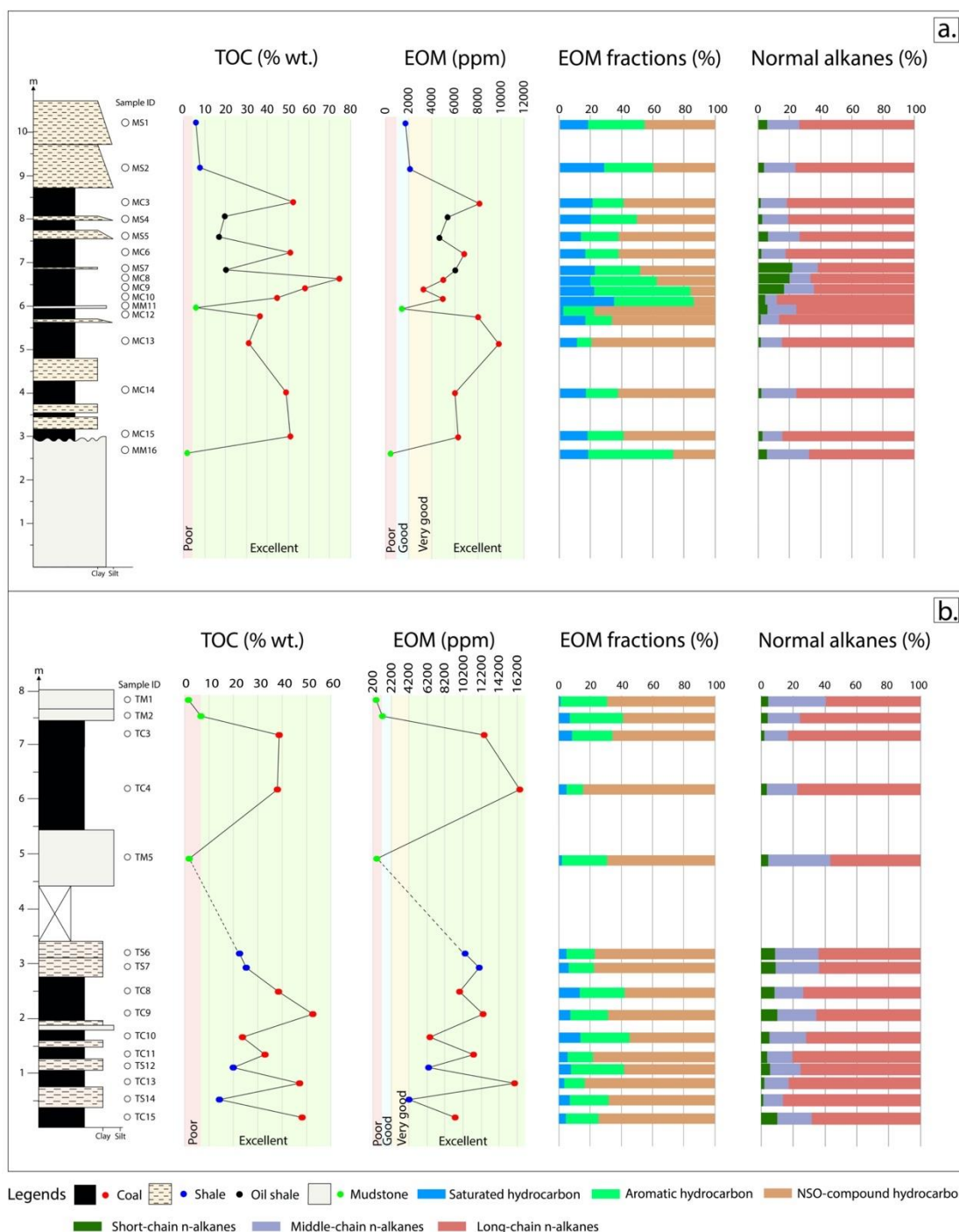


Figure 57 The lithostratigraphy correlated with TOC (% wt.) and EOM (ppm) contents and EOM fractions of (a) Mae Teep coal mine, (b) Mae Than coal mine.

In summary, the geochemical characteristic data such as TOC, EOM and EOM fractions are used to estimate organic richness in rocks. The results of coals, shales and oil shales are compared to the previous studies (Table 11). The compared results seem likely that coals commonly contain high TOC and EOM contents. The NSO compound hydrocarbon is the highest amount in EOM fractions followed by aromatic and saturated hydrocarbons, respectively. These compared results can be interpreted the organic richness and hydrocarbon generation potential in source rocks. Generally, coals exhibit high organic richness and contain excellent potential to be a petroleum source rock (Table 11). In addition to shales and oil shales, the previous works are consistent with this study (Table 12). Shales and oil shales are considered to contain moderate TOC and EOM contents. The EOM fractions exhibit the highest amount in NSO compounds followed by aromatic and saturated hydrocarbons, respectively. The organic richness of these rocks is evaluated as moderate amount of organic matter. Mostly, shales and oil shales are in the range of excellent hydrocarbon generation potential in source rocks (Table 12).

Table 11 The results of TOC, EOM and EOM fractions of coals compared to the previous studies.

Coal	Location	TOC (wt. %)	EOM	EOM fractions	Organic richness	Hydrocarbon potential
This study	Mae Teep basin, Northern Thailand	30.12- 73.71	High	NSO compounds > Aromatic > Saturated hydrocarbo ns	High	Excellent (TOC content > 4 wt. %) <sup>a</sup>
	Mae Than basin, Northern Thailand	23.48- 52.20				
Van Minh Le, 1994	Mae Moh basin, Northern Thailand	6.38- 31.11				
Hasiah and Abolins,	Buru Arang,	49.53- 57.61	-	-		

1998	Malaysia					
Ehinola et al., 2002	Benue Trough, Nigeria	14.80 - 48.40	-	-		
Petersen and Ratanastheinn, 2011	Bang Mark basin, Southern Thailand	36.90-48.85	-	-		
Alias et al., 2012	Sabah, Malaysia	51.20-77.70	Very high	NSO compounds > Aromatic > Saturated hydrocarbons		
Hos-Çebi and Korkmaz, 2013	North Anatolia, Turkey	35.35 - 68.51	High			
Mustapha et al., 2017	Northeast Sabah, Malaysia	55.70 - 62.37	High			
Gogoi et al., 2020	Meghalaya, India	49.81 - 70.12	-	-		

<sup>a</sup>Peters and Cassa, 1994

Table 12 The results of TOC, EOM and EOM fractions of shales and oil shales compared to the previous studies.

Shale and oil shale	Location	TOC (wt. %)	EOM	EOM fractions	Organic richness	Hydrocarbon potential
This study	Mae Teep basin, Northern Thailand	4.82-19.49	High	NSO compounds > Aromatic > Saturated hydrocarbons	Moderate	Excellent (TOC content > 4 wt. %) <sup>a</sup>
	Mae Than basin, Northern Thailand	14.00-24.87				
Van Minh Le, 1994	Mae Moh basin,	17.54-31.11				

	Northern Thailand					
Curiale and Gibling, 1993	Mae Sot basin, Northern Thailand	0.89 - 22.40				
Hasiah and Abolins, 1998	Buru Arang, Malaysia	8.76 - 10.42	-	-		

<sup>a</sup>Peters and Cassa, 1994

## 5.2 Type of organic matter

Based on organic geochemistry, gas chromatograms were obtained by using GC-MS analysis provide total ion current (TIC) in various ion chromatograms depend on mass-to-charge ratio ( $m/z$ ). In terms of  $m/z$  85, n-alkanes and isoprenoids are prevalent in the chromatograms which are useful to imply type of organic matter. Long-chain n-alkanes ( $>nC_{27}$ ) are the main components of plants waxes (Tissot and Welte, 1984) and are considered as biomarkers for higher terrestrial plants. Long-chain n-alkanes are derived from diagenetic transformation of even-numbered carboxylic acids and alcohols presented in leaf and cuticular waxes. In addition, some freshwater algae are also typically found in long-chain n-alkanes (Gülz et al., 1992; Peters et al., 2005; Rieley et al., 1993). Mid-chain n-alkanes ( $C_{21-26}$ ) are biological precursors of vascular plants, microalgae and cyanobacteria (Matsumoto et al., 1990). Aquatic macrophytes contain  $C_{23}$  and  $C_{25}$  n-alkanes (Ficken et al., 2000). Some fossil conifer species' cones and shoots including *Taxodium balticum*, *Arthrotaxis couttsiae* and *Pinus paleostrobus* contain high amounts of mid-chain n-alkanes (Otto and Simoneit, 2001). Short-chain n-alkanes are mainly present in algae and microorganism (Cranwell, 1977). In this study, the studied samples from both basins show the distribution of n-alkanes in unimodal pattern ranging from  $nC_{12}$  to  $nC_{35}$ . The high amount of long-chain n-alkanes in all samples indicates terrestrial higher plants are the main source of n-alkanes (Figure 58).



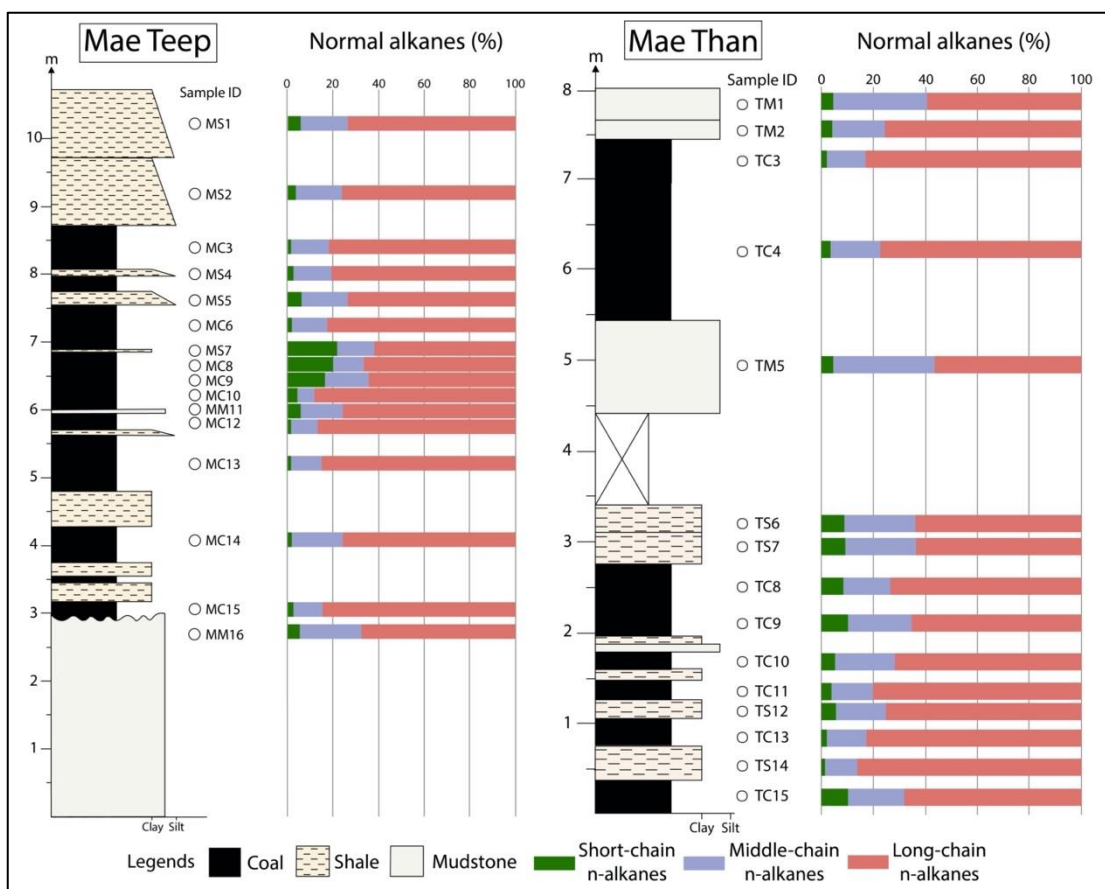


Figure 58 The lithology correlates with the percentage of n-alkanes from (a) Mae Teep samples (b) Mae Than samples.

The CPI values are higher or lower than 1.0 indicates immature stage while CPI closes to 1.0 point to a mature stage (Peter and Moldowan, 1993). In the reducing environment, dominant n-fatty acids, alcohols and phytol over decarboxylation causing the predominance of even-numbered n-alkanes over odd-numbered n-alkanes (CPI<1.0) (Tissot and Welte, 1984). In contrast to oxidizing environment, more decarboxylation dominants over n-fatty acids, alcohol and phytol showing the result of the predominance of odd-numbered n-alkanes over even-numbered n-alkanes (CPI>1.0) (Tissot and Welte, 1984). In addition, land plant associated material showed the predominance of odd-numbered n-alkanes with CPI ~ 5-10 (Commendatore et al., 2012; Kanzari et al., 2014). Marine microorganisms contain CPI values closed to 1.0 (Kennicutt II et al., 1987). In this study, CPI values are in the C<sub>25</sub>-C<sub>35</sub> range containing high index (more than 3.0) with the predominance of odd-carbon numbered n-alkanes (Figure 59). The results of CPI in all samples have

suggested that odd over even n-alkanes provides a high contribution of land plants to precursor of organic matter which is deposited under oxidizing environment (Tissot and Welte, 1984). Also, the studied samples are evaluated as an immature stage (Peter and Moldowan, 1993).

For ACL data, the length of n-alkane chain is indicative of vegetation type that are mainly derived from terrigenous leaf lipids. The lipids in leaf from forest plants generally contain shorter chain-length than those of leaf from grasslands (Cranwell, 1973). The value of ACL from plant leaf waxes is dependent on some factors including aridity, temperature, rainfall and vegetation changes. Herbaceous types are mainly contributed with C<sub>31</sub> or C<sub>33</sub> n-alkanes, resulting in higher value of ACL compared to those of woody plants (Rommerskirchen et al., 2006). In addition, the change of vegetation types controls the ACL value. The chain-length of terrestrial higher plants is longer than aquatic macrophytes (Ficken et al., 2000). As the ACL results of this study, the depositional environment may combine of terrestrial and aquatic settings due to the presence of relative odd-numbered n-alkanes between C<sub>25</sub>-C<sub>33</sub> n-alkanes. Also, there is little difference in the depositional environment in both basins based on the constant ACL values from samples (Figure 59) (Sakari et al., 2008).

For the proxy ratio ( $P_{aq}$ ), this index is an indicator of organic matter source input by using the relative amounts of odd-numbered between C<sub>23</sub>-C<sub>31</sub> n-alkanes. Submerged and/or floating macrophytes compose abundances of mid-chain length, C<sub>23</sub> and C<sub>25</sub> n-alkanes, showing high  $P_{aq}$  value (more than 0.4). While, emerged macrophytes are typically dominated by the long-chain length homologues (>C<sub>29</sub>) which contain low  $P_{aq}$  value, ranging from 0.1 to 0.4 (Ficken et al., 2000). As the results, the  $P_{aq}$  ratios of studied samples from both coal mines contain lower than 0.4 except mudstones (Sample ID TM1 and TM5). Thus, emerged macrophytes (terrestrial higher plants) are mainly dominant for organic matter input (Figure 59).

In addition, the TAR is a ratio of the relative variation of terrestrial and aquatic sources of n-alkanes based on the abundance of long-chain and short-chain n-alkanes. The predominance of odd-numbered long-chain n-alkanes (C<sub>27</sub>, C<sub>28</sub> and C<sub>31</sub>) is an indicator of the debris of terrestrial higher plants (Rieley et al., 1991). In contrast, odd-numbered short-chain n-alkanes (C<sub>15</sub>, C<sub>17</sub> and C<sub>19</sub>) is prevalent to

aquatic organic matter source (Jaffé et al., 2001). The low TAR ratio is generally present in the contribution of marine source input. In this study, the TAR ratio of all samples is higher than two, indicating organic matter derived from the terrigenous source (Figure 59) (Silva et al., 2008).

Natural n-alkanes ratio (NAR) contributes the relative amounts between natural and petroleum n-alkanes (Mille et al., 2007). NAR is a ratio that indicates by using n-alkanes related to even-numbered n-alkanes in order to differentiate petroleum hydrocarbons and crude oils from natural n-alkanes. The value of NAR is close to zero represents organic matter source derived from petroleum or crude oils, while NAR value closes to 1 indicating nature organic matter occurrence. In this study, the NAR results of all samples exhibit as a natural organic matter from terrestrial higher plants (Figure 59).

In summary, the main contribution is an emerged material including detrital of higher plants from land nearby basin associated with minor submerged aquatic algae in the basin based on CPI, ACL,  $P_{aq}$  and TAR (Figure 59). In addition, Mae Teep samples can be divided into 4 units. Unit A is mudstone showing low CPI and ACL values, and high  $P_{aq}$  and TAR values. Unit B comprises shale formation interbedded with coal seams with high CPI,  $P_{aq}$  and TAR values. Unit C is thick coal seams interbedded with thin shale and oil shale showing fluctuation values of CPI, ACL,  $P_{aq}$  and TAR. Unit D consists of thick shale with moderate CPI, ACL and  $P_{aq}$  values (Figure 59a). In other hand, Mae Than samples are classified 5 units based on CPI, ACL,  $P_{aq}$  and TAR values including unit A coal seams interbedded with shale, unit B thick shale, unit C and unit E thick mudstone and unit D thick coal seam (Figure 59b).

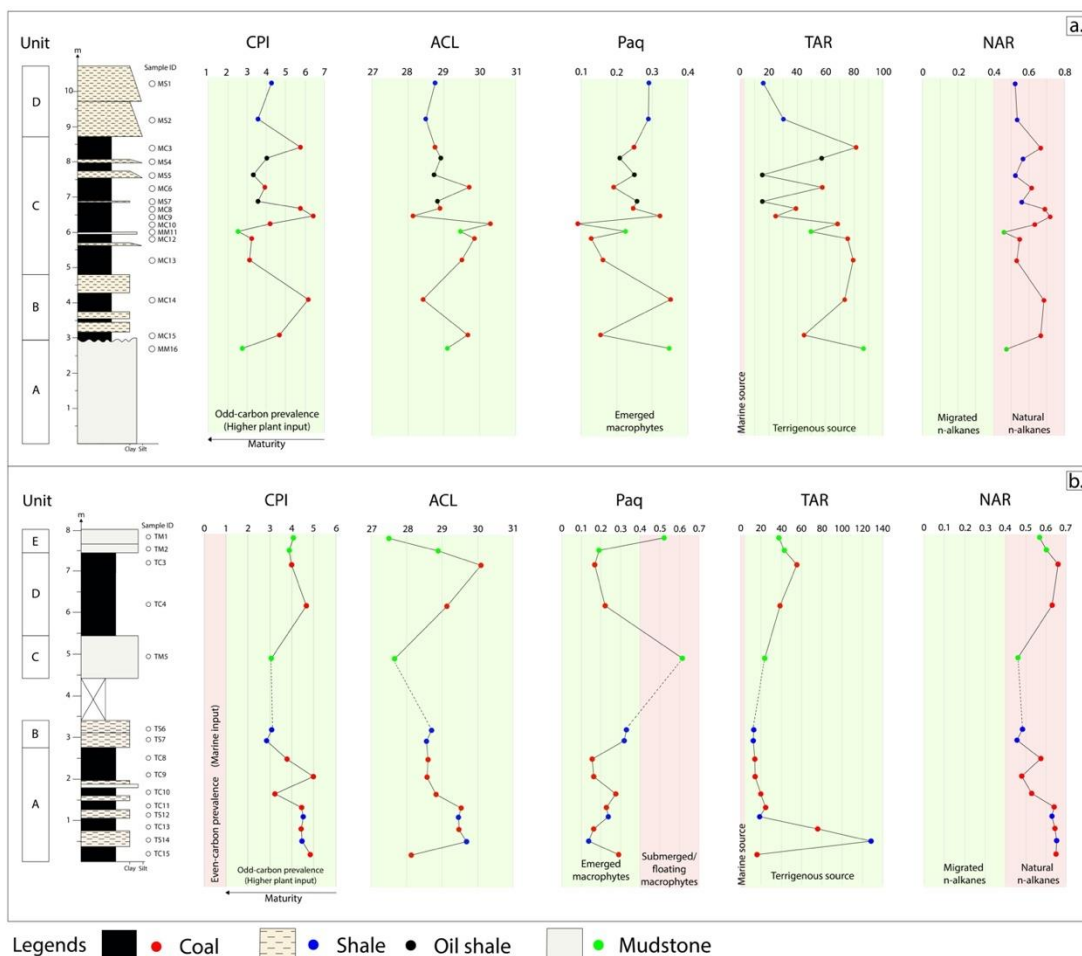


Figure 59 The lithology correlates with CPI, ACL,  $P_{aq}$ , TAR and NAR of (a) Mae Teep coal mine (b) Mae Than coal mine.

The n-alkane distributions and related parameters of this study are compared with the previous works in order to estimate organic matter inputs. It seems likely that the studied coals are coincided with other coal studies that the main contribution is higher plants due to the presence of long-chain n-alkanes and high CPI. Some studies use the different methods such as the maceral composition to imply organic matter inputs. The association of algae material reveals in some coal studies (Table 13). Also, the shales and oil shales are investigated and compared with other works. The studied shales are also mainly typical of higher plants with minor algae based on n-alkane distribution and CPI. Some works purposed that algae and planktonic materials are the main contribution of shales and oil shales.

Table 13 The results of n-alkane distribution, CPI and type of organic matter of coals compared to the previous studies.

Coal	Location	n-alkane distribution	CPI	Type of organic matter
This study	Mae Teep basin, Northern Thailand	Long chain > mid-chain > short-chain n-alkanes	3.60-7.04	Higher plants
	Mae Than basin, Northern Thailand		3.44-6.20	
Van Minh Le, 1994	Mae Moh basin, Northern Thailand		0.90-3.00	
Hasiah and Abolins, 1998	Buru Arang, Malaysia		1.10-1.44	
Ehinola et al., 2002	Benue Trough, Nigeria		1.00-1.07	Higher plants and algae
Petersen and Ratanasthein, 2011	Bang Mark basin, Southern Thailand	Maceral composition study	-	Higher plants
Alias et al., 2012	Sabah, Malaysia	Long chain > mid-chain > short-chain n-alkanes	1.19-1.41	
Hos-Çebi and Korkmaz, 2013	North Anatolia, Turkey		-	
Mustapha et al., 2017	Northeast Sabah, Malaysia		1.30-3.97	
Gogoi et al., 2020	Meghalaya, India	Maceral composition study	-	

Table 14 The results of n-alkane distribution, CPI and type of organic matter of shales and oil shales compared to the previous studies.

Shale and oil shale	Location	n-alkane distribution	CPI	Type of organic matter
This study	Mae Teep basin, Northern Thailand	Long chain > mid-chain >	3.52-4.10	Higher plants

	Mae Than basin, Northern Thailand	short-chain n- alkanes	3.30-5.67	
Van Minh Le, 1994	Mae Moh basin, Northern Thailand	<sup>13</sup> C isotope study		Algae
Curiale and Gibling, 1993	Mae Sot basin, Northern Thailand	Long chain > mid-chain > short-chain n- alkanes	Higher than 1	Higher plants and algae
Hasiah and Abolins, 1998	Buru Arang, Malaysia		1.13-1.25	Planktonic and higher plants

### 5.3 Maturity of organic matter related to coal rank

In this study, biomarkers and non-biomarkers are alternatively used to evaluate organic matter maturity in the samples during lithification or diagenetic process. Biomarker maturity parameters can be evaluated using terpane and sterane distributions obtained from m/z 191 and m/z 217, respectively (El Diasty et al., 2016; El Nady, 2008). The maturity results from both study areas are used to correlate the coal rank of the samples. The biomarker parameters include Ts/(Ts+Tm), moretane/hopane, C<sub>31</sub> homohopane isomerization and C<sub>29</sub> steranes isomerization.

Ts (C<sub>27</sub> 18 $\alpha$ (H)-22, 29, 30-trisnorneohopane) and Tm (C<sub>27</sub> 17 $\alpha$ (H)-22, 29, 30-trisnorneohopane) are used for thermal maturity assessment by the ratio of Ts/(Ts+Tm) relatively controlled to some extent by lithology oxicity of the depositional environment (Seifert and Moldowan, 1979). Ts is more stable to thermal maturity than Tm (Hunt, 1991). The Ts/(Ts+Tm) ratio increases with increasing maturity. The values of Ts/(Ts+Tm) ratio range between 0.35 and 0.95, reflecting mature organic matter (Peters et al., 2005). The lithology variation may influence the value of this ratio, in which clay-rich siliciclastic source rocks are generally higher value than carbonate rocks (Peter and Moldowan, 1993; Waples and Machiharia, 1991). According to the study area, all samples are siliciclastic rocks mainly derived from terrestrial higher plants, thus the value of ratio tends to be more directly controlled by thermal maturity compared to lithology. The samples in this study are divided into three types based on lithology: coal, shale and mudstone. As the result, all samples from both basins represent that organic matter is immature to early mature stage at the present day (Figure 60) (Peters et al., 2005).

The  $17\beta$ ,  $21\alpha(\text{H})$ -moretane is thermally less stable than  $17\alpha(\text{H})$ ,  $21\beta(\text{H})$ -hopane. Moretane can convert to hopane with increasing maturity (Hunt, 1991). Thus, the ratio decreases with higher maturation which can be applicable to the immature-early mature range (Kvenvolden and Simoneit, 1990; Peters et al., 2005) and moretane/hopane ratio less than 0.15 indicates mature stage in organic matter (Waples and Machiharia, 1991). This ratio values about 0.8 in immature stage and around 0.15-0.05 in mature stage. As the results, coals from both basins are in mature stage at the present day (Figure 60).

In addition, homohopane isomerization ratio is one of biomarker maturity indicators obtained by ratio of the configuration of homohopane isomers between biological form (22R) and geological form (22S). As maturity increases, the 22R homohopane convert to the 22S isomer. The  $22\text{S}/(22\text{S}+22\text{R})$  homohopane ratio ranging from 0 to 0.6 indicates an increase in maturity. Ratio ranges between 0.50 and 0.54 suggesting the early oil-generation stage and can be reached from 0.57 to 0.67 for oil window maturity (Seifert and Moldowan, 1979). The homohopane isomerization can be calculated from any or all of  $\text{C}_{31}$ - $\text{C}_{35}$  homohopane. In this study,  $\text{C}_{31}$  homohopane is only present in all samples based on triterpene and terpane distribution obtained by  $m/z$  191 ion chromatogram. Therefore,  $\text{C}_{31}$  homohopane is used to assess organic matter maturity and the results show that coals from both basins are in immature to early mature stage at the present day (Figure 61) (Peters and Moldowan, 1991).

Moreover, biomarker ratios such as  $20\text{S}/(20\text{S}+20\text{R})$  and  $(\beta\beta/\beta\beta+\alpha\alpha)$  for  $\text{C}_{29}$  steranes are also used to evaluate the level of maturity in organic matter. In the  $\alpha\alpha$   $\text{C}_{29}$  steranes, the proportion of two epimers between biological form (22R) and geological form (22S) change depend on the degree of maturity. The 20S form is greater stable relative to the 20R form during maturation (Dahl et al., 1993). The 20S increases as the result of 20R change configuration into 20S when increasing maturity (Hunt, 1991). The  $\text{C}_{29}$   $20\text{S}/(20\text{S}+20\text{R})$  ratio increases with increasing maturity ranging from 0 to 0.5 and values between 0.52 and 0.55 at equilibrium (Hunt, 1991). This equilibrium ratio is related to be at or before the peak of oil-generative window, while the  $\text{T}_s/(\text{T}_s+\text{T}_m)$  ratio can reach the endpoint value in which beyond the peak of oil-generative window (Peters and Moldowan, 1991). Thus, the ratio of  $\text{C}_{29}$

$20S/(20S+20R)$  remains constant at equilibrium value after reaching the peak of oil window, whereas  $Ts/(Ts+Tm)$  ratio increases with increasing thermal maturity. Another maturity parameter is the ratio of  $\beta\beta/\beta\beta+\alpha\alpha$  derived from  $\beta\beta$  and  $\alpha\alpha$  of  $C_{29}$  steranes due to the isomerization at C-14 and C-17 in both 20S and 20R. As maturity increases, the  $\alpha\alpha$   $C_{29}$  sterane is biological produce converted gradually into the mixture of  $\alpha\alpha$  and  $\beta\beta$ . The ratios increase from 0 to 0.7 with increasing thermal maturity and reach around 0.67-0.71 at equilibrium (Hunt, 1991; Seifert and Moldowan, 1986; Waples and Machiharia, 1991). The low amounts of  $\beta\beta/\beta\beta+\alpha\alpha$  show a low level of organic matter maturity that confirmed other biomarkers maturity indicators (Figure 62).

Biomarker maturity ratios are coincided to EOM/TOC ratio that increases when increasing maturity (Tissot and Welte, 1984). In addition, the presence of low percentage of saturated hydrocarbon as well as high amounts of NSO-compounds in EOM content (Figure 57) (Dević and Popović, 2013). The CPI values also represent low maturity containing high CPI values (more than 3.0) in all samples (Figure 59) (Peter and Moldowan, 1993). In the log plot diagrams, low maturity is confirmed as high isoprenoid/n-alkane ratios (Figure 62) (Shanmugam, 1985; Waples, 1985). Based on m/z 191 chromatograms on all samples, hopane, one of pentacyclic is relatively higher than  $C_{19}$  tricyclic terpane in concentration, thus this ratio confirms immaturity of organic matter (Figure 53 and 55).

Based on biomarker maturity ratios mentioned above, these are coincided to the previous works. According to Fabiańska and Kurkiewicz (2013), lignite coals from Poland are higher amount of  $C_{31}$  homohopane 22R than  $C_{31}$  homohopane 22S, reflecting very low values of  $C_{31}$   $22S/(22S+22R)$  ratio. This ratio indicates that lignite coals from Poland are in immature stage. In addition to Alias et al. (2012), coals from Sabah, Malaysia show the  $Tm$  ( $C_{27}17\alpha(H)-22,29,30$ -trisnorhopane) predominates over  $Ts$  ( $C_{27}18\alpha(H)-22,29,30$ -trisnorhopane) with high  $Tm/Ts$  ratios. Moretane/hopane ratios are present in low values, indicating coals are at early stage of oil maturity window (Table 15).



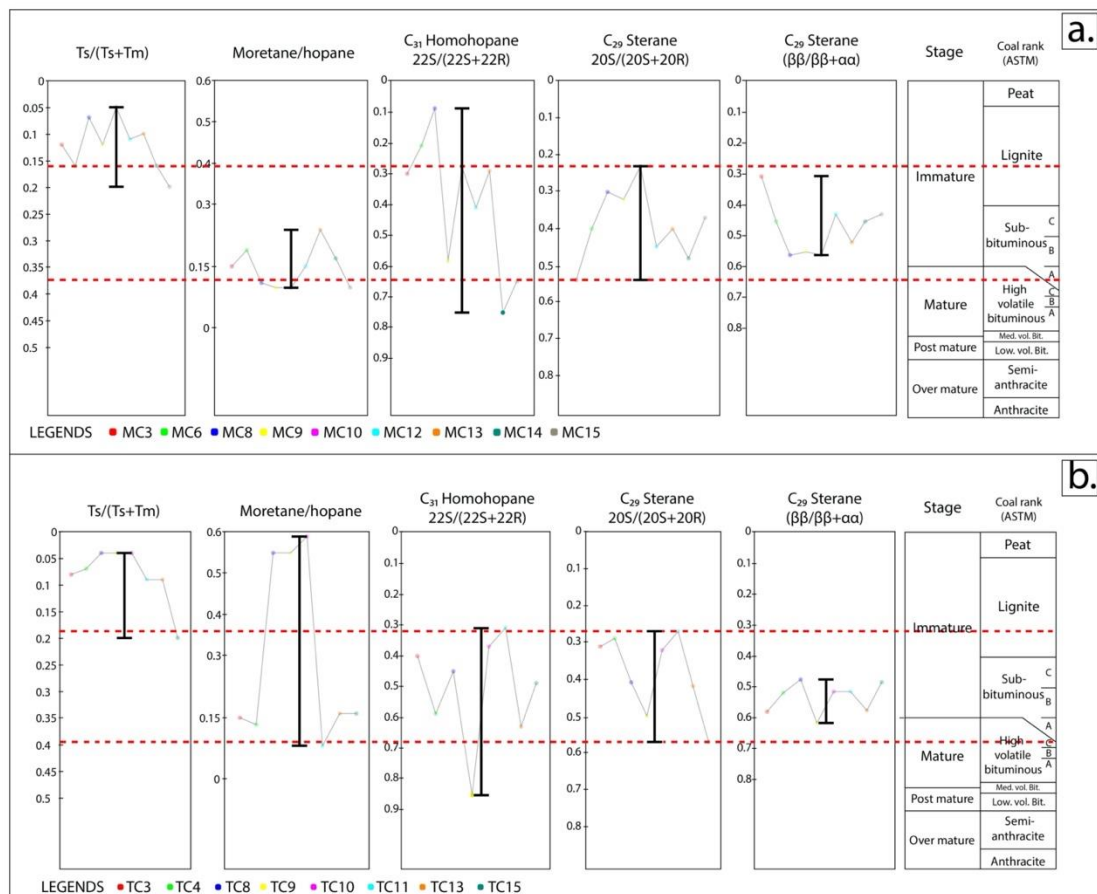


Figure 60 The intersection of maturity biomarker parameters indicates immature to early mature stage at the present day.

In summary, these biomarker maturity parameters are plotted and overlapped to evaluate maturity, showing in the range of immature to early mature in the present day (Figure 60). Also, these ratios can be related to coal rank in comparison of American Society for Testing and Materials (ASTM). In this study, coals from both basins are related to lignite to sub-bituminous A coal which is consistent to coal rank from the previous studies (Ducrocq et al., 1995; Muenlek, 1992b; Ratanasthien, 1984). In addition, the study of thermal maturity is compared to the related coal studies (Table 15). The coal rank studies use several different maturity indicators such as biomarkers, spores and pollen, vitrinite reflectance and pyrolysis to assess the thermal maturity of coals. The maturity can be equivalent to coal rank based on ASTM. The coals from various works exhibit that the higher coal rank depends on the higher thermal maturity (Table 15).

Table 15 The maturity indicator and thermal maturity related to coal rank compared to the previous studies.

<b>Coal</b>	<b>Location</b>	<b>Maturity indicator</b>	<b>Thermal maturity</b>	<b>Coal rank</b>
This study	Mae Teep basin, Northern Thailand	Biomarkers	Immature-early mature	Lignite - subbituminous A
	Mae Than basin, Northern Thailand			
Van Minh Le, 1994	Mae Moh basin, Northern Thailand	Spores and pollen and vitrinite reflectance	Immature	Lignite
Hasiah and Abolins, 1998	Buru Arang, Malaysia	Biomarkers and vitrinite reflectance		
Ehinola et al., 2002	Benue Trough, Nigeria	Biomarkers, vitrinite reflectance and pyrolysis	Mature - overmature	Bituminous
Petersen and Ratanasthein, 2011	Bang Mark basin, Southern Thailand	Vitrinite reflectance and pyrolysis	Immature	Lignite
Alias et al., 2012	Sabah, Malaysia	Biomarkers, vitrinite reflectance and pyrolysis	Immature - early mature	Subbituminous B - high volatile bituminous C
Hos-Çebi and Korkmaz, 2013	North Anatolia, Turkey	Biomarkers and pyrolysis		Subbituminous A - high volatile bituminous C
Mustapha et al., 2017	Northeast Sabah, Malaysia	Biomarkers, spores and pollen, vitrinite reflectance and pyrolysis		Lignite
Gogoi et al., 2020	Meghalaya, India	Vitrinite reflectance and pyrolysis	Immature	Lignite - subbituminous

#### 5.4 Depositional environment

The sterane distribution obtained by using  $m/z$  217 ion chromatograms is used to indicate organic matter inputs. The steranes are derived from sterols that originate from higher plants and algae (Waples and Machihara, 1991) but they are rare in prokaryotic organisms (Huang and Meinschein, 1979; Seifert and Moldowan, 1979; Volkman, 1986). Generally, steranes are used to study photosynthetic biota with regular steranes as an indicator of organic matter sources and depositional environments. The  $C_{27}$  steranes prevalent related to marine phytoplankton influence, while  $C_{28}$  steranes indicate lacustrine environment associated with algae, yeast, fungi and plankton (Waples and Machihara, 1991). A predominance of  $C_{29}$  steranes is associated with terrestrial higher plants contribution as well as brown and green algae (Volkman, 1986). However, microalgae or cyanobacteria are presented in high amount of  $C_{29}$  steranes (Volkman and Maxwell, 1986). The relative amounts of  $C_{27}$ ,  $C_{28}$  and  $C_{29}$  regular steranes are converted into relative percentages and plotted in a ternary diagram (Figure 61). Accumulation and preservation of organic matter occurs overwhelmingly in aquatic environments, both terrestrial (often lacustrine) and marine settings. In fact, terrestrial biomarkers are considered to be preserved preferentially in marine sediments compared to marine lipids (Damsté et al., 2002; Prah et al., 2003). Thus, terrestrial source can combine with aquatic source (i.e. lacustrine and marine). In this study, all samples from both basins show the highest proportion of  $C_{29}$  regular sterane more than 60 % compared with  $C_{28}$  and  $C_{27}$  regular steranes, respectively ( $C_{29} > C_{28} > C_{27}$ ). Thus, both basins have similar depositional setting as terrestrial environment.

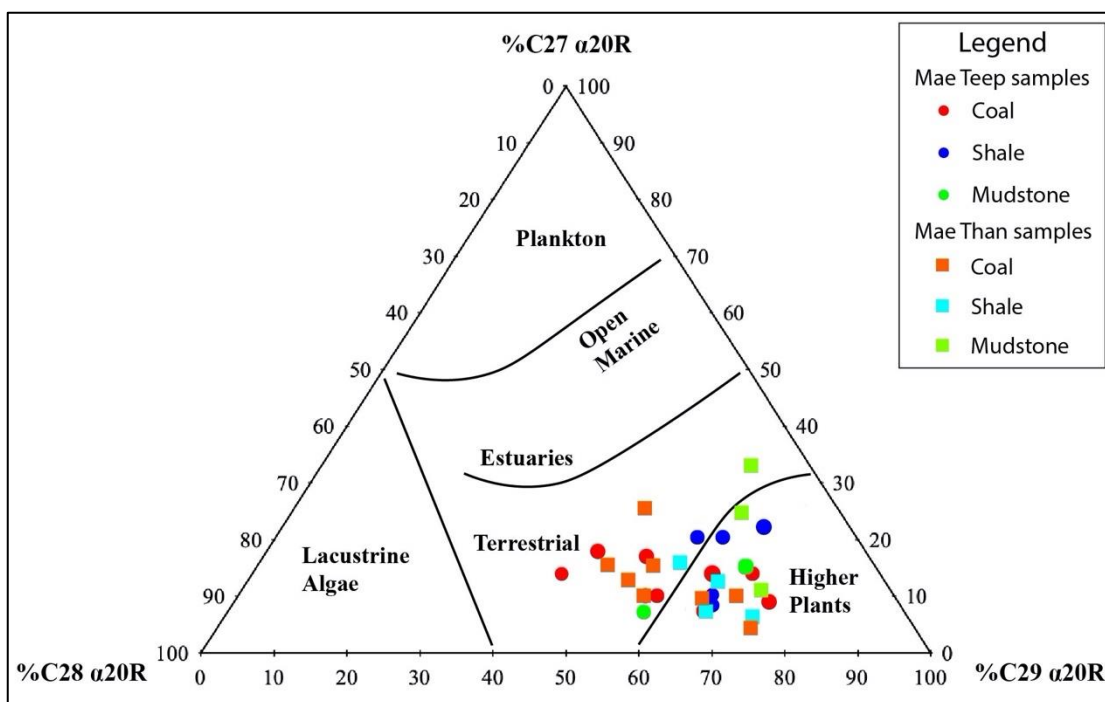


Figure 61 The ternary diagram showing the relative of C<sub>27</sub>, C<sub>28</sub> and C<sub>29</sub> regular steranes. The red, blue and green circle dots represent coal, shale and mudstone from Mae Teep coal mine. The orange, light blue and light green square dots represent coal, shale and mudstone from Mae Than coal mine (Huang and Meinschein, 1979).

Isoprenoids such as pristane (Pr) and phytane (Ph) against n-alkanes can be generally used as ratios of  $pr/nC_{17}$  and  $ph/C_{18}$  with the log plot of  $pr/nC_{17}$  versus  $ph/C_{18}$  proposed by Shanmugam (1985). The log plot provides types of organic matter, paleoenvironmental conditions, maturity level and biodegradation degree as shown in Figure 62. Isoprenoids are generally more resistant to biodegradation than n-alkanes (Waples, 1985). Pr and Ph may be high amount as the result of alteration from n-alkanes via microbial activity or high biodegradation (Peters and Moldowan, 1993). In contrast, n-alkanes can be found in high amount when increasing maturity (Waples, 1985). As the Mae Teep coal mine results, the depositional conditions can be separated based on lithology. Coals and mudstones are mainly present in oxidizing terrestrial environment, while shales are indicative of reducing algal aquatic environment. In contrast to Mae Than samples, there are various conditions in all lithology. Coals are in the range of suboxic terrestrial and algal aquatic mixed environment, whereas shales slightly fall in more reducing algal aquatic environment.

Mudstones are present in oxidizing terrestrial environment. In addition, coal formation is compared between Mae Teep and Mae Than basins based on the isoprenoid/n-alkane plot. Mae Teep coals are likely to have higher oxidizing condition than Mae Than coals (Figure 62).

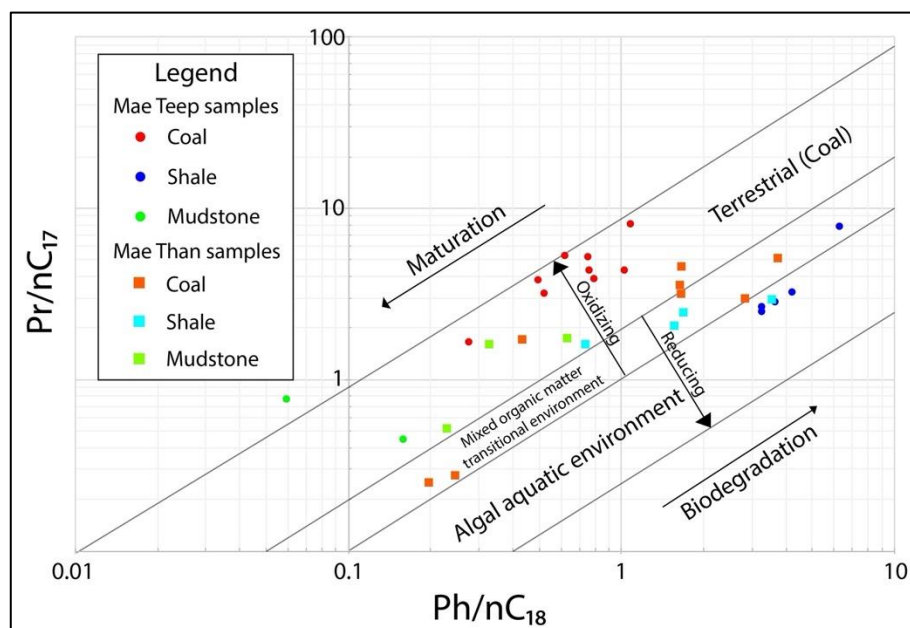


Figure 62 The log plot of  $Ph/nC_{18}$  versus  $Pr/nC_{17}$  of both Mae Teep and Mae Than samples (Shanmugam, 1985). The circle and square points denote Mae Teep and Mae Than samples, respectively.

In terms of paleoenvironmental conditions, pristane ( $C_{19}H_{40}$ ) and phytane ( $C_{20}H_{42}$ ) are regular isoprenoids provided by m/z 85 chromatogram. These isoprenoids are derived from the phytol side chain of chlorophyll molecule (Miles, 1989). The phytol can be transformed into pristane in oxidizing condition and/or into phytane in reducing condition of depositional environment. The pristane/phytane ratio ( $Pr/Ph$ ) is used to suggest paleoenvironmental conditions of the source rocks and organic matter source (Chandra et al., 1994; Large and Gize, 1996; Powell, 1988) and are considered as potential indicators of the redox conditions during sedimentation and diagenesis (Didyk et al., 1978). According to (Didyk et al., 1978), the  $Pr/Ph$  ratio values lower than 1.0 represented the anoxic condition associated with hypersaline or carbonate environment (Peter and Moldowan, 1993), while oxic condition values more than 3.0 including prevalence of terrigenous input (Peters et al., 2005). In

addition, intermediate or suboxic condition ranges from 1.0 to 3.0 (Waseda and Nishita, 1998). As the Mae Teep samples, there are difference in the conditions of depositional environment which can be separated based on lithology. Coals, shales and mudstones relatively indicate oxic, anoxic and suboxic conditions, respectively (Figure 63a). However, Mae Than samples show various conditions in all lithology. The studied samples are mostly common in suboxic and anoxic conditions, except coal (sample ID TC15) (Figure 63b). Wood fragment can be preserved in shale under anoxic condition during the deposition (Figure 51).

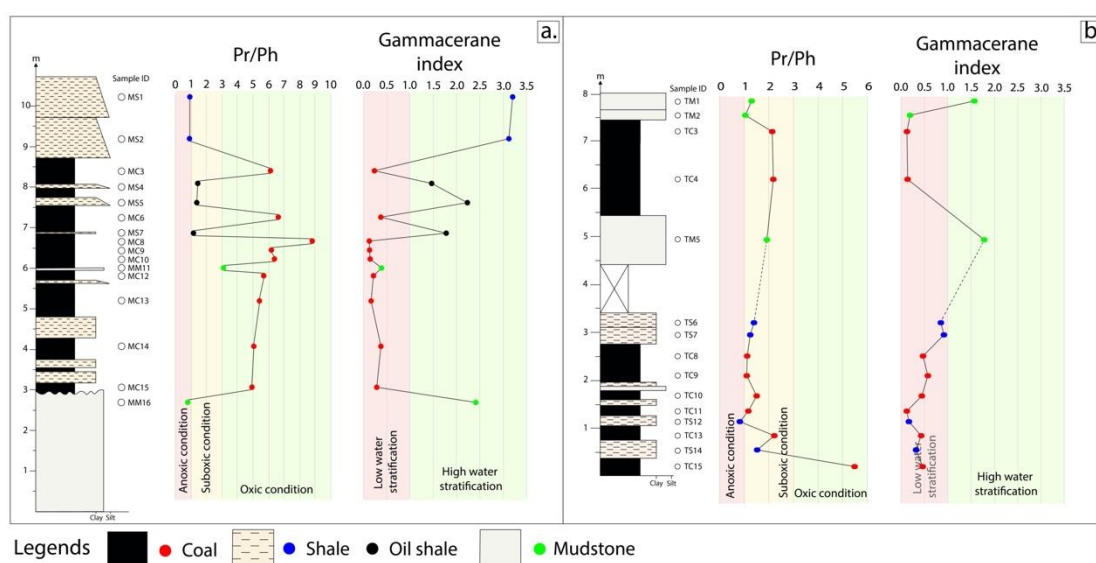


Figure 63 The lithostratigraphy correlates with pr/ph ratio and gammacerane index of (a) Mae Teep coal mine, (b) Mae Than coal mine.

Furthermore, gammacerane is a major biomarker for interpretation of lacustrine and marine types in sediments. Also, it can be used to evaluate as an indicator of salinity of water column and a marker for photic zone under anoxic condition during deposition (Sinninghe Damste et al., 1995). Gammacerane is generally derived from tetrahymanol in bacterivorous ciliates living at the boundary between high salinity water lower layer and less salinity water upper layer (Brassell et al., 1983). The gammacerane index can be calculated by gammacerane/17 $\alpha$ (H)-hopane ratio. The high ratio value reflecting a highly saline depositional environment associated with evaporitic carbonate deposition and low terrigenous input (Peters and Moldowan, 1991). Gammacerane is also typical of hypersaline in marine and non-marine depositional environments (Moldowan et al., 1985). However, the relatively

high amount of gammacerane can be found in freshwater lacustrine sediments (Sinninghe Damsté et al., 1995). Thus, gammacerane index is indicative of water-column stratification. As the Mae Teep results, gammacerane index can be separated based on lithology. Coals, shales and mudstones relatively indicate low, high and moderate water stratifications, respectively (Figure 63a). In contrast to Mae Than results, all samples mostly fall in low stratification, except mudstones (sample ID TM1 and TM5) (Figure 63b).

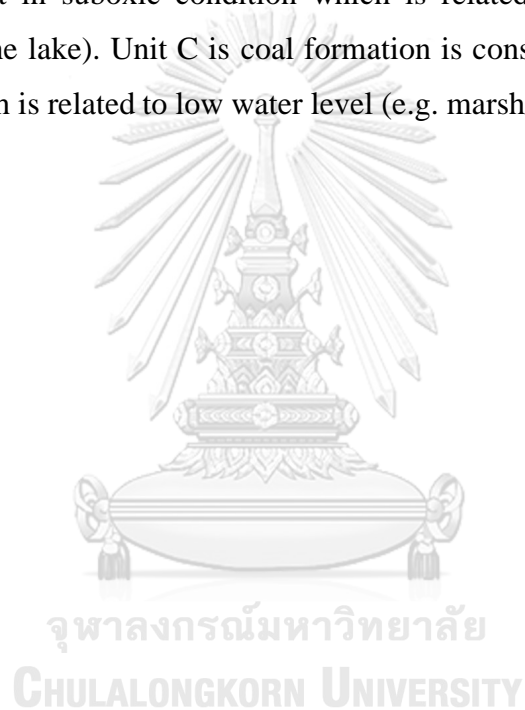
In summary, gammacerane index is plotted and compared to Pr/Ph ratio in order to indicate the relationship between lithology and water level during the deposition (Hunt, 1991; Peter and Moldowan, 1993; Waples and Machihara, 1991). There are similar trends of gammacerane index and Pr/Ph ratio from both basins. The greater pr/ph ratio in samples show the lower gammacerane index suggesting oxygen level related to the water stratification in the basin (Figure 63). The coal formation is contributed to require more oxygen level in shallow water in the basin. While, the shale formation is typical of low amount of oxygen level in bottom of the basin. In addition, the high gammacerane index in Mae Teep shales is regarded as an indicator of highly reducing and hypersaline conditions in stratified water column (Moldowan et al., 1985) and/or different stratified lacustrine setting (Sinninghe Damsté et al., 1995). Thus, the two main water layers control the coexistence of coal and shale formation including high-oxygen water layer and oxygen deficient layer (Figure 65).

### **5.5 Comparison between Mae Teep and Mae Than basins**

In this study, Mae Teep and Mae Than basins are interpreted that coal formation requires high level of oxygen content, probably related to suboxic to oxic condition of depositional environment (Figure 64). The difference in coal formation in these two basins is the different redox condition in the individual basins. Local water level within basins may be controlled the organic matter inputs and coal formation. In addition, the basin geometry can be one of the main factors to control local water level within the basins. Generally, shales samples in this study are interpreted to be deposited under anoxic condition in high water level. Consequently, this condition provides algal materials originated from bloom of planktonic algae settling to the bottom of the basin where is little to no oxygen content. In addition, the

formation of oil shale can be found in Mae Teep basin which can lead to the fact that aquatic algae are a major source for oil generation (Li et al., 2016; Tissot and Welte, 1984). Mudstones contain low amount of organic matter based on low TOC and EOM contents. The formation is deposited mostly in suboxic condition during the low productivity.

The schematic models proposed in this study can be grouped into three lithology. Unit A is shale and oil shale formation deposited in anoxic condition which is related to high water level (deep part of the lake). Unit B is mudstone formation is commonly present in suboxic condition which is related to moderate water level (shallow part of the lake). Unit C is coal formation is considered as oxic conditional environment which is related to low water level (e.g. marsh/bog near the lake) (Figure 64).





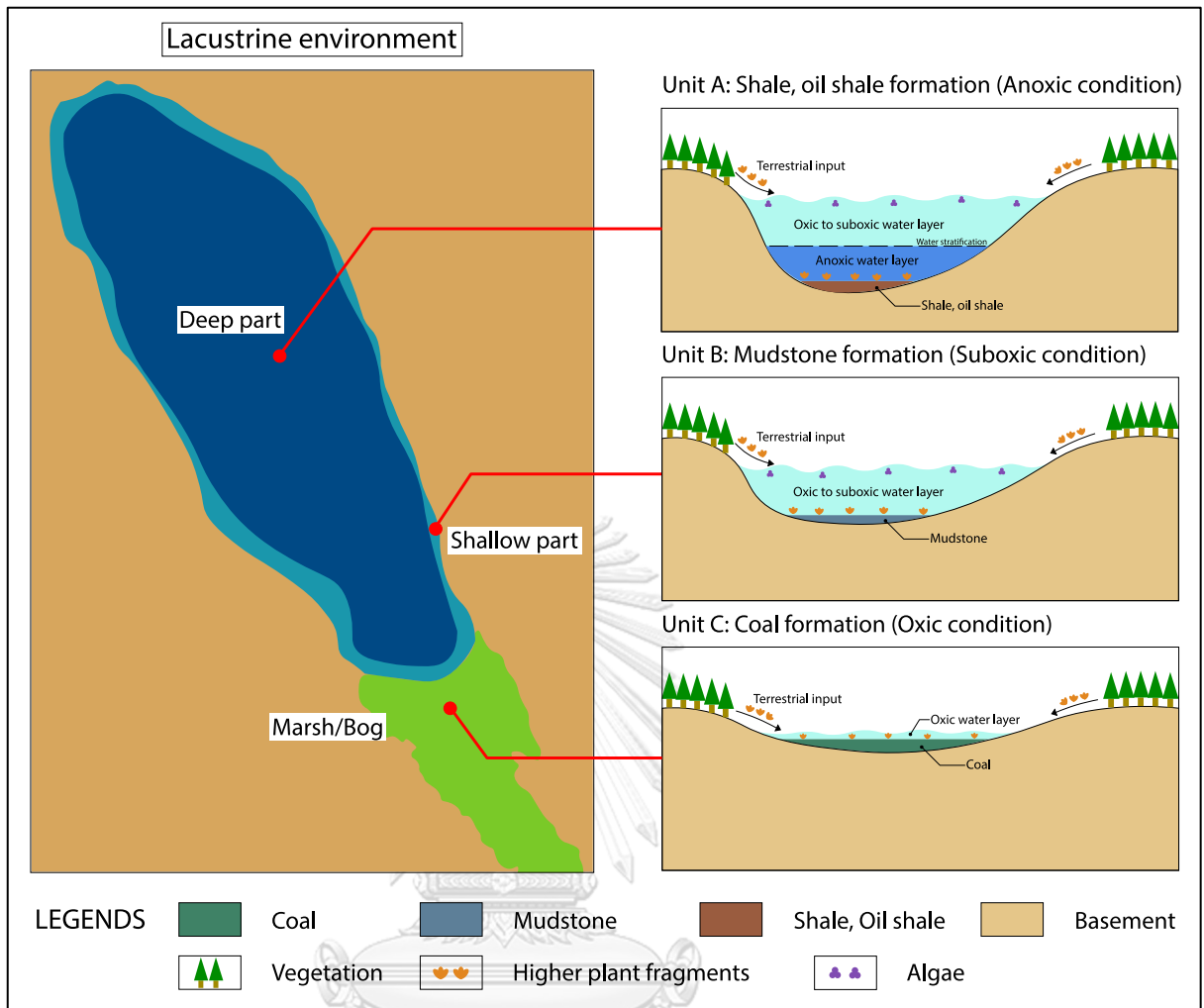


Figure 64 The schematic model of three different types units provide the different lithotypes formation including Unit A: Shale and oil shale formation, Unit B: Mudstone formation and Unit C: Coal formation related to deep part, shallow part and marsh/bog in lacustrine environment, respectively (Setyobudi et al., 2016).

In comparison, Mae Teep basin is likely characterized by a small basin with a steep slope margin during the sediment deposition (Figure 65). Thus, a slight increase in the water level may shift from marsh/bog near the lake to shallow part of lake which is related to oxic and suboxic condition (Figure 64). The rise of water level in the steep basin may easily develop anoxic-deep water in the middle of the basin. The development can be occurred shale and oil shale formation. In contrast to Mae than basin, the basin is considered as a large basin with a gentle slope margin (Figure 65). The shift of water level may have little influence in the change of the depositional

conditions. As the water level increase, the condition is difficult to shift from oxic to anoxic. Thus, oil shale formation may not find in Mae than basin.

The schematic model is purposed for illustrate and separate between Mae Teep and Mae Than basins based on the basin geometry. The model consists of lakes with bordering marsh/bog and two layers of water stratification including oxic to suboxic and anoxic layers in the middle of lake (Figure 65). The difference in lithology such as coals, shales and mudstones and the study of biomarkers suggest that there is the fluctuation of dry and rainy seasons of tropical climate during the deposition of sediments in these basins (Friederich et al., 2016). The depositional environments of these two basins have been open lakes adjacent to marsh/bog areas in which provides source of vegetation (Figure 64).

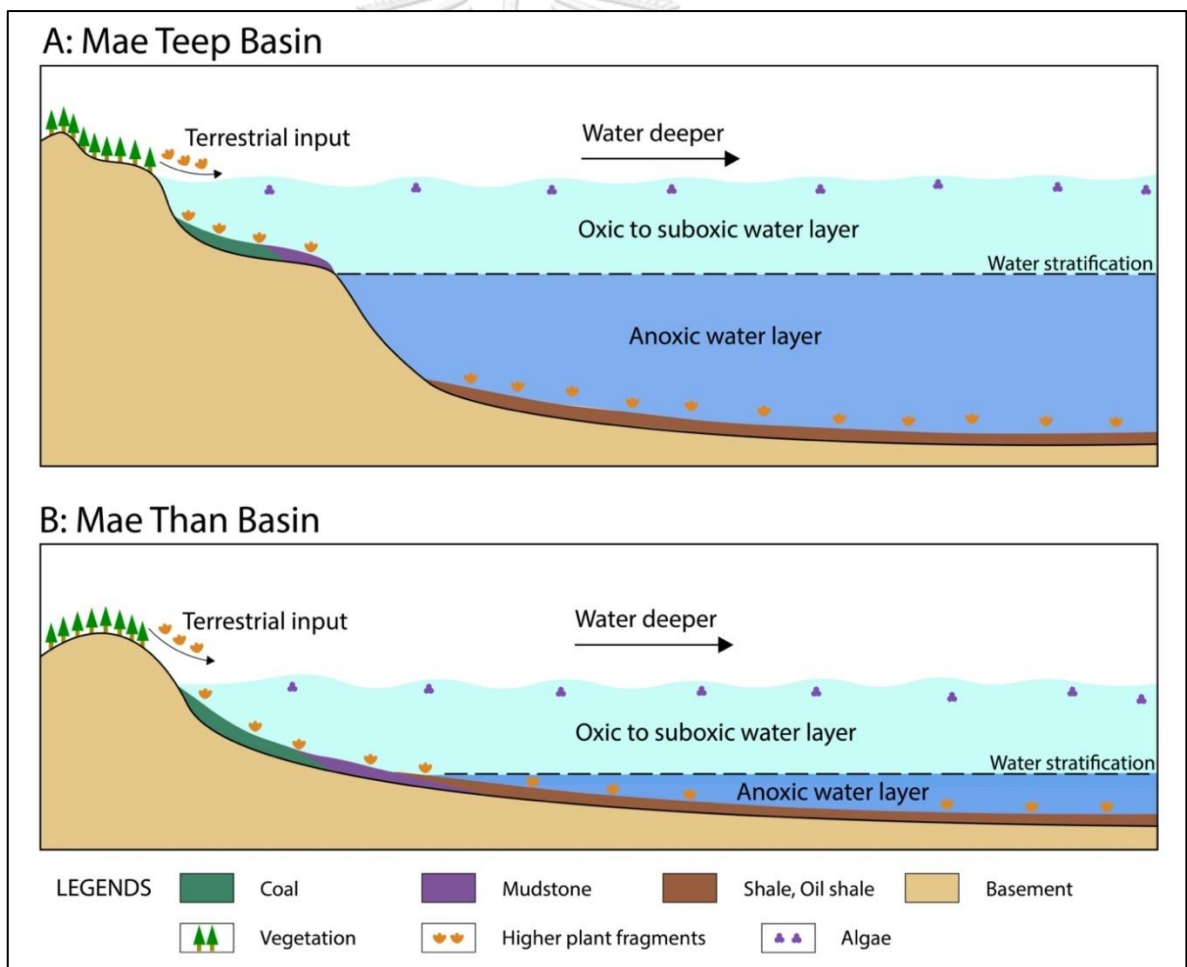


Figure 65 The schematic model of relative water level dependent on environmental conditions in (a) Mae Teep basin and (b) Mae Than basin, showing the difference in basin geometry (Yin et al., 2019).

Furthermore, the previous coal studies of the depositional environments and their conditions are compared to this study. The coal formation can be occurred in various environments, particularly terrestrial swamp lake. The depositional conditions mostly vary from suboxic to oxic condition to deposit coal formation. Some studies reveal that coals can be formed in anoxic with marine environment and/or marine influence (Table 16). In addition to oil shale and shale formation, the rocks are mostly typical of anoxic to suboxic condition. The lake environment is commonly found in this formation (Table 17).

Table 16 The depositional environments and their conditions of coals compared to the previous studies.

<b>Coal</b>	<b>Location</b>	<b>Condition</b>	<b>Environment</b>
This study	Mae Teep basin, Northern Thailand	Oxic	Marsh/Bog near lake
	Mae Than basin, Northern Thailand	Suboxic - oxic	Marsh/Bog near lake- shallow part of lake
Van Minh Le, 1994	Mae Moh basin, Northern Thailand	Suboxic - oxic	Swamp forest/lake
Hasiah and Abolins, 1998	Buru Arang, Malaysia	Suboxic	Swamp freshwater lake
Ehinola et al., 2002	Benue Trough, Nigeria	Oxic	Shallow marine
Petersen and Ratanasthein, 2011	Bang Mark basin, Southern Thailand	Anoxic	Freshwater peat mire with minor saline water
Alias et al., 2012	Sabah, Malaysia	Oxic	Terrestrial with minor marine influence
Hos-Çebi and Korkmaz, 2013	North Anatolia, Turkey	Suboxic	Lacustrine swamps
Mustapha et al., 2017	Northeast Sabah, Malaysia	Anoxic - oxic	Mangrove to lower coastal plain
Gogoi et al., 2020	Meghalaya, India	Oxic - anoxic	Wet swamp with marine influence

Table 17 The depositional environments and their conditions of shales and oil shales compared to the previous studies.

Shale and oil shale	Location	Condition	Environment
This study	Mae Teep basin, Northern Thailand	Anoxic - suboxic	Deep part of lake
	Mae Than basin, Northern Thailand	Suboxic	Deep to shallow part of lake
Van Minh Le, 1994	Mae Moh basin, Northern Thailand	Anoxic - suboxic	Swamp forest/lake
Curiale and Gibling, 1993	Mae Sot basin, Northern Thailand	Anoxic	Lacustrine
Hasiah and Abolins, 1998	Buru Arang, Malaysia	Anoxic - suboxic	Flooding lake

In summary, the biomarker distributions and their related parameters can be characterized the organic geochemistry of the studied samples. The results of biomarker parameters are shown in Table 18 and compared between Mae Teep and Mae Than samples. As those results, the rocks of this study from Mae Teep and Mae Than basins can be interpreted and divided based on lithology. Each lithology exhibits the difference in organic richness, organic matter inputs, thermal maturity, depositional environment and its condition (Table 19). The studied coals can be evaluated coal rank from the thermal maturity assessment based on ASTM (Table 19).

Table 18 The organic geochemical characteristics of the studied samples based on biomarkers and related parameters.

Lithology	Coal		Shale and oil shale		Mudstone	
Location	Mae Teep	Mae Than	Mae Teep	Mae Than	Mae Teep	Mae Than
TOC (wt. %)	30.12- 73.71	23.48- 52.20	4.82- 19.49	14.00- 24.87	0.88- 4.92	0.59-5.98
EOM	High		Moderate	High	Low	
EOM fractions	NSO-compounds > Aromatic > Saturated hydrocarbons					
n-alkane distribution	Long-chain > Mid-chain > Short-chain n-alkanes					
CPI	Moderate-	Moderate	Moderate		Low	Moderate

	high				
ACL	Moderate (narrow range)				
P <sub>aq</sub>	Low				Low-moderate
TAR	High				
NAR	High				
Sterane distribution	C <sub>29</sub> > C <sub>28</sub> > C <sub>27</sub>				
Pr/nC <sub>17</sub>	High		Moderate		Low
Ph/nC <sub>18</sub>	Moderate	High	High	Moderate	Low
Pr/Ph	High	Moderate	Low	Moderate	Moderate
Gammacerane index	Low		Moderate-high	Low-moderate	Moderate

Table 19 The interpretation of organic geochemical characteristics of the studied samples.

Lithology	Coal		Shale and oil shale		Mudstone	
Location	Mae Teep	Mae Than	Mae Teep	Mae Than	Mae Teep	Mae Than
Organic richness	High		Moderate		Low	
Type of organic matter	Terrestrial higher plants		Terrestrial higher plants with minor fresh water algae		Terrestrial higher plants	
Thermal maturity	Immature-early mature					
Coal rank	Lignite-subbituminous A		-			
Condition	Oxic	Suboxic-oxic	Anoxic-suboxic	Suboxic	Oxic	
Environment	Marsh/Bog near lake	Marsh/Bog near lake-shallow part of lake	Deep part of lake	Deep to shallow part of lake	Shallow part of lake	

## Chapter VI

### Conclusions

The organic matter quantitative analysis of the studied samples mostly exhibits high amount of organic matter which meets a good to excellent hydrocarbon generation potential for source rocks, except some mudstone samples based on TOC and EOM contents.

The biomarkers and their related parameters exhibit distributions and abundances performed by using GC-MS analysis. The studied samples from Mae Teep and Mae Than basins are analyzed to characterize these parameters in order to interpret types of organic matter, depositional environments and their conditions and to assess thermal maturity of the coal samples.

For thermal maturity assessment, the coal samples from both Mae Teep and Mae Than basins are immature to early mature stage at the present day based on biomarker maturity indicators and are equivalent to lignite – subbituminous A coal based on ASTM coal rank.

The n-alkane distribution and their related parameters provide the types of organic matter. The organic matters are mainly contributed of terrestrial higher plants with minor fresh water algae in all studied samples.

Based on isoprenoid/n-alkane, Pr/Ph ratio, gammacerane index and regular steranes, the depositional environments and their conditions are interpreted that the Mae Teep coals occur in oxidizing terrestrial environment, whereas the Mae Than coals are typical of mixed terrestrial and aquatic environment under suboxic condition. Shale in both basins exhibit to deposit in suboxic to anoxic aquatic environment. During the low productivity, mudstones can be occurred mostly in suboxic condition, showing low amount of organic matter. An association of algae in the high water level or deep water lake with anoxic condition may lead to oil shale formation.

## Appendix

Table 20 The peak identification of triterpene and terpane distribution.

Peak	Formula	Weight	Identification
a	C <sub>27</sub> H <sub>46</sub>	370	18 $\alpha$ ,21 $\beta$ -22,29,30-Trisnorhopane (Ts)
b	C <sub>27</sub> H <sub>46</sub>	370	17 $\alpha$ ,21 $\beta$ -22,29,30-Trisnorhopane (Tm)
b	C <sub>29</sub> H <sub>50</sub>	398	17 $\alpha$ ,21 $\beta$ -30-Norhopane
d	C <sub>29</sub> H <sub>50</sub>	398	29Ts
e	C <sub>29</sub> H <sub>50</sub>	398	18 $\alpha$ ,17 $\alpha$ -Methyl-28,30-dinorhopane
f	C <sub>29</sub> H <sub>50</sub>	398	Oleanane
g	C <sub>29</sub> H <sub>50</sub>	398	17 $\beta$ ,21 $\alpha$ -30-Normortane
h	C <sub>30</sub> H <sub>52</sub>	412	30Ts
i	C <sub>30</sub> H <sub>52</sub>	412	17 $\alpha$ ,21 $\beta$ -Hopane
j	C <sub>30</sub> H <sub>52</sub>	412	17 $\beta$ ,21 $\alpha$ -Moretane
k	C <sub>31</sub> H <sub>54</sub>	426	17 $\alpha$ ,21 $\beta$ -30-Homohopane (22S)
l	C <sub>30</sub> H <sub>52</sub>	412	Gammacerane
m	C <sub>31</sub> H <sub>54</sub>	426	17 $\alpha$ ,21 $\beta$ -30-Homohopane (22R)

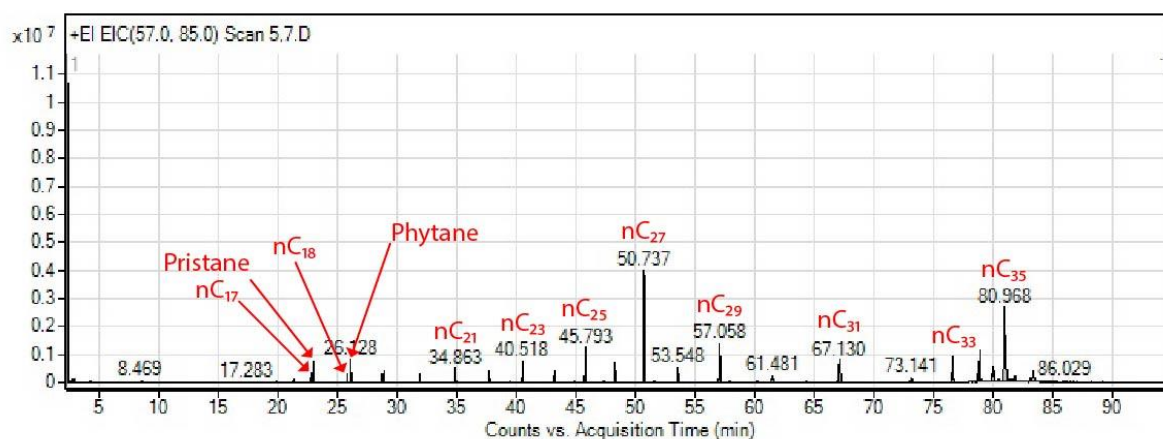
Table 21 The peak identification of sterane distribution.

Identification	Formula	Weight
Cholestane	C <sub>27</sub> H <sub>48</sub>	372
Ergostane	C <sub>28</sub> H <sub>50</sub>	386
Stigmastane -5 $\alpha$ -Stigmastane (20S) -5 $\alpha$ ,14 $\beta$ ,17 $\beta$ -Stigmastane (20R) -5 $\alpha$ ,14 $\beta$ ,17 $\beta$ -Stigmastane (20S) -5 $\alpha$ -Stigmastane (20R)	C <sub>29</sub> H <sub>52</sub>	400
C <sub>30</sub> sterane	C <sub>30</sub> H <sub>54</sub>	414

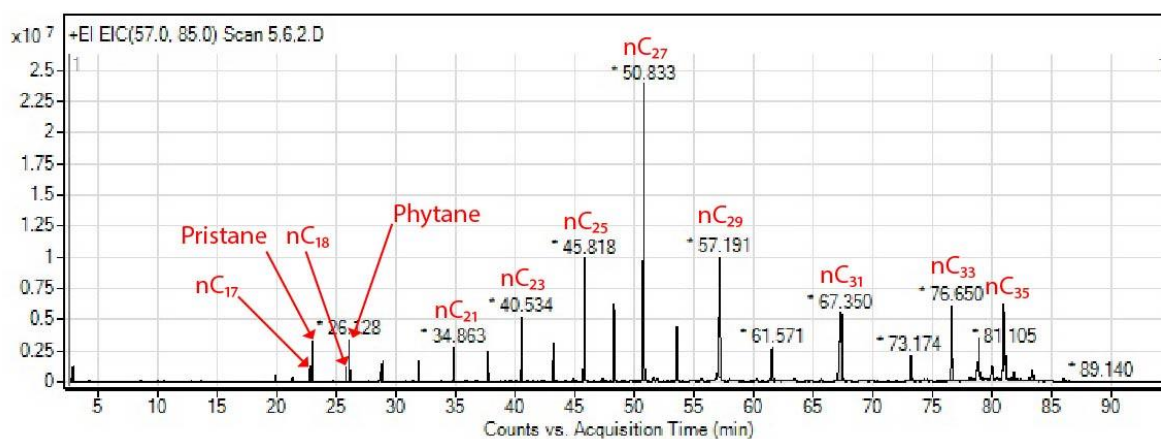
## 1. m/z 85 ion chromatograms showing n-alkane and isoprenoid distribution

### 1.1 Location: Mae Teep coal mine

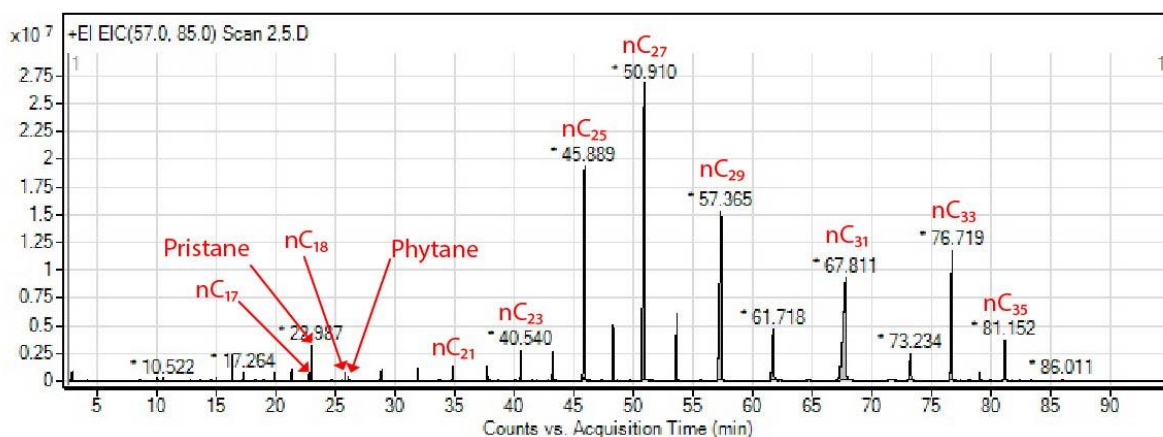
#### Sample ID MS1 Shale



#### Sample ID MS2 Shale

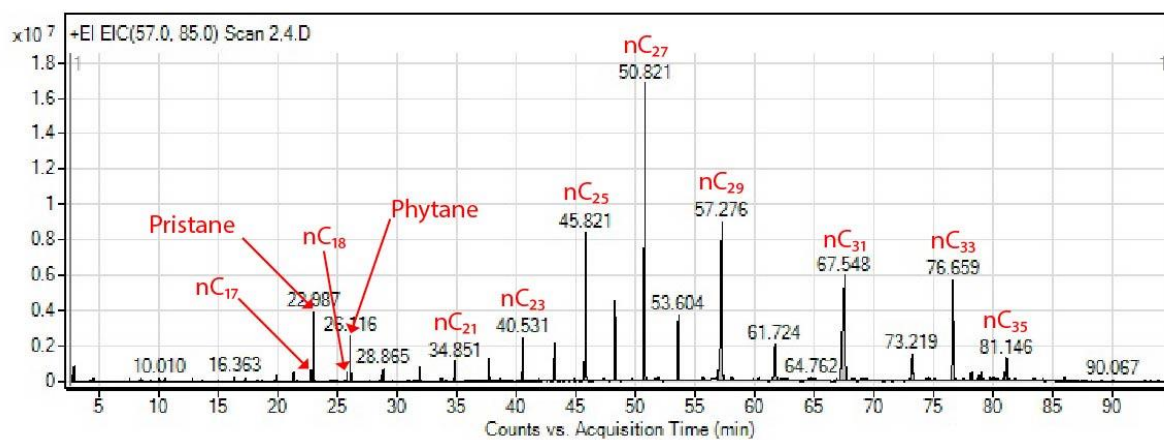


#### Sample ID MC3 Coal

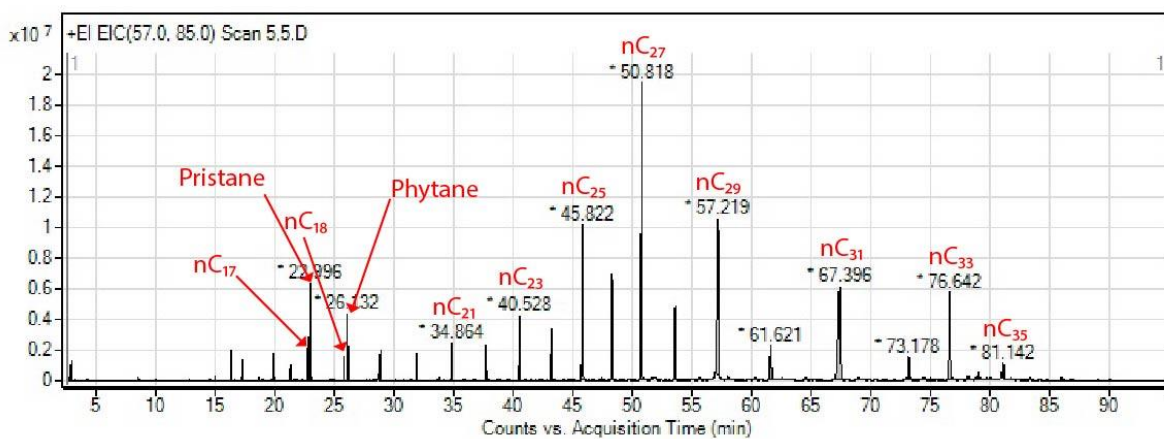




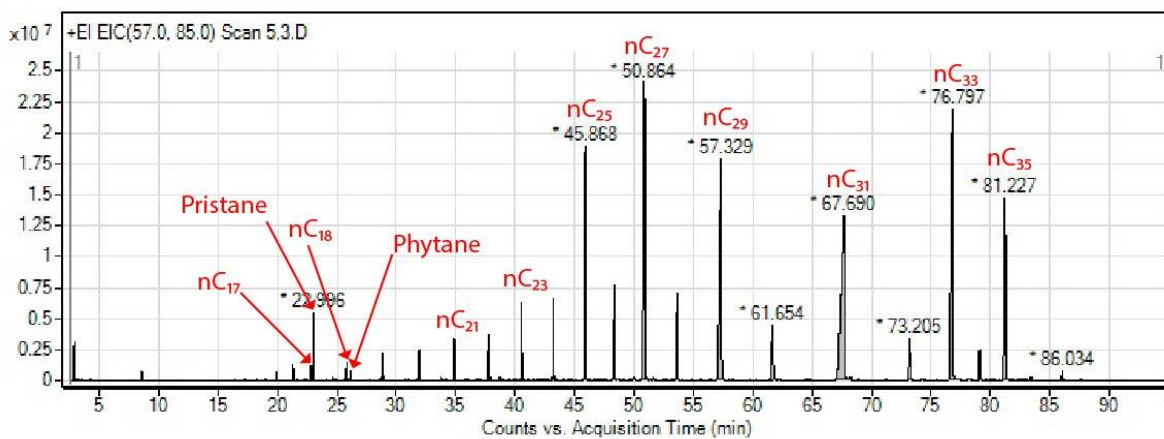
## Sample ID MS4 Oil shale



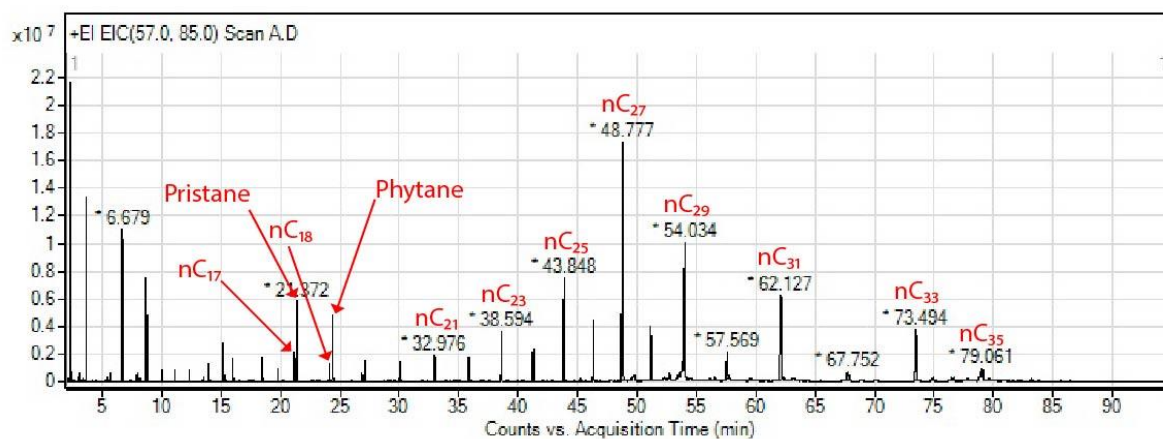
## Sample ID MS5 Oil shale



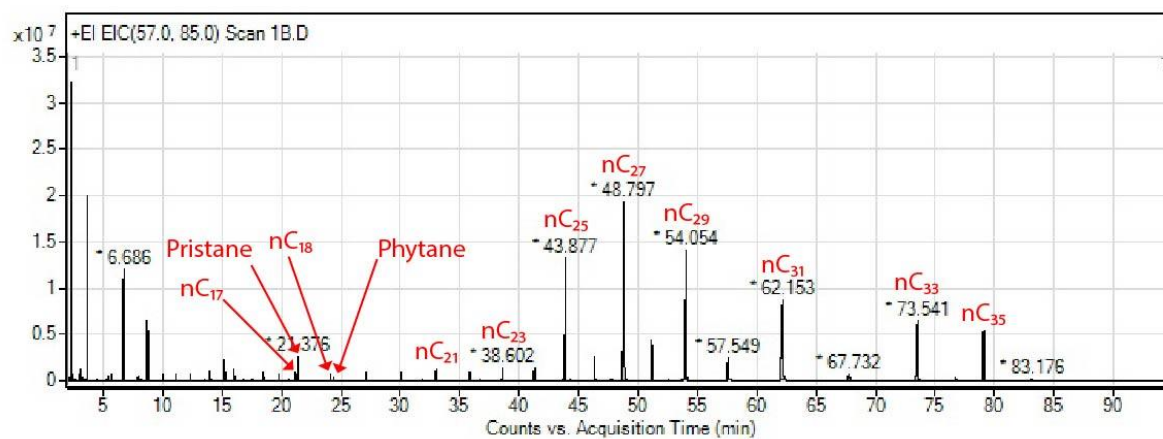
## Sample ID MC6 Coal



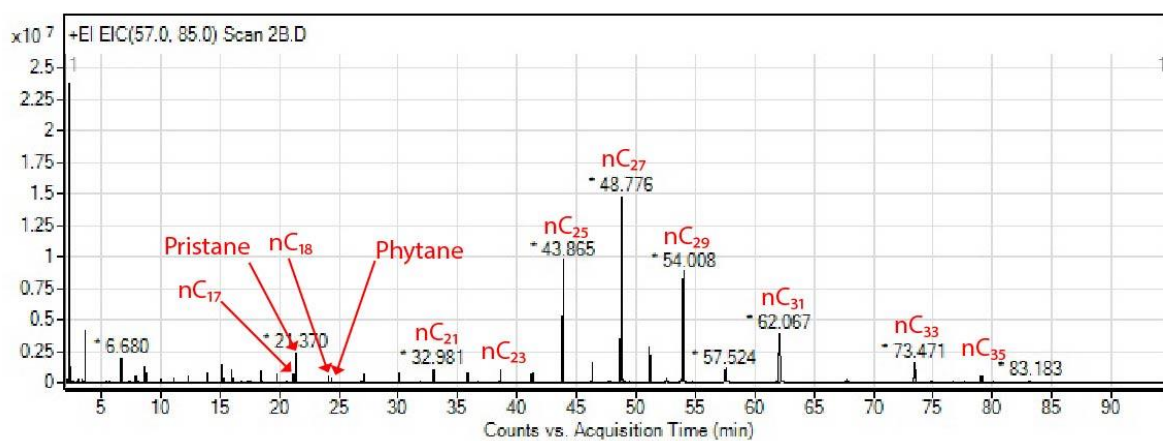
## Sample ID MS7 Oil shale



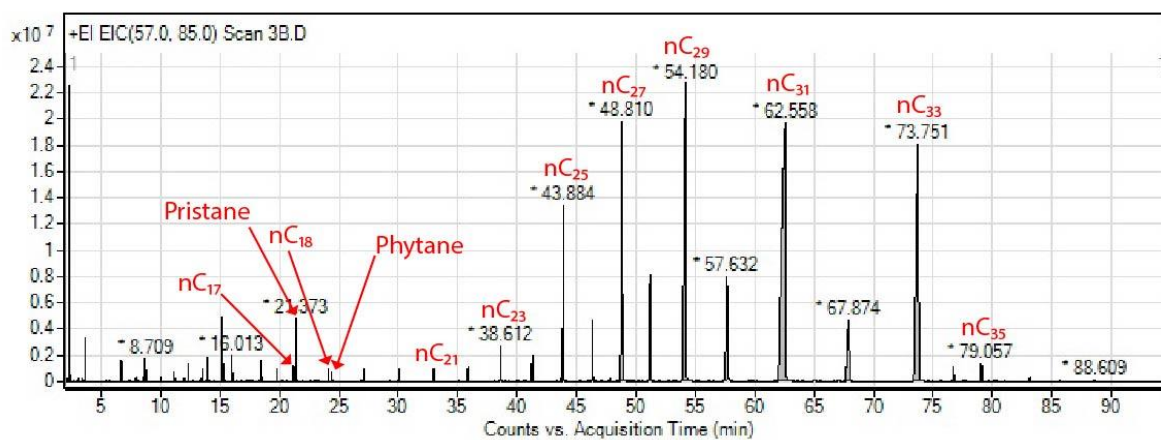
## Sample ID MC8 Coal



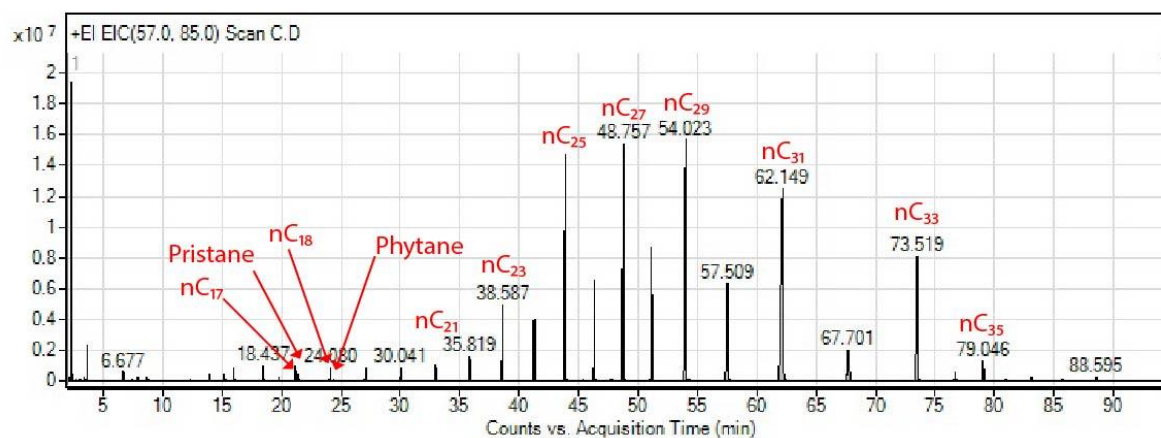
## Sample ID MC9 Coal



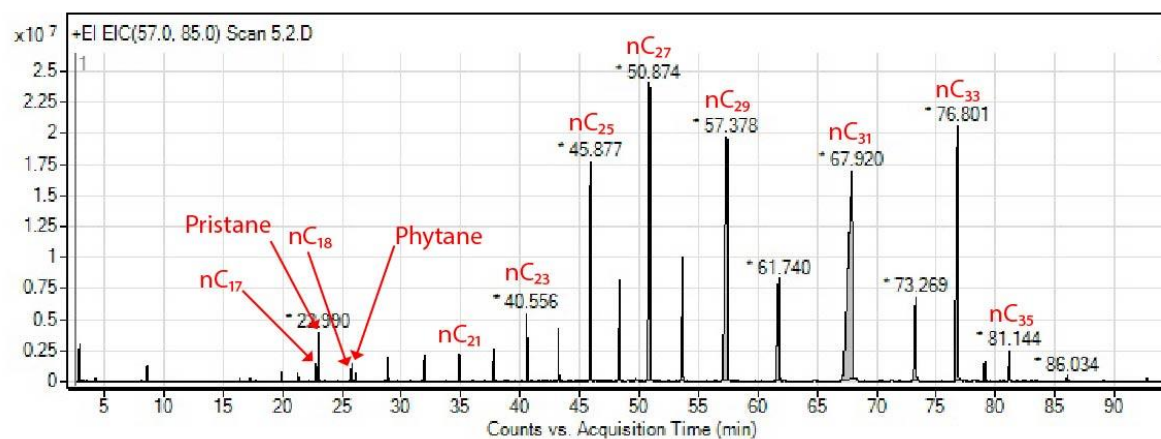
## Sample ID MC10 Coal



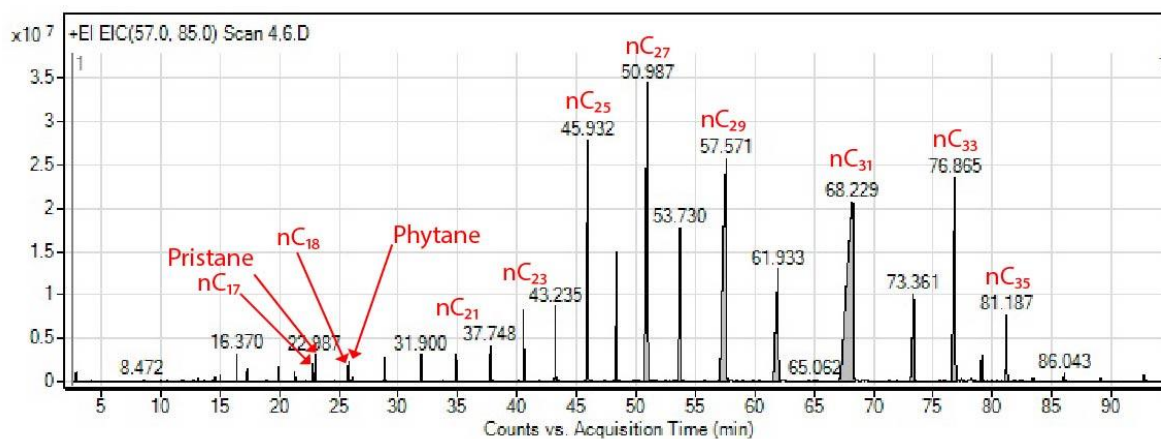
## Sample ID MM11 Mudstone



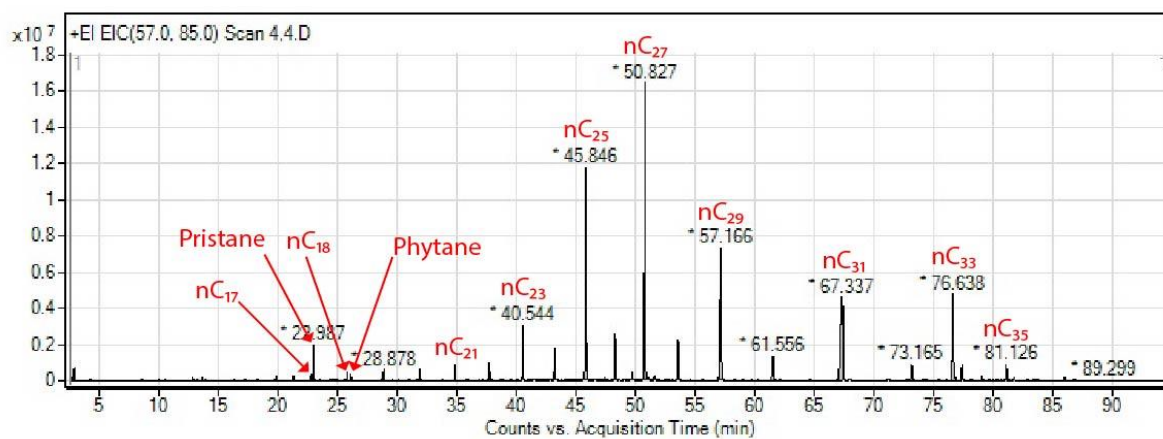
## Sample ID MC12 Coal



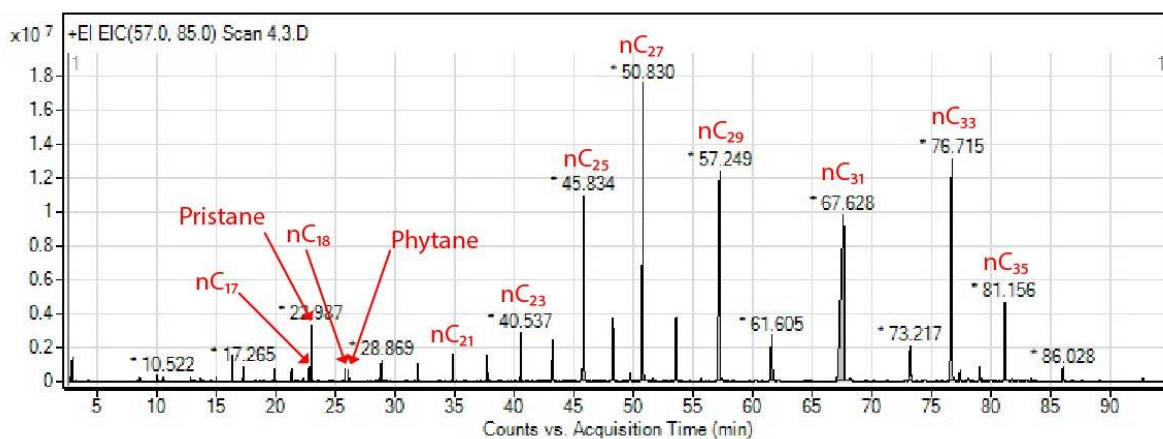
## Sample ID MC13 Coal



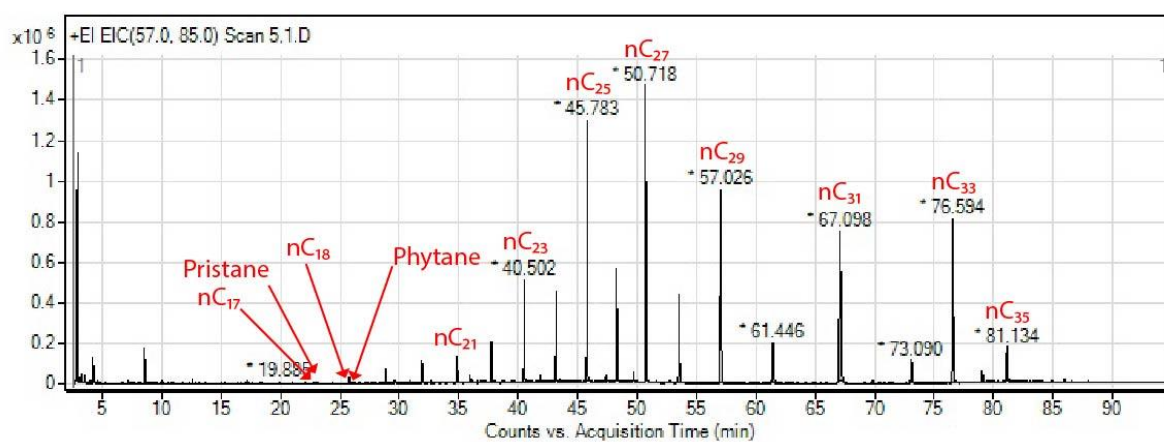
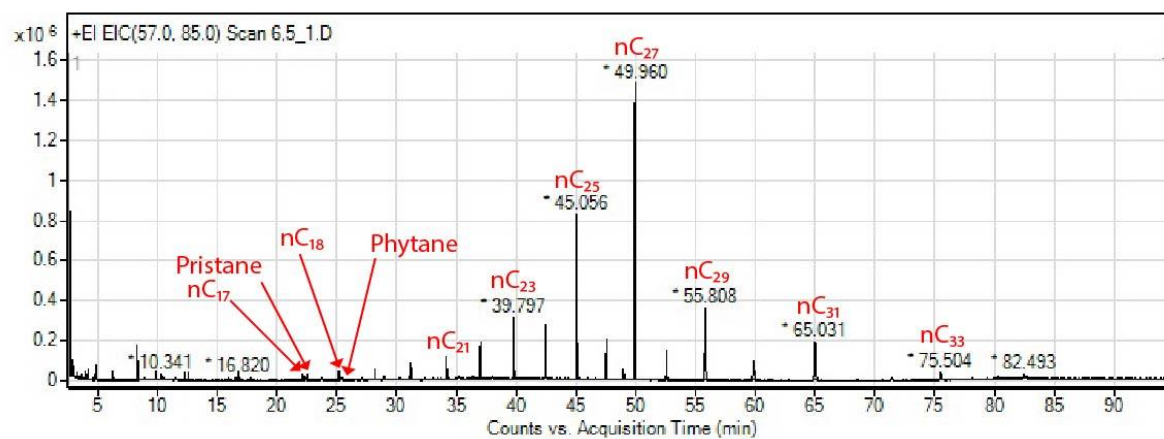
## Sample ID MC14 Coal



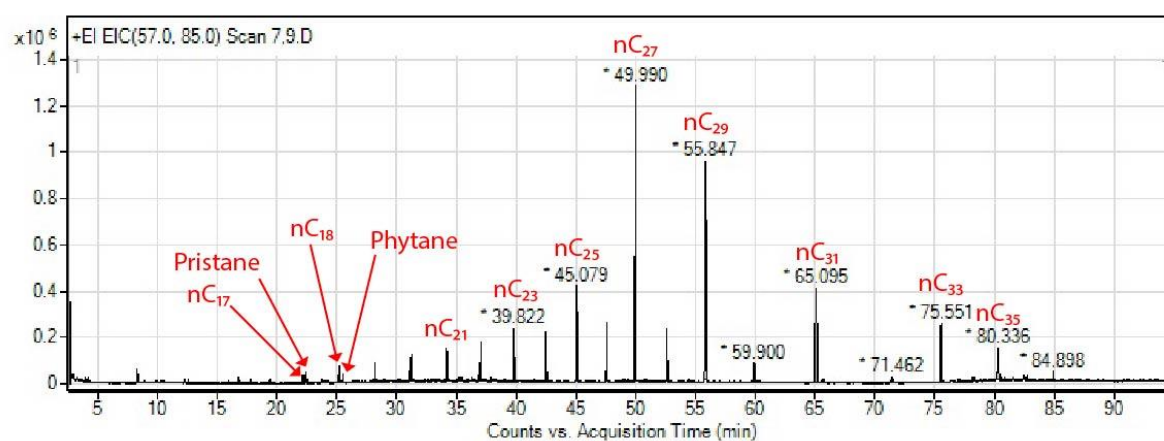
## Sample ID MC15 Coal



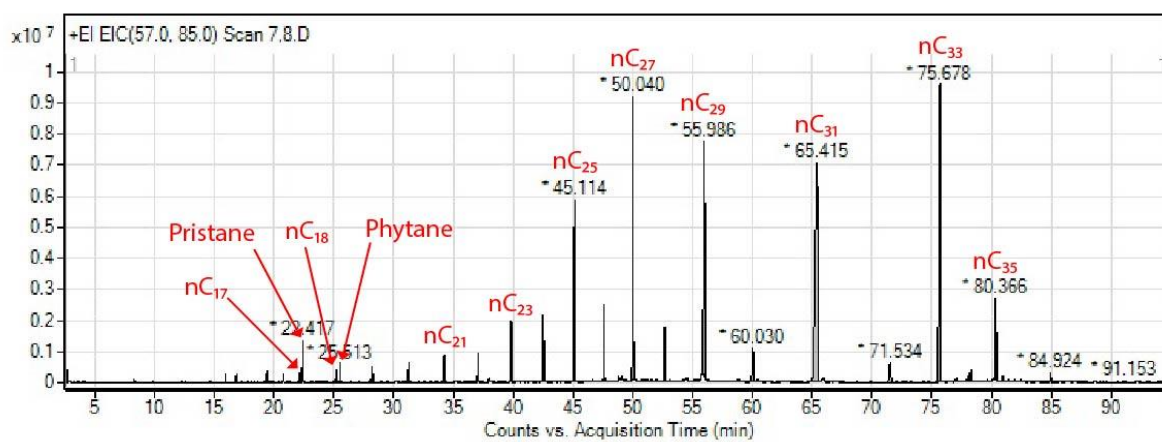
## Sample ID MM16 Mudstone


 1.2 Location: Mae Than coal mine  
 Sample ID TM1 Mudstone


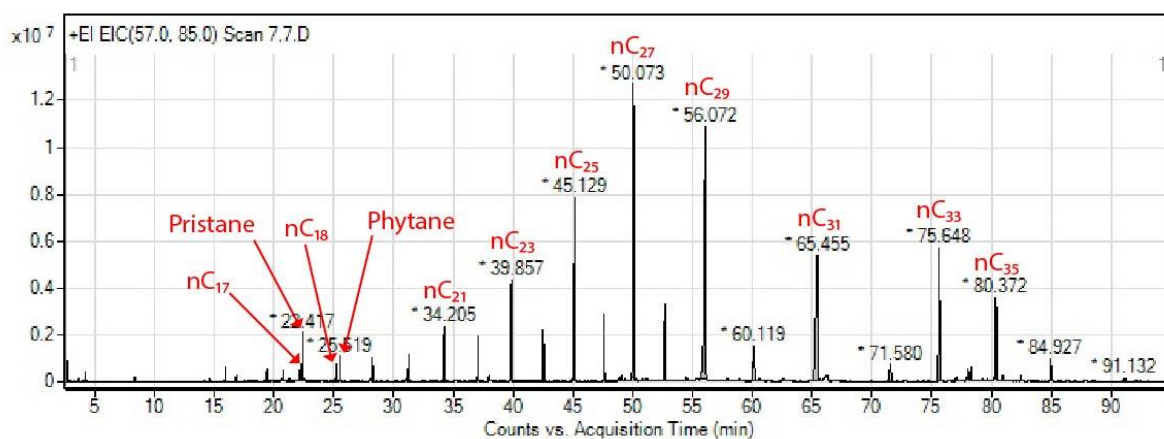
## Sample ID TM2 Mudstone



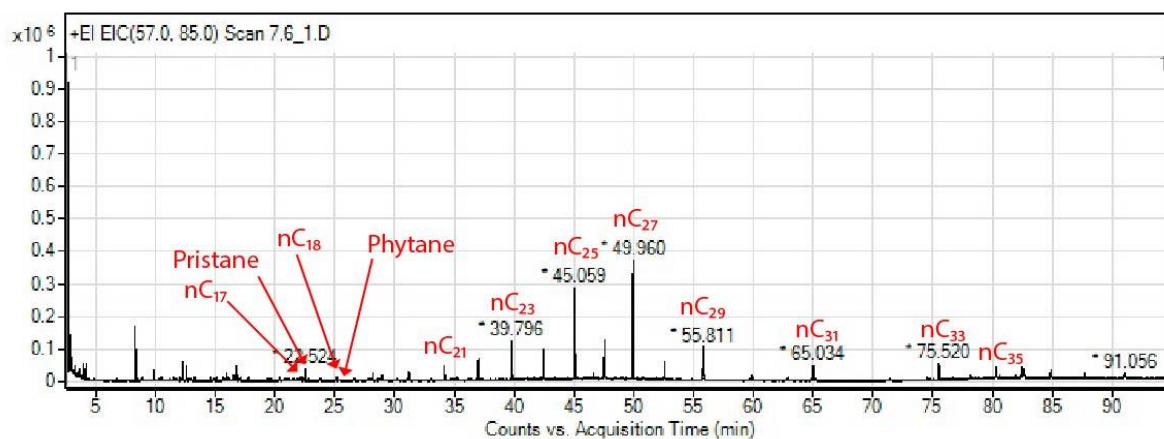
## Sample ID TC3 Coal



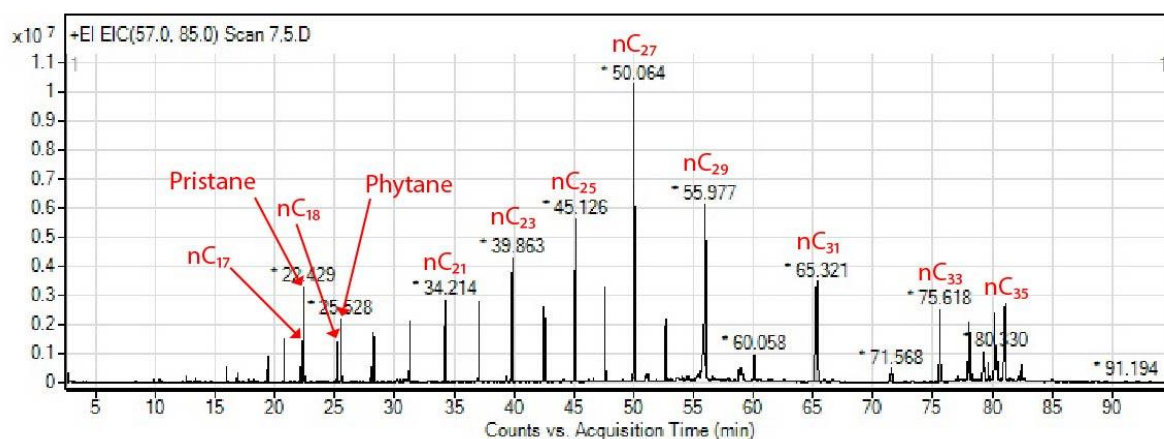
## Sample ID TC4 Coal



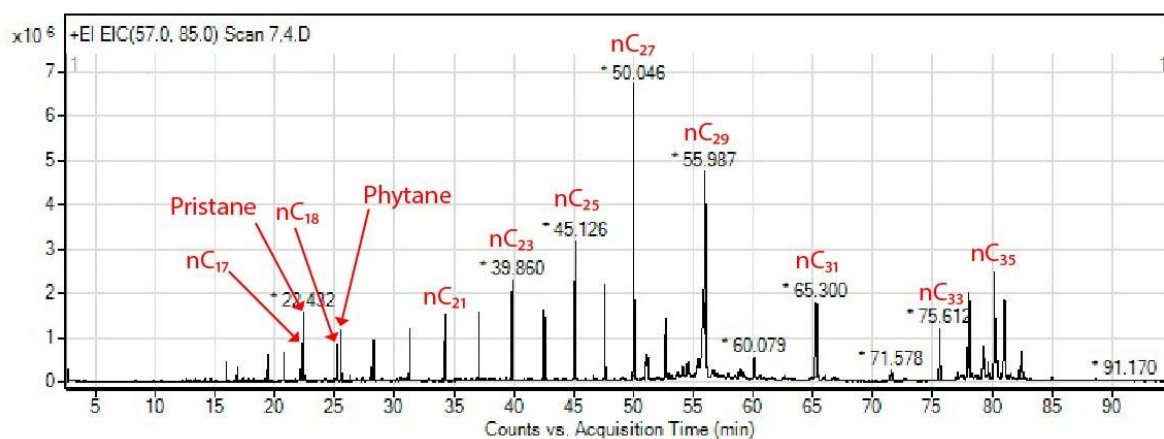
## Sample ID TM5 Mudstone



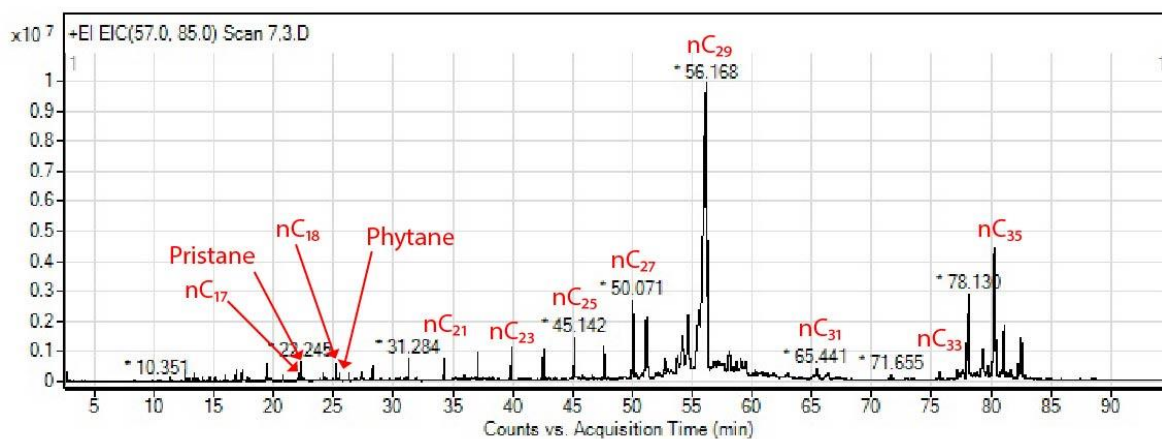
## Sample ID TS6 Shale



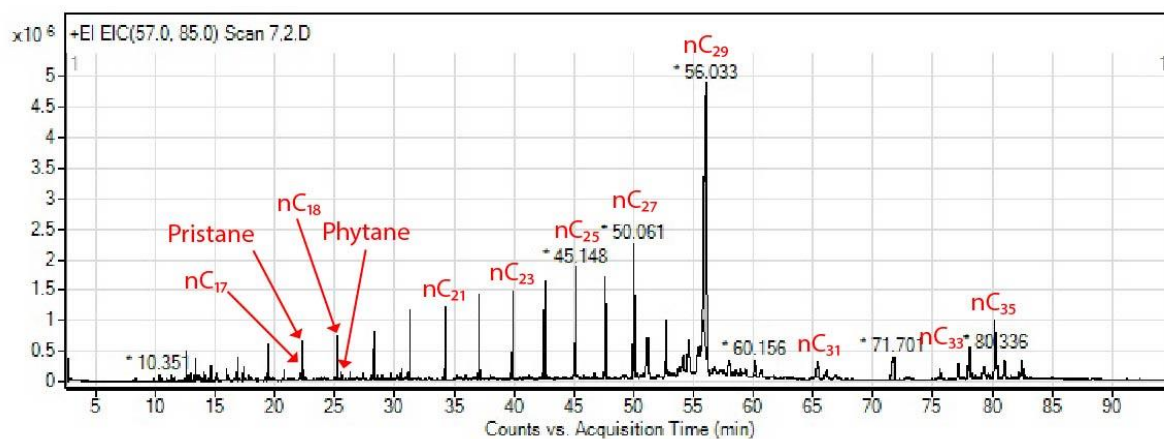
## Sample ID TS7 Shale



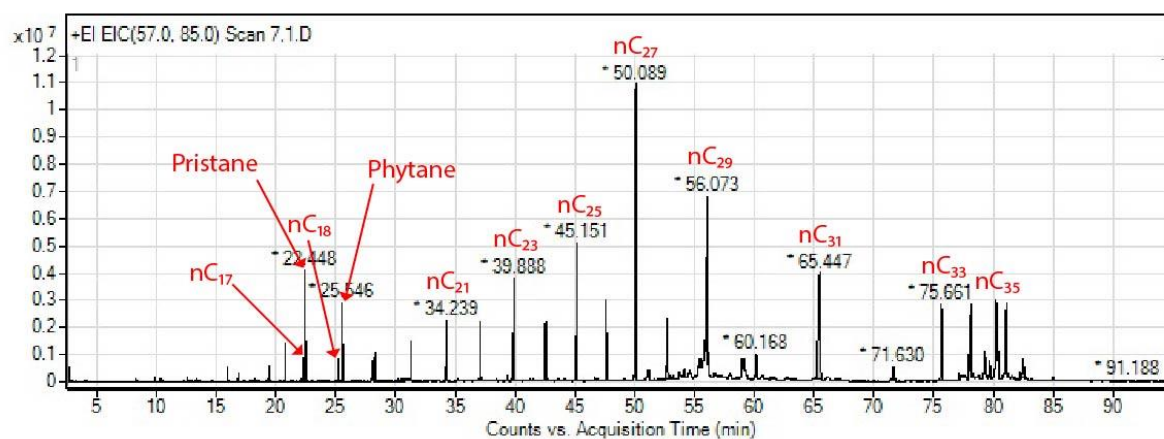
## Sample ID TC8 Coal



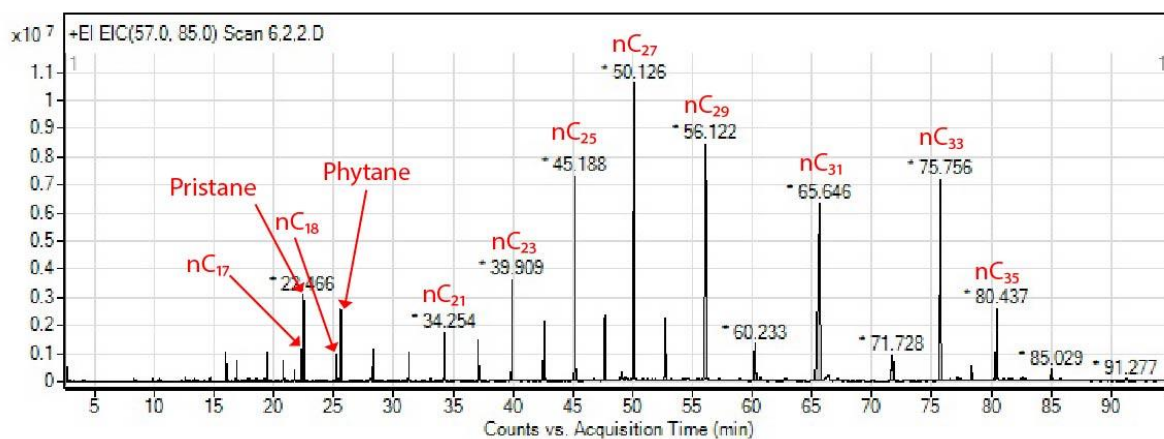
Sample ID TC9 Coal



Sample ID TC10 Coal

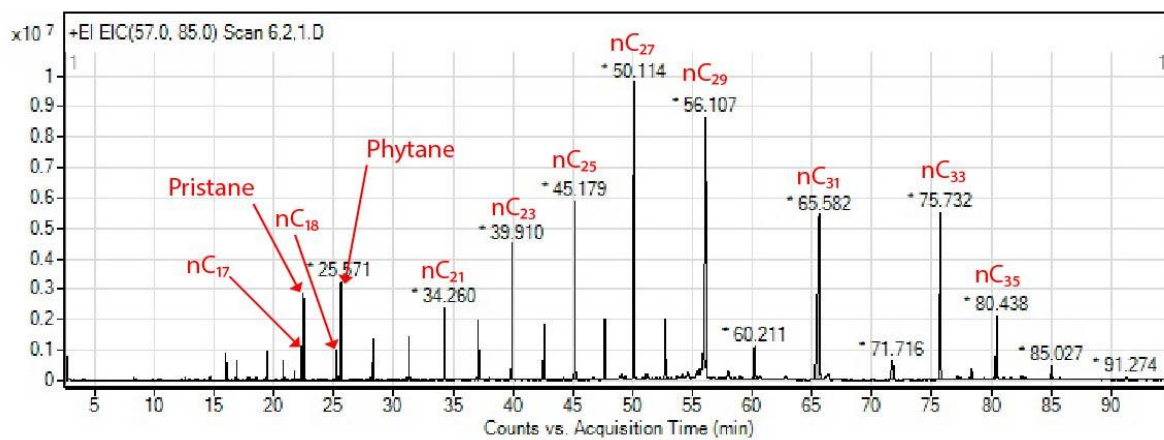


Sample ID TC11 Coal

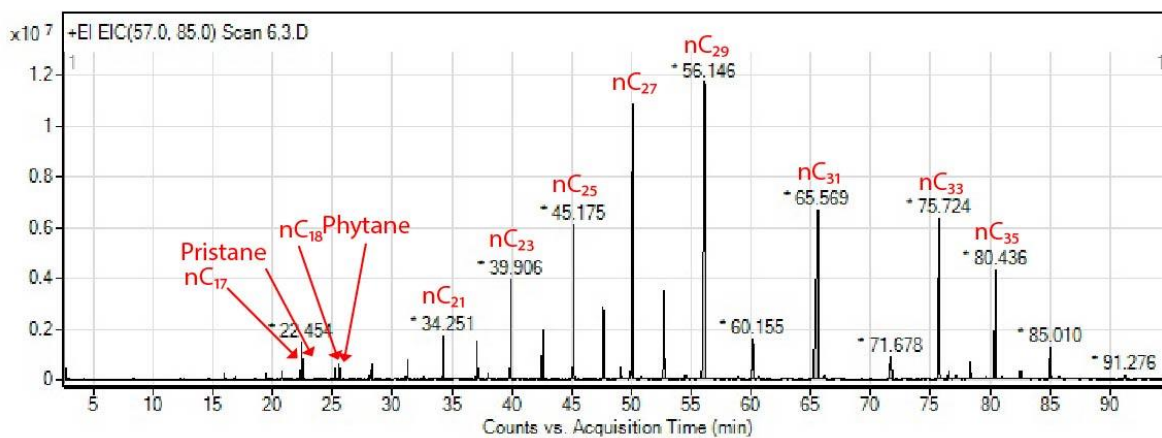




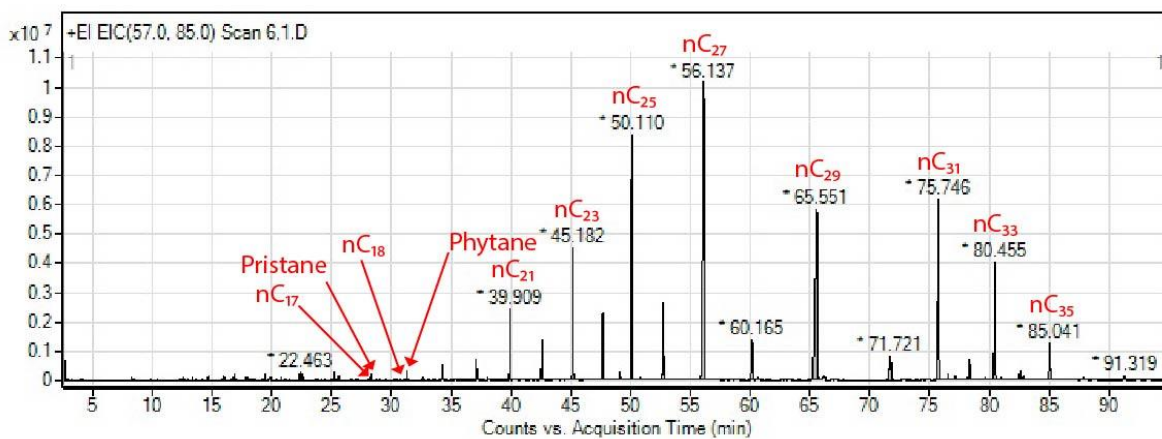
## Sample ID TS12 Shale



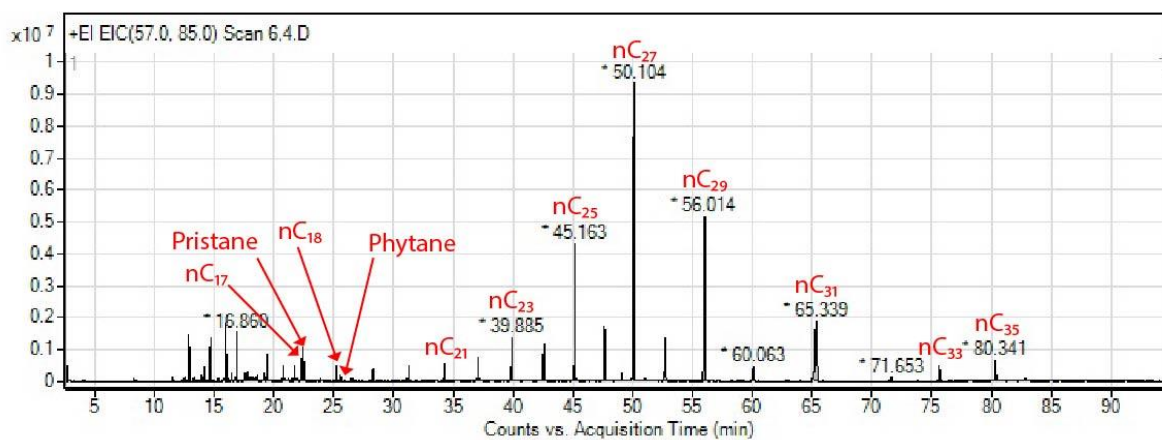
## Sample ID TC13 Coal



## Sample ID TS14 Shale



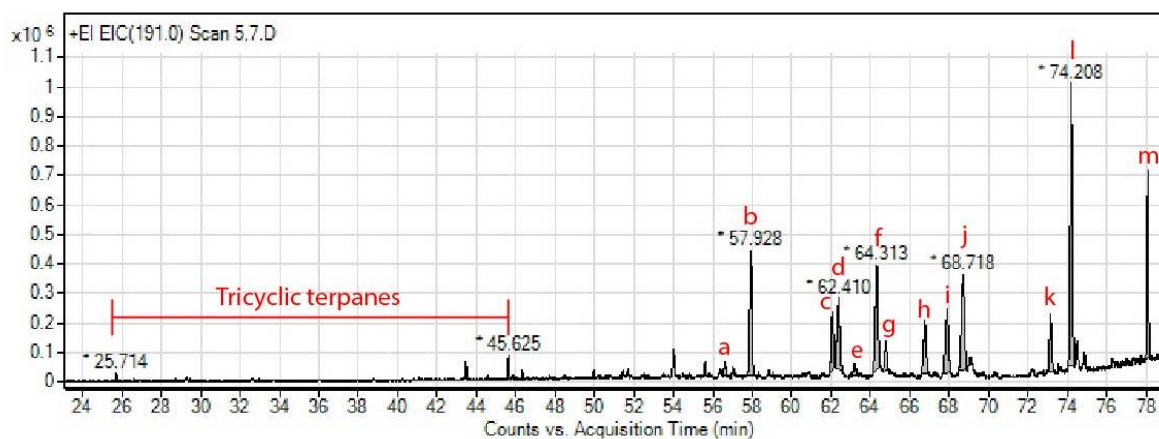
## Sample ID TC15 Coal



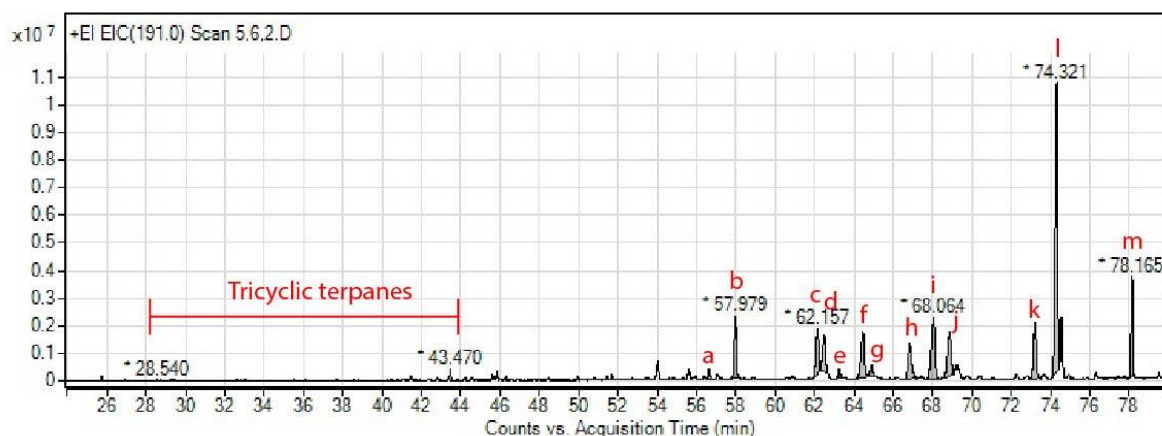
## 2. m/z 191 ion chromatograms showing terpane and triterpene distribution

## 2.1 Location: Mae Teep coal mine

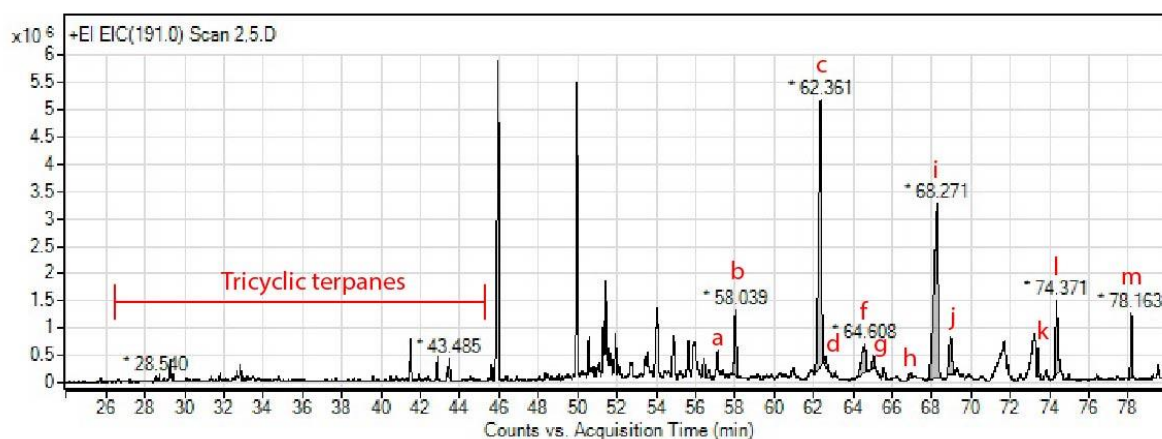
## Sample ID MS1 Shale



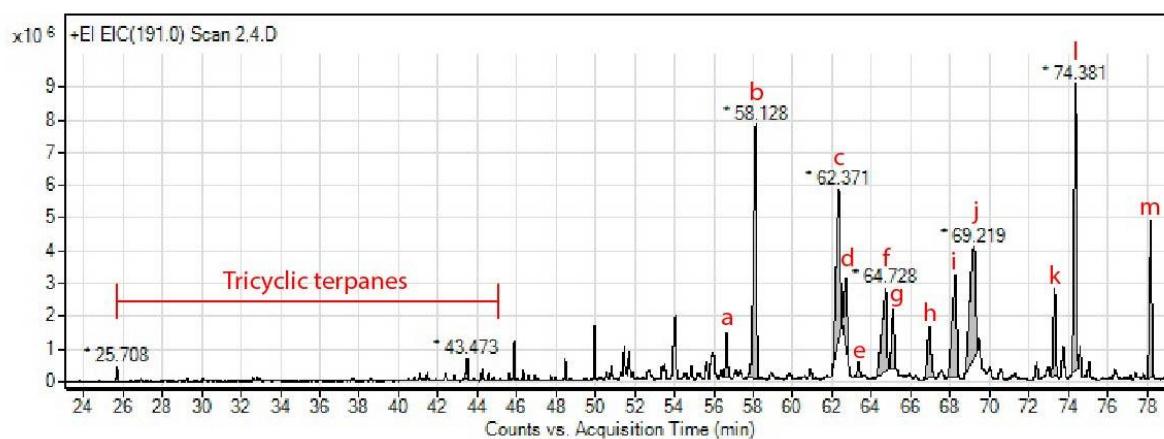
## Sample ID MS2 Shale



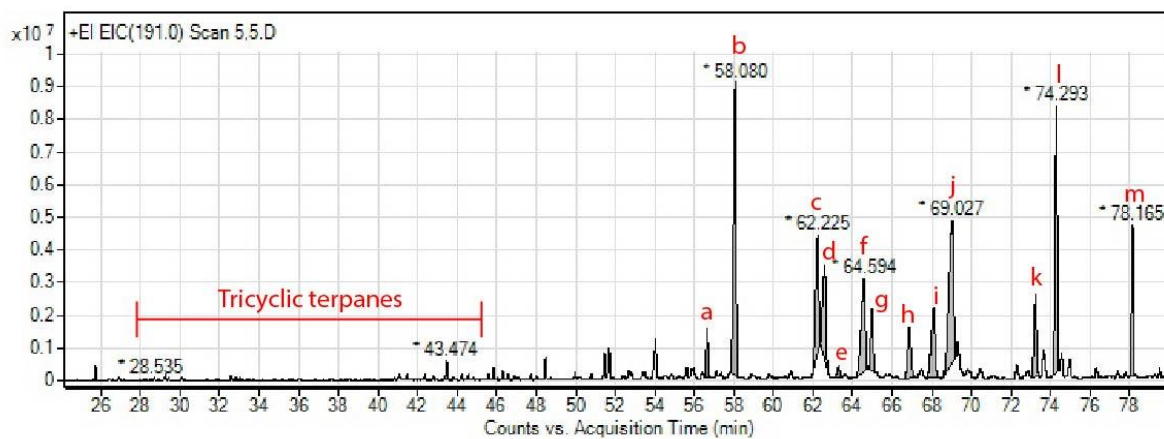
## Sample ID MC3 Coal



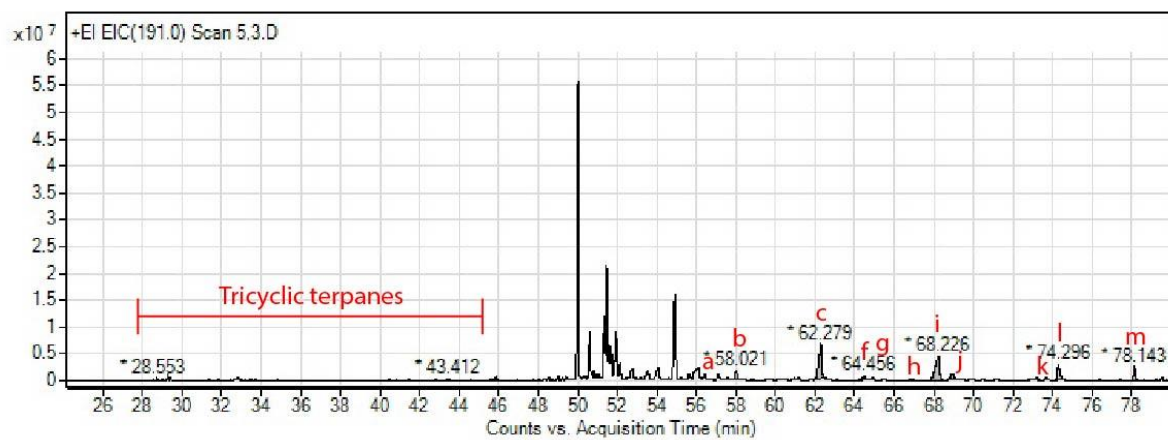
## Sample ID MS4 Oil shale



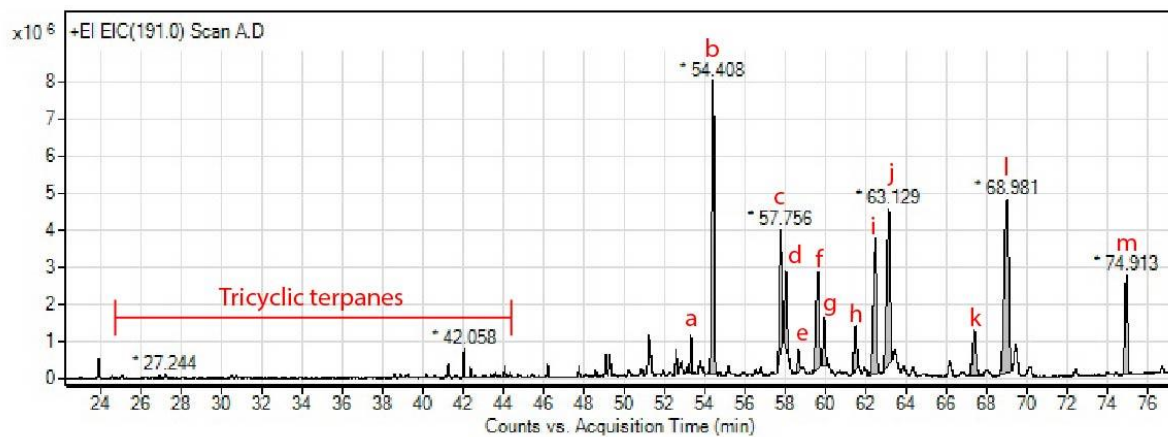
## Sample ID MS5 Oil shale



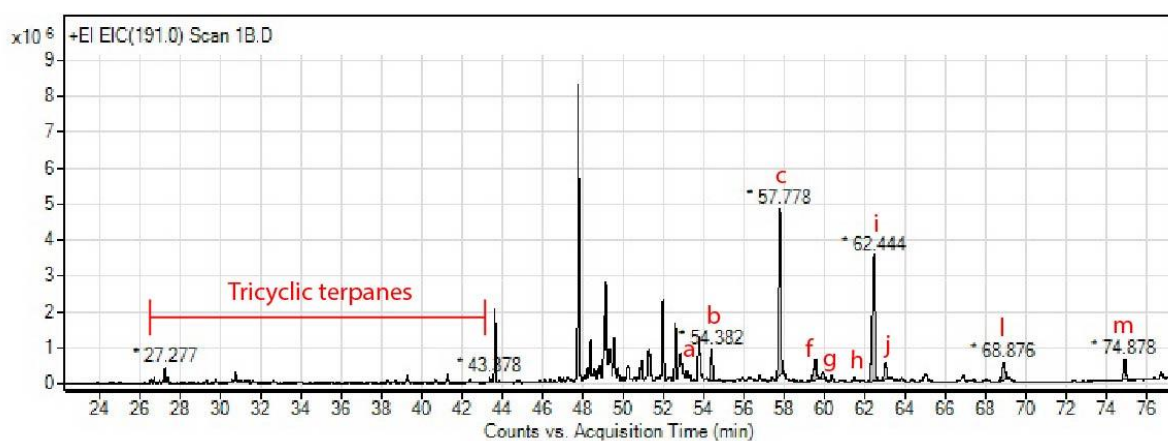
## Sample ID MC6 Coal



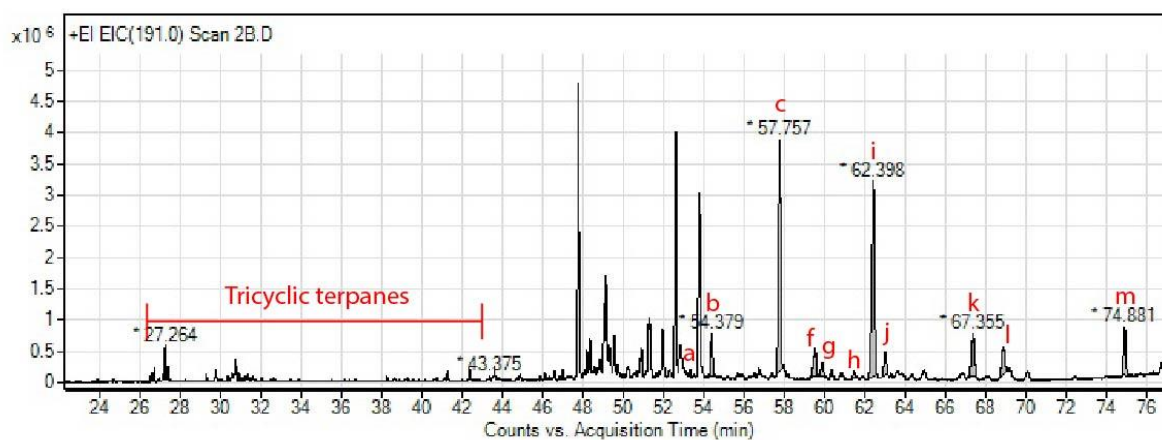
## Sample ID MS7 Oil shale



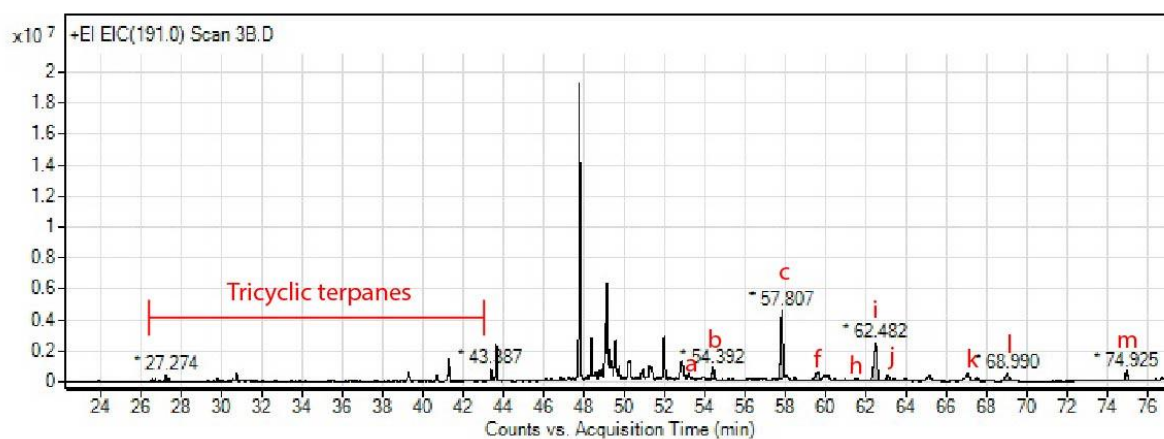
## Sample ID MC8 Coal



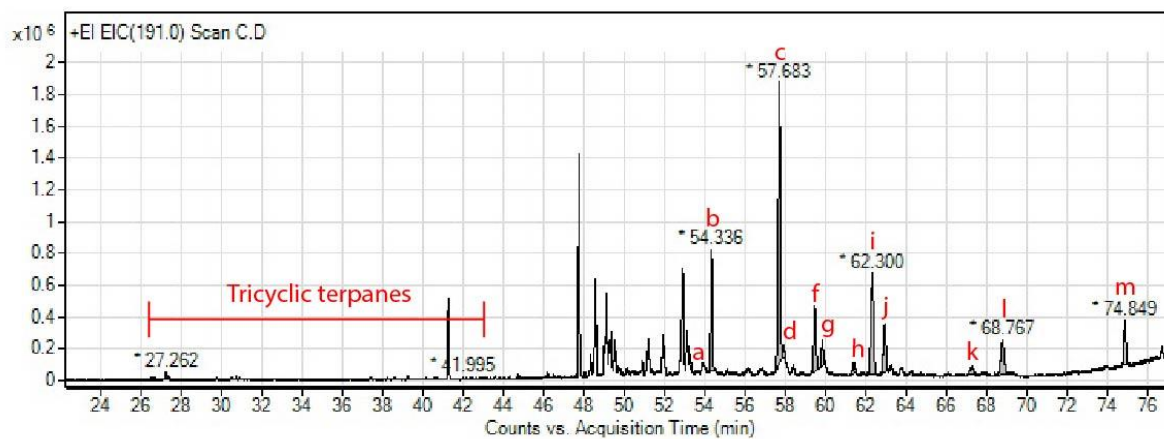
## Sample ID MC9 Coal



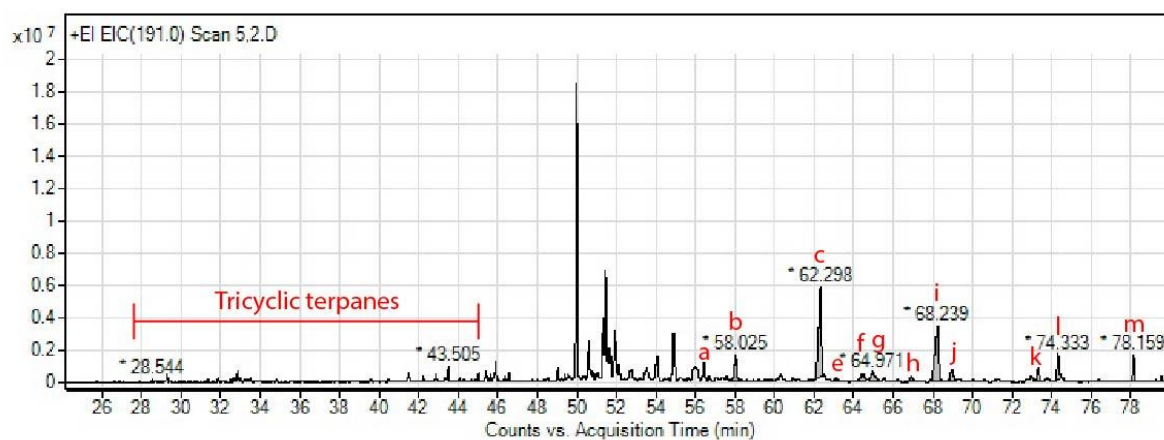
## Sample ID MC10 Coal



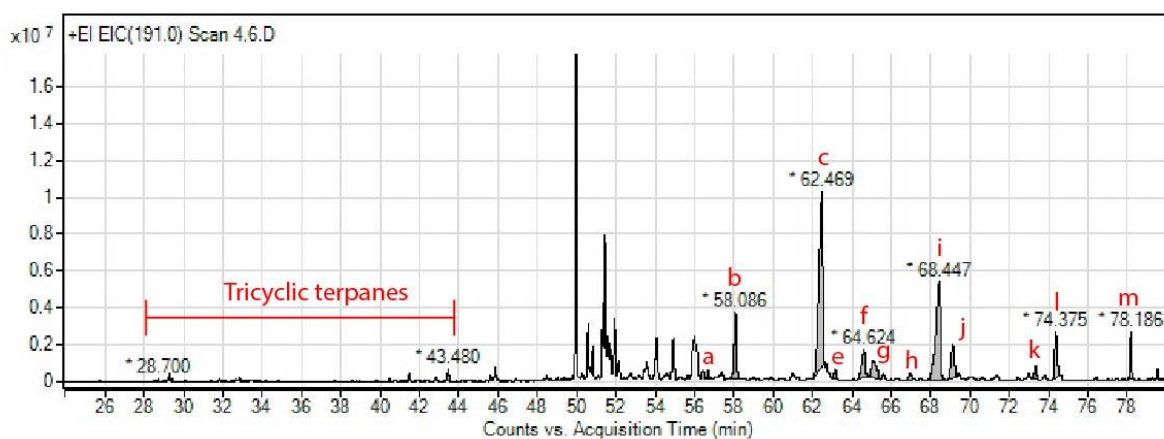
## Sample ID MM11 Mudstone



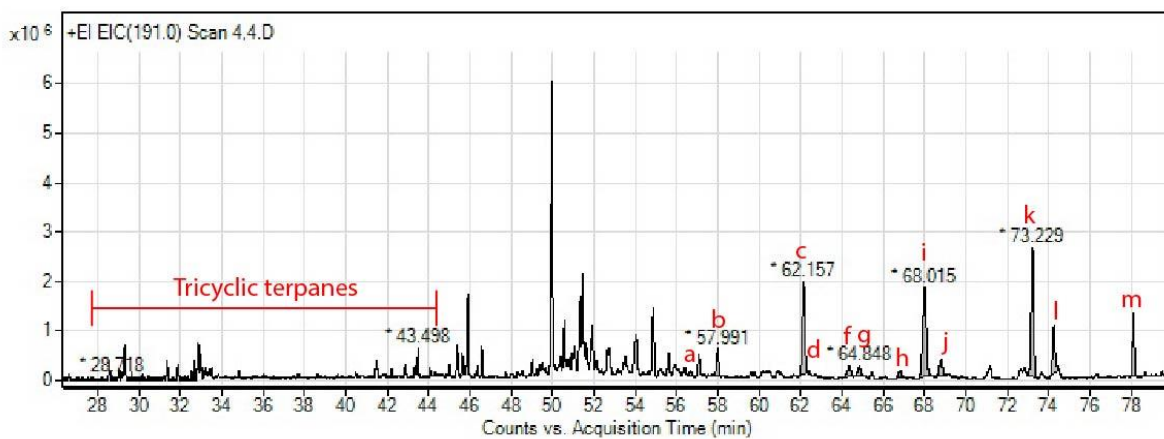
## Sample ID MC12 Coal



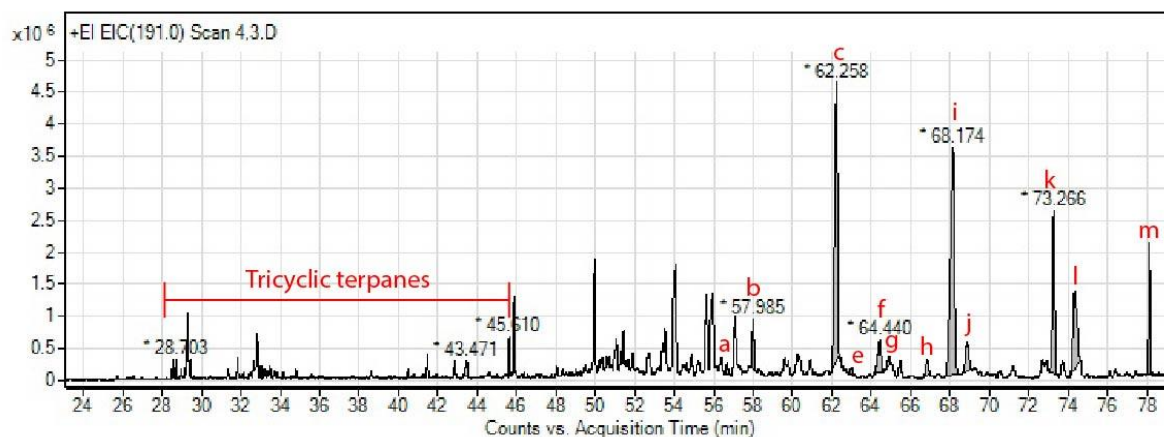
## Sample ID MC13 Coal



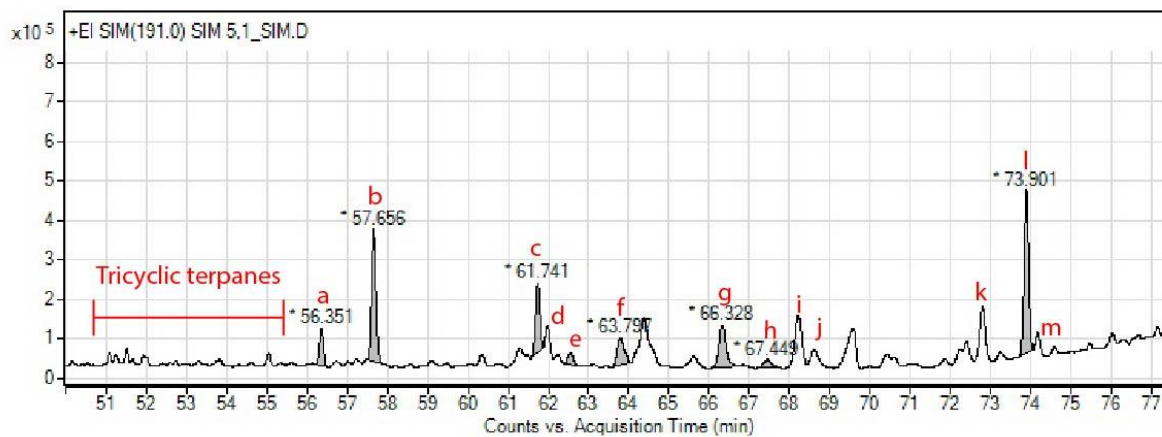
## Sample ID MC14 Coal



## Sample ID MC15 Coal

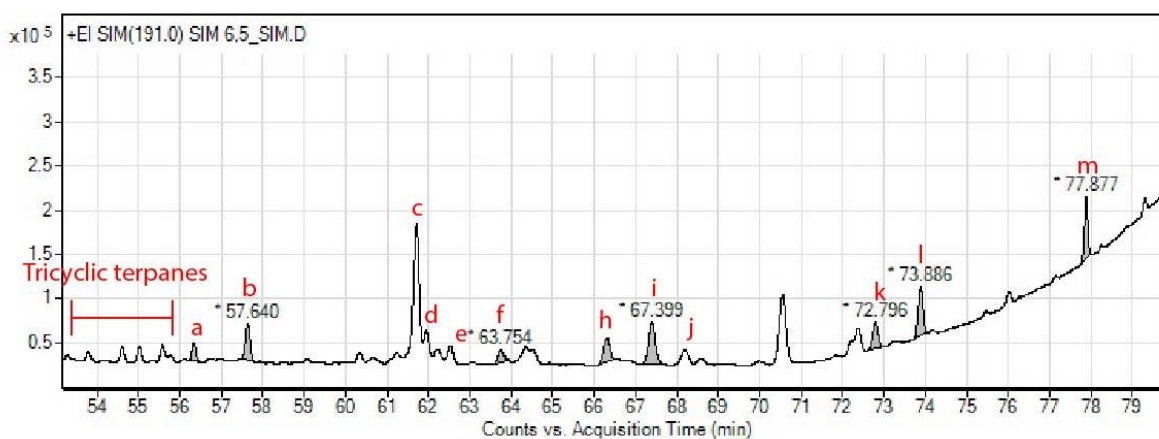


## Sample ID MM16 Mudstone

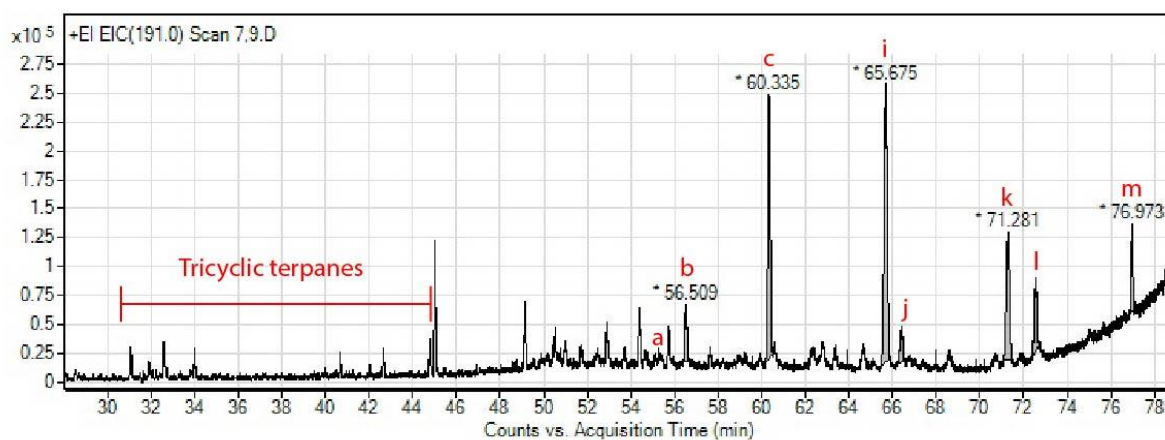


## 2.2 Location: Mae Than coal mine

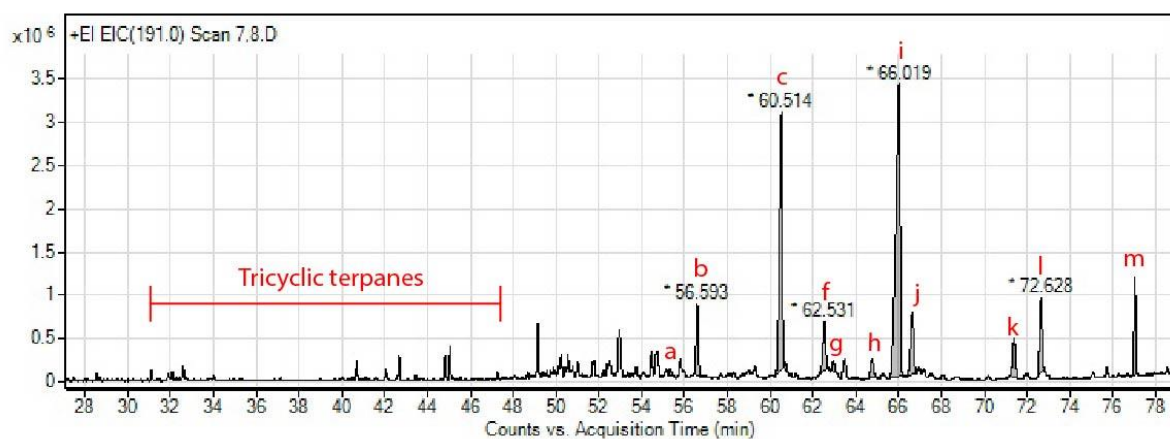
## Sample ID TM1 Mudstone



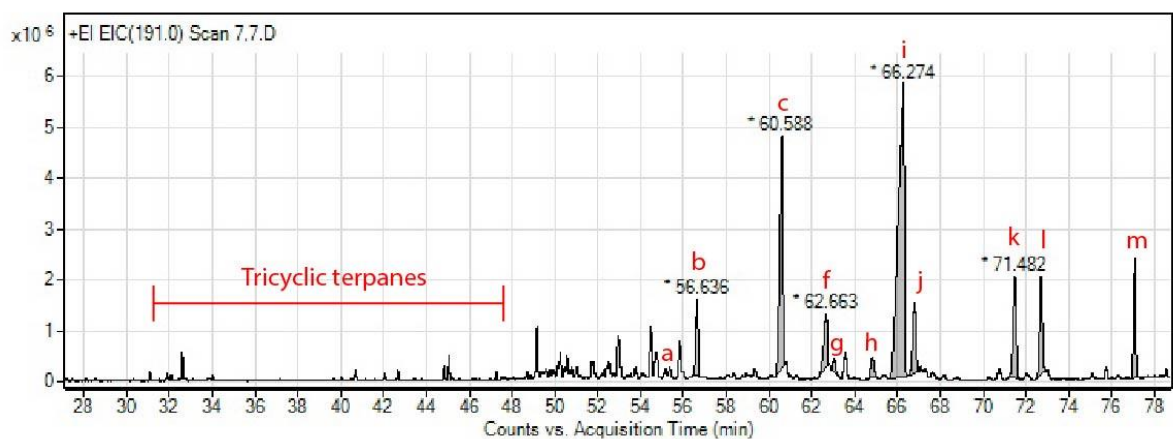
## Sample ID TM2 Mudstone



## Sample ID TC3 Coal

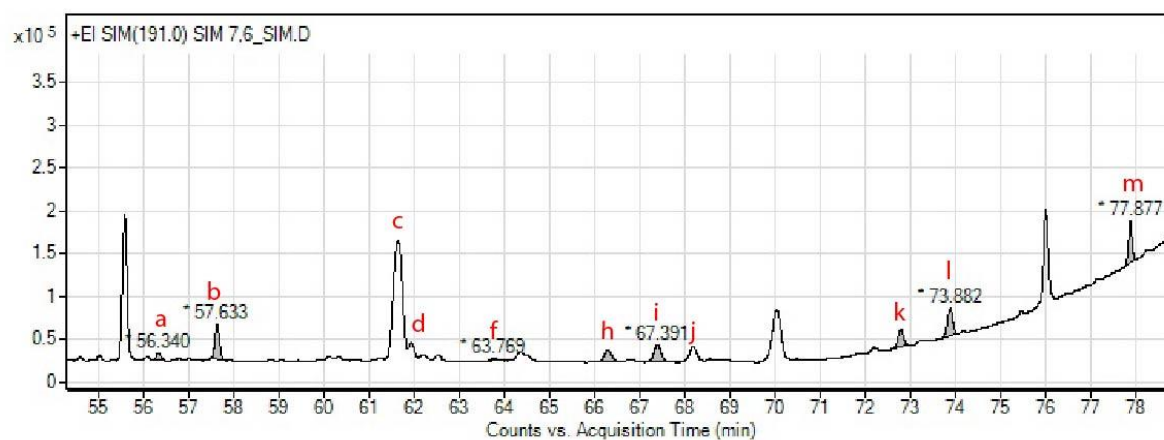


## Sample ID TC4 Coal

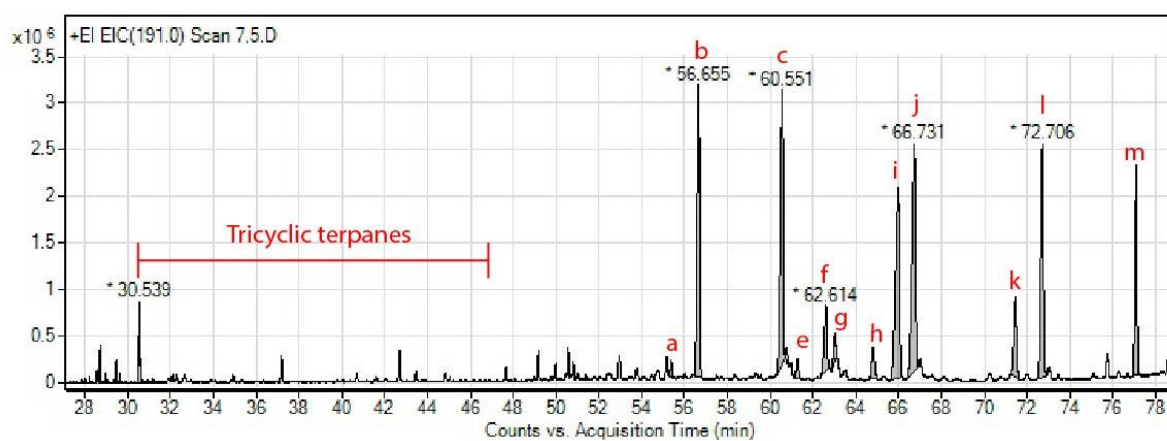




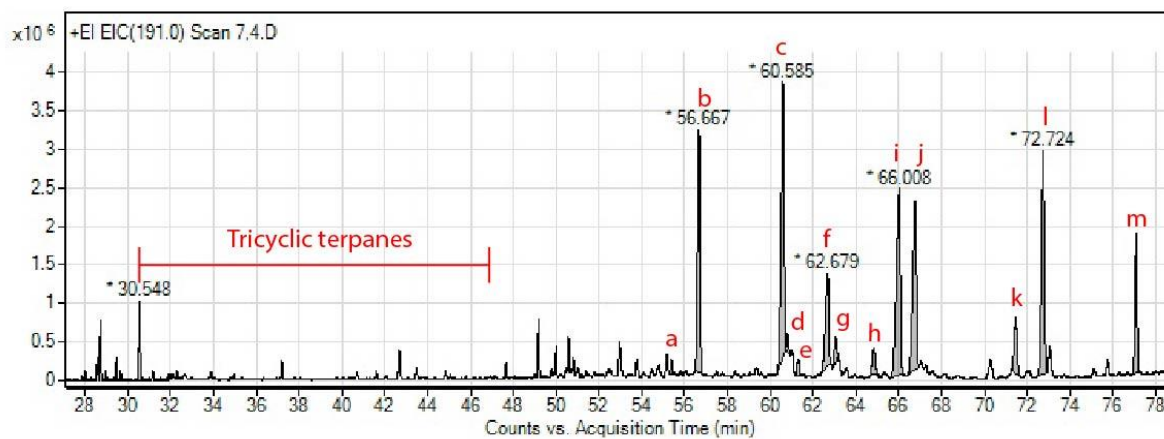
## Sample ID TM5 Mudstone



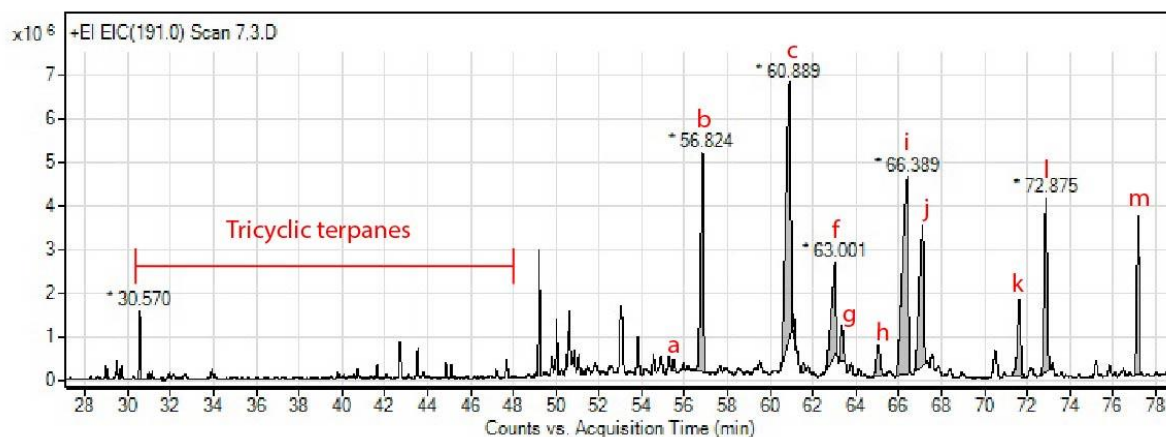
## Sample ID TS6 Shale



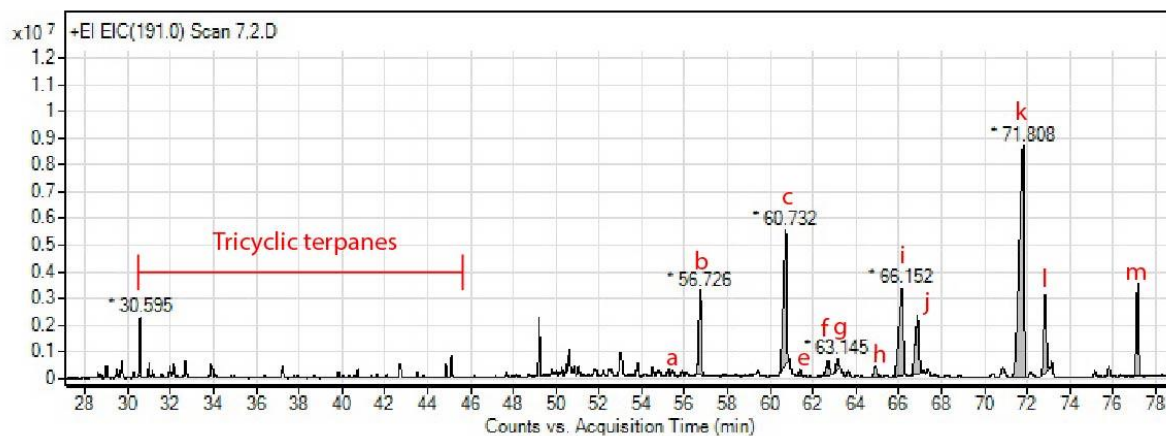
## Sample ID TS7 Shale



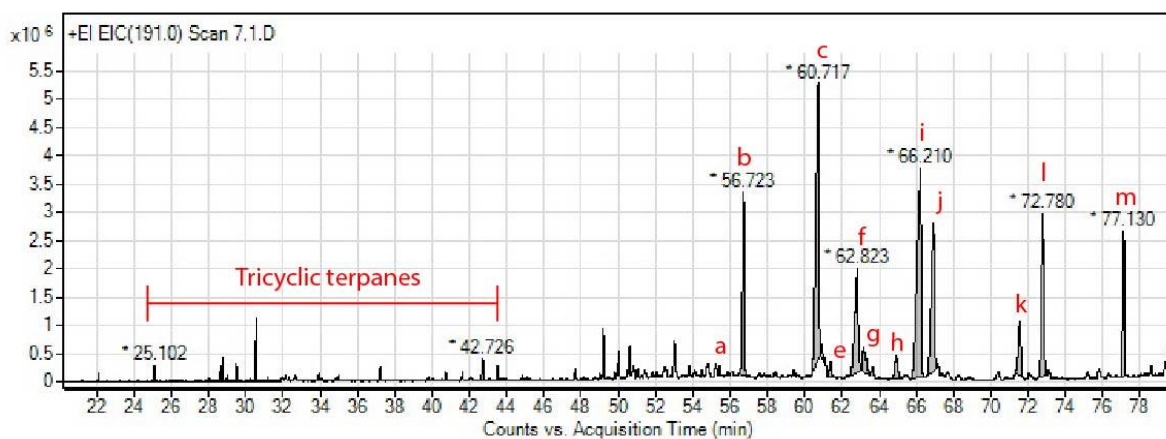
## Sample ID TC8 Coal



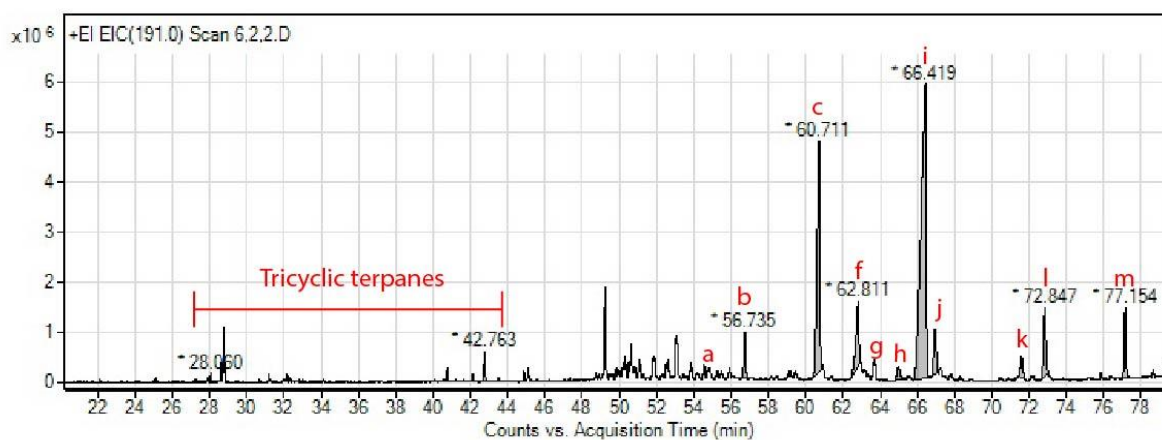
## Sample ID TC9 Coal



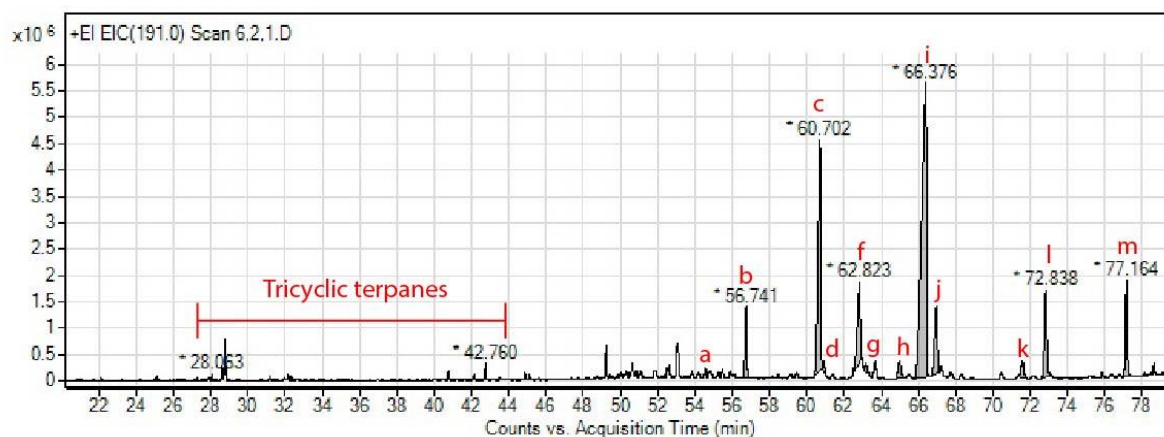
## Sample ID TC10 Coal



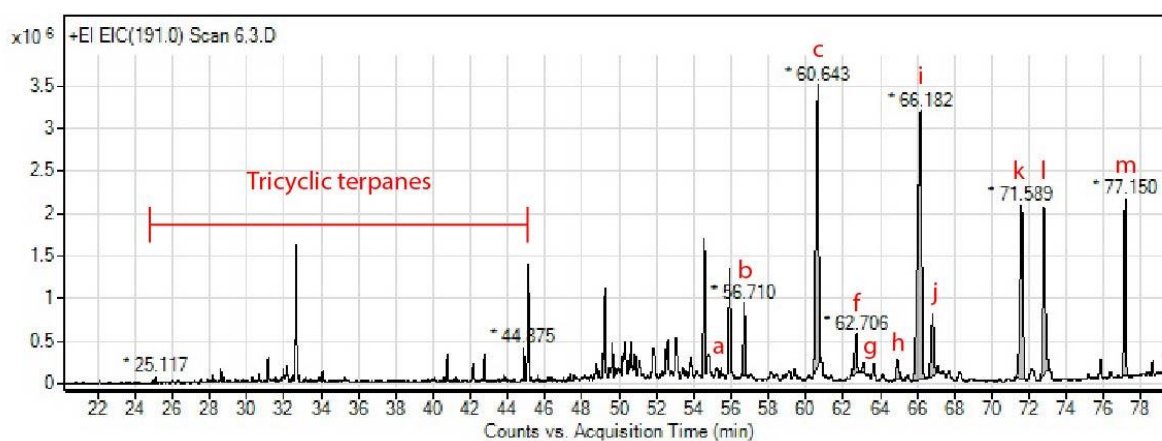
## Sample ID TC11 Coal



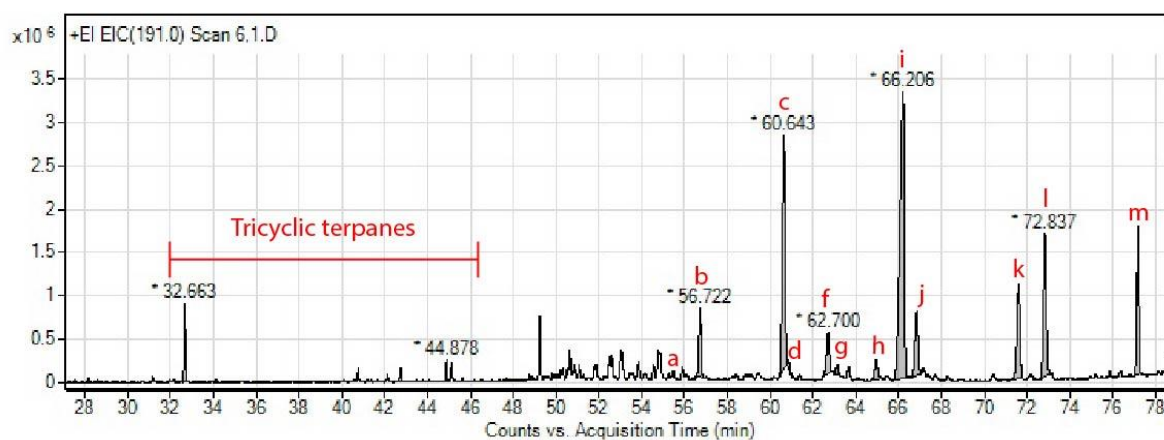
## Sample ID TS12 Shale



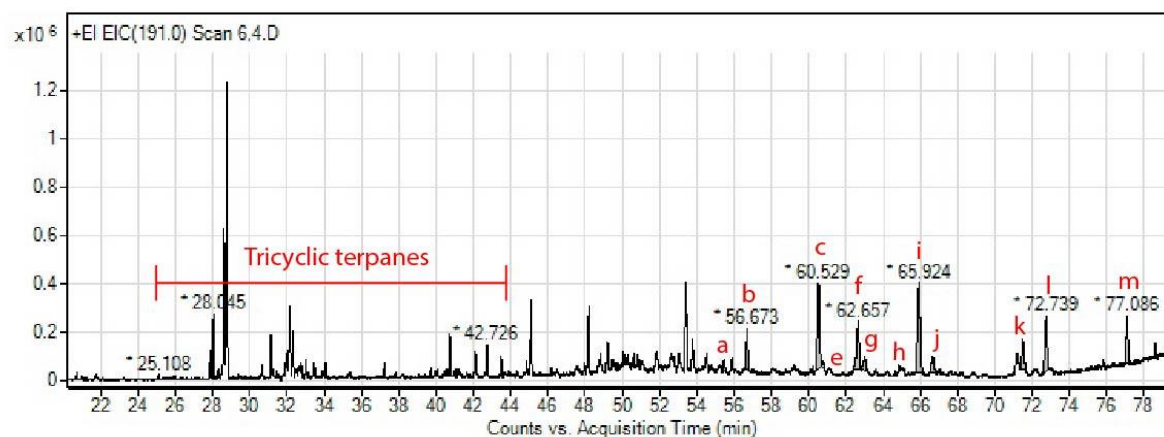
## Sample ID TC13 Coal



## Sample ID TS14 Shale



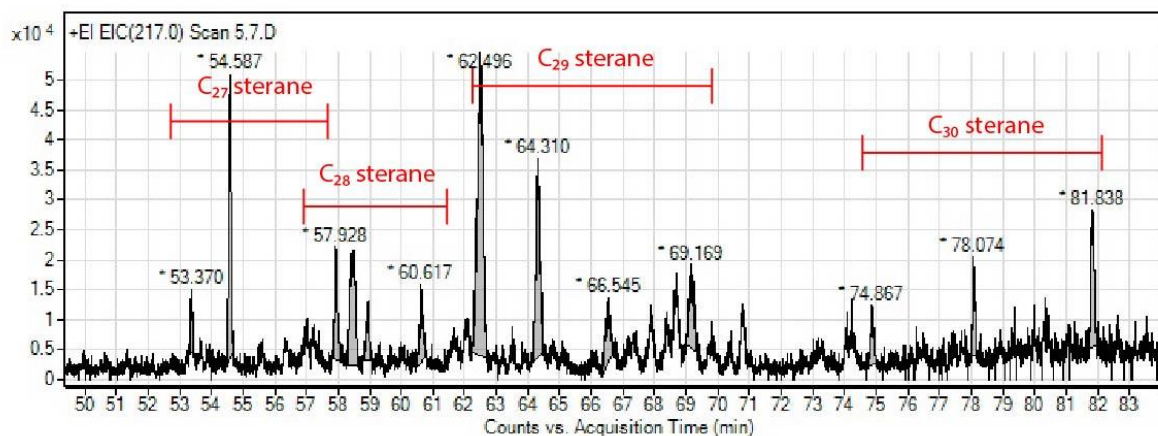
## Sample ID TC15 Coal



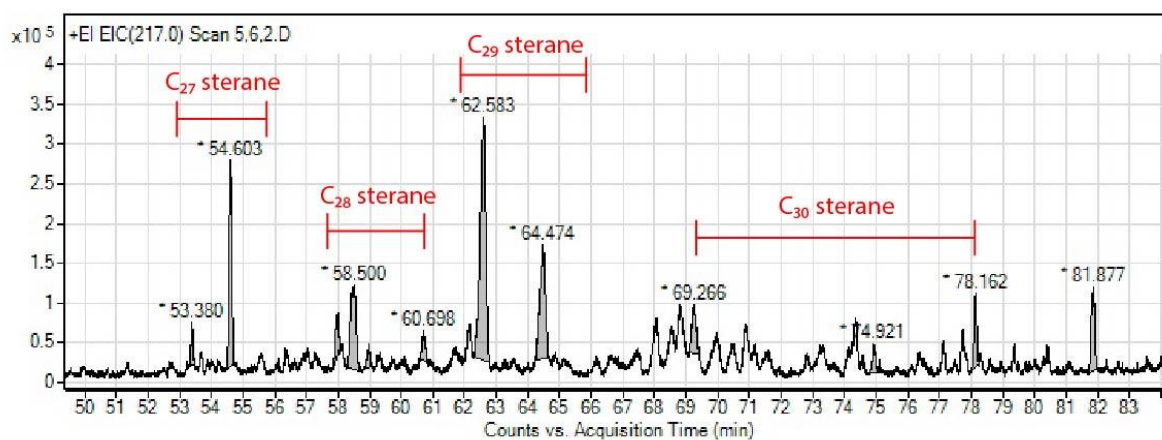
## 3. m/z 217 ion chromatograms showing and sterane distribution

## 3.1 Location: Mae Teep coal mine

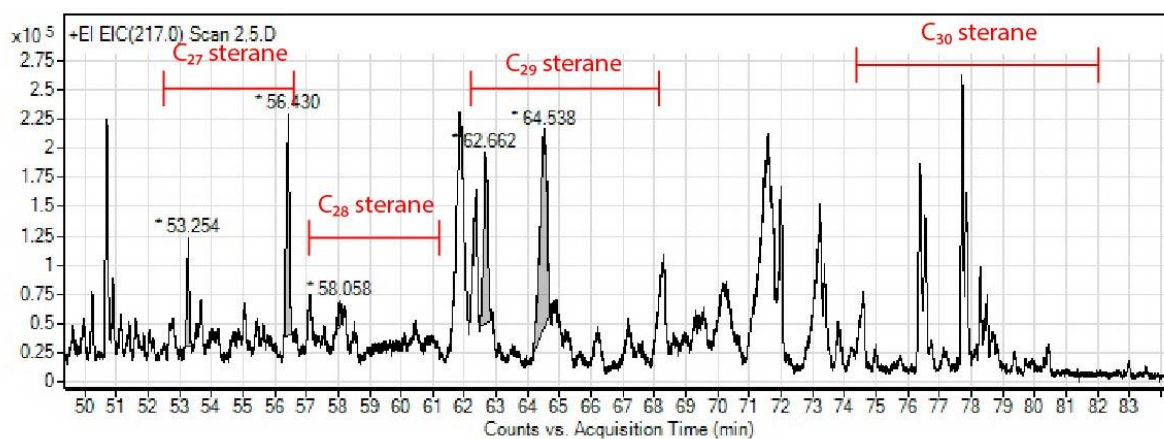
## Sample ID MS1 Shale



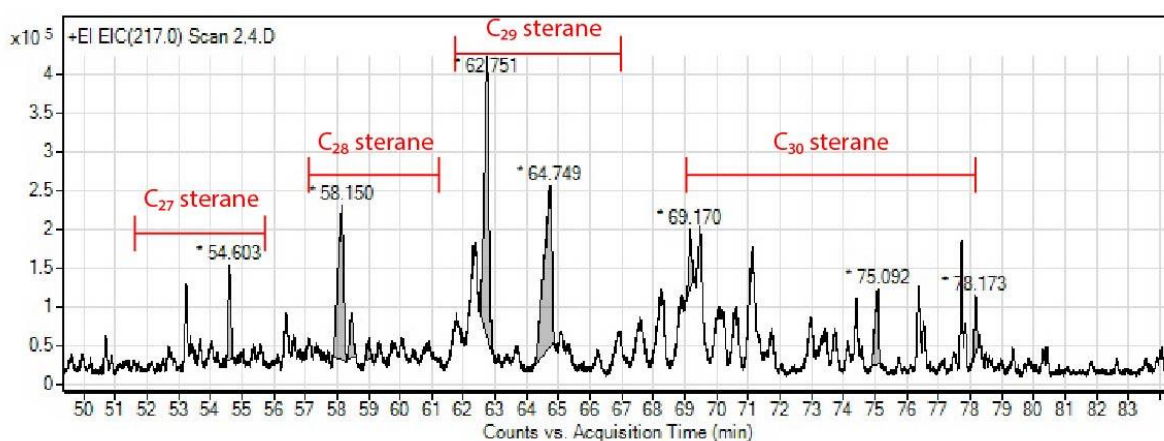
## Sample ID MS2 Shale



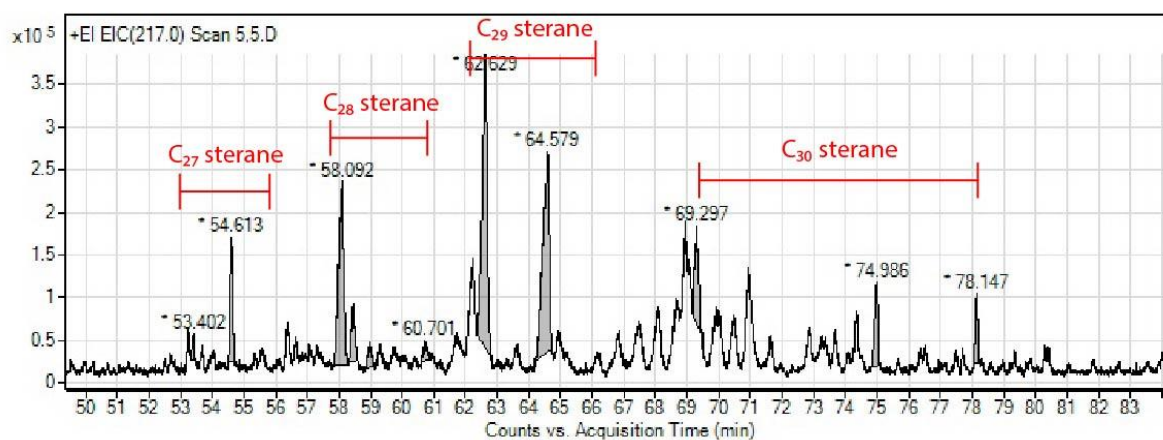
## Sample ID MC3 Coal



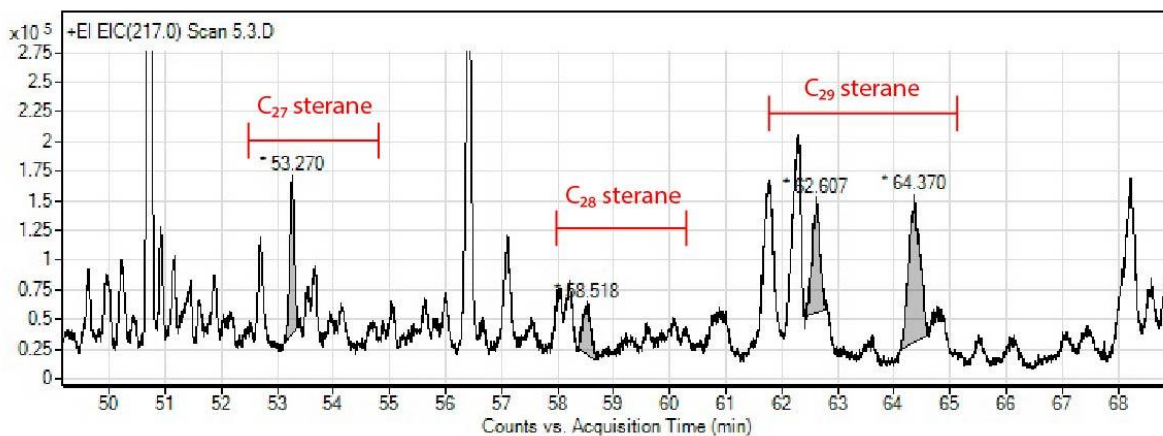
## Sample ID MS4 Oil shale



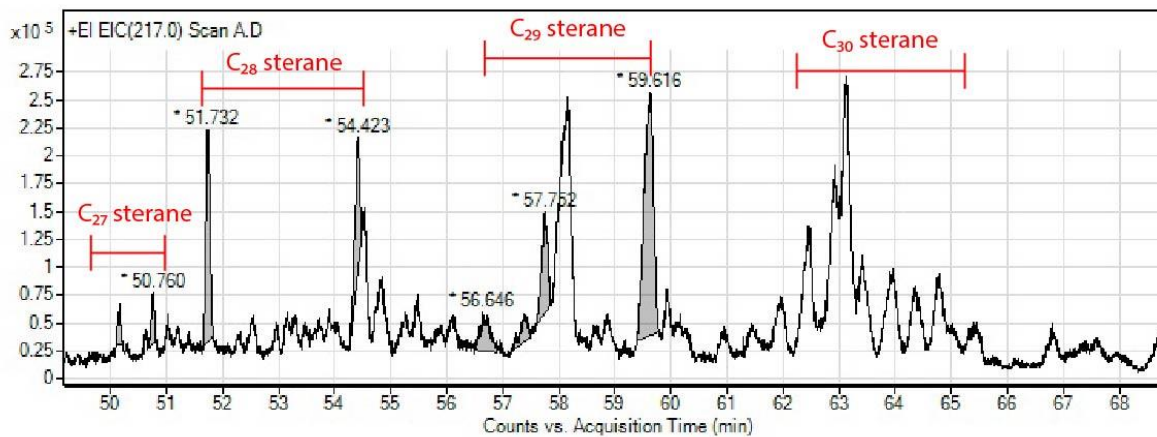
## Sample ID MS5 Oil shale



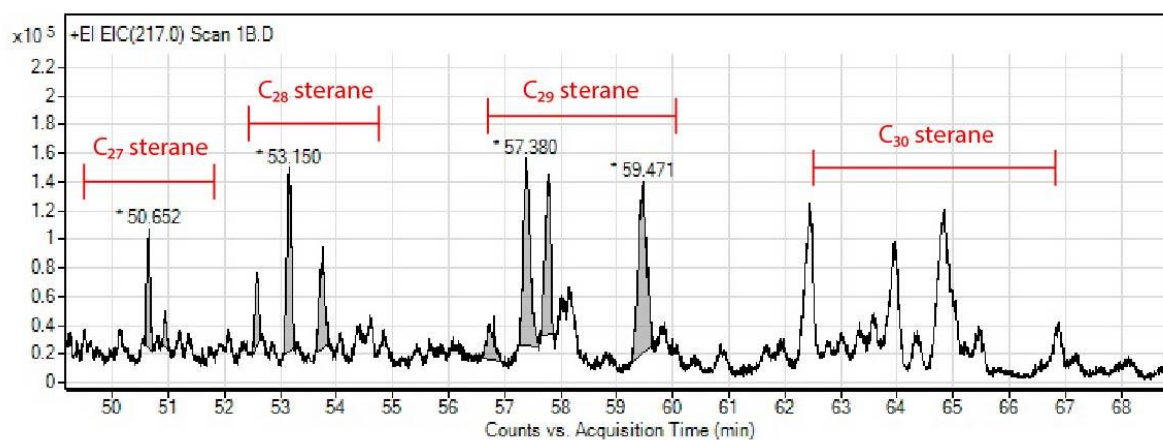
## Sample ID MC6 Coal



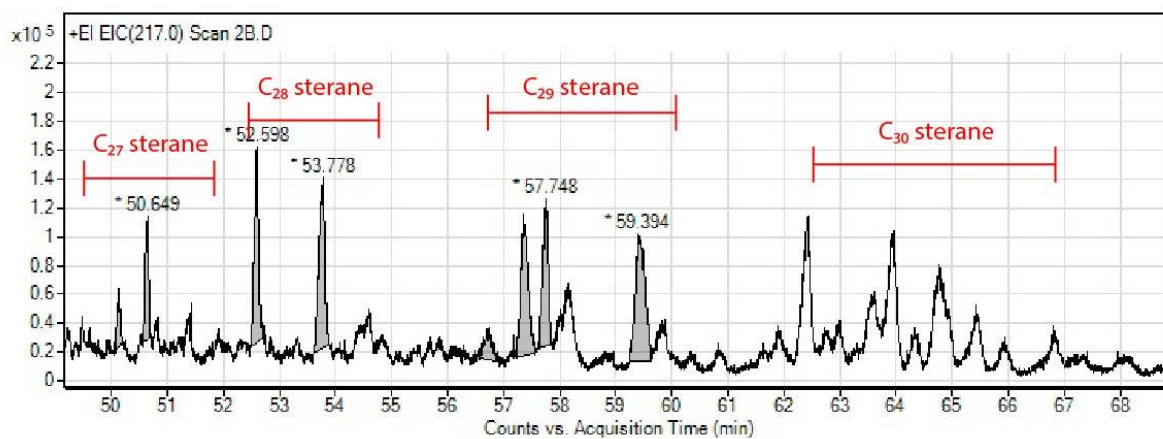
## Sample ID MS7 Oil shale



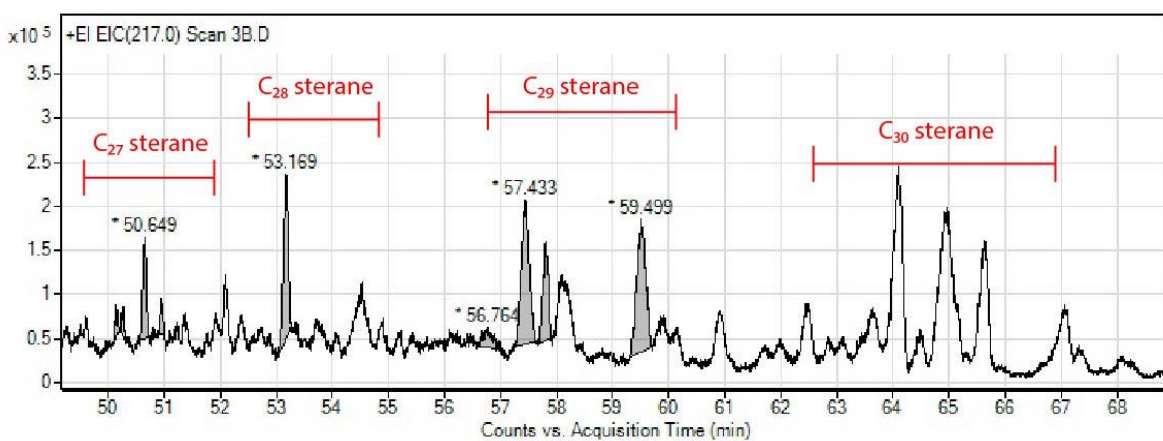
## Sample ID MC8 Coal



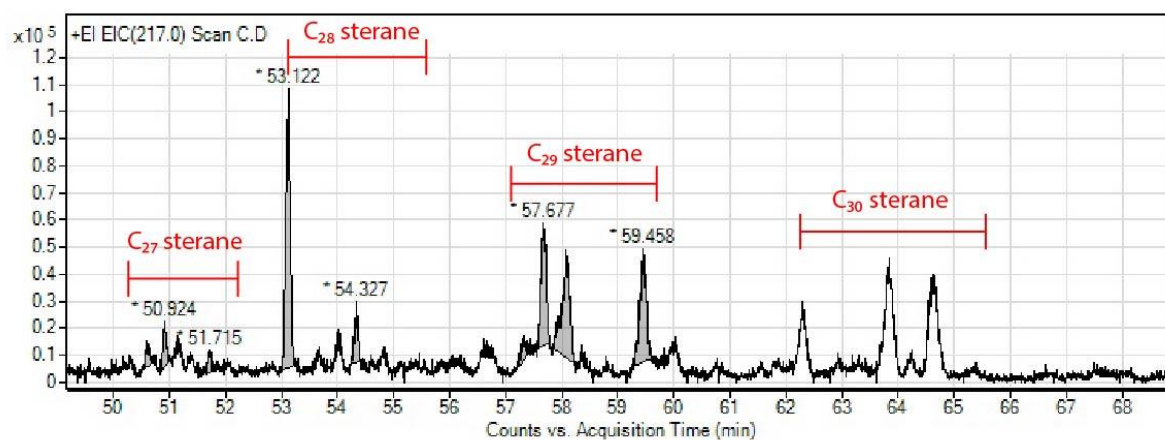
## Sample ID MC9 Coal



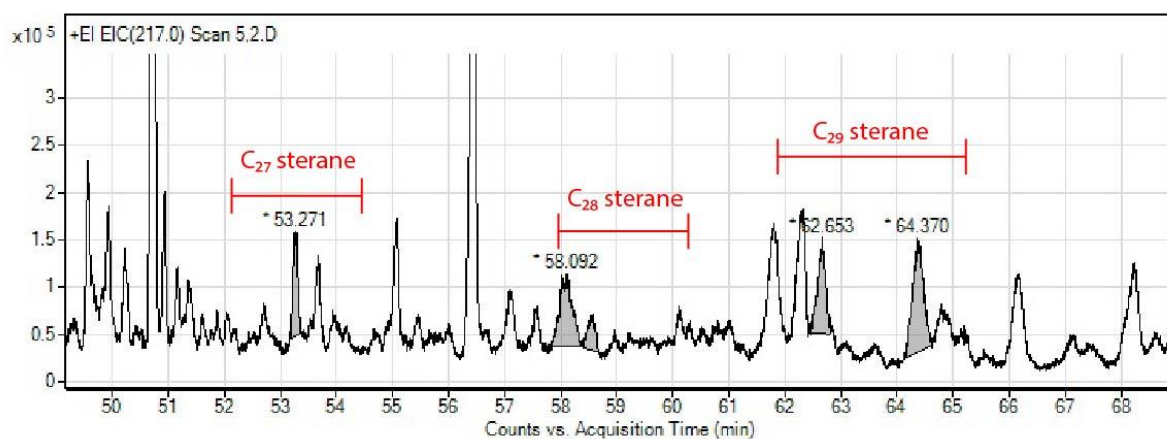
## Sample ID MC10 Coal



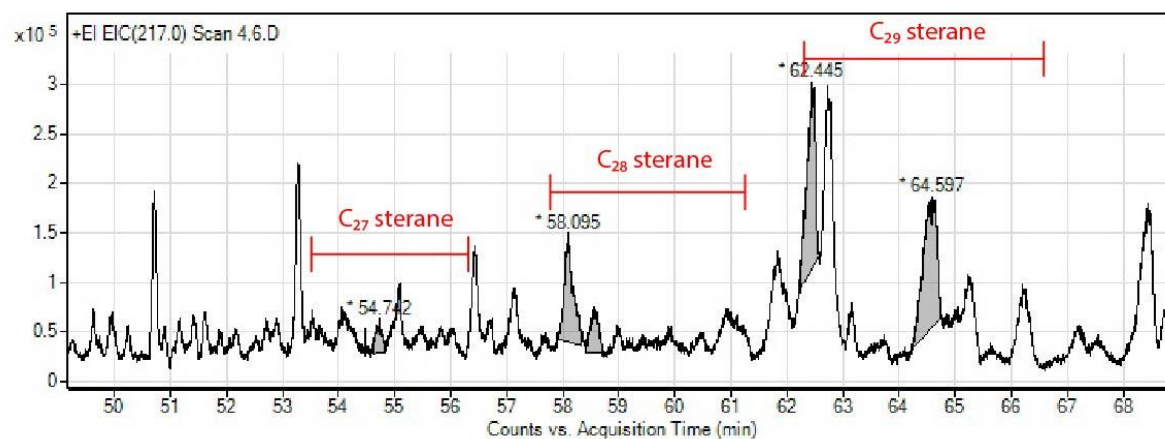
## Sample ID MM11 Mudstone



## Sample ID MC12 Coal

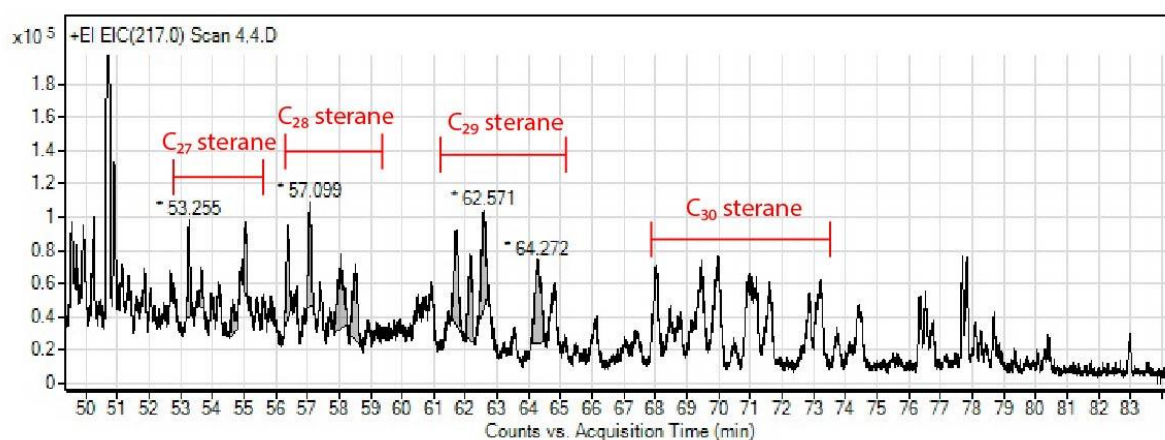


## Sample ID MC13 Coal

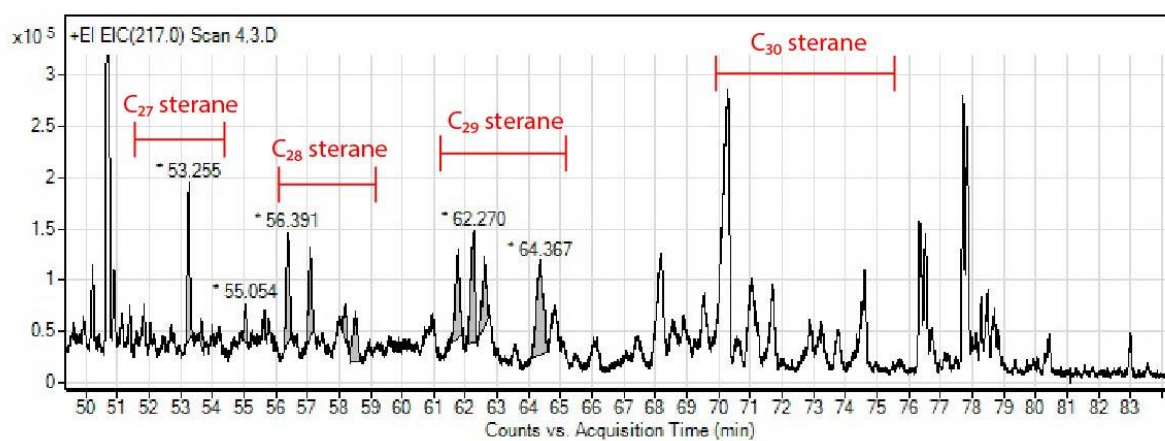




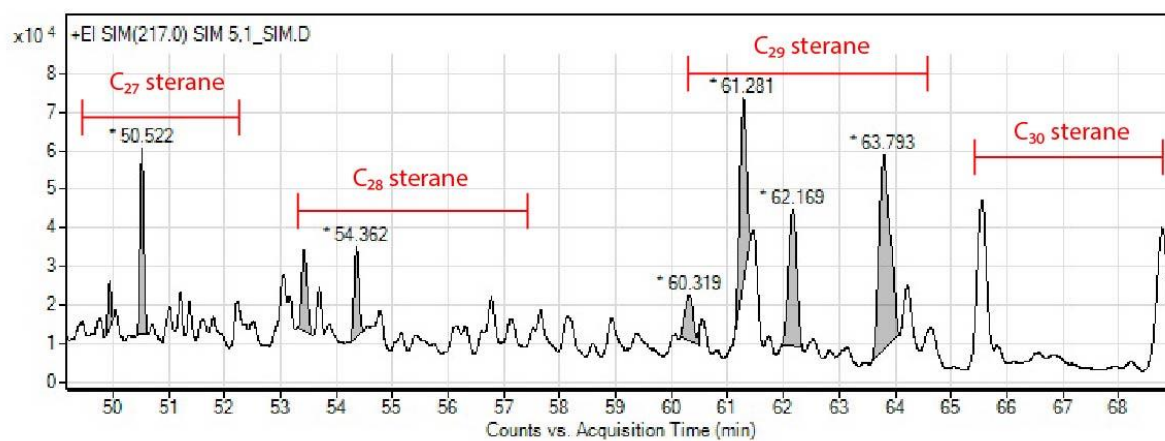
## Sample ID MC14 Coal



## Sample ID MC15 Coal

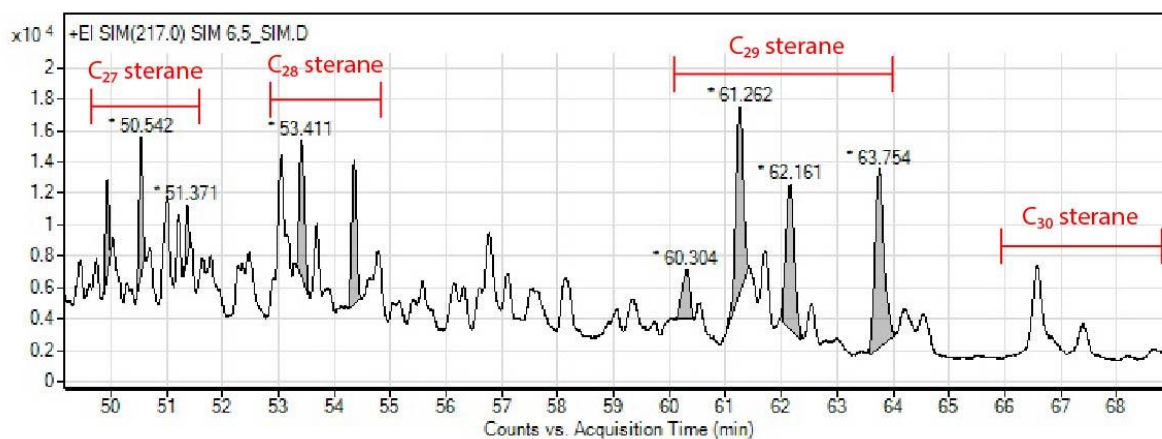


## Sample ID MM16 Mudstone

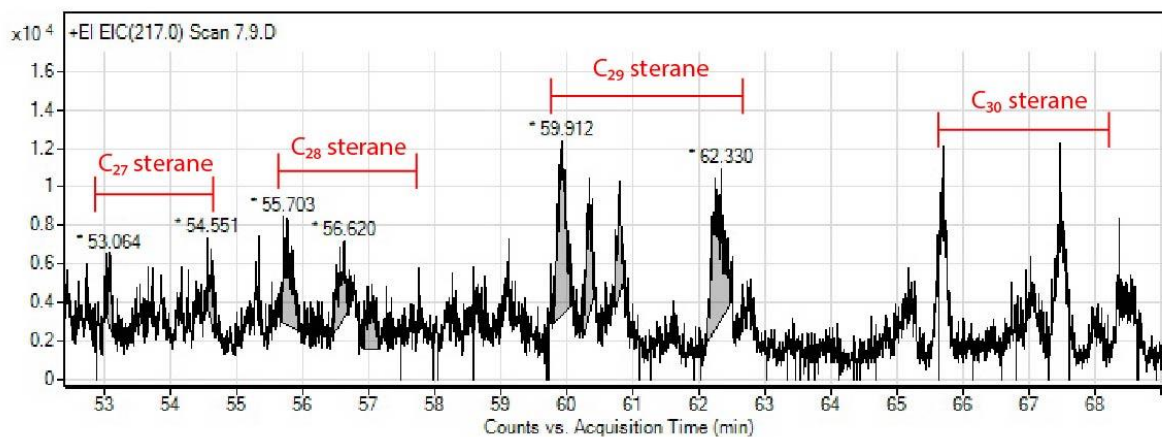


## 3.2 Location: Mae Than coal mine

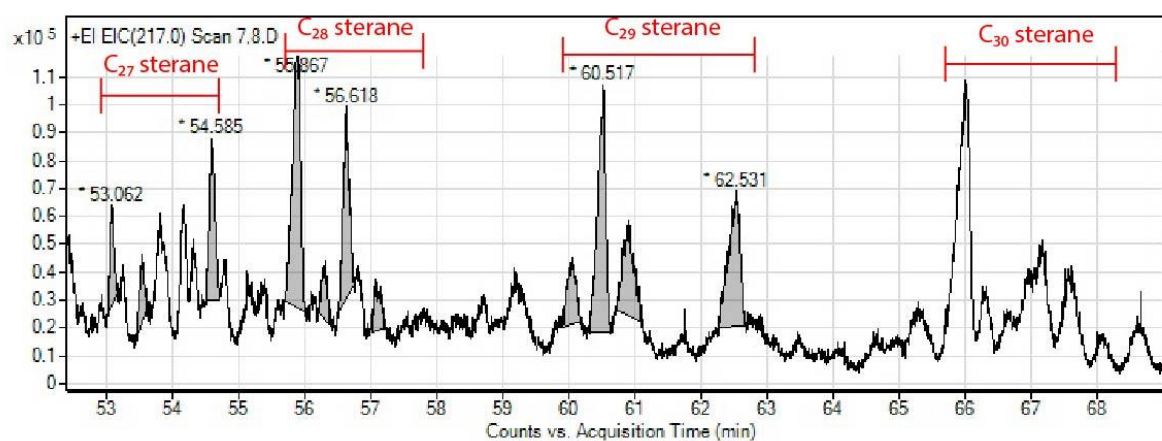
Sample ID TM1 Mudstone



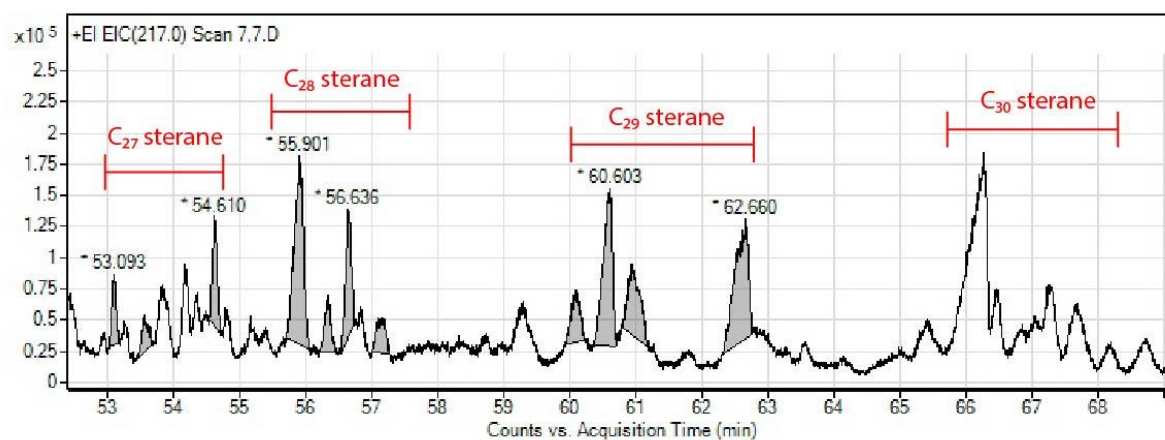
Sample ID TM2 Mudstone



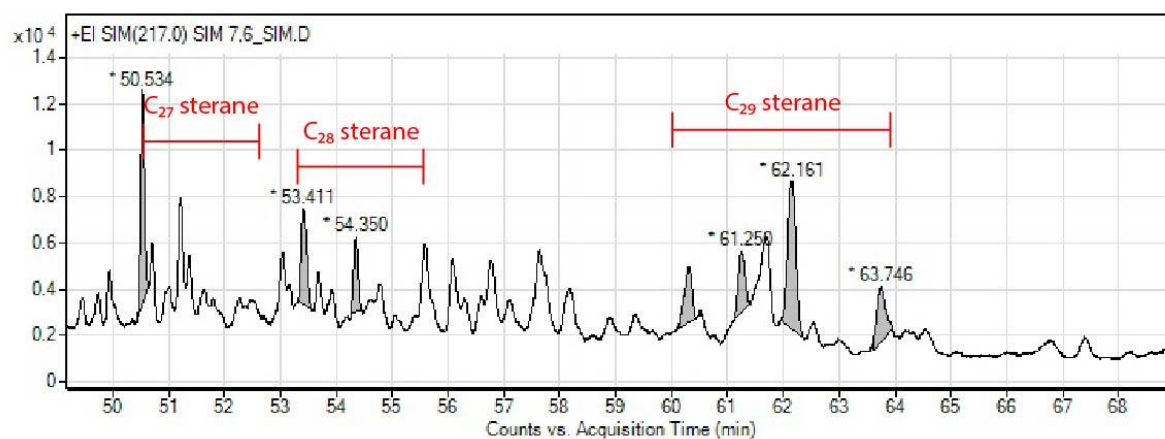
Sample ID TC3 Coal



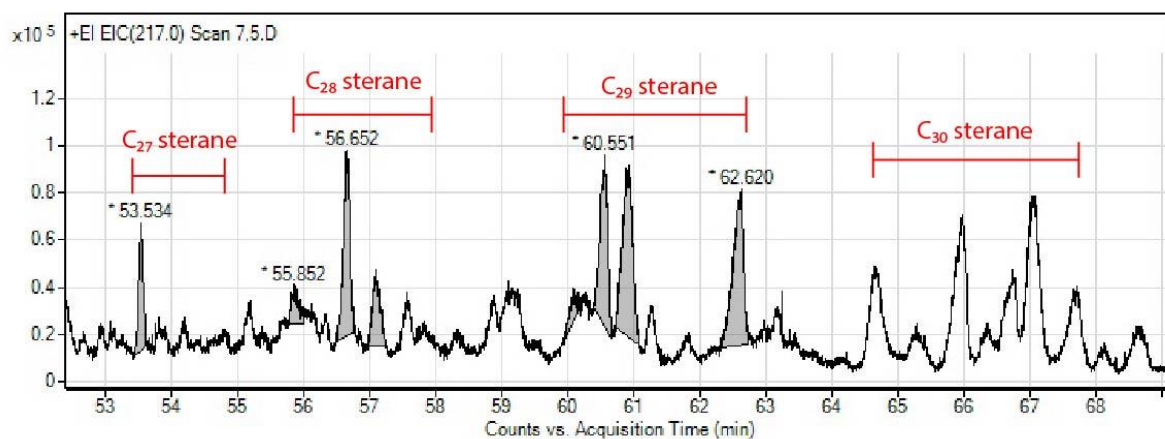
## Sample ID TC4 Coal



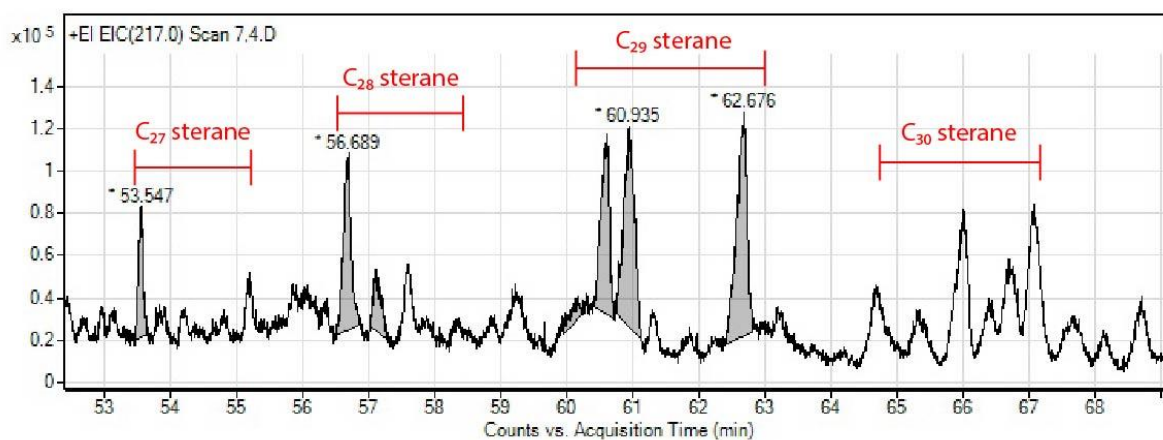
## Sample ID TM5 Mudstone



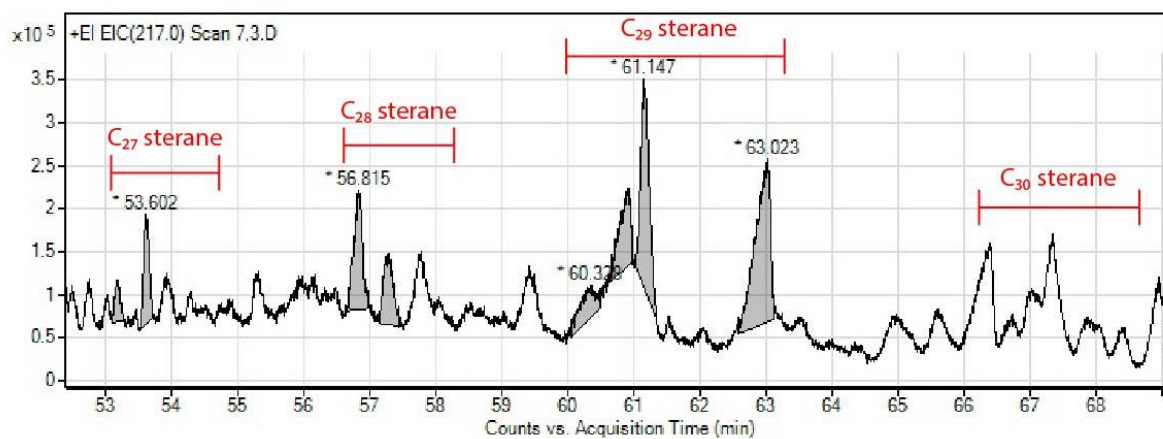
## Sample ID TS6 Shale



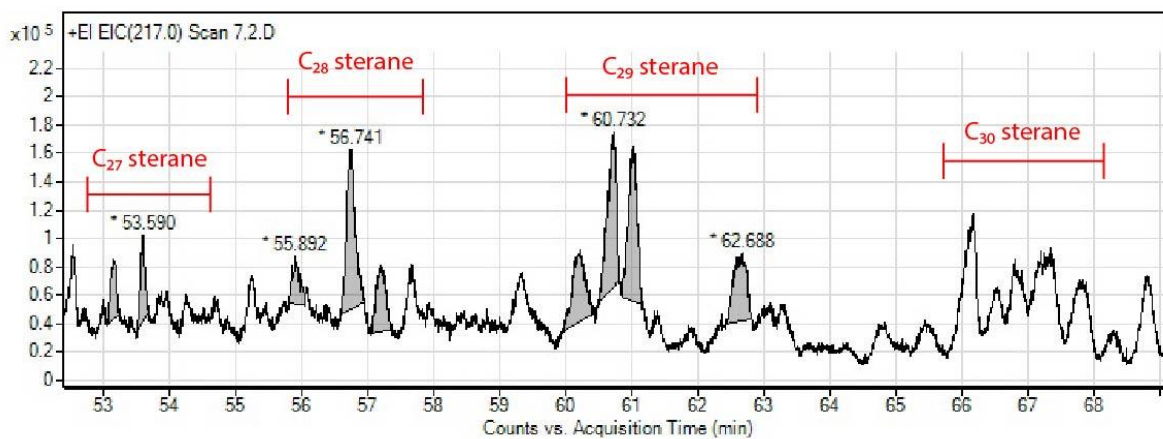
## Sample ID TS7 Shale



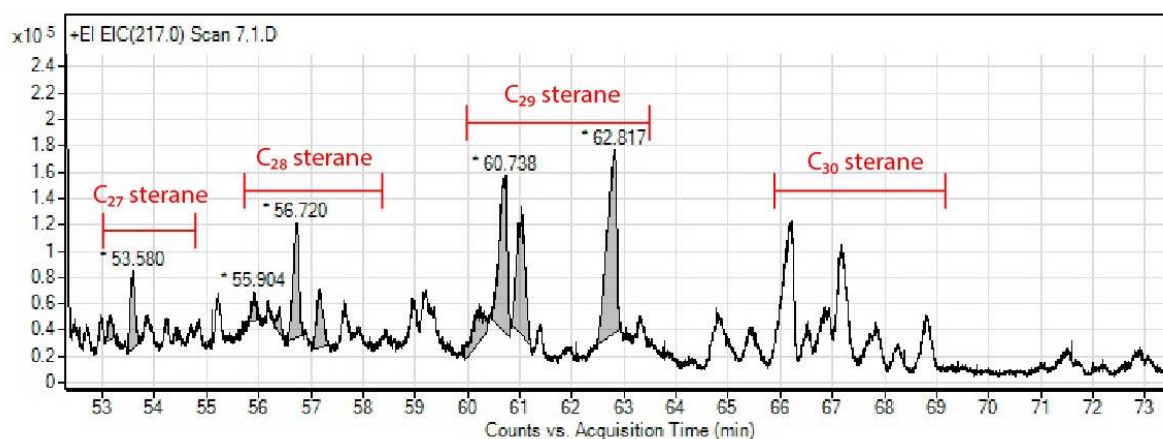
## Sample ID TC8 Coal



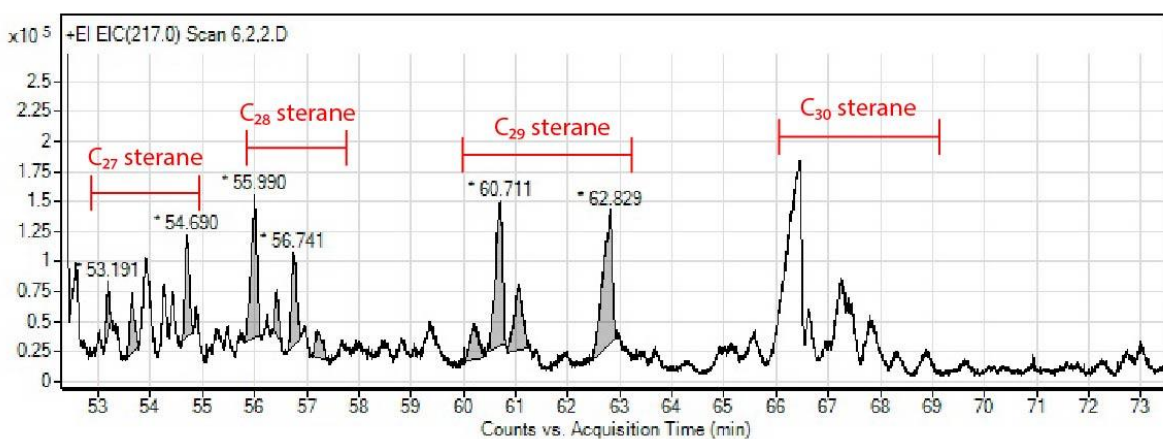
## Sample ID TC9 Coal



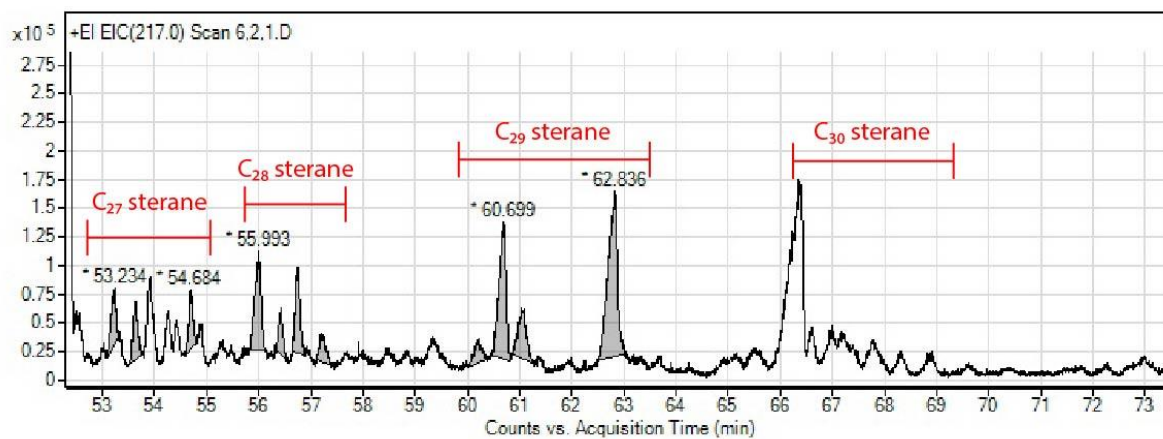
## Sample ID TC10 Coal



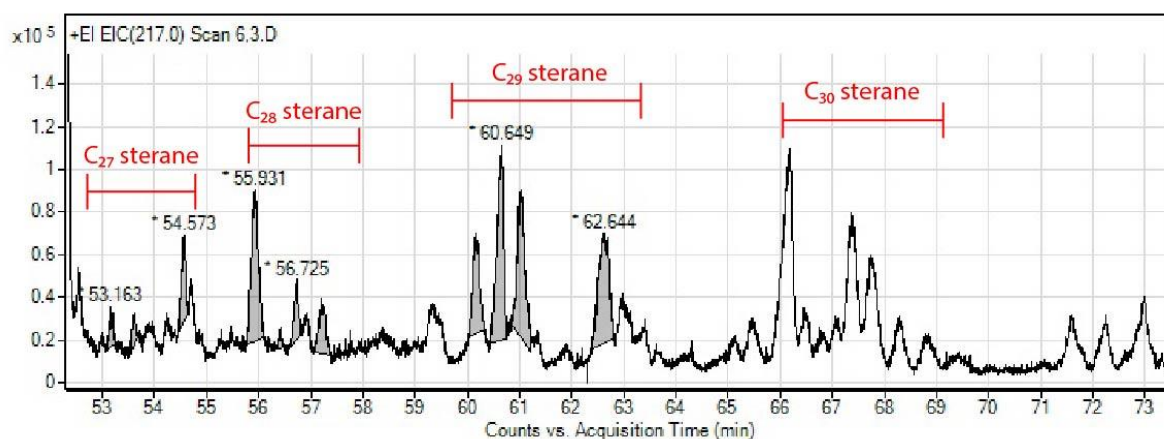
## Sample ID TC11 Coal



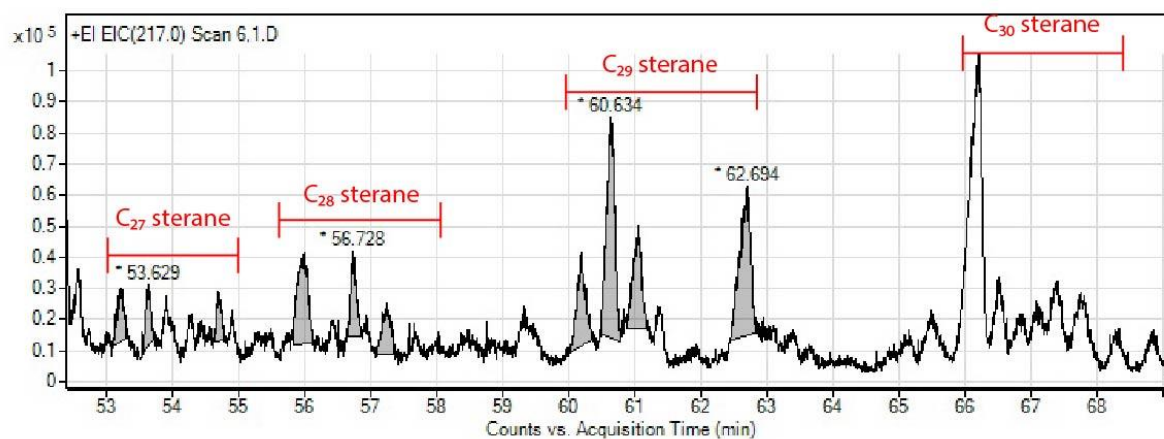
## Sample ID TS12 Shale



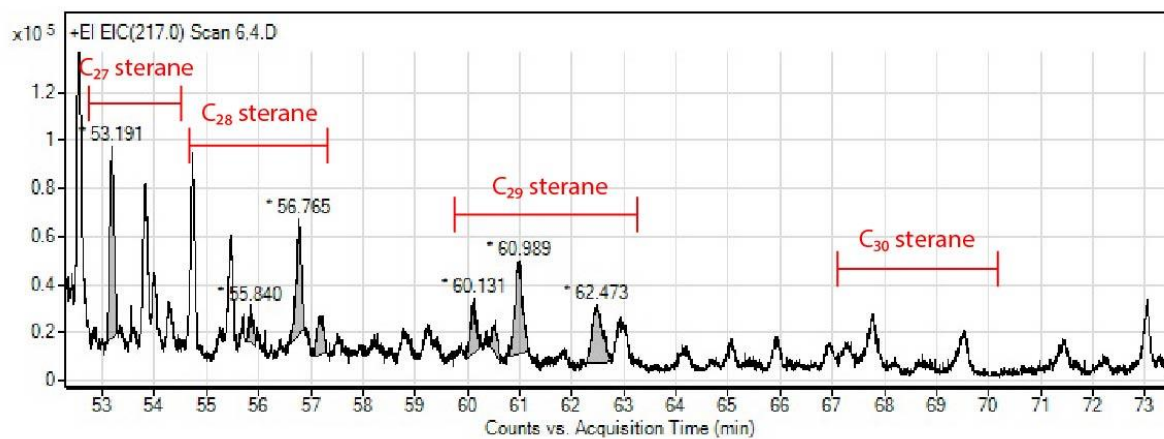
Sample ID TC13 Coal



Sample ID TS14 Shale



Sample ID TC15 Coal



## REFERENCES

- Alias, F. L., Abdullah, W. H., Hakimi, M. H., Azhar, M. H., and Kugler, R. L. (2012). Organic geochemical characteristics and depositional environment of the Tertiary Tanjong Formation coals in the Pinangah area, onshore Sabah, Malaysia. *International Journal of Coal Geology*, 104, 9-21.
- ASTM. (1991). *Annual Book of ASTM Standards. Sec 05.05. Standard Test Method for Gross Calorific Value of Coal and Coke by Adiabatic Bomb Calorimeter*.
- Audley-Charles, M. (1988). Evolution of the southern margin of Tethys (North Australian region) from early Permian to late Cretaceous. *Geological Society, London, Special Publications*, 37(1), 79-100.
- Barber, A., and Crow, M. (2003). An evaluation of plate tectonic models for the development of Sumatra. *Gondwana Research*, 6(1), 1-28.
- Barber, A., Crow, M., and De Smet, M. (2005). Tectonic evolution. *Geological Society, London, Memoirs*, 31(1), 234-259.
- Bates, R. L., and Jackson, J. A. (1987). Glossary of geology.
- Boreham, C. J., and Powell, T. G. (1993). Petroleum Source Rock Potential of Coal and Associated Sediments: Qualitative and Quantitative Aspects: Chapter 6.
- Bourbonniere, R. A., and Meyers, P. A. (1996). Sedimentary geolipid records of historical changes in the watersheds and productivities of Lakes Ontario and Erie. *Limnology and Oceanography*, 41(2), 352-359.
- Brassell, S., Eglinton, G., and Maxwell, J. (1983). The geochemistry of terpenoids and steroids. *Biochemical Society Transactions*, 11(5), 575-586.
- Bray, E. E., and Evans, E. D. (1965). Hydrocarbons in non-reservoir-rock source beds. *AAPG Bulletin*, 49(3), 248-257.
- Brooks, J., Gould, K., and Smith, J. (1969). Isoprenoid hydrocarbons in coal and petroleum. *Nature*, 222(5190), 257-259.
- Bustin, R. M., Cameron, A., Grieve, D., and Kalkreuth, W. (1985). *Coal petrology: its principles, methods, and applications*.
- Chamchoy, P. (2014). *Petroleum Geochemistry of Huai Hin Lat Formation, Northeastern Thailand*. Chulalongkorn University,
- Chandra, K., Mishra, C., Samanta, U., Gupta, A., and Mehrotra, K. (1994). Correlation of different maturity parameters in the Ahmedabad-Mehsana block of the Cambay basin. *Organic Geochemistry*, 21(3-4), 313-321.
- Chaodumrong, P., Ukakimapan, Y., Snansieng, S., Janmaha, S., Pradidtan, S., and Leow, N. S. (1983). *A review of the Tertiary sedimentary rocks of Thailand*. Paper presented at the Workshop on stratigraphic correlation of Thailand and Malaysia.
- Charusiri, P., and Pum-Im, S. (2009). Cenozoic tectonic evolution of major sedimentary basins in Central, Northern, and the Gulf of Thailand. *BEST*, 2(1&2), 40-62.
- Chu, G., Xiao, L., Jin, Z., Lin, M., and Blokhin, M. G. (2015). The relationship between trace element concentrations and coal-forming environments in the No. 6 coal seam, Haerwusu Mine, China. *Energy Exploration & Exploitation*, 33(1), 91-104.
- Clark, J., RC, and Blumer, M. (1967). DISTRIBUTION OF n-PARAFFINS IN MARINE ORGANISMS AND SEDIMENT 1. *Limnology and Oceanography*, 12(1), 79-87.

- Clayton, J. (1993). Composition of Crude Oils Generated from Coals and Coaly Organic Matter in Shales: Chapter 8.
- Commendatore, M. G., Nievas, M. L., Amin, O., and Esteves, J. L. (2012). Sources and distribution of aliphatic and polyaromatic hydrocarbons in coastal sediments from the Ushuaia Bay (Tierra del Fuego, Patagonia, Argentina). *Marine environmental research*, 74, 20-31.
- Connan, J., Bouroullec, J., Dessort, D., and Albrecht, P. (1986). The microbial input in carbonate-anhydrite facies of a sabkha palaeoenvironment from Guatemala: a molecular approach. *Organic Geochemistry*, 10(1-3), 29-50.
- Coster, P., Benammi, M., Chaimanee, Y., Yamee, C., Chavasseau, O., Emonet, E.-G., and Jaeger, J.-J. (2010). A complete magnetic-polarity stratigraphy of the Miocene continental deposits of Mae Moh Basin, northern Thailand, and a reassessment of the age of hominoid-bearing localities in northern Thailand. *GSA Bulletin*, 122(7-8), 1180-1191.
- Cranwell, P. (1977). Organic geochemistry of Cam Loch (Sutherland) sediments. *Chemical Geology*, 20, 205-221.
- Cranwell, P. (1984). Lipid geochemistry of sediments from Upton Broad, a small productive lake. *Organic Geochemistry*, 7(1), 25-37.
- Cranwell, P., Eglinton, G., and Robinson, N. (1987). Lipids of aquatic organisms as potential contributors to lacustrine sediments—II. *Organic Geochemistry*, 11(6), 513-527.
- Cranwell, P. A. (1973). Chain-length distribution of n-alkanes from lake sediments in relation to post-glacial environmental change. *Freshwater Biology*, 3(3), 259-265.
- Dahl, J., Moldowan, J. M., and Sundararaman, P. (1993). Relationship of biomarker distribution to depositional environment: Phosphoria Formation, Montana, USA. *Organic Geochemistry*, 20(7), 1001-1017.
- Dai, S., Bechtel, A., Eble, C. F., Flores, R. M., French, D., Graham, I. T., Hood, M. M., Hower, J. C., Korasidis, V. A., and Moore, T. A. (2020). Recognition of peat depositional environments in coal: A review. *International Journal of Coal Geology*, 219, 103383.
- Damsté, J. S. S., Rijpstra, W. I. C., Hopmans, E. C., Prahl, F. G., Wakeham, S. G., and Schouten, S. (2002). Distribution of membrane lipids of planktonic Crenarchaeota in the Arabian Sea. *Applied and Environmental Microbiology*, 68(6), 2997-3002.
- Dević, G. J., and Popović, Z. V. (2013). Biomarker and micropetrographic investigations of coal from the Krepoljin Brown Coal Basin Serbia. *International Journal of Coal Geology*, 105, 48-59.
- Didyk, B., Simoneit, B., Brassell, S. t., and Eglinton, G. (1978). Organic geochemical indicators of palaeoenvironmental conditions of sedimentation. *Nature*, 272(5650), 216-222.
- Dommain, R., Couwenberg, J., and Joosten, H. (2011). Development and carbon sequestration of tropical peat domes in south-east Asia: links to post-glacial sea-level changes and Holocene climate variability. *Quaternary Science Reviews*, 30(7-8), 999-1010.
- Donmuang, K., Asnachinda, P., Limtrakun, P., and Khandarosa, B. R. a. W. (2014). Mineralogical Variation of Sedimentary Clay Deposit at Mae Than Mine, Ban



- Mae Than, Amphoe Mae Tha, Lampang Province, Thailand. *J. Appl. Geol. Geophys.*, 2, 16-21.
- Ducrocq, S., Chaimanee, Y., Suteethorn, V., and Jaeger, J.-J. (1995). Mammalian faunas and the ages of the continental Tertiary fossiliferous localities from Thailand. *Journal of Southeast Asian Earth Sciences*, 12(1-2), 65-78.
- Durand, B. (1980). *Kerogen: Insoluble organic matter from sedimentary rocks*: Editions technip.
- El Diasty, W. S., El Beialy, S., Mahdi, A., and Peters, K. (2016). Geochemical characterization of source rocks and oils from northern Iraq: Insights from biomarker and stable carbon isotope investigations. *Marine and Petroleum Geology*, 77, 1140-1162.
- El Nady, M. (2008). Biomarkers assessment of crude oils and extracts from Jurassic-Cretaceous rocks, North Qattara Depression, North Western Desert, Egypt. *Petroleum science and technology*, 26(9), 1063-1082.
- Erik, N. Y., and Sancar, S. (2010). Relationships between coal-quality and organic-geochemical parameters: A case study of the Hafik coal deposits (Sivas Basin, Turkey). *International Journal of Coal Geology*, 83(4), 396-414.
- Fabiańska, M. J., and Kurkiewicz, S. (2013). Biomarkers, aromatic hydrocarbons and polar compounds in the Neogene lignites and gangue sediments of the Konin and Turoszów Brown Coal Basins (Poland). *International Journal of Coal Geology*, 107, 24-44.
- Fenton, C. H., Charusiri, P., and Wood, S. H. (2003). Recent paleoseismic investigations in Northern and Western Thailand. *Annals of Geophysics*.
- Ferm, J., and Horne, J. (1979). Carboniferous depositional environments in the Appalachian region: Columbia. *Department of Geology, University of South Carolina*.
- Ferm, J., and Weisenfluh, G. (1989). Evolution of some depositional models in Late Carboniferous rocks of the Appalachian coal fields. *International Journal of Coal Geology*, 12(1-4), 259-292.
- Ferm, J. C. (1976). Depositional models in coal exploration and development.
- Ficken, K. J., Li, B., Swain, D., and Eglinton, G. (2000). An n-alkane proxy for the sedimentary input of submerged/floating freshwater aquatic macrophytes. *Organic Geochemistry*, 31(7-8), 745-749.
- Friederich, M. C., Moore, T. A., and Flores, R. M. (2016). A regional review and new insights into SE Asian Cenozoic coal-bearing sediments: Why does Indonesia have such extensive coal deposits? *International Journal of Coal Geology*, 166, 2-35.
- Gasse, F. (1990). Tectonic and Climatic Controls on Lake Distribution and Environments in Afar from Miocene to Present: Chapter 2.
- Gibling, M., and Ratanasthien, B. (1980). Cenozoic basins of Thailand and their coal deposits: a preliminary report.
- Gibling, M., Ukakimaphan, Y., and Srisuk, S. (1981). Facies changes of coal and oil shale strata in the Cenozoic Mae Tip basin: open—file report 8105-2. *Dept. Geol. Sci-, Chiang Mai Univ.*
- Gibling, M. R., Tantisukrit, C., Uttamo, W., Thanasuthipitak, T., and Haraluck, M. (1985a). Oil Shale Sedimentology and Geochemistry in Cenozoic Mae Sot Basin, Thailand1. *AAPG Bulletin*, 69(5), 767-780. doi:10.1306/AD462808-

16F7-11D7-8645000102C1865D

- Gibling, M. R., Ukakimaphan, Y., and Srisuk, S. (1985b). Oil Shale and Coal in Intermontane Basins of Thailand1. *AAPG Bulletin*, 69(5), 760-766.  
doi:10.1306/AD462803-16F7-11D7-8645000102C1865D
- Greb, S. F. (2006). *Coal and the Environment* (Vol. 10): Amer Geological Inst.
- Greenwood, P. F., Arouri, K. R., and George, S. C. (2000). Tricyclic terpenoid composition of Tasmanites kerogen as determined by pyrolysis GC-MS. *Geochimica et Cosmochimica Acta*, 64(7), 1249-1263.
- Gülz, P.-G., Müller, E., Schmitz, K., Marner, F.-J., and Güth, S. (1992). Chemical composition and surface structures of epicuticular leaf waxes of *Ginkgo biloba*, *Magnolia grandiflora* and *Liriodendron tulipifera*. *Zeitschrift für Naturforschung C*, 47(7-8), 516-526.
- Hardie, L. A., Smoot, J. P., and Eugster, H. P. (1978). Saline lakes and their deposits: a sedimentological approach. In *Modern and ancient lake sediments* (Vol. 2, pp. 7-41): Blackwell Oxford.
- Hayes, J., Freeman, K. H., Popp, B. N., and Hoham, C. H. (1990). Compound-specific isotopic analyses: a novel tool for reconstruction of ancient biogeochemical processes. *Organic Geochemistry*, 16(4-6), 1115-1128.
- Hintze, P., Buhler, C., Schuerger, A., Calle, L., and Calle, C. (2010). Alteration of five organic compounds by glow discharge plasma and UV light under simulated Mars conditions. *Icarus*, 208, 749-757. doi:10.1016/j.icarus.2010.03.015
- Hoffmann, C., Foster, C., Powell, T., and Summons, R. (1987). Hydrocarbon biomarkers from Ordovician sediments and the fossil alga *Gloeocapsomorpha prisca* Zalesky 1917. *Geochimica et Cosmochimica Acta*, 51(10), 2681-2697.
- Horne, J., Ferm, J., Caruccio, F., and Baganz, B. (1978). Depositional models in coal exploration and mine planning in Appalachian region. *AAPG Bulletin*, 62(12), 2379-2411.
- Huang, W.-Y., and Meinschein, W. G. (1979). Sterols as ecological indicators. *Geochimica et Cosmochimica Acta*, 43(5), 739-745.  
doi:[https://doi.org/10.1016/0016-7037\(79\)90257-6](https://doi.org/10.1016/0016-7037(79)90257-6)
- Hunt, J. M. (1991). Generation of gas and oil from coal and other terrestrial organic matter. *Organic Geochemistry*, 17(6), 673-680.
- Hunt, J. M. (1995). Petroleum geochemistry and geology.
- Hutton, A., Kantsler, A., Cook, A., and McKirdy, D. (1980). Organic matter in oil shales. *The APPEA Journal*, 20(1), 44-67.
- ICCP. (1971). International Handbook of Coal Petrography. In: Centre National de Recherche Scientifique Paris.
- ICCP. (1998). The new vitrinite classification (ICCP System 1994). *Fuel*, 77(5), 349-358.
- ICCP. (2001). Handbook Coal Petr. suppl. to 2nd ed. ICCP. 1998. The new vitrinite classification (ICCP System 1994). *Fuel*, 77, 349-358.
- Jaffé, R., Mead, R., Hernandez, M. E., Peralba, M. C., and DiGuida, O. A. (2001). Origin and transport of sedimentary organic matter in two subtropical estuaries: a comparative, biomarker-based study. *Organic Geochemistry*, 32(4), 507-526.
- Jarvie, D. M. (1991a). Total organic carbon (TOC) analysis: Chapter 11 Geochemical methods and exploration.
- Jarvie, D. M. (1991b). Total organic carbon (TOC) analysis: Chapter 11: Geochemical

methods and exploration.

- Jeng, W.-L., and Huh, C.-A. (2008). A comparison of sedimentary aliphatic hydrocarbon distribution between East China Sea and southern Okinawa Trough. *Continental Shelf Research*, 28(4-5), 582-592.
- Jia, J., Liu, Z., Bechtel, A., Strobl, S. A., and Sun, P. (2013). Tectonic and climate control of oil shale deposition in the Upper Cretaceous Qingshankou Formation (Songliao Basin, NE China). *International Journal of Earth Sciences*, 102(6), 1717-1734.
- Jin, X. (1994). Sedimentary and paleogeographic significance of Permo-Carboniferous sequences in western Yunnan, China. *Geologisches Institut der Universitaet zu Koeln Sonderveroeffentlichungen*, 99, 1-136.
- Jones, R. (1987). Organic facies.
- Kanzari, F., Syakti, A., Asia, L., Malleret, L., Piram, A., Mille, G., and Doumenq, P. (2014). Distributions and sources of persistent organic pollutants (aliphatic hydrocarbons, PAHs, PCBs and pesticides) in surface sediments of an industrialized urban river (Huveaune), France. *Science of the Total Environment*, 478, 141-151.
- Kennicutt II, M., Barker, C., Brooks, J., DeFreitas, D., and Zhu, G. (1987). Selected organic matter source indicators in the Orinoco, Nile and Changjiang deltas. *Organic Geochemistry*, 11(1), 41-51.
- Khositchaisri, W. (2012). *Petroleum geochemistry of Huai Hin Lat formation in Amphoe Nam Nao, Changwat Phetchabun and Amphoe Chumpae, Changwat Khon Kaen, Thailand*. Chulalongkorn University,
- Killops, S. D., and Killops, V. J. (2013). *Introduction to organic geochemistry*: John Wiley & Sons.
- Kvenvolden, K. A., and Simoneit, B. R. (1990). Hydrothermally Derived Petroleum: Examples from Guaymas Basin, Gulf of California, and Escanaba Trough, Northeast Pacific Ocean (1). *AAPG Bulletin*, 74(3), 223-237.
- Kwansiririkul, K., Singharajwarapan, F., Mackay, R., Ramingwong, T., and Wongpornchai, P. (2004). Vulnerability assessment of groundwater resources in the Lampang Basin of Northern Thailand. *J Environ Hydrol*, 12(23), 1-15.
- Large, D., and Gize, A. (1996). Pristane/phytane ratios in the mineralized Kupferschiefer of the Fore-Sudetic Monocline, southwest Poland. *Ore Geology Reviews*, 11(1-3), 89-103.
- Levine, J. R. (1993). Coalification: the evolution of coal as source rock and reservoir rock for oil and gas: Chapter 3.
- Li, Z., Li, X., Li, Y., Yu, J., Wang, D., Lv, D., Wang, P., Liu, Y., Liu, H., and Wu, X. (2016). Mechanisms of accumulation and coexistence of coal and oil shale in typical basins. *Energy Exploration & Exploitation*, 34(3), 360-377. doi:10.1177/0144598716631663
- Liu, R., Liu, Z., Sun, P., Xu, Y., Liu, D., Yang, X., and Zhang, C. (2015). Geochemistry of the Eocene Jijuntun Formation oil shale in the Fushun Basin, northeast China: Implications for source-area weathering, provenance and tectonic setting. *Geochemistry*, 75(1), 105-116.
- Mackenzie, A., Hoffmann, C., and Maxwell, J. (1981). Molecular parameters of maturation in the Toarcian shales, Paris Basin, France—III. Changes in aromatic steroid hydrocarbons. *Geochimica et Cosmochimica Acta*, 45(8), 1345-1355.

- Mastalerz, M., Goodman, A., and Chirdon, D. (2012). Coal lithotypes before, during, and after exposure to CO<sub>2</sub>: Insights from direct Fourier transform infrared investigation. *Energy & fuels*, 26(6), 3586-3591.
- Matsuda, H., and Koyama, T. (1977). Early diagenesis of fatty acids in lacustrine sediments—I. Identification and distribution of fatty acids in recent sediment from a freshwater lake. *Geochimica et Cosmochimica Acta*, 41(6), 777-783.
- Matsumoto, G. I., Akiyama, M., Watanuki, K., and Torii, T. (1990). Unusual distributions of long-chain n-alkanes and n-alkenes in Antarctic soil. *Organic Geochemistry*, 15(4), 403-412.
- Maxwell, J., Cox, R., Eglinton, G., Pillinger, C., Ackman, R., and Hooper, S. (1973). Stereochemical studies of acyclic isoprenoid compounds—II The role of chlorophyll in the derivation of isoprenoid-type acids in a lacustrine sediment. *Geochimica et Cosmochimica Acta*, 37(2), 297-313.
- Meinschein, W. (1969). Hydrocarbons—saturated, unsaturated and aromatic. In *Organic Geochemistry* (pp. 330-356): Springer.
- Mello, M., Telnaes, N., Gaglianone, P., Chicarelli, M., Brassell, S., and Maxwell, J. (1988). Organic geochemical characterisation of depositional palaeoenvironments of source rocks and oils in Brazilian marginal basins. In *Organic Geochemistry In Petroleum Exploration* (pp. 31-45): Elsevier.
- Metcalf, I. (1991). Late Palaeozoic and Mesozoic palaeogeography of southeast Asia. *Palaeogeography, Palaeoclimatology, Palaeoecology*, 87(1-4), 211-221.
- Metcalf, I. (2006). Palaeozoic and Mesozoic tectonic evolution and palaeogeography of East Asian crustal fragments: the Korean Peninsula in context. *Gondwana Research*, 9(1-2), 24-46.
- Metcalf, I. (2011). Tectonic framework and Phanerozoic evolution of Sundaland. *Gondwana Research*, 19(1), 3-21.
- Meyers, P. A., and Ishiwatari, R. (1993). Lacustrine organic geochemistry—an overview of indicators of organic matter sources and diagenesis in lake sediments. *Organic Geochemistry*, 20(7), 867-900.
- Miles, J. A. (1989). *Illustrated glossary of petroleum geochemistry*: Oxford University Press, USA.
- Mille, G., Asia, L., Guiliano, M., Malleret, L., and Doumenq, P. (2007). Hydrocarbons in coastal sediments from the Mediterranean sea (Gulf of Fos area, France). *Marine pollution bulletin*, 54(5), 566-575.
- Moldowan, J. M., Seifert, W. K., and Gallegos, E. J. (1985). Relationship between petroleum composition and depositional environment of petroleum source rocks. *AAPG Bulletin*, 69(8), 1255-1268.
- Moore, P. D. (1989). The ecology of peat-forming processes: a review. *International Journal of Coal Geology*, 12(1-4), 89-103.
- Morley, C. (2001). Combined escape tectonics and subduction rollback—back arc extension: a model for the evolution of Tertiary rift basins in Thailand, Malaysia and Laos. *Journal of the Geological Society*, 158(3), 461-474.
- Morley, C. (2009). Evolution from an oblique subduction back-arc mobile belt to a highly oblique collisional margin: the Cenozoic tectonic development of Thailand and eastern Myanmar. *Geological Society, London, Special Publications*, 318(1), 373-403.
- Morley, C. (2017). The impact of multiple extension events, stress rotation and inherited

- fabrics on normal fault geometries and evolution in the Cenozoic rift basins of Thailand. *Geological Society, London, Special Publications*, 439(1), 413-445.
- Morley, C., Charusiri, P., and Watkinson, I. (2011). Tertiary structure. *The Geology of Thailand, Geological Society of London, Memoir*, 273-334.
- Morley, C., Haranya, C., Phoosongsee, W., Pongwapee, S., Kornsawan, A., and Wonganan, N. (2004). Activation of rift oblique and rift parallel pre-existing fabrics during extension and their effect on deformation style: examples from the rifts of Thailand. *Journal of Structural Geology*, 26(10), 1803-1829.
- Morley, C., Woganan, N., Sankumarn, N., Hoon, T., Alief, A., and Simmons, M. (2001). Late Oligocene–Recent stress evolution in rift basins of northern and central Thailand: implications for escape tectonics. *Tectonophysics*, 334(2), 115-150.
- Morley, C. K. (2015). Five anomalous structural aspects of rift basins in Thailand and their impact on petroleum systems. *Geological Society, London, Special Publications*, 421(1), 143-168.
- Moustafa, Y. M., and Morsi, R. E. (2012). Biomarkers. In *Chromatography and its applications*: IntechOpen.
- Muenlek, S. (1992a). *Coal geology of Mae Than basin Amphoe Mae Tha, Lampang*. Paper presented at the Proceedings of a National Conference on Geologic Resources of Thailand: Potential for Future Development. Department of Mineral Resources, Bangkok.
- Muenlek, S. (1992b). *Coal Geology of Mae Than Basin, Amphoe Mae Tha, Lampang*. Paper presented at the Proceedings of a National Conference on Geologic Resources of Thailand: Potential for Future Development. Department of Mineral Resources, Bangkok.
- Mukhopadhyay, P. K., and Hatcher, P. G. (1993). Composition of Coal: Chapter 4.
- Otto, A., and Simoneit, B. R. (2001). Chemosystematics and diagenesis of terpenoids in fossil conifer species and sediment from the Eocene Zeitz formation, Saxony, Germany. *Geochimica et Cosmochimica Acta*, 65(20), 3505-3527.
- Peter, K., and Moldowan, J. (1993). The biomarker guide. *Interpreting Molecular*.
- Peters, K., and Moldowan, J. (1991). Effects of source, thermal maturity, and biodegradation on the distribution and isomerization of homohopanes in petroleum. *Organic Geochemistry*, 17(1), 47-61.
- Peters, K. E., and Cassa, M. R. (1994). Applied source rock geochemistry: Chapter 5: Part II. Essential elements.
- Peters, K. E., Peters, K. E., Walters, C. C., and Moldowan, J. (2005). *The biomarker guide* (Vol. 1): Cambridge University Press.
- Petersen, H., Foopattanakamol, A., and Ratanasthien, B. (2006). Petroleum potential, thermal maturity and the oil window of oil shales and coals in Cenozoic rift basins, central and northern Thailand. *Journal of Petroleum Geology*, 29, 337-360. doi:10.1111/j.1747-5457.2006.00337.x
- Petersen, H. I., Nytoft, H. P., and Nielsen, L. H. (2004). Characterisation of oil and potential source rocks in the northeastern Song Hong Basin, Vietnam: indications of a lacustrine-coal sourced petroleum system. *Organic Geochemistry*, 35(4), 493-515.
- Philippi, G. (1965). On the depth, time and mechanism of petroleum generation. *Geochimica et Cosmochimica Acta*, 29(9), 1021-1049.

- Piyasin, S. (1972). Geology of Changwat Lampang Sheet, scale 1: 250,000. *DMR (Department of Mineral Resources of Thailand) Report, 14*, 98.
- Polachan, S., Praditnan, S., Tongtaow, C., Janmaha, S., Intarawijitr, K., and Sangsuwan, C. (1991). Development of Cenozoic basins in Thailand. *Marine and Petroleum Geology, 8*(1), 84-97.
- Polachan, S., and Sattayarak, N. (1989). *Strike-slip tectonics and the development of Tertiary basins in Thailand*. Paper presented at the International symposium on intermontane basins: geology and resources.
- Powell, T. (1988). Pristane/phytane ratio as environmental indicator. *Nature, 333*(6174), 604-604.
- Powell, T., and Mokirdy, D. (1973). The effect of source material, rock type and diagenesis on the n-alkane content of sediments. *Geochimica et Cosmochimica Acta, 37*(3), 623-633.
- Poynter, J., and Eglinton, G. (1990). *14. Molecular composition of three sediments from hole 717c: The Bengal fan*. Paper presented at the Proceedings of the Ocean Drilling Program: Scientific results.
- Prahl, F., Cowie, G., De Lange, G., and Sparrow, M. (2003). Selective organic matter preservation in “burn-down” turbidites on the Madeira Abyssal Plain. *Paleoceanography, 18*(2).
- Quinty, F., and Rochefort, L. (2003). *Peatland restoration guide: Canadian Sphagnum Peat Moss Association*.
- Racey, A. (2011). Chapter 13. *Petroleum geology*. In: Ridd MF, Barber AJ & Crow MJ (eds) *Geology of Thailand*. Geological Society, London, 251, 392.
- Ratanasthien, B. (1984). *Spore and pollen dating of some Tertiary coal and oil deposits in northern Thailand*. Paper presented at the Conference on Applications of Geology to National Development, Chulalongkorn University. Bangkok, 1984.
- Ratanasthien, B. (2011). *Coal deposits*.
- Ratanasthien, B., Kandharosa, W., Chompusri, S., and Chartprasert, S. (1999). Liptinite in coal and oil source rocks in northern Thailand. *Journal of Asian Earth Sciences, 17*(1), 301-306. doi:[https://doi.org/10.1016/S0743-9547\(98\)00067-1](https://doi.org/10.1016/S0743-9547(98)00067-1)
- Rhodes, B. P., Conejo, R., Benchawan, T., Titus, S., and Lawson, R. (2005). Palaeocurrents and provenance of the Mae Rim Formation, Northern Thailand: implications for tectonic evolution of the Chiang Mai basin. *Journal of the Geological Society, 162*(1), 51-63.
- Rieley, G., Collier, R. J., Jones, D. M., Eglinton, G., Eakin, P. A., and Fallick, A. E. (1991). Sources of sedimentary lipids deduced from stable carbon-isotope analyses of individual compounds. *Nature, 352*(6334), 425-427.
- Rieley, G., Collister, J. W., Stern, B., and Eglinton, G. (1993). Gas chromatography/isotope ratio mass spectrometry of leaf wax n-alkalines from plants of differing carbon dioxide metabolisms. *Rapid Communications in Mass Spectrometry, 7*(6), 488-491.
- Rohrssen, M., Gill, B. C., and Love, G. D. (2015). Scarcity of the C30 sterane biomarker, 24-n-propylcholestane, in Lower Paleozoic marine paleoenvironments. *Organic Geochemistry, 80*, 1-7. doi:<https://doi.org/10.1016/j.orggeochem.2014.11.008>
- Sakari, M., Zakaria, M. P., Lajis, N. H., Mohamed, C. A. R., Bahry, P. S., Anita, S., and Chandru, K. (2008). Characterization, distribution, sources and origins of

- aliphatic hydrocarbons from surface sediment of Prai Strait, Penang, Malaysia: A widespread anthropogenic input. *Environment Asia*, 2, 1-14.
- Schopf, J. M. (1956). A definition of coal. *Economic geology*, 51(6), 521-527.
- Searle, M., Morley, C., Ridd, M., Barber, A., and Crow, M. (2011). Tectonic and thermal evolution of Thailand in the regional context of SE Asia. *The Geology of Thailand. Geological Society, London*, 539, 571.
- Seifert, W., and Moldowan, J. (1986). Use of biological markers in petroleum exploration. *Methods in geochemistry and geophysics*, 24, 261-290.
- Seifert, W. K., and Moldowan, J. M. (1979). The effect of biodegradation on steranes and terpanes in crude oils. *Geochimica et Cosmochimica Acta*, 43(1), 111-126.
- Setyobudi, P. T., Suandhi, P. A., Tarigan, Z. L., Bachtiar, A., Jayanti, A. G. R., and Budin, L. (2016). Sedimentology And Limnology of Singkarak and Toba Lakes, Sumatra, Indonesia: Depositional and Petroleum System Model for Tropical Fluvio-Lacustrine and Volcanic Related Rift Basins in Southeast Asia.
- Shanmugam, G. (1985). Significance of Coniferous Rain Forests and Related Organic Matter in Generating Commercial Quantities of Oil, Gippsland Basin, Australia. *AAPG bulletin*, 69(8), 1241-1254.
- Simão, G., and Kalkreuth, W. (2015). Petrographic and Chemical Characterization of the Bonito Seam and its Beneficiation Products, South Santa Catarina Coalfield—Brazil. *Energy Exploration & Exploitation*, 33(1), 75-90.
- Sinninghe Damsté, J. S., Kenig, F., Koopmans, M. P., Koster, J., Schouten, S., Hayes, J., and de Leeuw, J. W. (1995). Evidence for gammacerane as an indicator of water column stratification. *Geochimica et Cosmochimica Acta*, 59(9), 1895-1900.
- Sivavong, V. (2009). Coal demand/supply outlook in Thailand. (In: Conference Proceedings of the 2009APEC Clean Fossil Energy Technical and Policy Seminar— Clean Coal: Moving Towards Zero Emissions, Inchon).
- Sleutel, S., De Neve, S., Singier, B., and Hofman, G. (2007). Quantification of organic carbon in soils: a comparison of methodologies and assessment of the carbon content of organic matter. *Communications in Soil Science and Plant Analysis*, 38(19-20), 2647-2657.
- Snansieng, S. (1979). Exploration and use of lignite in the north (in Thai): Geological Society of Thailand Special Paper. *Year*, 2522, 25-38.
- Sone, M., and Metcalfe, I. (2008). Parallel Tethyan sutures in mainland Southeast Asia: new insights for Palaeo-Tethys closure and implications for the Indosinian orogeny. *Comptes Rendus Geoscience*, 340(2-3), 166-179.
- Songtham, W., Ratanasthien, B., Mildenhall, D. C., Singharajwarapan, S., and Kandharosa, W. (2003). Oligocene-Miocene climatic changes in northern Thailand resulting from extrusion tectonics of Southeast Asian landmass. *Science Asia*, 29(3), 221-233.
- Songtham, W., Ratanasthien, B., Watanasak, M., Mildenhall, D. C., Singharajwarapan, S., and Kandharosa, W. (2005). Tertiary basin evolution in northern Thailand: A palynological point of view. *Natural History Bulletin of the Siam Society*, 53(1), 17-32.
- Stach, E., Mackowsky, M.-T., Teichmuller, M., Taylor, G., Chandra, D., and Teichmuller, R. (1982). Stach's textbook of coal petrology: Gebruder Borntraeger. *Berlin*, 535p.

- Stanton, R., Moore, T. A., Warwick, P. D., Crowley, S., and Flores, R. M. (1989). Comparative facies formation in selected coal beds of the Powder River Basin.
- Staub, J. R., and Esterle, J. S. (1994). Peat-accumulating depositional systems of Sarawak, East Malaysia. *Sedimentary Geology*, 89(1-2), 91-106.
- Stauffer, E., Dolan, J., and Newman, R. (2008a). Chapter 8-Gas Chromatography and Gas Chromatography—Mass Spectrometry. *Fire debris analysis*, 235-293.
- Stauffer, E., Dolan, J. A., and Newman, R. (2008b). CHAPTER 9 - Interpretation of Data Obtained from Neat Ignitable Liquids. In E. Stauffer, et al. (Eds.), *Fire Debris Analysis* (pp. 295-354). Burlington: Academic Press.
- Stefanova, M., Magnier, C., and Velinova, D. (1995). Biomarker assemblage of some Miocene-aged Bulgarian lignite lithotypes. *Organic Geochemistry*, 23(11-12), 1067-1084.
- Stefanova, M., Marinov, S., and Magnier, C. (1999). Aliphatic biomarkers from Miocene lignites desulphurization. *Fuel*, 78(12), 1395-1406.
- Stopes, M. C. C. (1935). *On the petrology of banded bituminous coal*: Verlag nicht ermittelbar.
- Styan, W. t., and Bustin, R. (1983). Petrography of some Fraser river delta peat deposits: coal maceral and microlithotype precursors in temperate-climate peats. *International Journal of Coal Geology*, 2(4), 321-370.
- Summons, R. E., Brassell, S. C., Eglinton, G., Evans, E., Horodyski, R. J., Robinson, N., and Ward, D. M. (1988). Distinctive hydrocarbon biomarkers from fossiliferous sediment of the late Proterozoic Walcott member, Chuar Group, Grand Canyon, Arizona. *Geochimica et Cosmochimica Acta*, 52(11), 2625-2637.
- Sun, P., Sachsenhofer, R. F., Liu, Z., Strobl, S. A. I., Meng, Q., Liu, R., and Zhen, Z. (2013). Organic matter accumulation in the oil shale- and coal-bearing Huadian Basin (Eocene; NE China). *International Journal of Coal Geology*, 105, 1-15. doi:<https://doi.org/10.1016/j.coal.2012.11.009>
- Sýkorová, I., Pickel, W., Christanis, K., Wolf, M., Taylor, G. H., and Flores, D. (2005). Classification of huminite—ICCP System 1994. *International Journal of Coal Geology*, 62(1), 85-106. doi:<https://doi.org/10.1016/j.coal.2004.06.006>
- Tapponnier, P., Peltzer, G., and Armijo, R. (1986). On the mechanics of the collision between India and Asia. *Geological Society, London, Special Publications*, 19(1), 113-157.
- Taylor, G. H., Teichmüller, M., Davis, A., Diessel, C., Littke, R., and Robert, P. (1998). Organic petrology.
- Teichmüller, M. (1989). The genesis of coal from the viewpoint of coal petrology. *International Journal of Coal Geology*, 12(1-4), 1-87.
- Ten Haven, H., De Leeuw, J., Rullkötter, J., and Damsté, J. S. (1987). Restricted utility of the pristane/phytane ratio as a palaeoenvironmental indicator. *Nature*, 330(6149), 641-643.
- Thowanich, S. (1997). Geology and mineralogy of the Mae Than ball clay deposit, Amphoe Mae Tha, Changwat Lampang. *Chulalongkorn University, Bangkok*.
- Tissot, B., and Welte, D. (1984). Petroleum formation and occurrence. Springer-Verlag, Berlin, (1984), 699.
- Travena, A., and Clark, R. (1986). Diagenesis of sandstone reservoirs of Pattani Basin. *Gulf of Thailand: AAPG Bulletin*, 70, 299-308.
- Tuo, J., Wang, X., Chen, J., and Simoneit, B. (2003). Aliphatic and diterpenoid



- hydrocarbons and their individual carbon isotope compositions in coals from the Liaohe Basin, China. *Organic Geochemistry*, 34(12), 1615-1625.
- van Krevelen, D. W. (1981). *Coal*.
- Volkman, J. K. (1986). A review of sterol markers for marine and terrigenous organic matter. *Organic Geochemistry*, 9(2), 83-99.
- Volkman, J. K., and Maxwell, J. R. (1986). Acyclic isoprenoids as biological markers. *Methods in geochemistry and geophysics*, 24, 1-42.
- Wang, L., Wang, C., Li, Y., Zhu, L., and Wei, Y. (2011). Sedimentary and organic geochemical investigation of tertiary lacustrine oil shale in the central Tibetan plateau: Palaeolimnological and palaeoclimatic significances. *International Journal of Coal Geology*, 86(2-3), 254-265.
- Wang, X.-D., Ueno, K., Mizuno, Y., and Sugiyama, T. (2001). Late Paleozoic faunal, climatic, and geographic changes in the Baoshan block as a Gondwana-derived continental fragment in southwest China. *Palaeogeography, Palaeoclimatology, Palaeoecology*, 170(3-4), 197-218.
- Waples, D., and Machihara, T. (1991). Biomarkers for Geologists. AAPG Methods in Exploration Series No. 9. *American Association of Petroleum Geologists, Tulsa, Oklahoma*.
- Waples, D. W. (1985). Organic Chemistry and Isotopes. In *Geochemistry in Petroleum Exploration* (pp. 19-30): Springer.
- Waples, D. W., and Machihara, T. (1991). Biomarkers for geologists.
- Waseda, A., and Nishita, H. (1998). Geochemical characteristics of terrigenous-and marine-sourced oils in Hokkaido, Japan. *Organic Geochemistry*, 28(1-2), 27-41.
- Watcharanantakul, R., and Morley, C. (2000). Syn-rift and post-rift modelling of the Pattani Basin, Thailand: evidence for a ramp-flat detachment. *Marine and Petroleum Geology*, 17(8), 937-958.
- Wilcox, D. A., Thompson, T. A., Booth, R. K., and Nicholas, J. (2007). Lake-level variability and water availability in the Great Lakes. *US Geological Survey Circular 1311*.
- Wopfner, H. (1996). Gondwana origin of the Baoshan and Tengchong terranes of west Yunnan. *Geological Society, London, Special Publications*, 106(1), 539-547.
- Xiao, S., Tian, Z., Wang, Y., Si, L., Zhang, L., and Zhou, D. (2018). Recent progress in the antiviral activity and mechanism study of pentacyclic triterpenoids and their derivatives. *Medicinal Research Reviews*, 38(3), 951-976.  
doi:10.1002/med.21484
- Xu, J., Liu, Z., Bechtel, A., Meng, Q., Sun, P., Jia, J., Cheng, L., and Song, Y. (2015). Basin evolution and oil shale deposition during Upper Cretaceous in the Songliao Basin (NE China): Implications from sequence stratigraphy and geochemistry. *International Journal of Coal Geology*, 149, 9-23.
- Yan, J., Jiang, X., and Han, X. (2009). Study on the characteristics of the oil shale and shale char mixture pyrolysis. *Energy & fuels*, 23(12), 5792-5797.
- Zhao, C., Zhao, B., Shi, Z., Xiao, L., Wang, D., Khanchuk, A. I., Ivanov, V. V., and Blokhin, M. G. (2014). Maceral, mineralogical and geochemical characteristics of the Jurassic coals in Ningdong Coalfield, Ordos Basin. *Energy Exploration & Exploitation*, 32(6), 965-987.

## VITA

**NAME** Patthapong Chaiseanwang

**DATE OF BIRTH** 10 Jan 1995

**PLACE OF BIRTH** Lampang, Thailand

**INSTITUTIONS ATTENDED** Bachelor of Science (Geology), Chulalongkorn University

**HOME ADDRESS** 146/52 The Thamm 1, Prachatorn road, Lat Krabang subdistrict, Lat Krabang district, Bangkok 10520



จุฬาลงกรณ์มหาวิทยาลัย  
CHULALONGKORN UNIVERSITY